Chapter 5

Response to SST Profile (PEAKED, CONTROL, QOBS, FLAT)

Again we create a multi-model mean which provides a summary of the response of the climate of the modeled aqua-planet to the different zonal SST profiles. The set of models in the multi-model mean is slightly different than the set defined in Chapter 4 for the CONTROL experiment alone. Here FRCGC and UKMO(N96) are excluded since they did not provide results for the PEAKED, QOBS and FLAT experiments. Thus the multi-model mean model for the CONTROL is slightly different than that used in Chapter 4. As mentioned at the beginning of Chapter 4 some impact of dropping models from the average can be determined by comparing statistics for the multi-model mean from the CONTROL experiment in different chapters. Again, different chapters include a different set of models in the multi-model mean because not all models submitted all experiments, and for the cross-experiment comparisons, the models in the multi-mean must be the same set. Of course, the standard deviations are calculated over the same set of models as the multi-model mean. The multi-model mean for the eddy statistics in this chapter (based on MF files) excludes CGAM, MRI and UKMO(48) as well as FRCGC and UKMO(N96).

5.1 Mean State

5.1.1 Zonal-Time Average Poleward Energy Transport

Figure 5.1 shows the zonal-time average poleward energy transport for the multi-model mean of the four experiments (PEAKED, CONTROL, QOBS, FLAT) and for Earth estimates. Figures 5.2, 5.3 and 5.4 show the total, atmosphere and ocean transports, respectively, for the individual models. The calculation of transport is described in Section 4.1.1.

5.1.2 Global-Time Averages and Budgets

Figures 5.5 and 5.6 plot the global-time average (GT data sets) as bar plots for each variable for the multi-model mean for the PEAKED, CONTROL, QOBS and FLAT experiments. The whiskers with each bar range from plus one to minus one multi-model standard deviation. The variables plotted are tppn, cppn, dppn, evap, emp, cld_frac, albedo, ps, cldw, cldi, sw_toa, lw_toa, ssw, slw, slh, ssh, rflux_toa, rflux_sfce and rflux.

Figures 5.7 through 5.25 show the global-time average of the same variables as bar plots for the individual models. The whiskers with each bar range from plus one to minus one standard deviation of the time series of the model daily-global averages. GSFC, LASG, MIT and MRI did not submit cloud water (cldw) or cloud ice (cldi). AGU did not submit cloud ice (cldi). Thus the blank panels in Figures 5.15 and 5.16.

5.1.3 Zonal-Time Averages, 2-D Fields

Figures 5.26 and 5.27 show zonal-time averages for the multi-model mean for single level fields from the SH data sets for the four experiments (PEAKED, CONTROL, QOBS, FLAT). The fields shown are tppn, cppn, dppn, evap, emp, cld_frac, albedo, ps, tauu, sw_toa, lw_toa, rflux_toa, ssw, slw, rflux_sfce, slh, ssh and rflux. Figures 5.28 through 5.46 show zonal-time averages for the individual models for the same single level fields for the four experiments (PEAKED, CONTROL, QOBS, FLAT). The multi-model mean is repeated on the plots for convenience.

5.1.4 Zonal-Time Averages, 3-D Fields

Figures 5.47 through 5.49 show u, t, v, om, q and rh for the multi-model mean and standard deviation from the ML data sets.. The columns of the figures have PEAKED, CONTROL, QOBS and FLAT. Figures 5.50 through 5.52 show the differences of PEAKED, QOBS and FLAT with the CONTROL along with the CONTROL for the multi-model mean.

The remainder of this section shows a sequence of plots for each variable. It starts with a pair of plots for u for each model from PEAKED (Figure 5.53) and the difference of each model minus the multi-model mean for u from PEAKED (Figure 5.54). These are followed by similar pairs for CONTROL, QOBS and FLAT. Note the CONTROL replicates Figure 4.17 and Figure 4.18 from Section 4.1.4. These eight figures for u are then followed by differences PEAKED−CONTROL, QOBS−CONTROL and FLAT−CONTROL for all models, giving a total of eleven figures for u (Figures 5.53−5.63). These eleven figures for u are then followed by eleven figures each for v (Figures 5.75−5.85), t (Figures 5.64−5.74), om (Figures 5.86−5.96), q (Figures 5.97−5.107) and rh (Figures 5.108−5.118). This pattern is easier to see in the List of Figures.

5.2 Maintenance of Zonal Mean State (PEAKED, CONTROL, QOBS, FLAT)

5.2.1 Dynamical Budgets (variances and co-variances)

This section compares the stationary mean (sm_) (co-)variances $[\overline{\alpha}]\left[\overline{\beta}\right]$, and the transient eddy (te_) (co-)variances, $\overline{[\alpha'^*\beta'^*]}$, (see Eqn. 2.9) for the PEAKED, CONTROL, QOBS and FLAT SST distributions (MF data sets). Figures 5.119 and 5.120 show the the multi-model mean and standard deviation of the stationary mean: sm_ of uu, vv, uv and vt. Figures 5.121 and 5.122 show the multi-model mean and standard deviation for the transient eddies: te_ of uu, vv, uv

and vt. Figures 5.123 through 5.130 the (co-)variances for the individual models: sm_ and te_ of uu, vv, uv and vt.

We also include graphs of (co-)variances at selected levels for the four experiments (PEAKED, CONTROL, QOBS and FLAT) on the same plot to show the important differences more clearly. For example Figure 5.131 shows the stationary mean u variance, which is just the square of the zonal average zonal wind u, to show the transition of the jet core as the SSTs change from PEAKED to CONTROL to QOBS to FLAT. The (co-)variances shown are sm_uu at 250mb, te_uv at 250mb, te_vt at 700mb, te_vq at 850mb, te_uom at 400mb, te_vom at 500mb, te_omt at 700mb and te_omq at 700mb.

5.2.2 Parameterization Forcing

Figures 5.139 through 5.144 show the parameterization temperature tendencies: t, t_conv, t_cld, t_turb, t_sw and t_lw from the PF data sets. Figures 5.145 through 5.148 show the parameterization specific humidity tendencies: q, q_conv, q_cld and q_turb. Figures 5.149 and 5.150 show the parameterization zonal momentum tendencies: u_conv and u_turb. Figures 5.151 and 5.152 show the parameterization meridional momentum tendencies: v_conv and v_turb.

5.3 Tropical Variability (PEAKED, CONTROL, QOBS, FLAT)

5.3.1 Wavenumber-Frequency Spectra

For the wavenumber-frequency diagrams in this Chapter the log of the power is averaged from 20°S to 20°N instead of from 10°S to 10°N as was done in Section 4.3.2 which considered the CONTROL experiment alone. This domain is chosen because much of the tropical precipitation in the FLAT experiment moves poleward of 10° latitude (see Figure 5.28.)

For the experiments in which the precipitation remains within the 10°S to 10°N region the effect of the larger domain is to reduce the average power somewhat. (Compare the CONTROL in Figures 4.91 through 4.94 with the CONTROL in Figures 5.153 through 5.156.) Otherwise, the averages over the two domains are rather similar in structure. Note that contour values are reduced in this Section relative to the plots in Section 4.3.2 which minimizes the appearance of the differences.

Figure 5.153 shows the wavenumber-frequency diagrams of symmetric modes of tropical precipitation (tppn) for PEAKED, CONTROL, QOBS and FLAT for each model. Figure 5.154 shows the anti-symmetric modes of tropical precipitation. Figures 5.155 and 5.156 show the symmetric and anti-symmetric modes of TOA longwave radiation (lw_toa), respectively.

5.3.2 Precipitation Frequency Distributions

Again, because much of the tropical precipitation in the FLAT experiment moves poleward of 10° latitude (Figure 5.28) the frequency distributions are calculated from 20°S to 20°N latitude instead of from 10°S to 10°N as was done in Section 4.3.3 which considered the CONTROL experiment alone. To see the effect of the larger domain on the frequency distributions of the

CONTROL where the tropical precipitation occurs within ±10° latitude, the CONTROL in Figures 5.157 and 5.158 in this section can be compared to Figure 4.95. Similarly the frequency distributions after averaging to a 5° grid (Figures 5.159 and 5.160) can be compared to Figure 4.97.

Figure 5.157 shows the fraction of time precipitation (tppn) is in 1 mm day^{-1} bins ranging from 0 to 120 mm day^{-1} for all models for PEAKED, CONTROL, QOBS and FLAT experiments. The fractions are calculated from the 6-hour averages from the TR data for all model grid points between -20° and +20° latitude. Figure 5.158 shows the fractions for 10 mm day^{-1} bins ranging from 0 to 1200 mm day^{-1}. Most models show a monotonic decrease in the fraction of larger precipitation rates from PEAKED to CONTROL to QOBS to FLAT experiments. This is consistent with the zonal mean (Figure 5.28) at the equator decreasing in a similar manner. Figures 5.159 and 5.160 show the frequency distributions calculated from the data after they have been conservatively averaged to a 5° latitude-longitude grid.

5.4 Extratropics (PEAKED, CONTROL, QOBS, FLAT)

5.4.1 Wavenumber-Frequency Spectra

Figure 5.161 compares the wavenumber-frequency plots for the PEAKED, CONTROL, QOBS and FLAT experiments for the multi-model mean at 30° latitude and 50° latitude for the meridional velocity at 250 mb (v250) from the TR data. The plots at 30° latitude look similar for the PEAKED, CONTROL and QOBS. The FLAT experiment has less power and the indication of preferred modes for certain wavenumbers is missing. However, the jet core is more poleward in the FLAT case as seen in Fig. 5.47. Therefore we also show the wavenumber-frequency diagrams at 50° latitude, slightly poleward of the core of the jet in the FLAT case. When examined at this latitude, the FLAT experiment has more power than the other cases. The power decreases from FLAT to QOBS to CONTROL to PEAKED as the jet shifts equatorward and the zonal wind at 50° decreases. Similar properties are seen in the anti-symmetric modes shown in Figure 5.162.

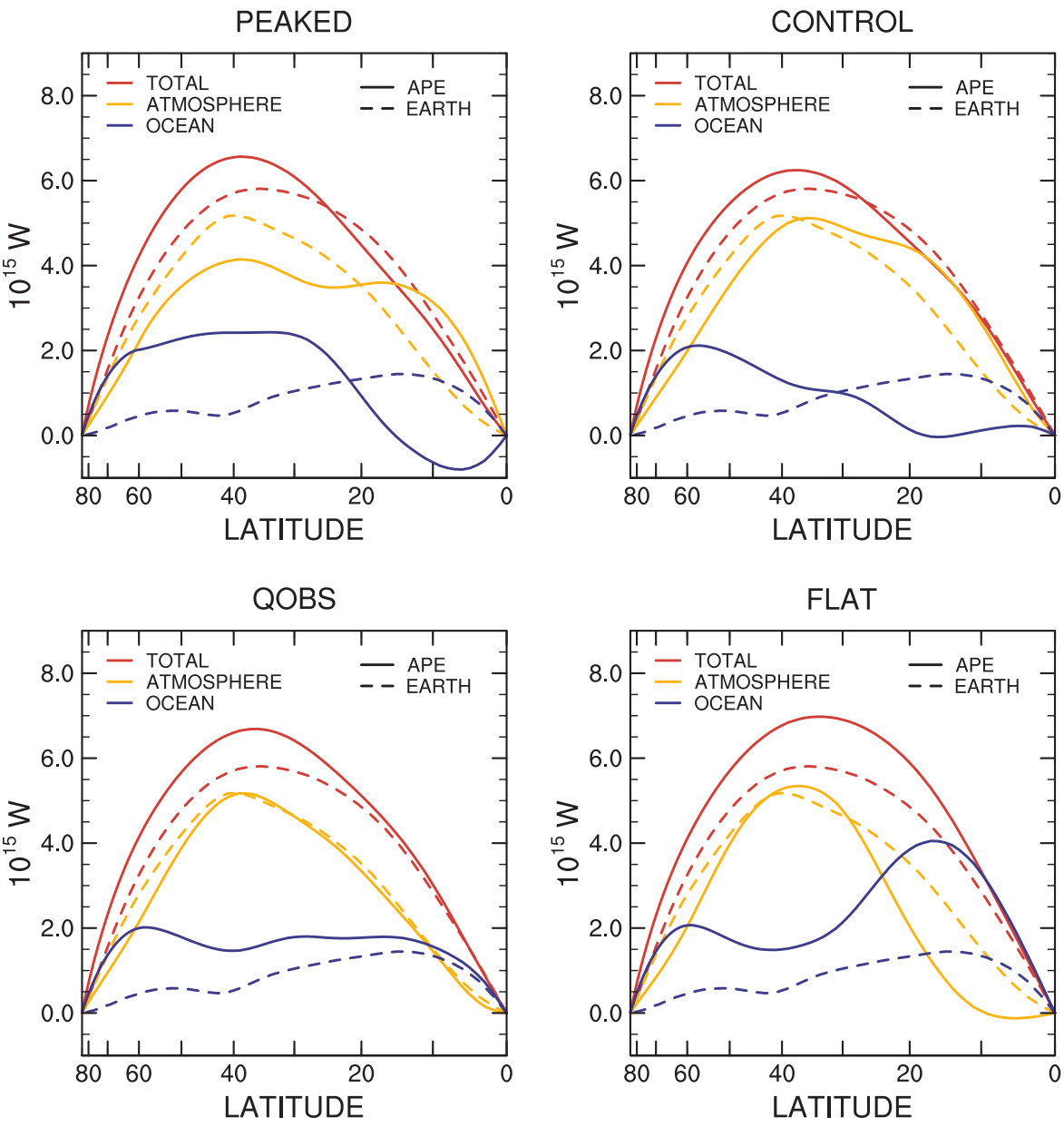

Figure 5.1: Multi-model mean zonal-time average poleward energy transports.

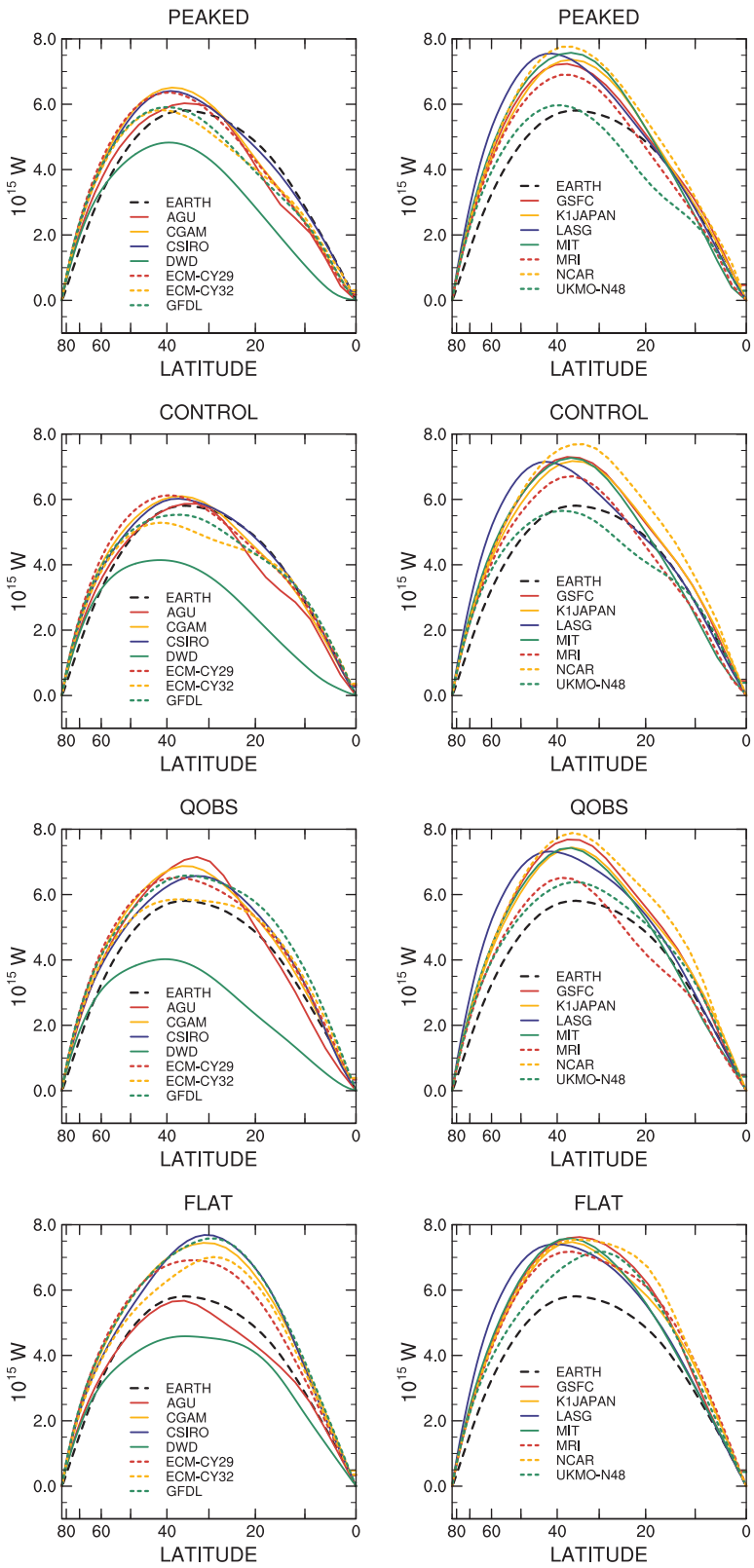

Figure 5.2: Individual model zonal-time average total poleward energy transport.

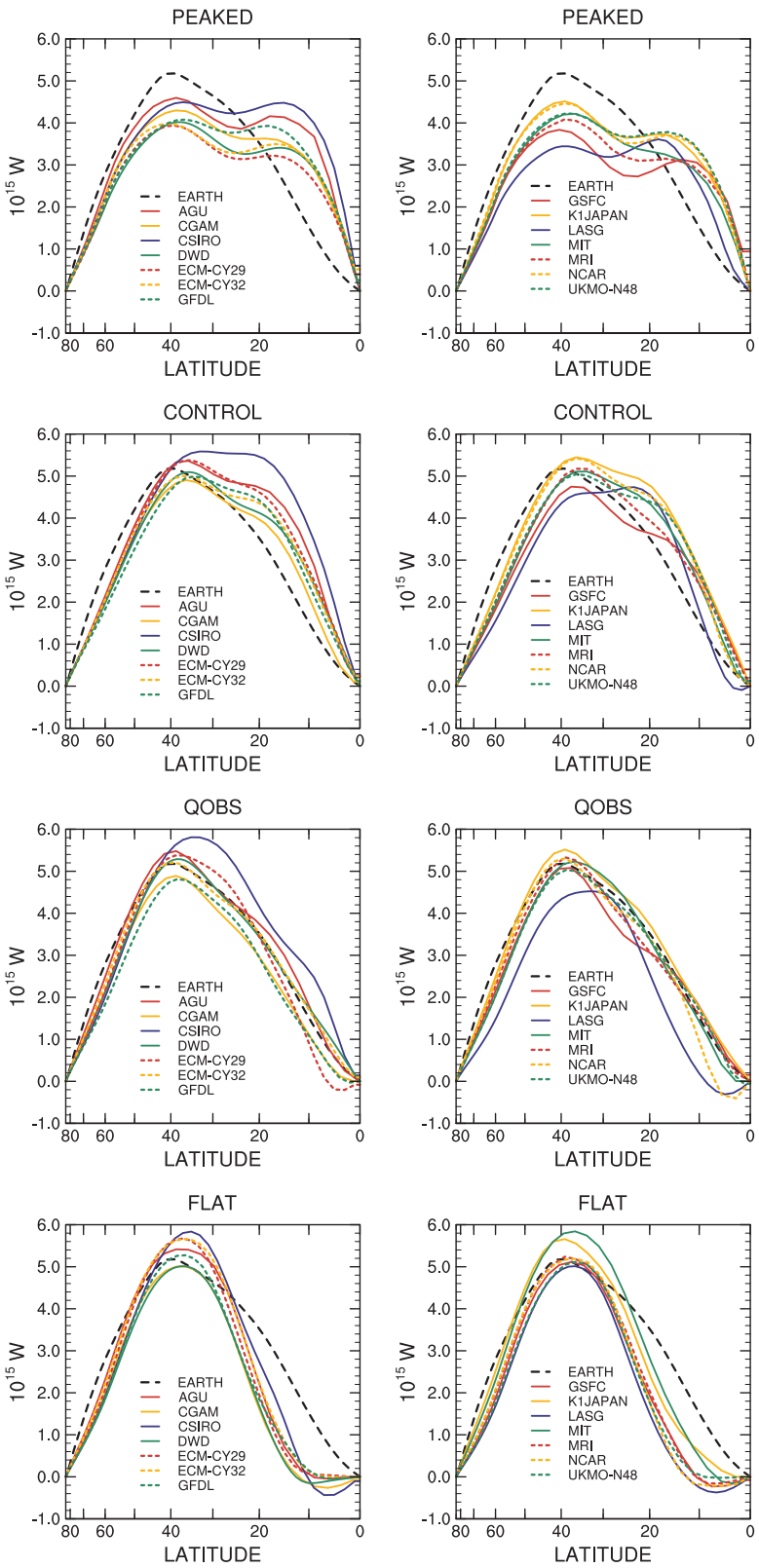

Figure 5.3: Individual model zonal-time average atmosphere poleward energy transport.

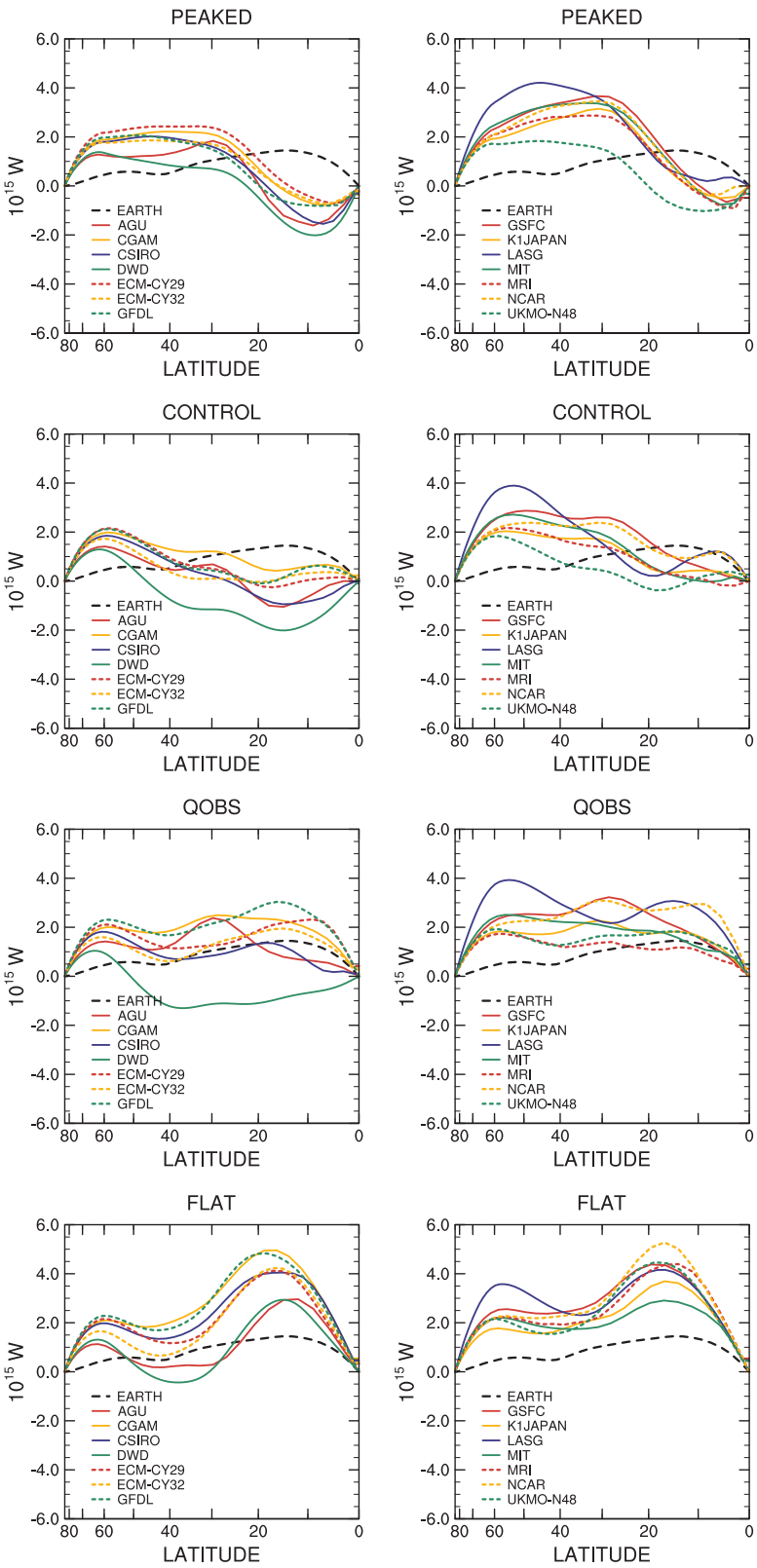

Figure 5.4: Individual model zonal-time average ocean poleward energy transport.

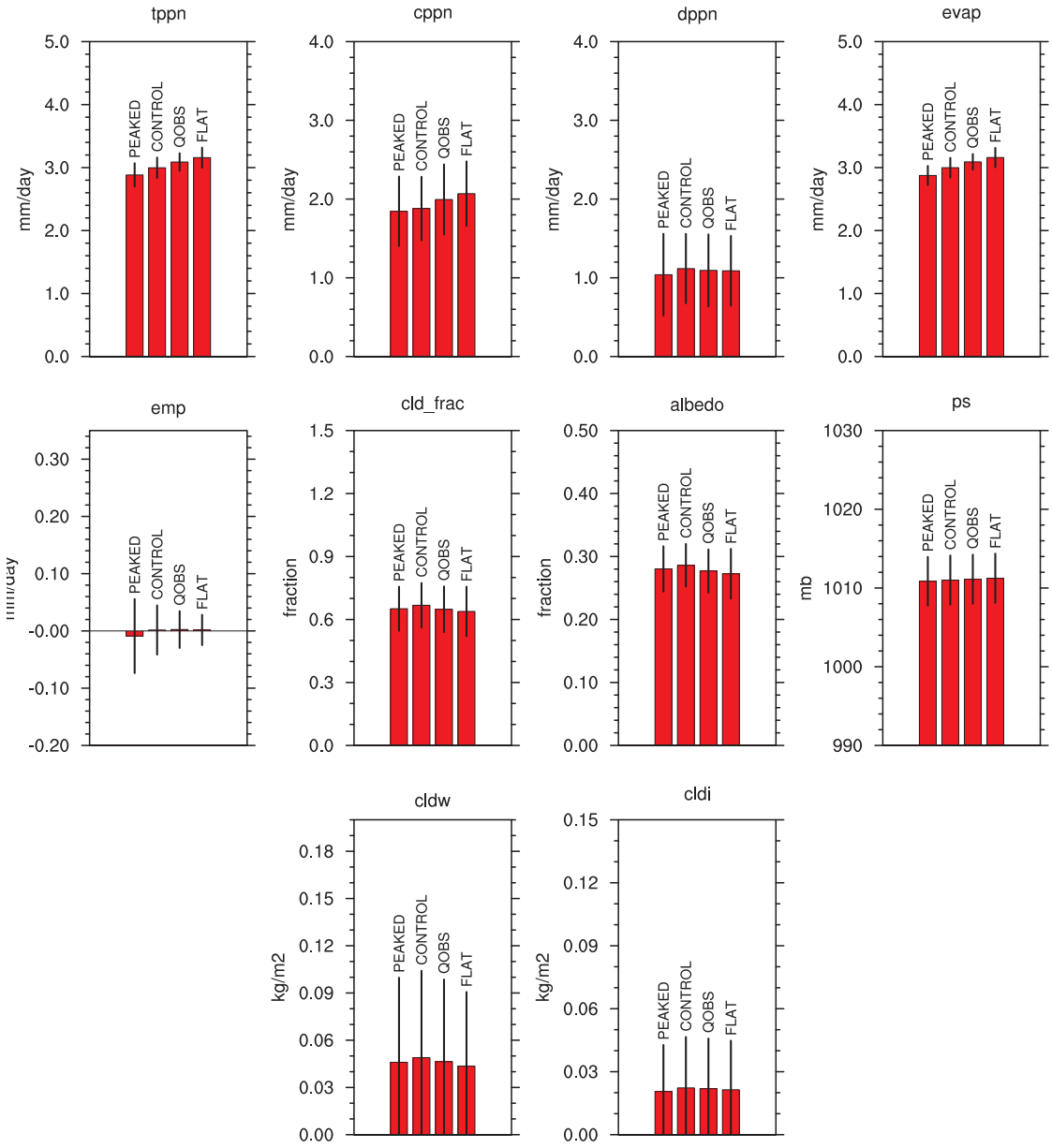

Figure 5.5: Multi-model mean global-time average total precipitation (tppn), convective precipitation (cppn), large-scale precipitation (dppn), evaporation (evap), evaporation minus precipitation (emp), cloud fraction (cld_frac), albedo (albedo), surface pressure (ps), cloud water (cldw) and cloud ice (cldi) from PEAKED, CONTROL, QOBS and FLAT SST distributions.

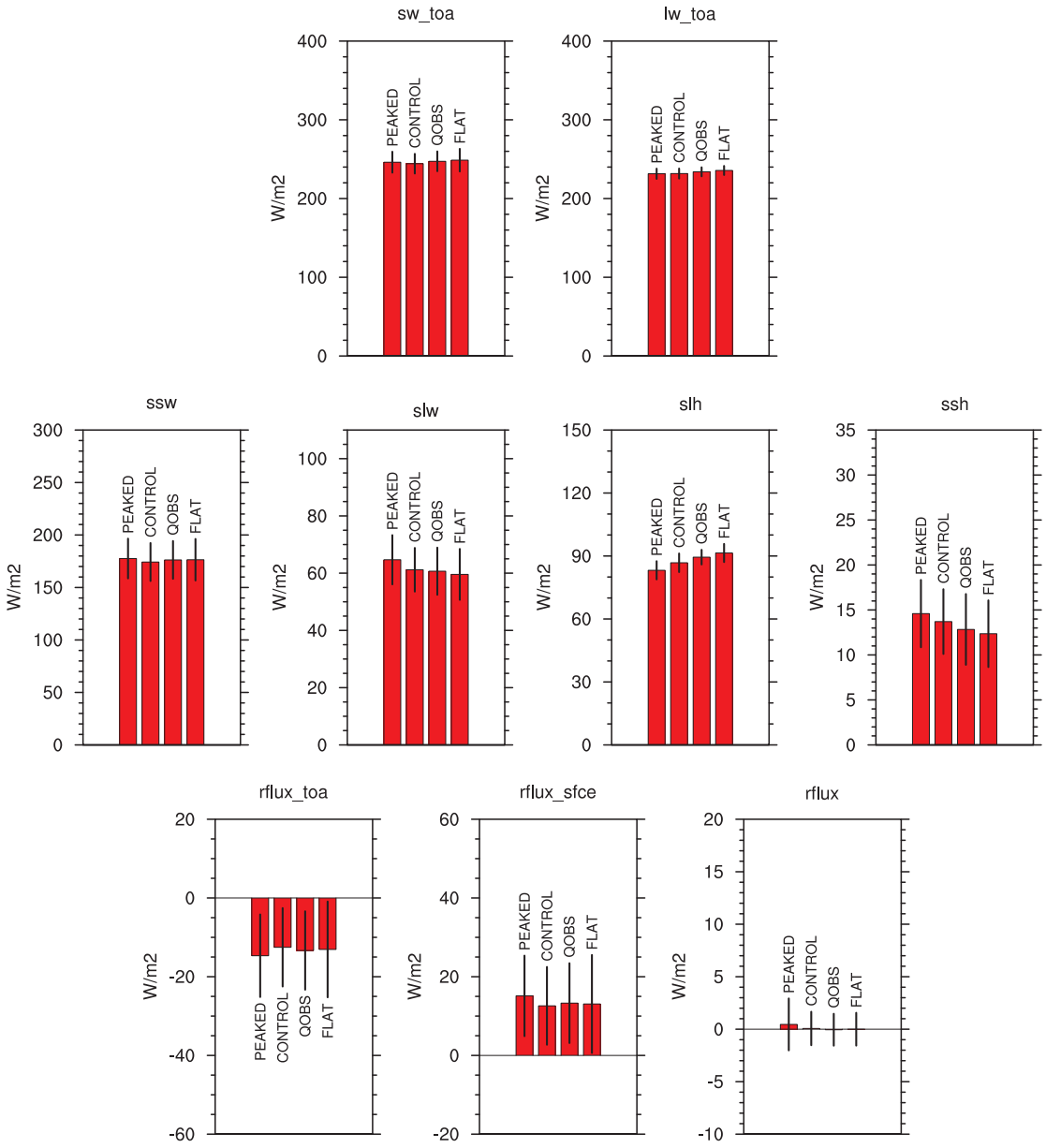

Figure 5.6: Multi-model mean global-time average TOA net shortwave (sw_toa, +ve downward), TOA net longwave (lw_toa, +ve upward), surface net shortwave (ssw, +ve downward), surface net longwave (slw, +ve upward), surface latent heat (slh), surface sensible heat (ssh), TOA residual (rflux_toa, +ve upward), surface residual (rflux_sfce, +ve downward) and net total (rflux, +ve out of atmosphere) fluxes from PEAKED, CONTROL, QOBS and FLAT SST distributions.

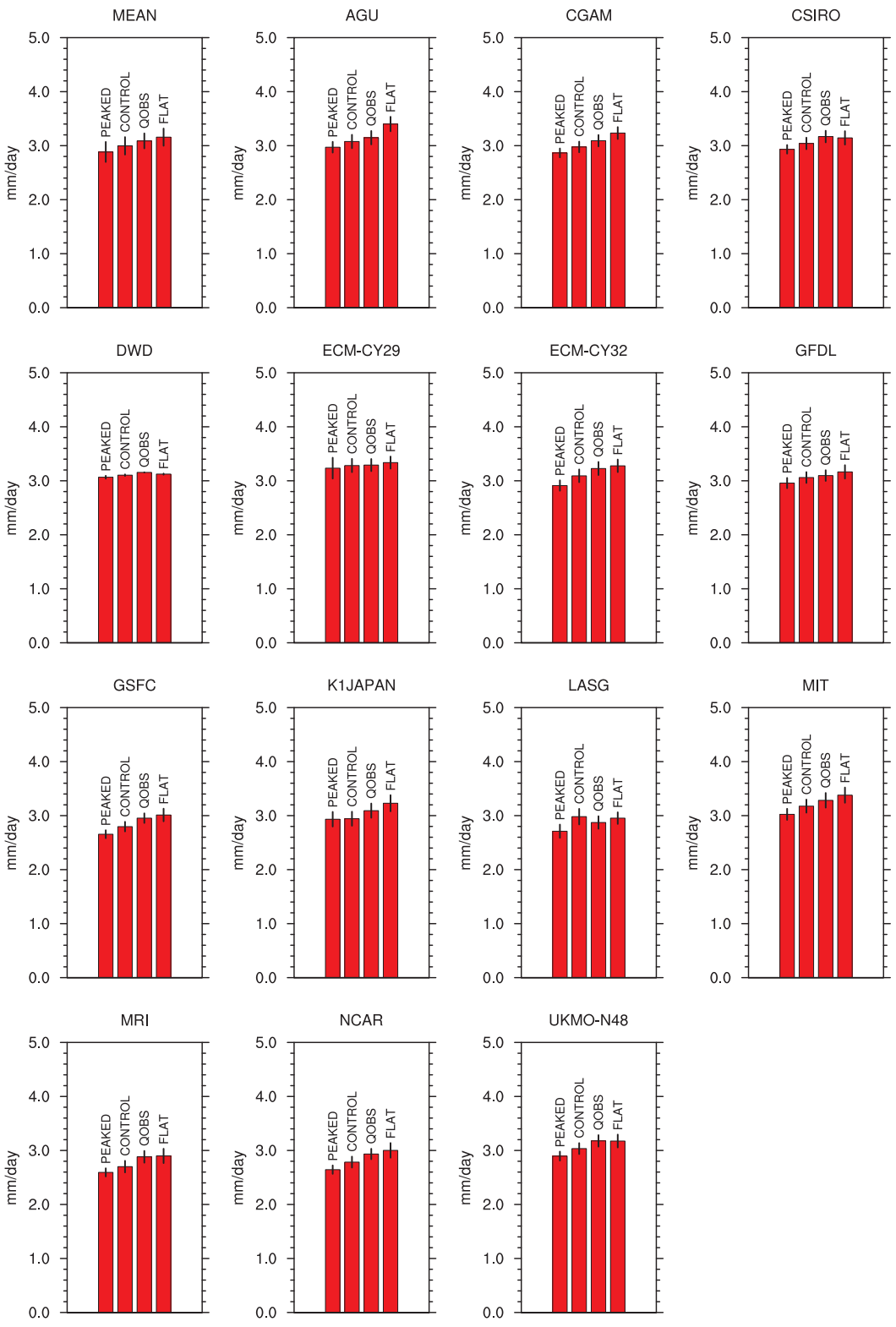

Figure 5.7: Global-time average precipitation (tppn) for individual models from PEAKED, CONTROL, QOBS and FLAT SST distributions (mm day^{-1}).

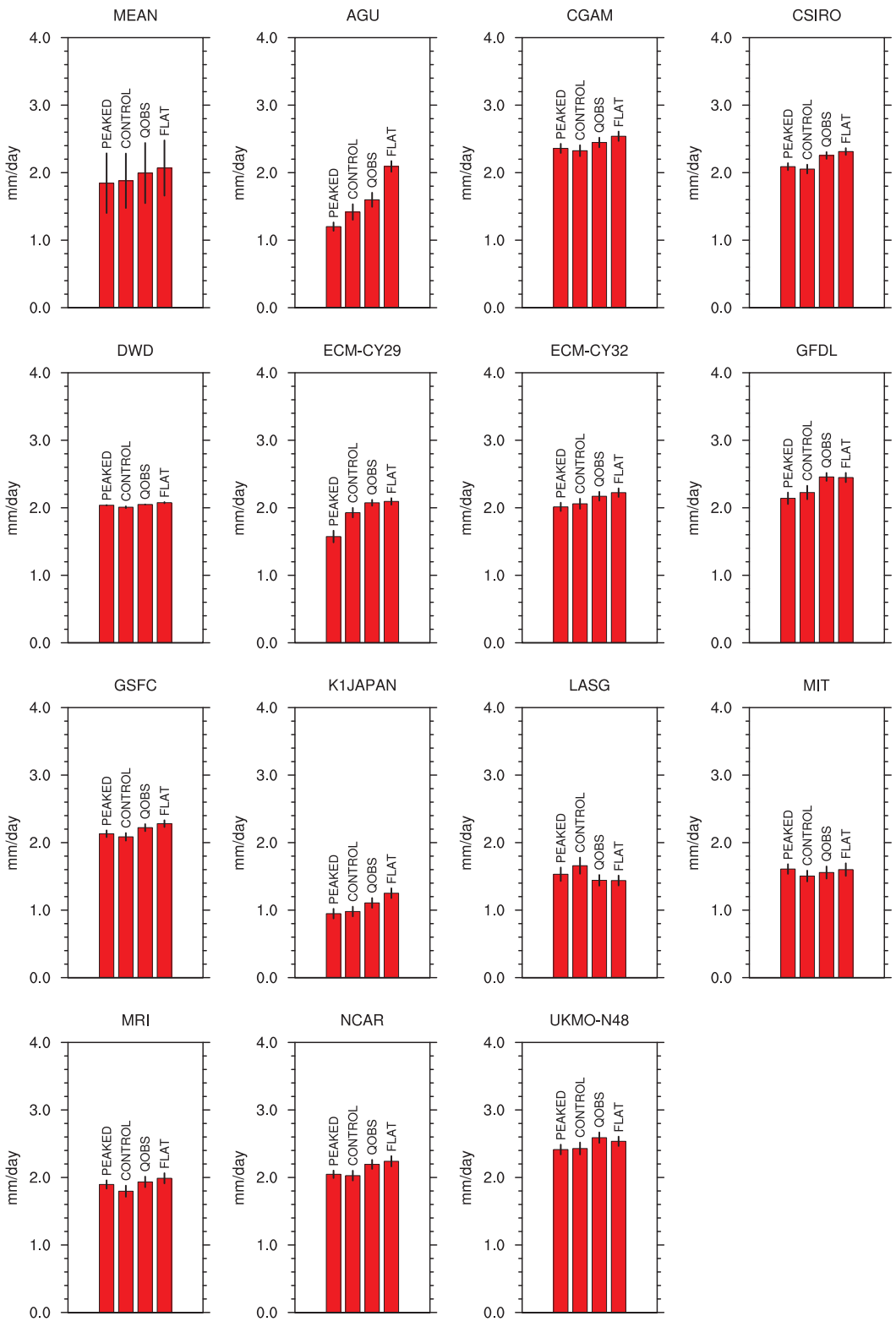

Figure 5.8: Global-time average convective precipitation (cppn) for individual models from PEAKED, CONTROL, QOBS and FLAT SST distributions (mm day^{-1}).

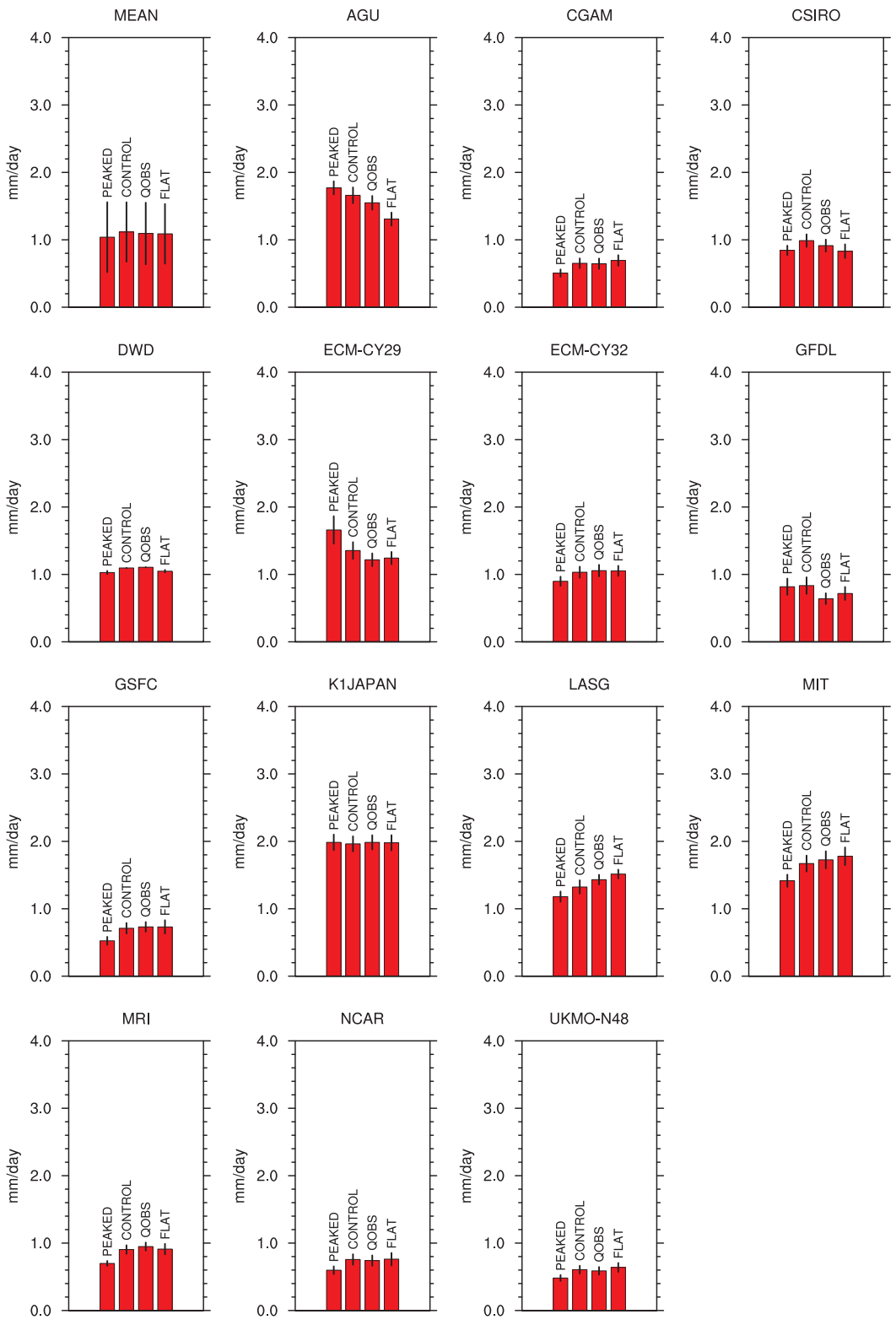

Figure 5.9: Global-time average large-scale precipitation (dppn) for individual models from PEAKED, CONTROL, QOBS and FLAT SST distributions (mm day^{-1}).

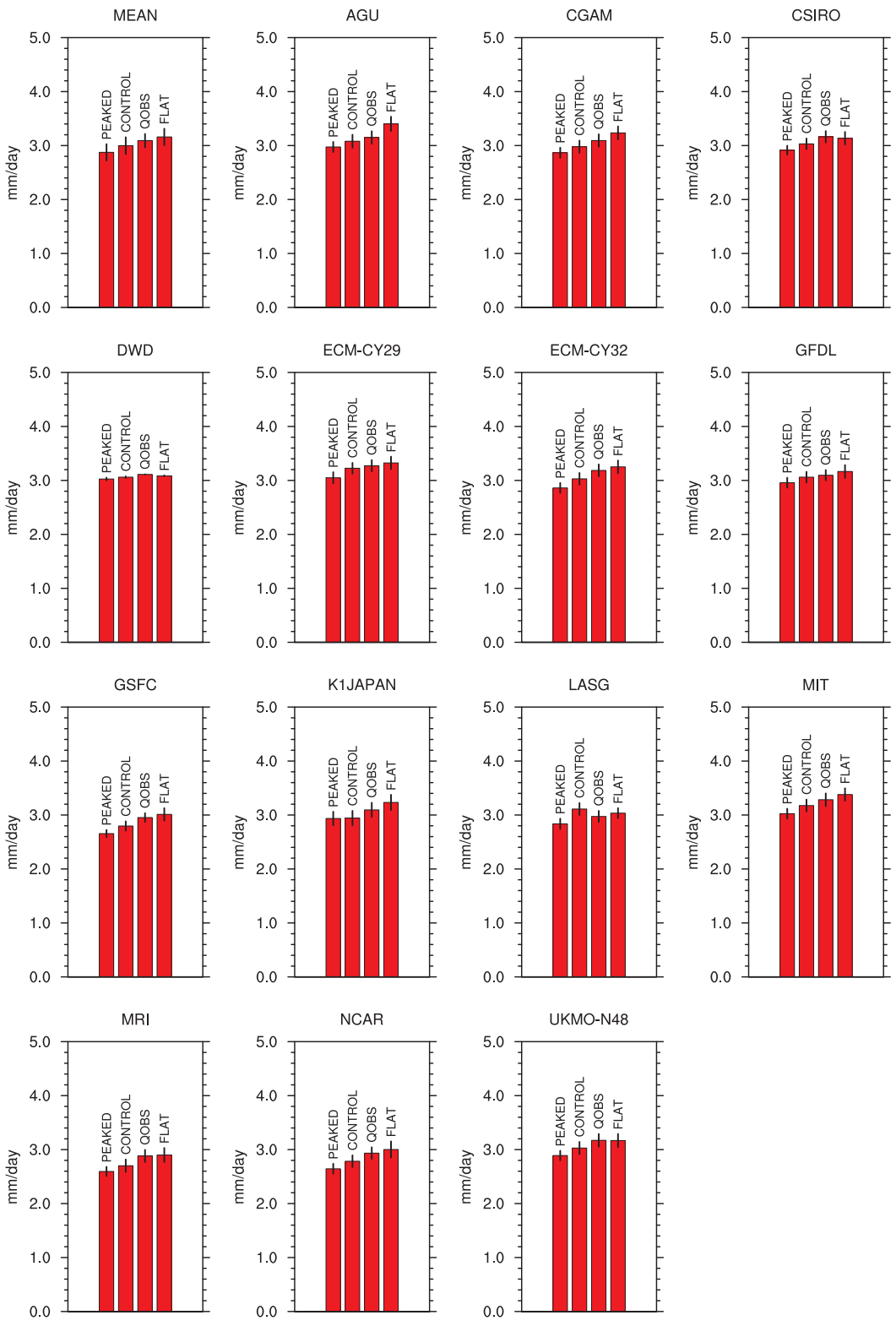

Figure 5.10: Global-time average evaporation (evap) for individual models from PEAKED, CONTROL, QOBS and FLAT SST distributions (mm day^{-1}).

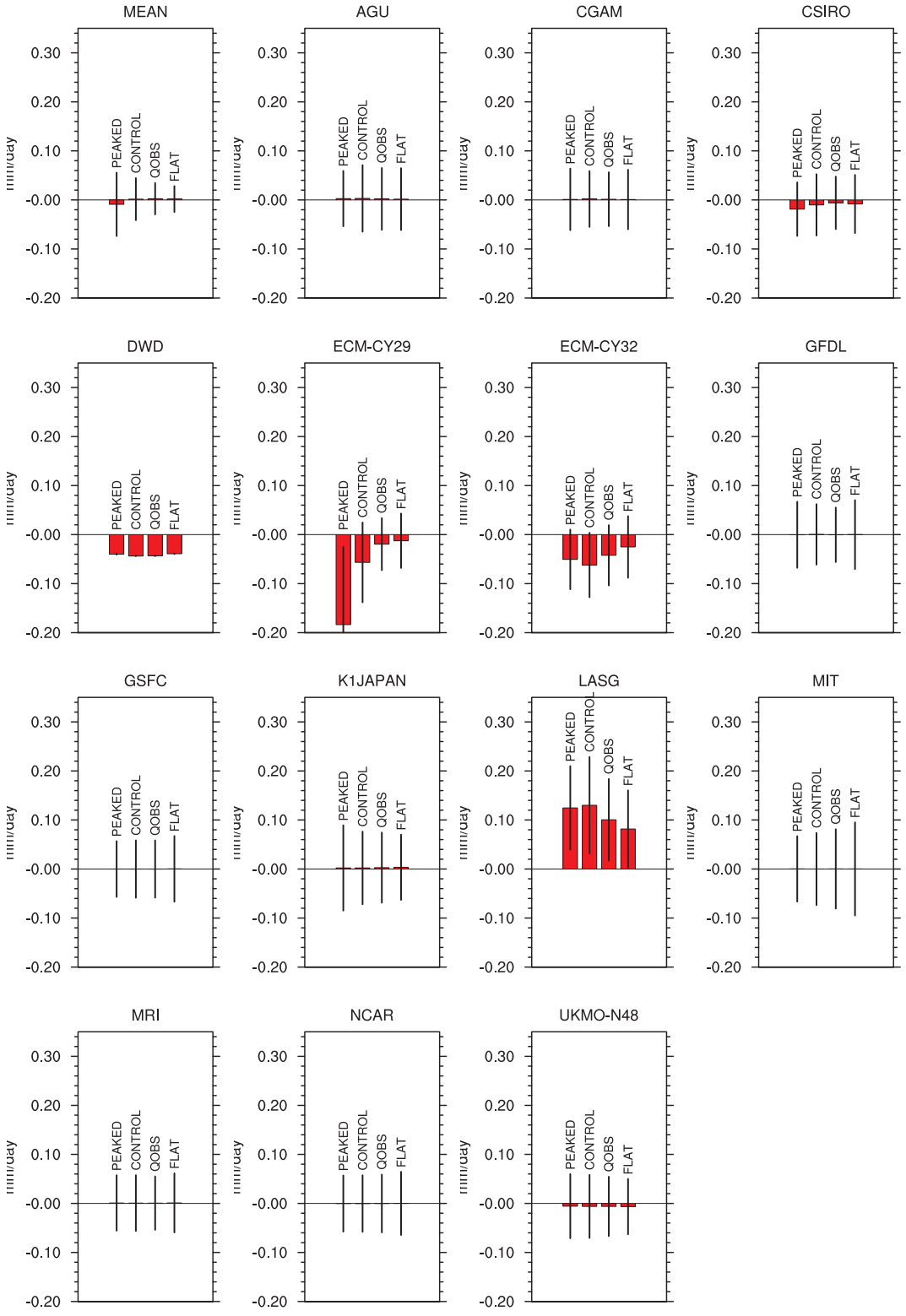

Figure 5.11: Global-time average evaporation minus precipitation (emp) for individual models from PEAKED, CONTROL, QOBS and FLAT SST distributions (mm day^{-1}).

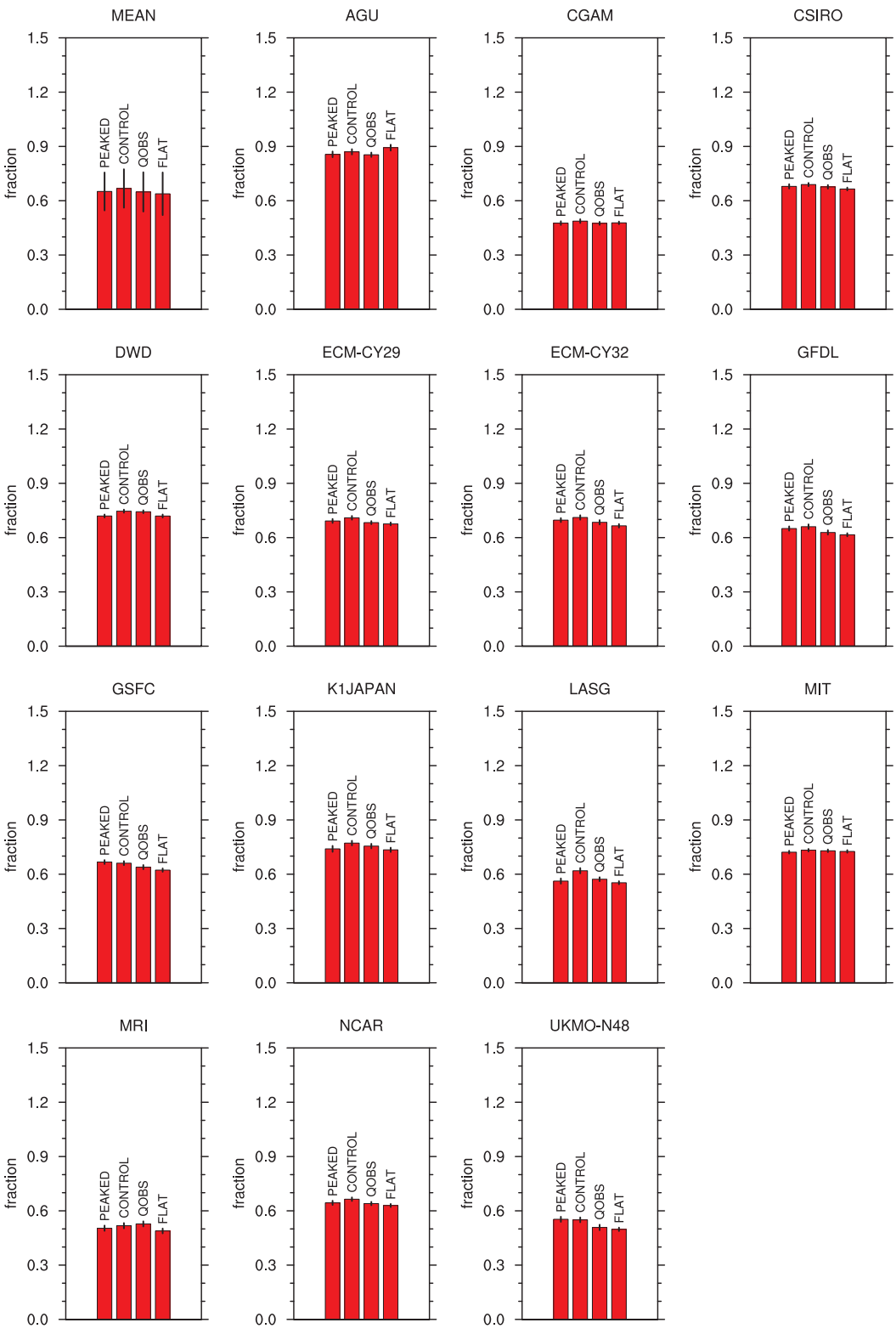

Figure 5.12: Global-time average cloud fraction (cld_frac) for individual models from PEAKED, CONTROL, QOBS and FLAT SST distributions (fraction).

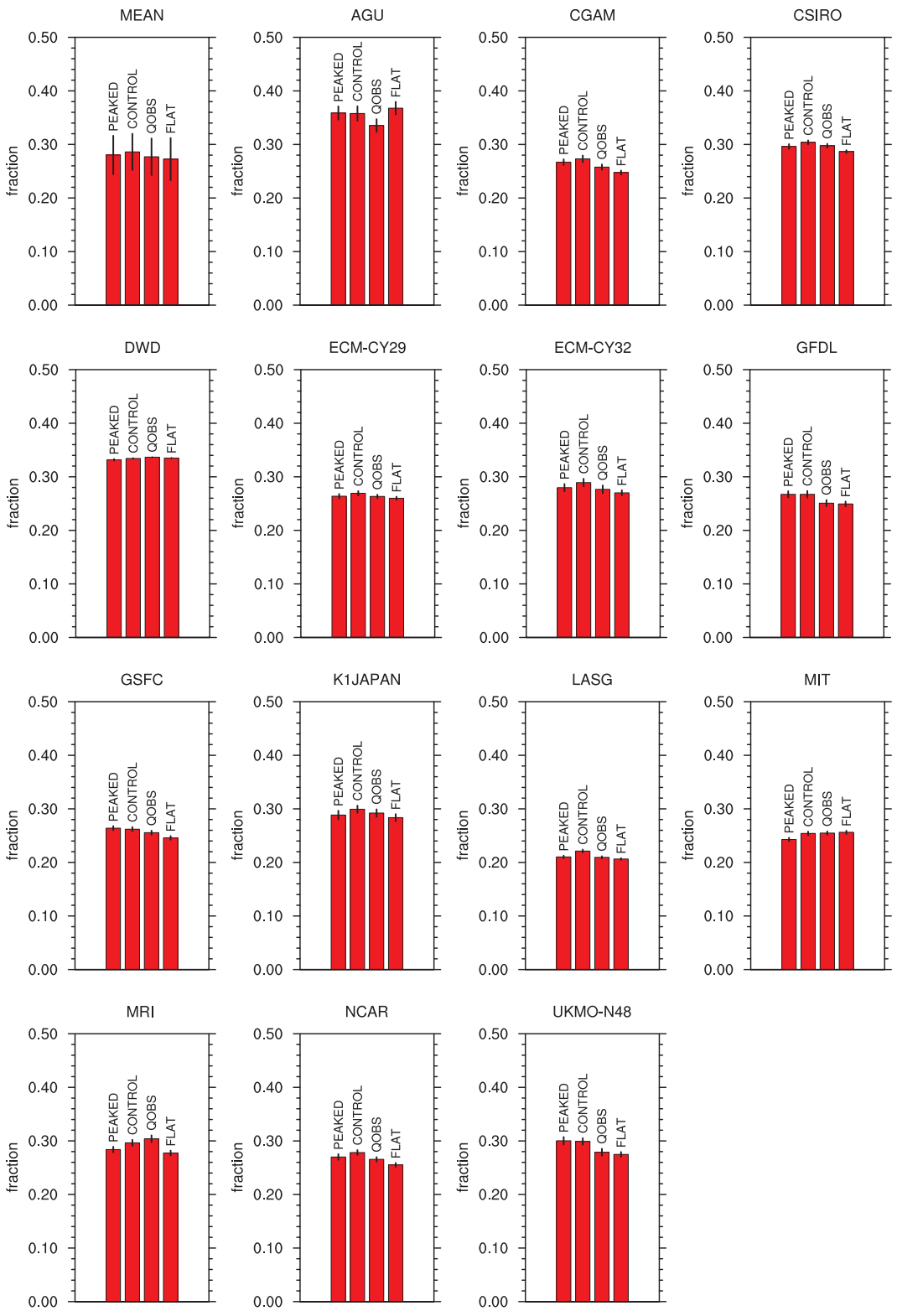

Figure 5.13: Global-time average albedo (albedo) for individual models from PEAKED, CONTROL, QOBS and FLAT SST distributions (fraction).

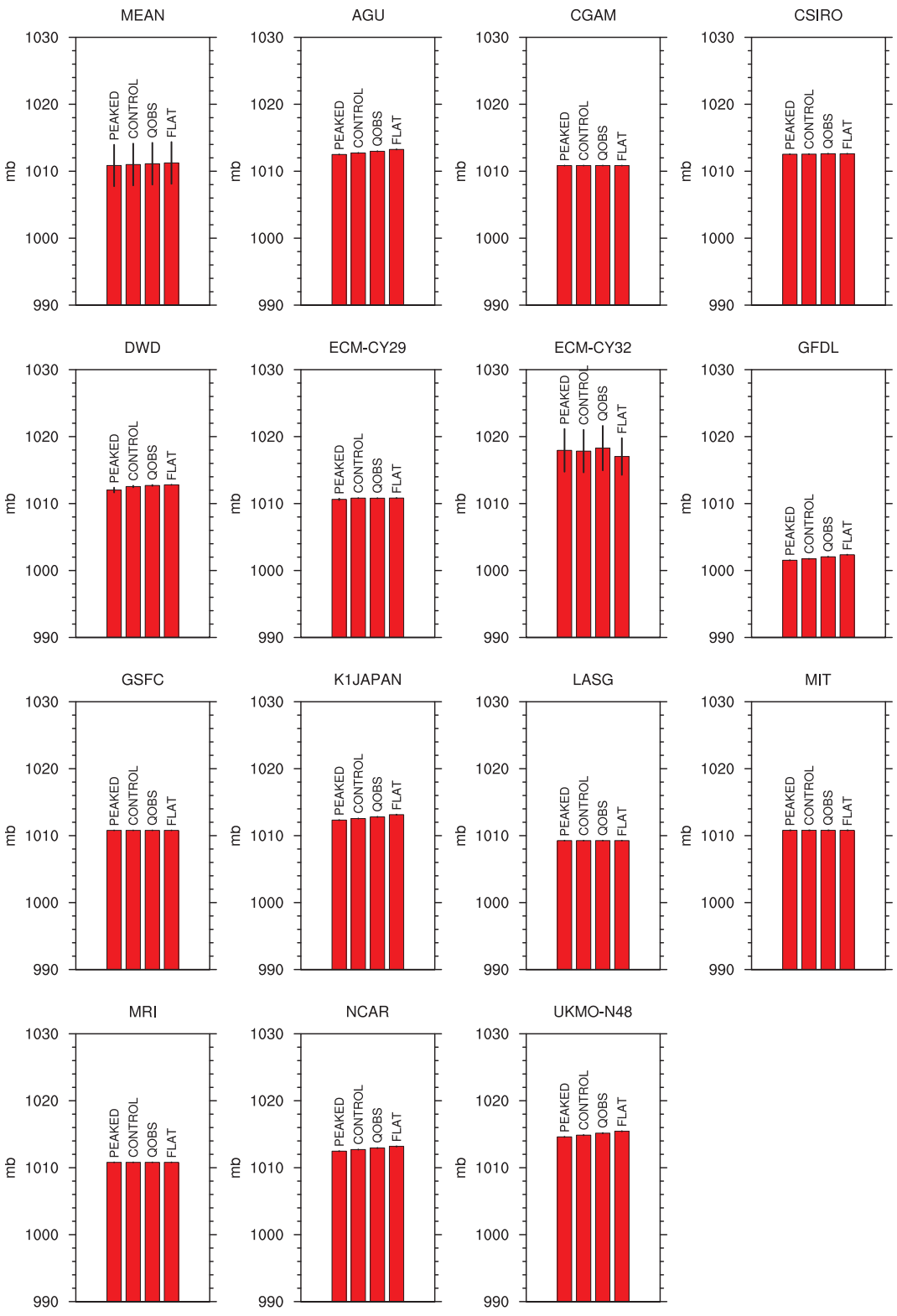

Figure 5.14: Global-time average surface pressure (ps) for individual models from PEAKED, CONTROL, QOBS and FLAT SST distributions (mb).

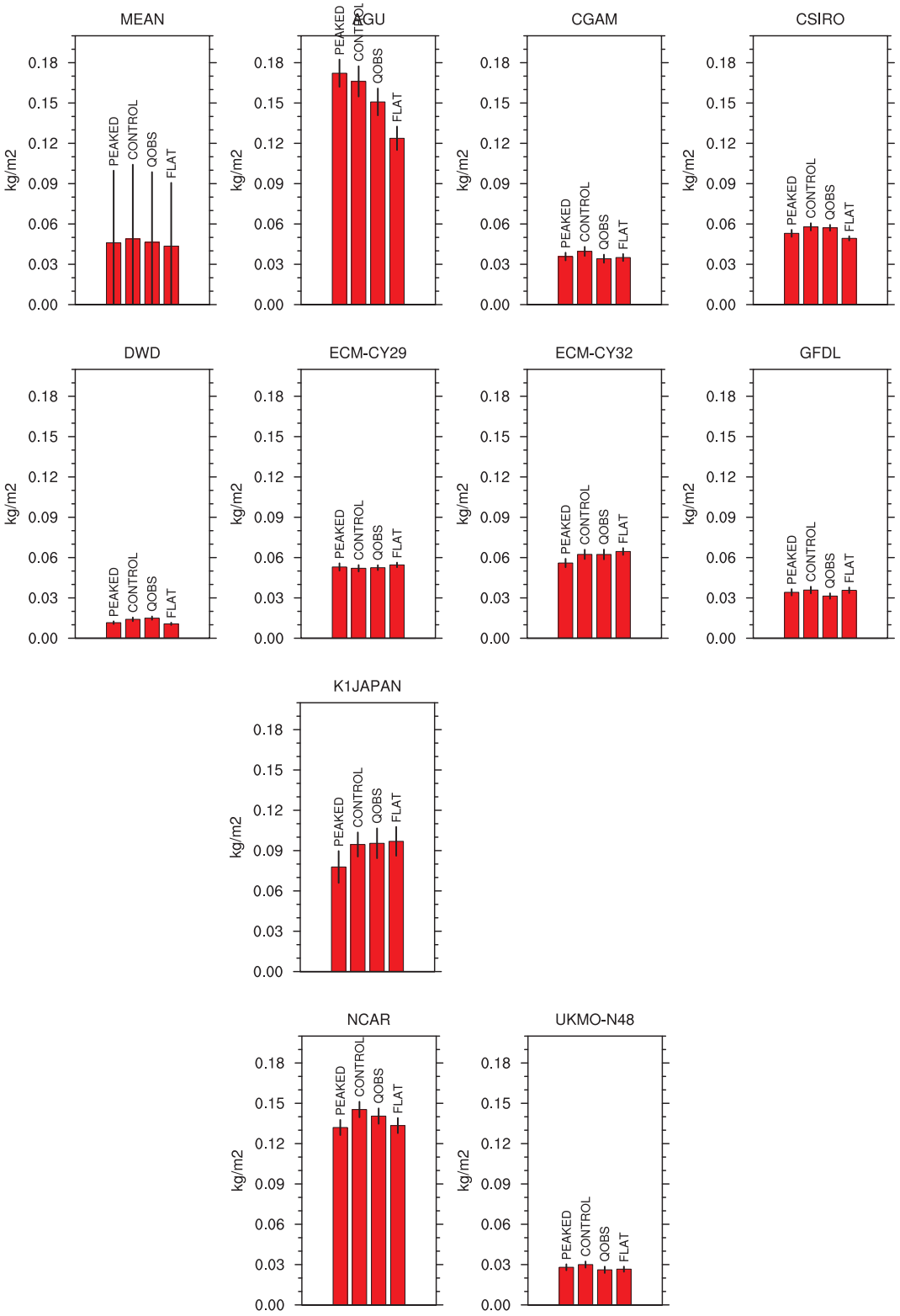

Figure 5.15: Global-time average cloud water (cldw) for individual models from PEAKED, CONTROL, QOBS and FLAT SST distributions (kg m^{-2}).

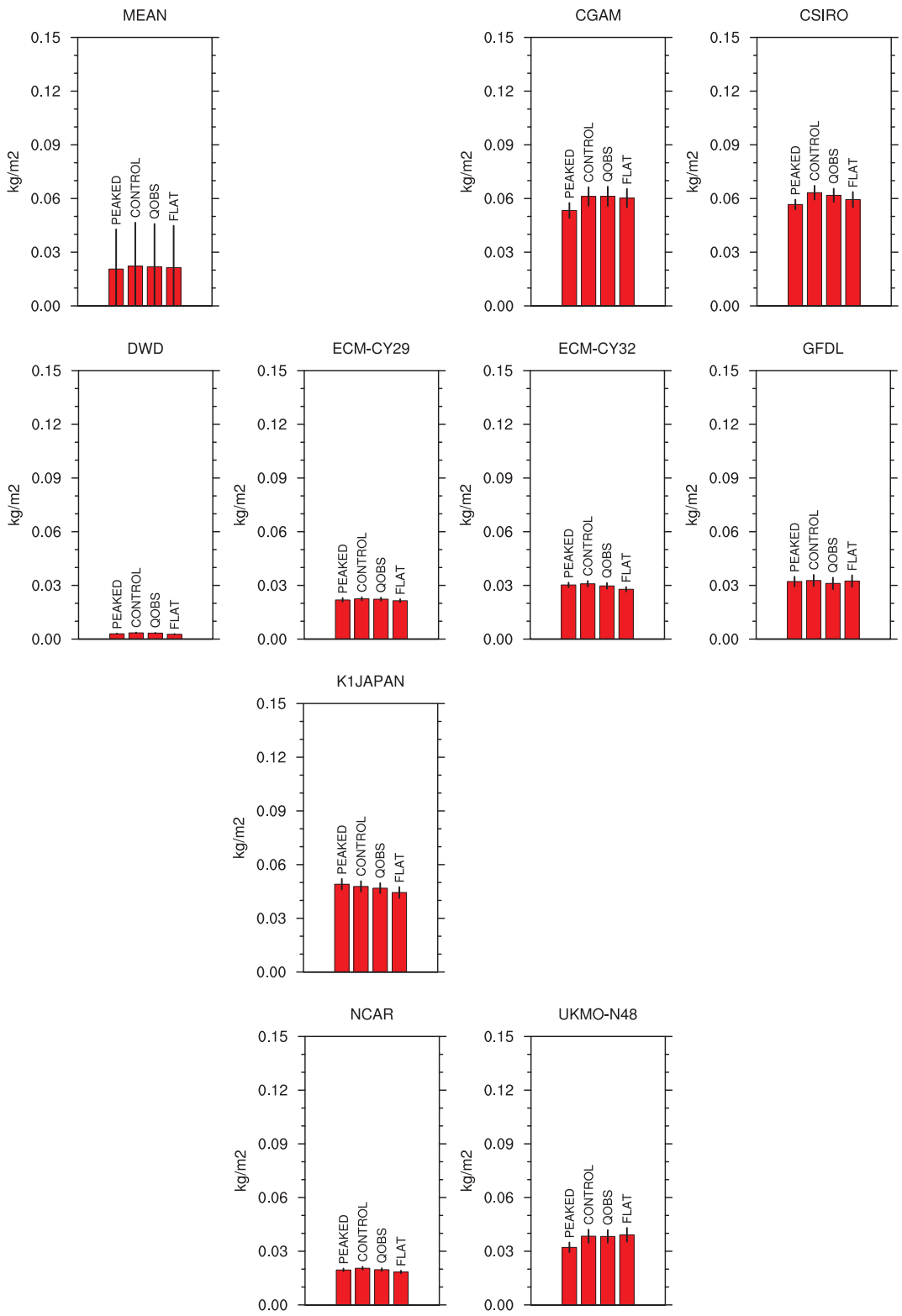

Figure 5.16: Global-time average cloud ice (cldi) for individual models from PEAKED, CONTROL, QOBS and FLAT SST distributions (kg m^{-2}).

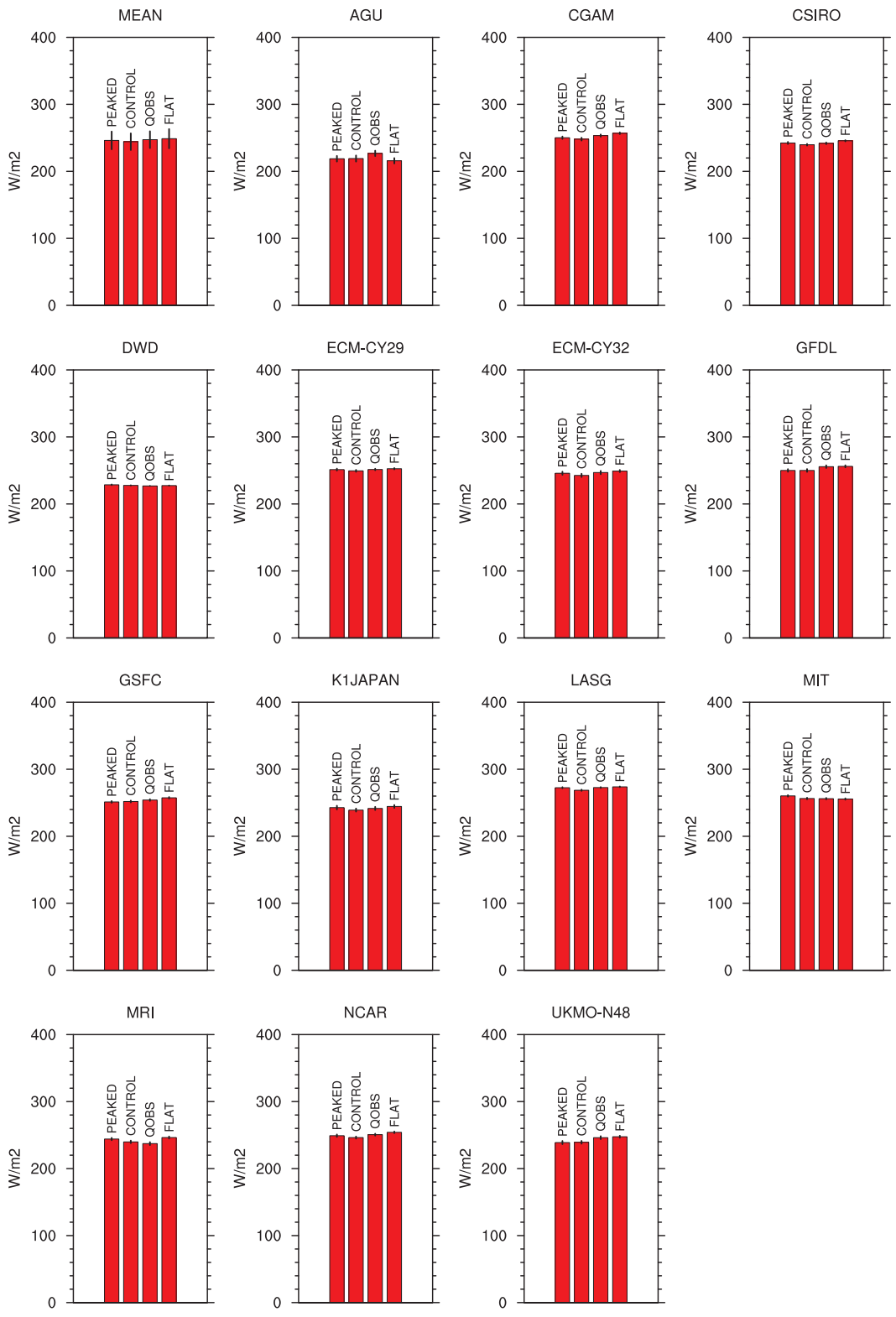

Figure 5.17: Global-time average TOA net shortwave radiation (sw_toa) for individual models from PEAKED, CONTROL, QOBS and FLAT SST distributions (W m^{-2}, +ve downward).

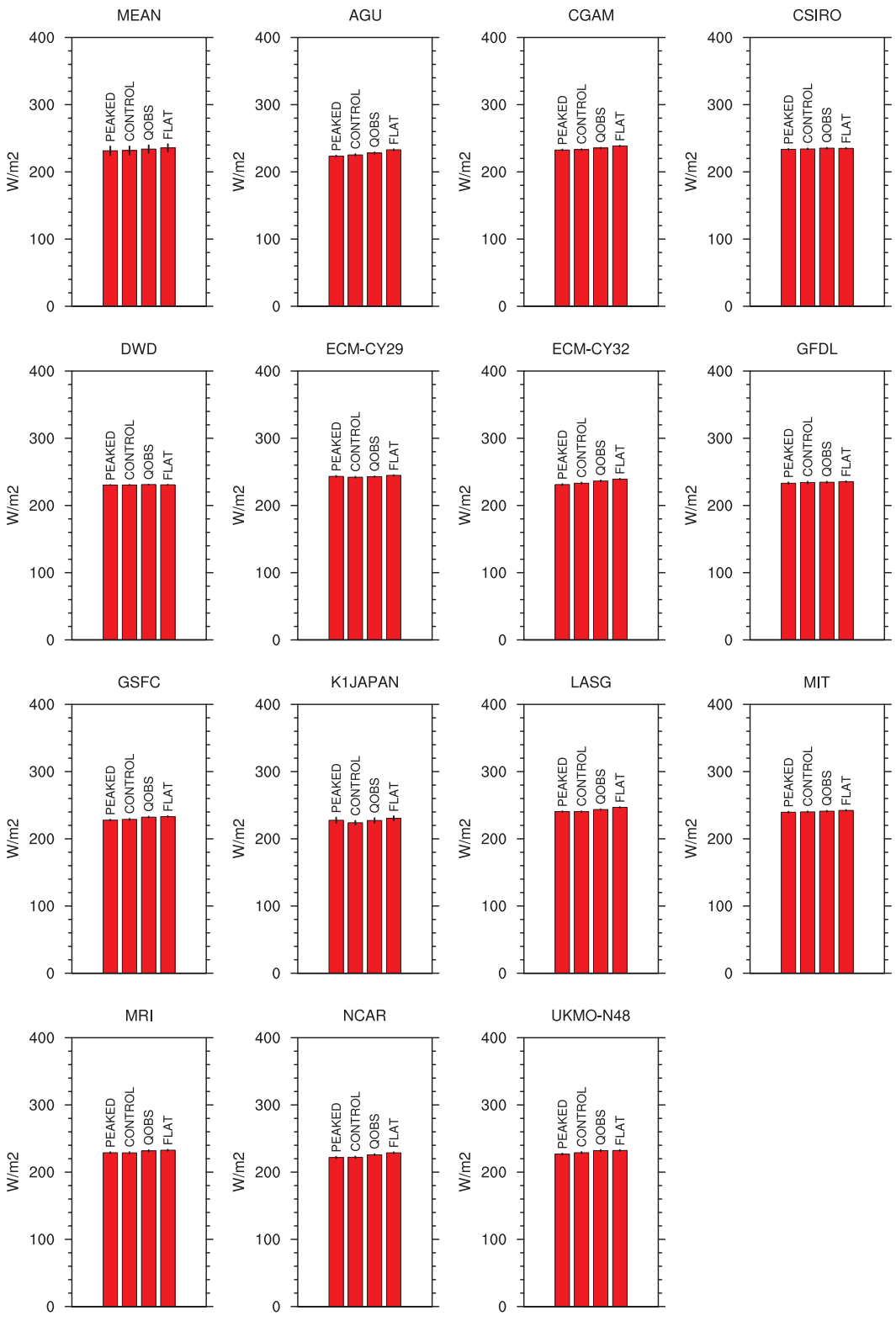

Figure 5.18: Global-time average TOA net longwave radiation (lw_toa) for individual models from PEAKED, CONTROL, QOBS and FLAT SST distributions (W m^{-2}, +ve upward).

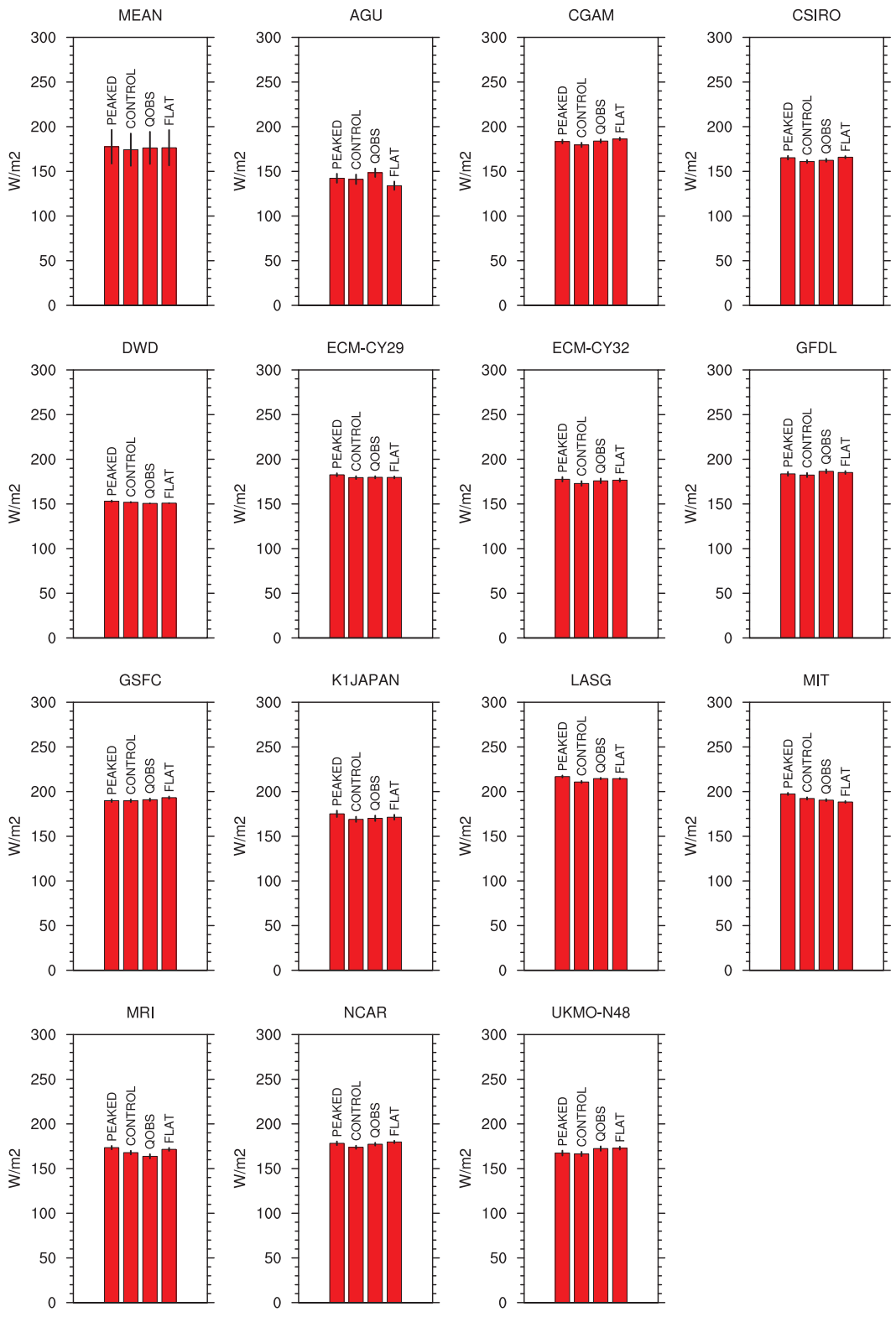

Figure 5.19: Global-time average surface net shortwave radiation (ssw) for individual models from PEAKED, CONTROL, QOBS and FLAT SST distributions (W m^{-2}, +ve downward).

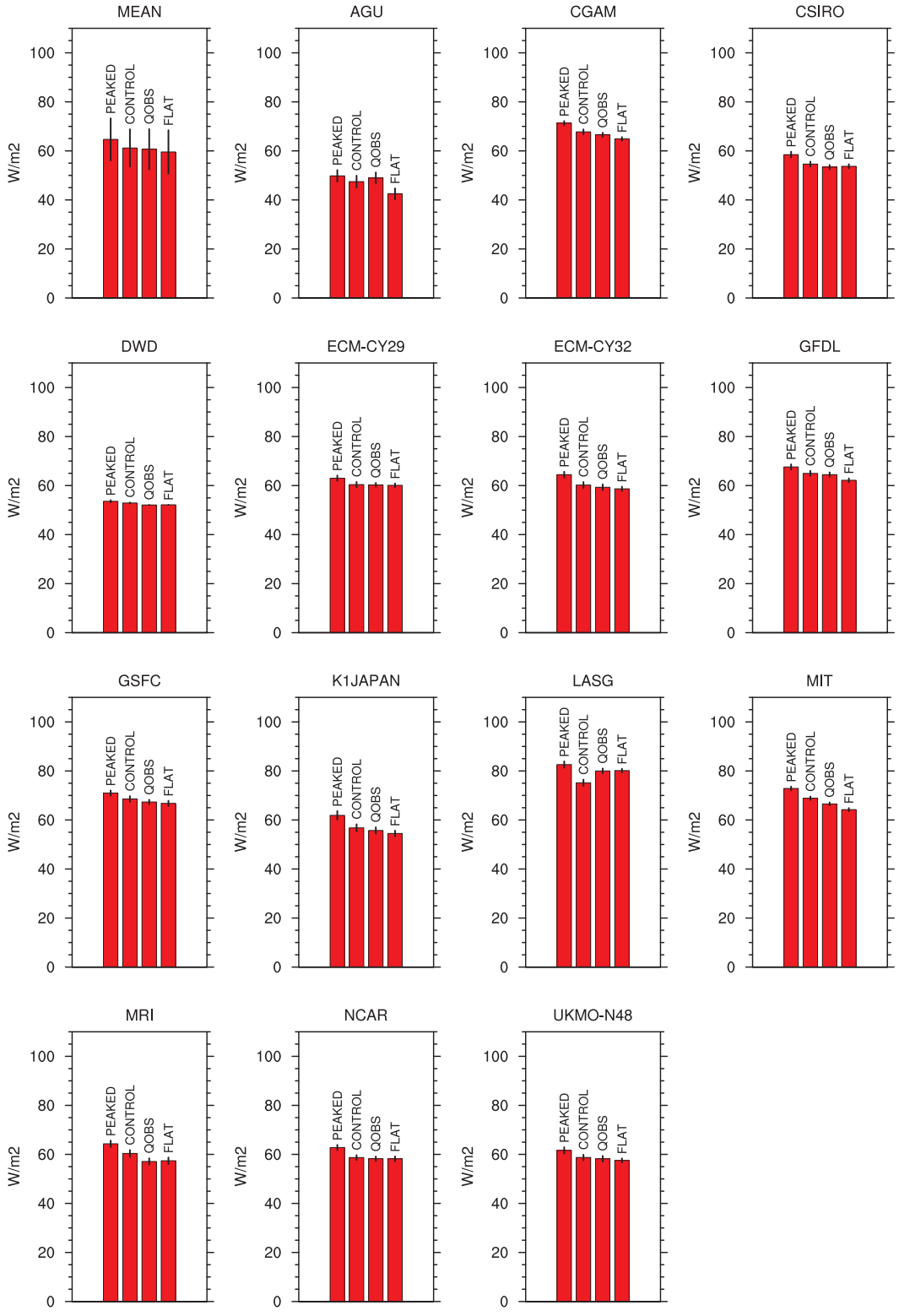

Figure 5.20: Global-time average surface net longwave radiation (slw) for individual models from PEAKED, CONTROL, QOBS and FLAT SST distributions (W m^{-2}, +ve upward).

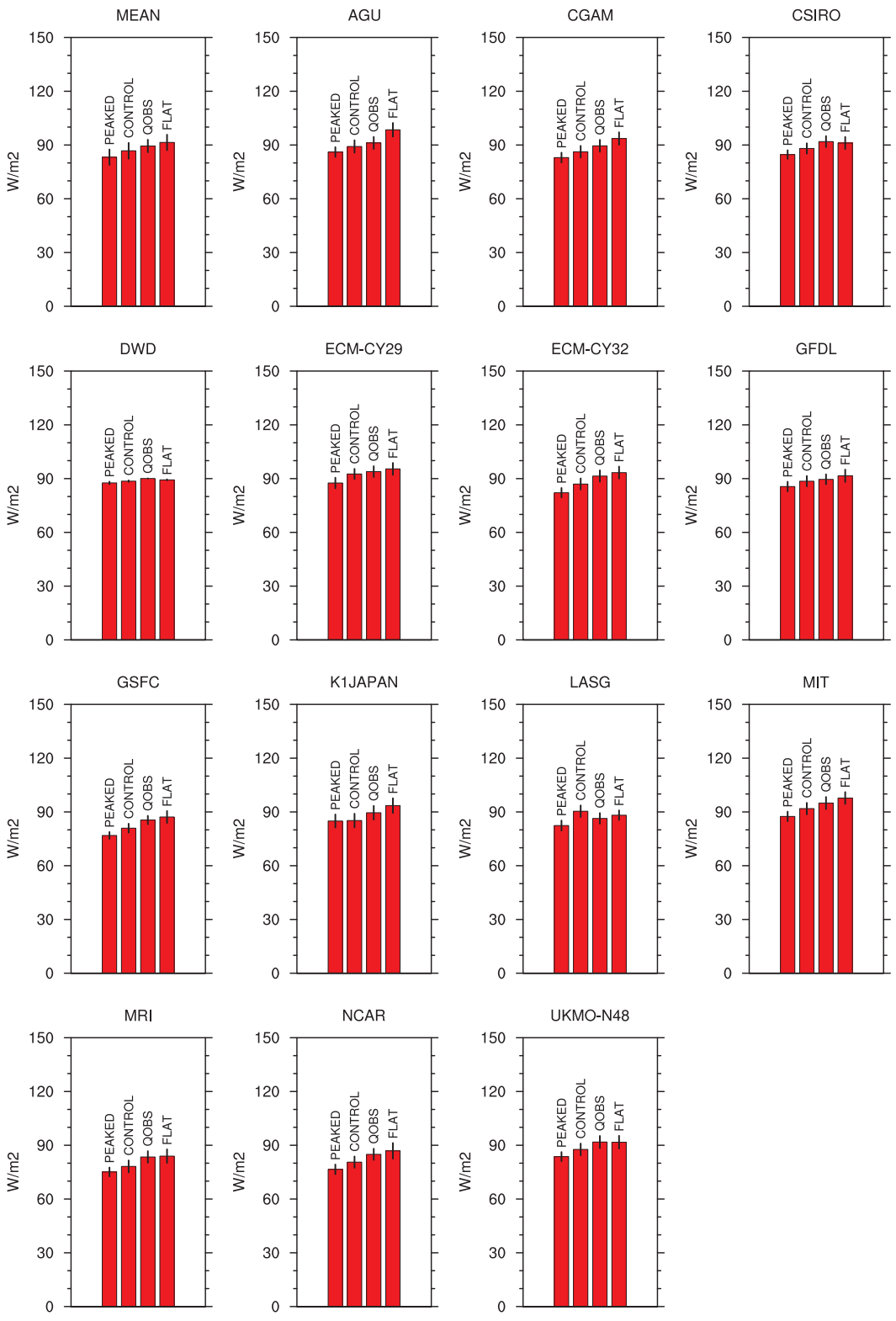

Figure 5.21: Global-time average surface latent heat flux (slh) for individual models from PEAKED, CONTROL, QOBS and FLAT SST distributions (W m^{-2}).

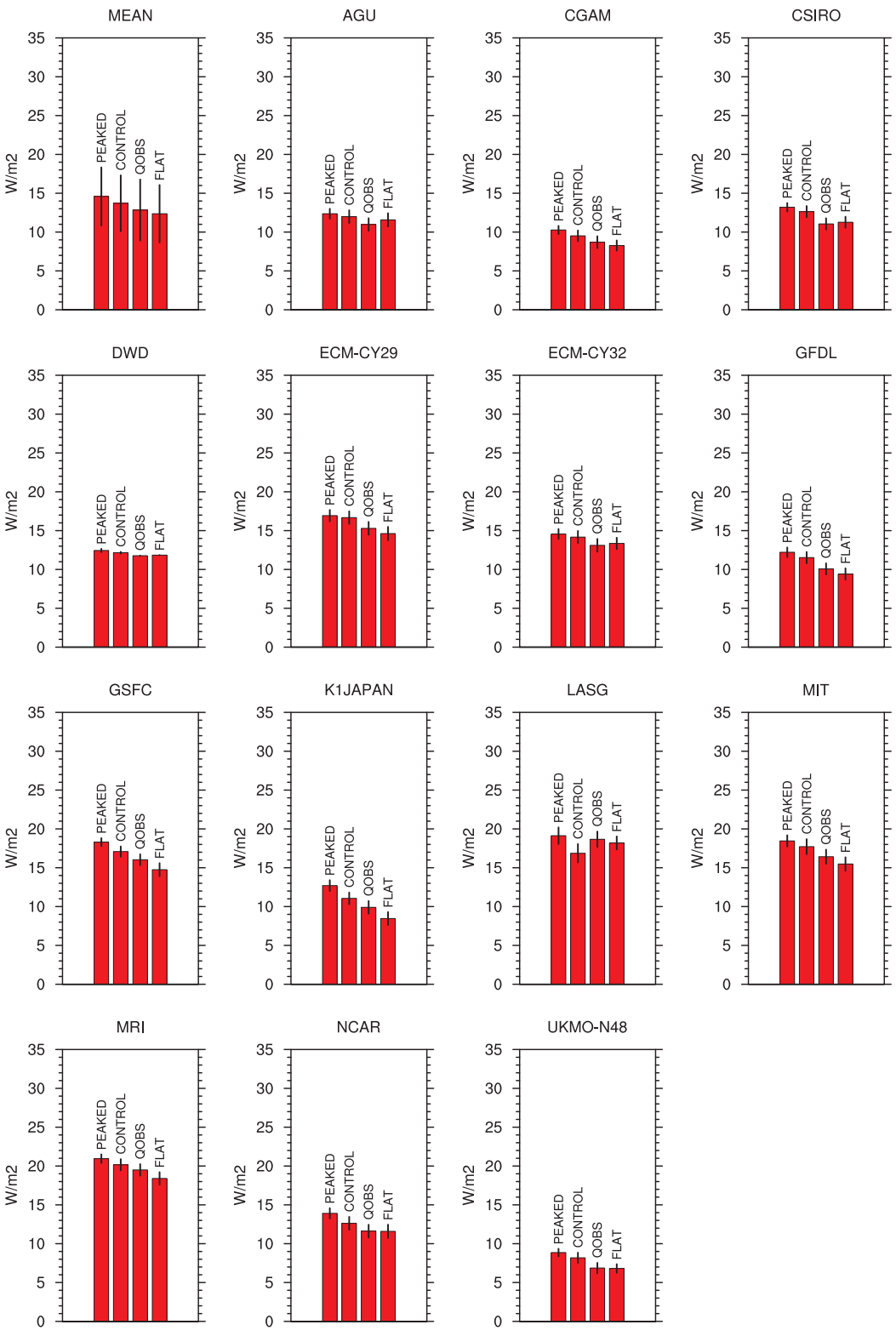

Figure 5.22: Global-time average surface sensible heat flux (ssh) for individual models from PEAKED, CONTROL, QOBS and FLAT SST distributions (W m^{-2}).

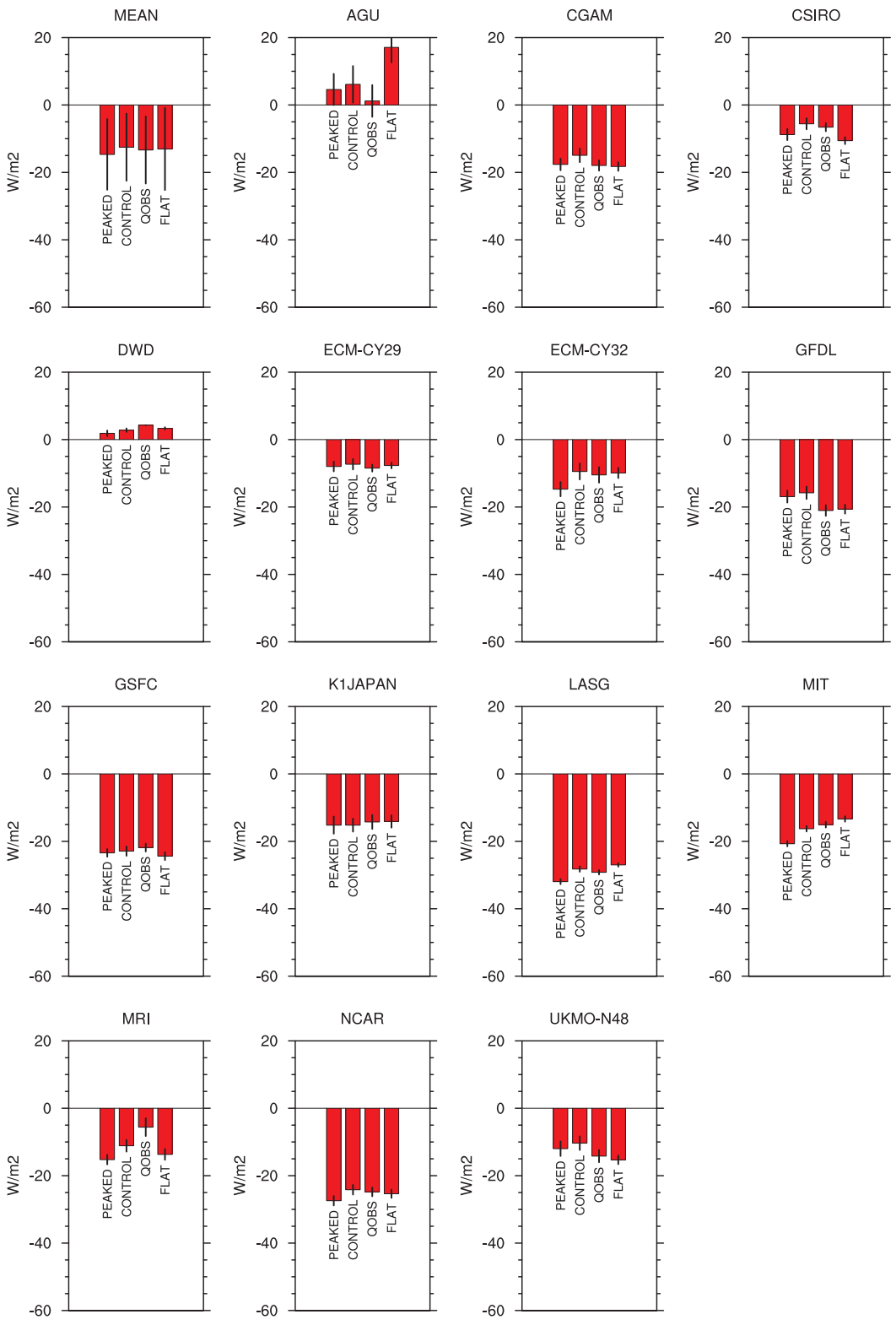

Figure 5.23: Global-time average TOA net radiation flux (rflux_toa) for individual models from PEAKED, CONTROL, QOBS and FLAT SST distributions (W m^{-2}, +ve upward).

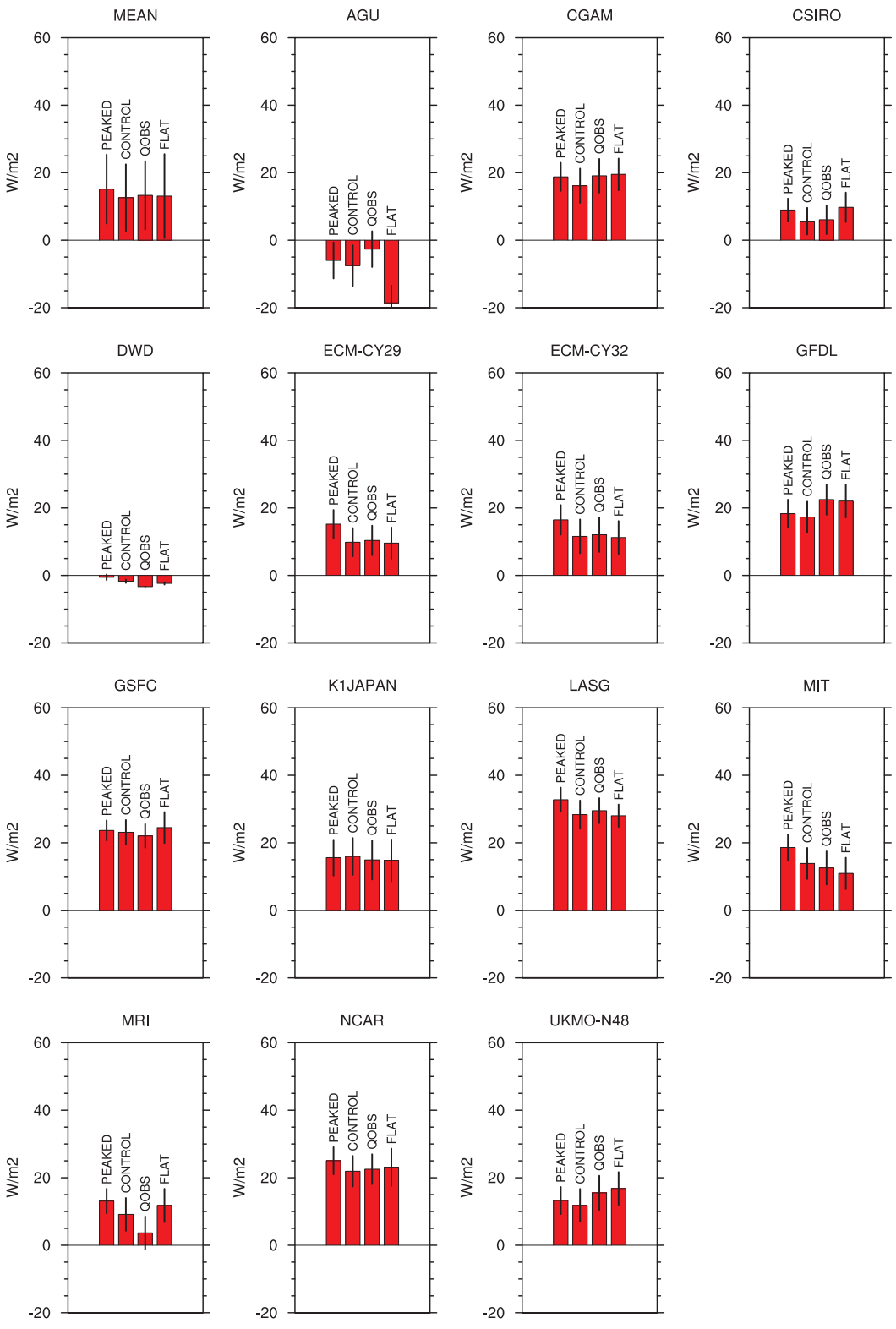

Figure 5.24: Global-time average surface net flux (rflux_sfce) for individual models from PEAKED, CONTROL, QOBS and FLAT SST distributions (W m^{-2}, +ve downward).

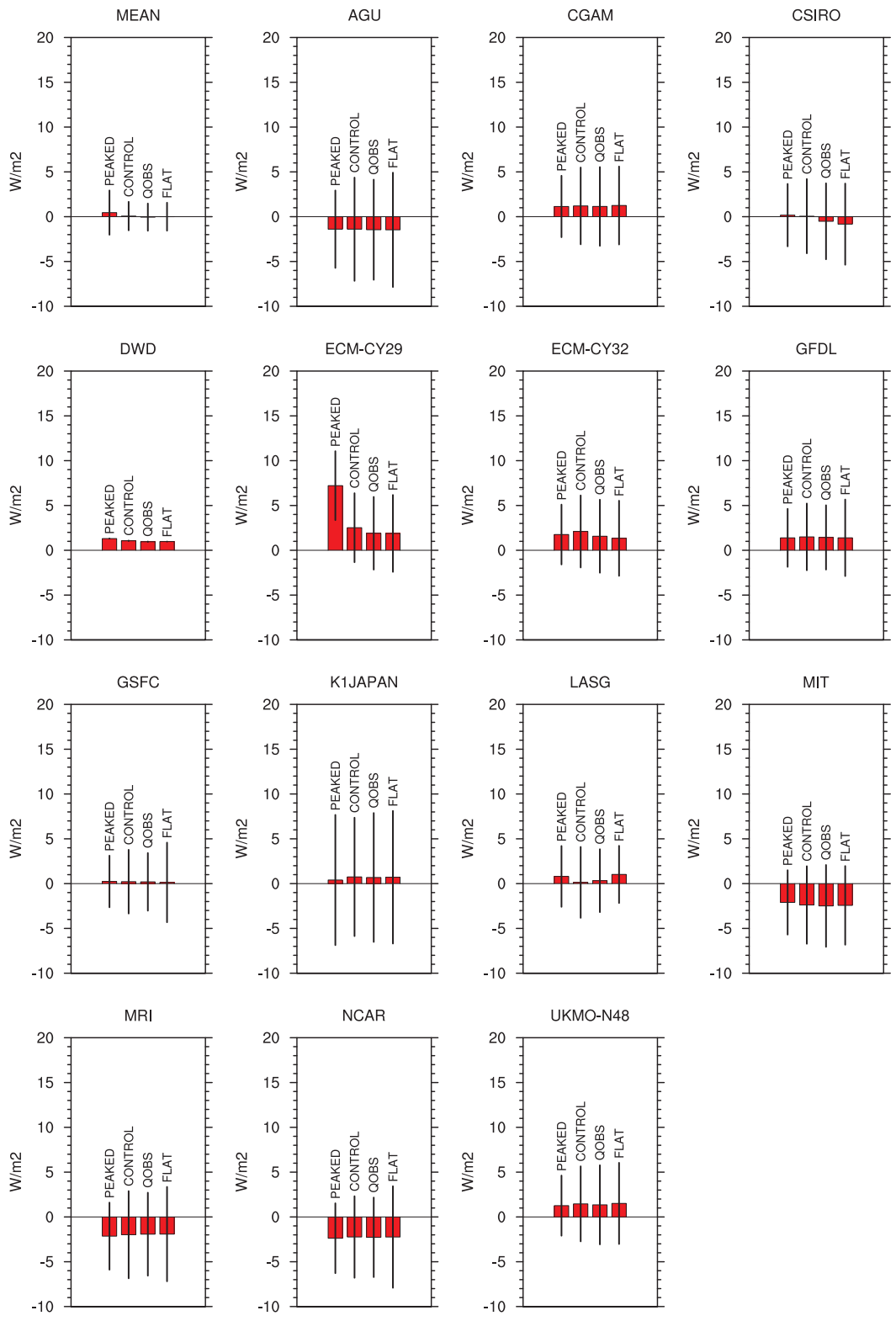

Figure 5.25: Global-time average net flux (rflux) for individual models from PEAKED, CONTROL, QOBS and FLAT SST distributions (W m^{-2}, +ve out of atmosphere).

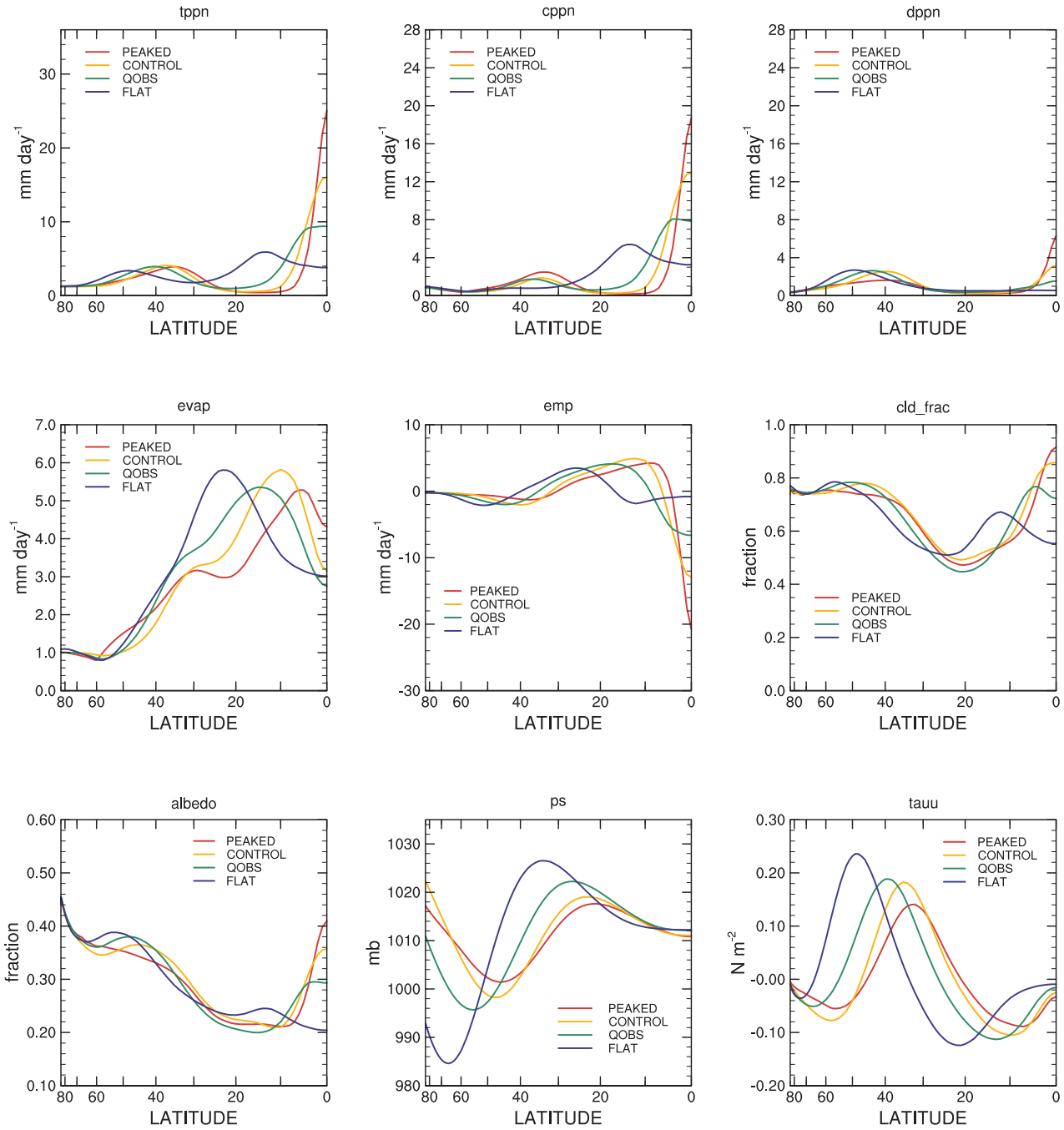

Figure 5.26: Multi-model mean zonal-time average total precipitation (tppn), convective precipitation (cppn), large-scale precipitation (dppn), evaporation (evap), evaporation minus precipitation (emp), cloud fraction (cld_frac), albedo (albedo), surface pressure (ps) and zonal surface stress (tauu) from PEAKED, CONTROL, QOBS and FLAT SST distributions.

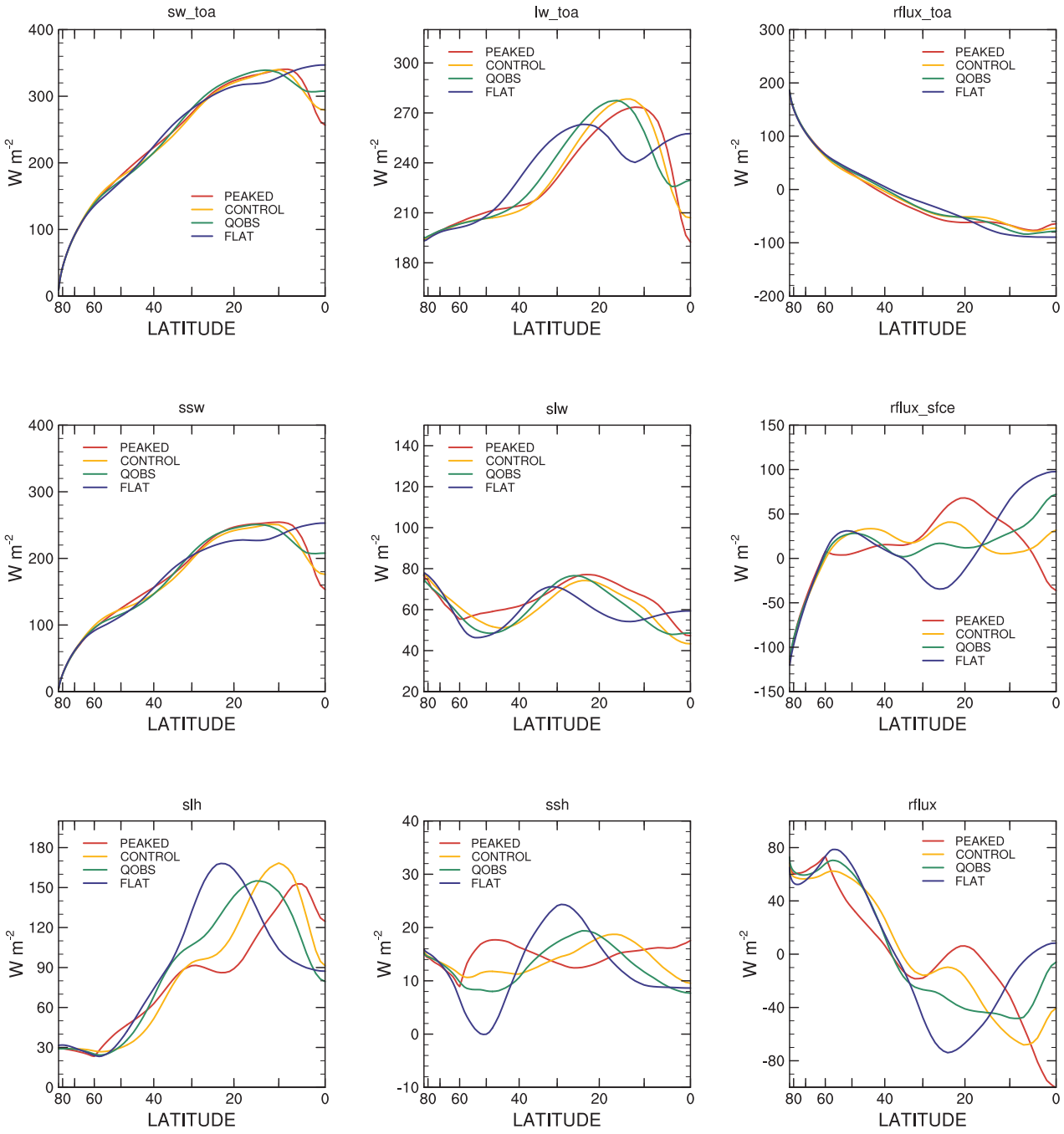

Figure 5.27: Multi-model mean zonal-time average TOA net shortwave (sw_toa, +ve downward), TOA net longwave (lw_toa, +ve upward), TOA residual (rflux_toa, +ve upward), surface net shortwave (ssw, +ve downward), surface net longwave (slw, +ve upward), surface residual (rflux_sfce, +ve downward), surface latent heat (slh), surface sensible heat (ssh) and net total (rflux, +ve out of atmosphere) fluxes from PEAKED, CONTROL, QOBS and FLAT SST distributions.

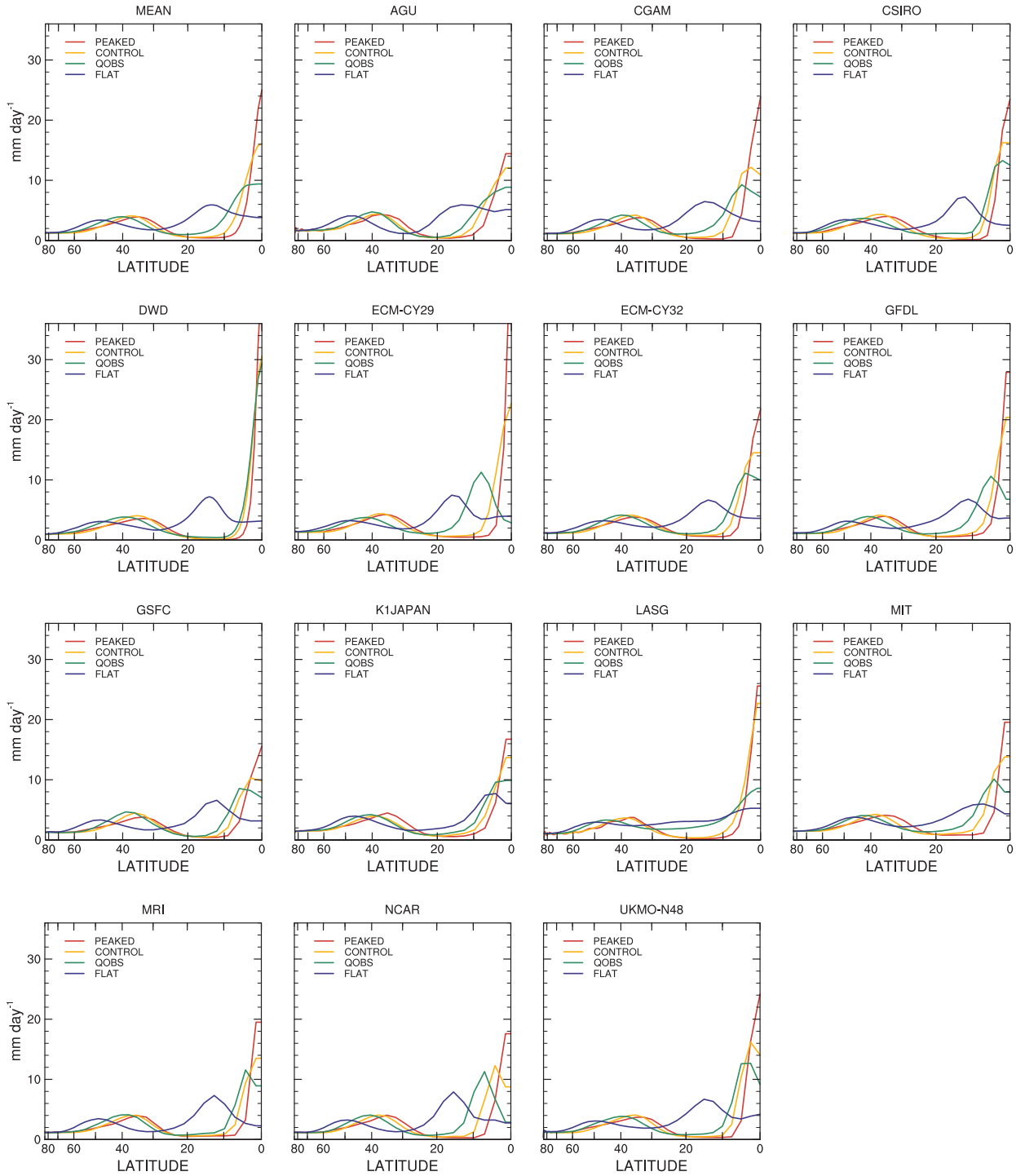

Figure 5.28: Zonal-time average precipitation (tppn) for individual models from PEAKED, CONTROL, QOBS and FLAT SST distributions, mm day^{-1}.

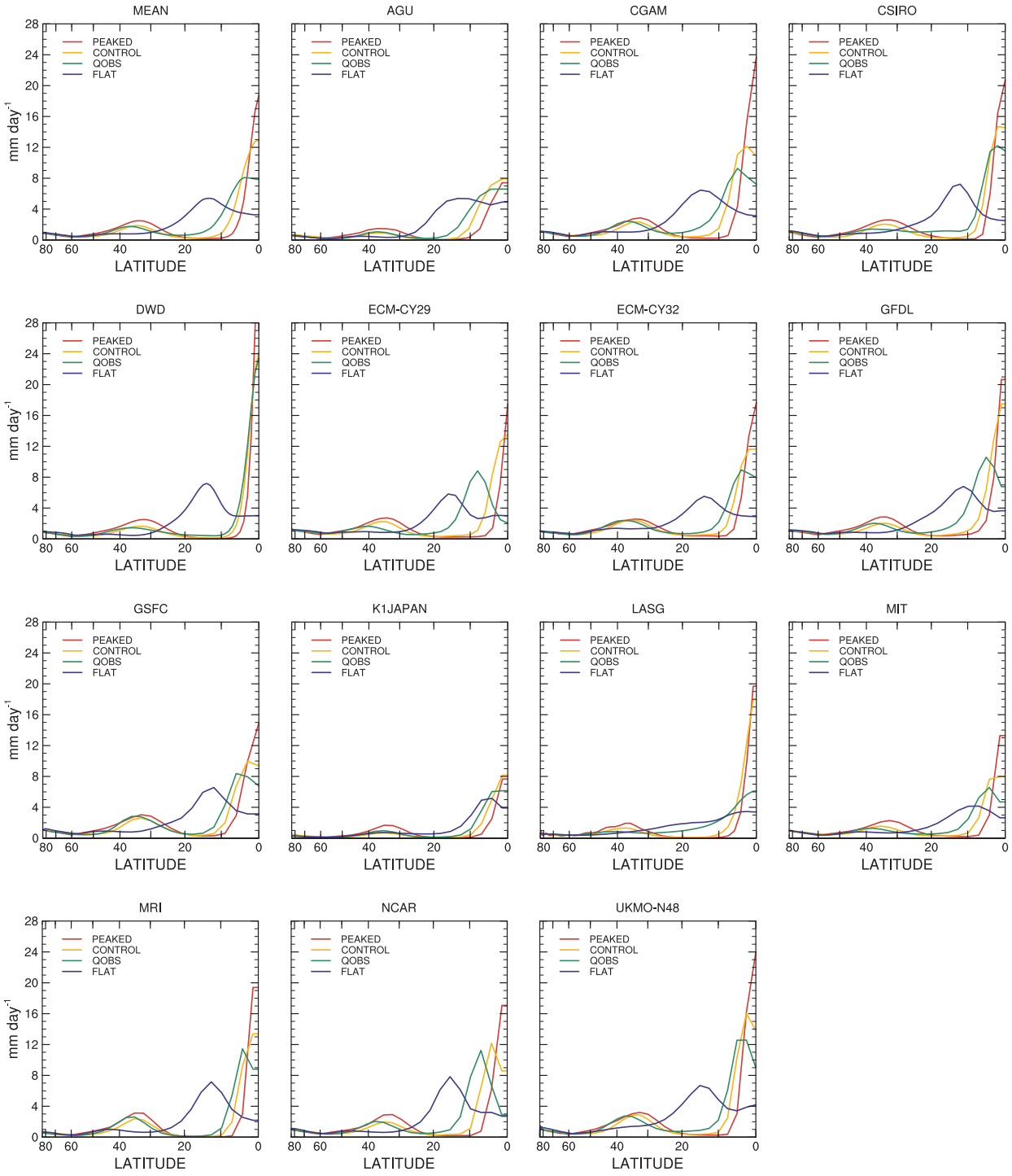

Figure 5.29: Zonal-time average convective precipitation (cppn) for individual models from PEAKED, CONTROL, QOBS and FLAT SST distributions, mm day^{-1}.

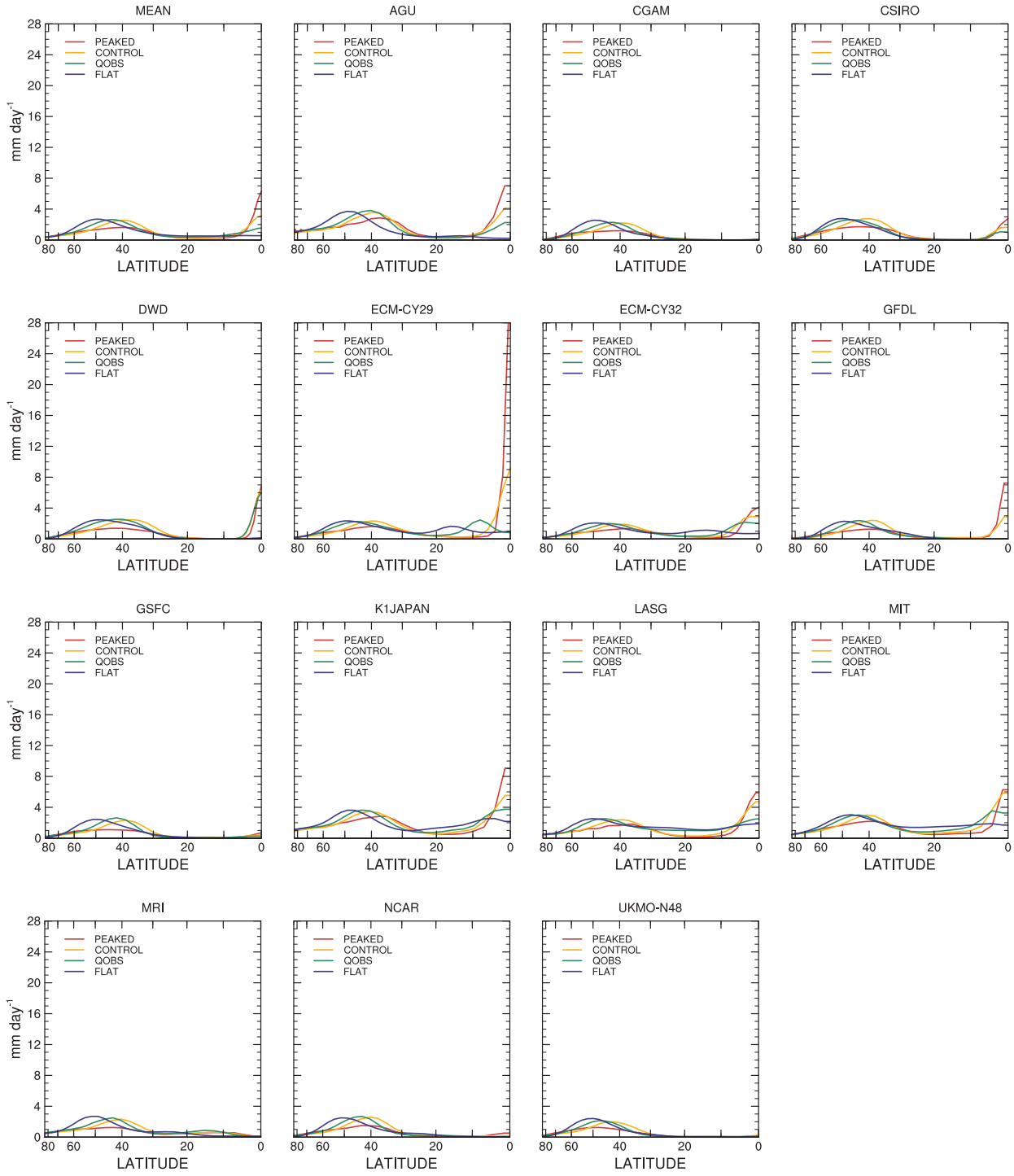

Figure 5.30: Zonal-time average large-scale precipitation (dppn) for individual models from PEAKED, CONTROL, QOBS and FLAT SST distributions, mm day^{-1}.

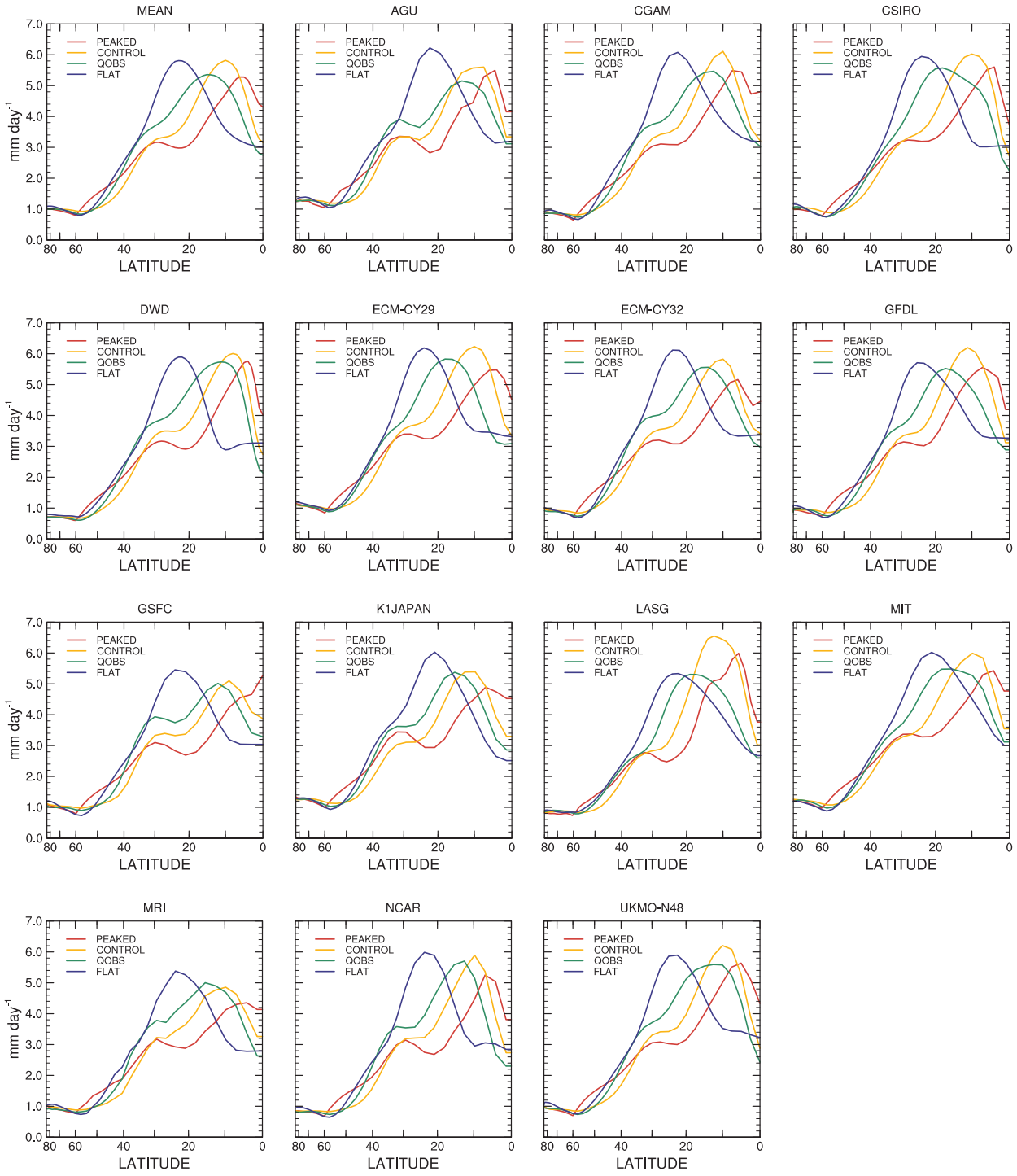

Figure 5.31: Zonal-time average evaporation (evap) for individual models from PEAKED, CONTROL, QOBS and FLAT SST distributions, mm day^{-1}.

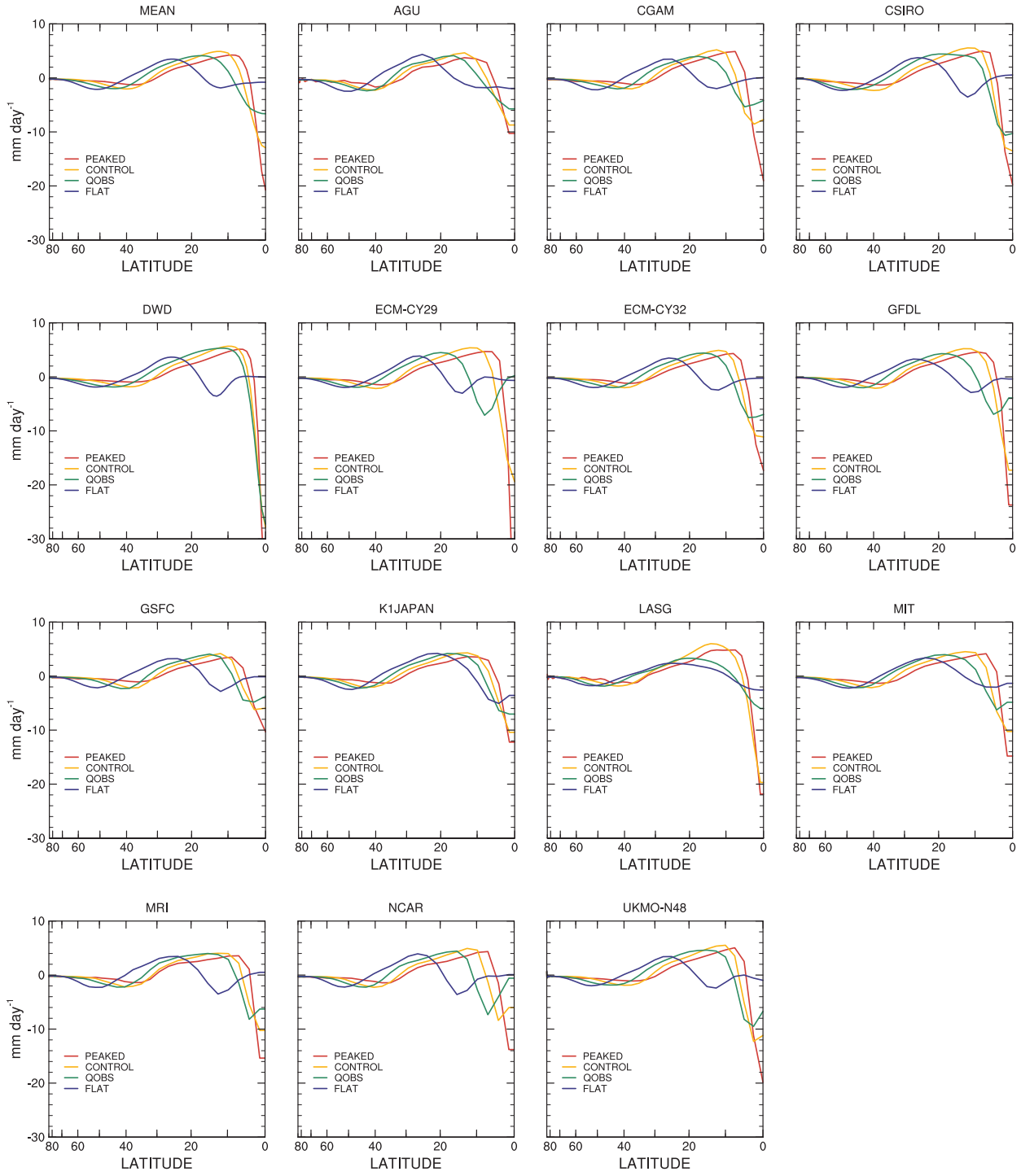

Figure 5.32: Zonal-time average evaporation minus precipitation (emp) for individual models from PEAKED, CONTROL, QOBS and FLAT SST distributions, mm day^{-1}.

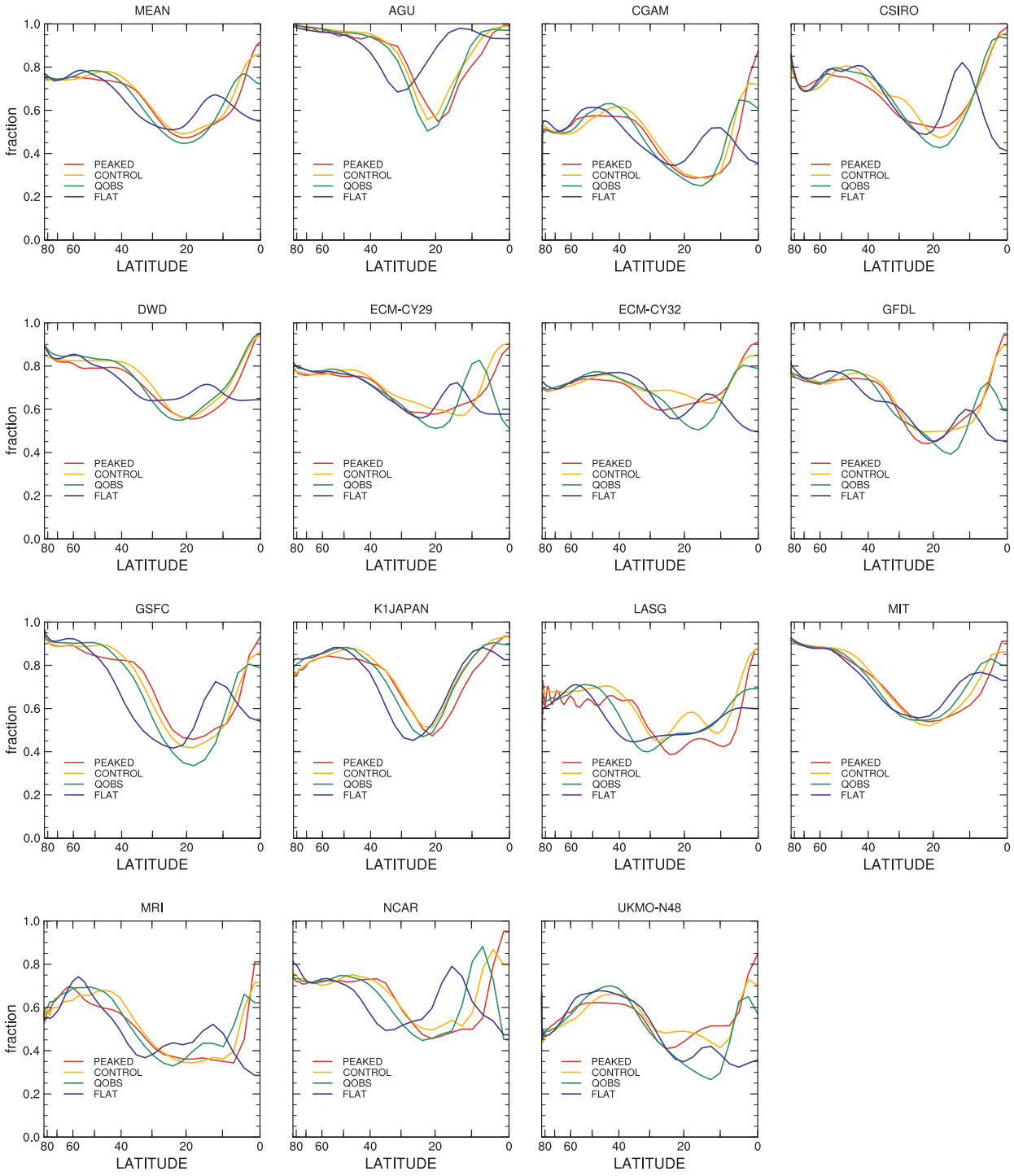

Figure 5.33: Zonal-time average cloud fraction (cld_frac) for individual models from PEAKED, CONTROL, QOBS and FLAT SST distributions, fraction.

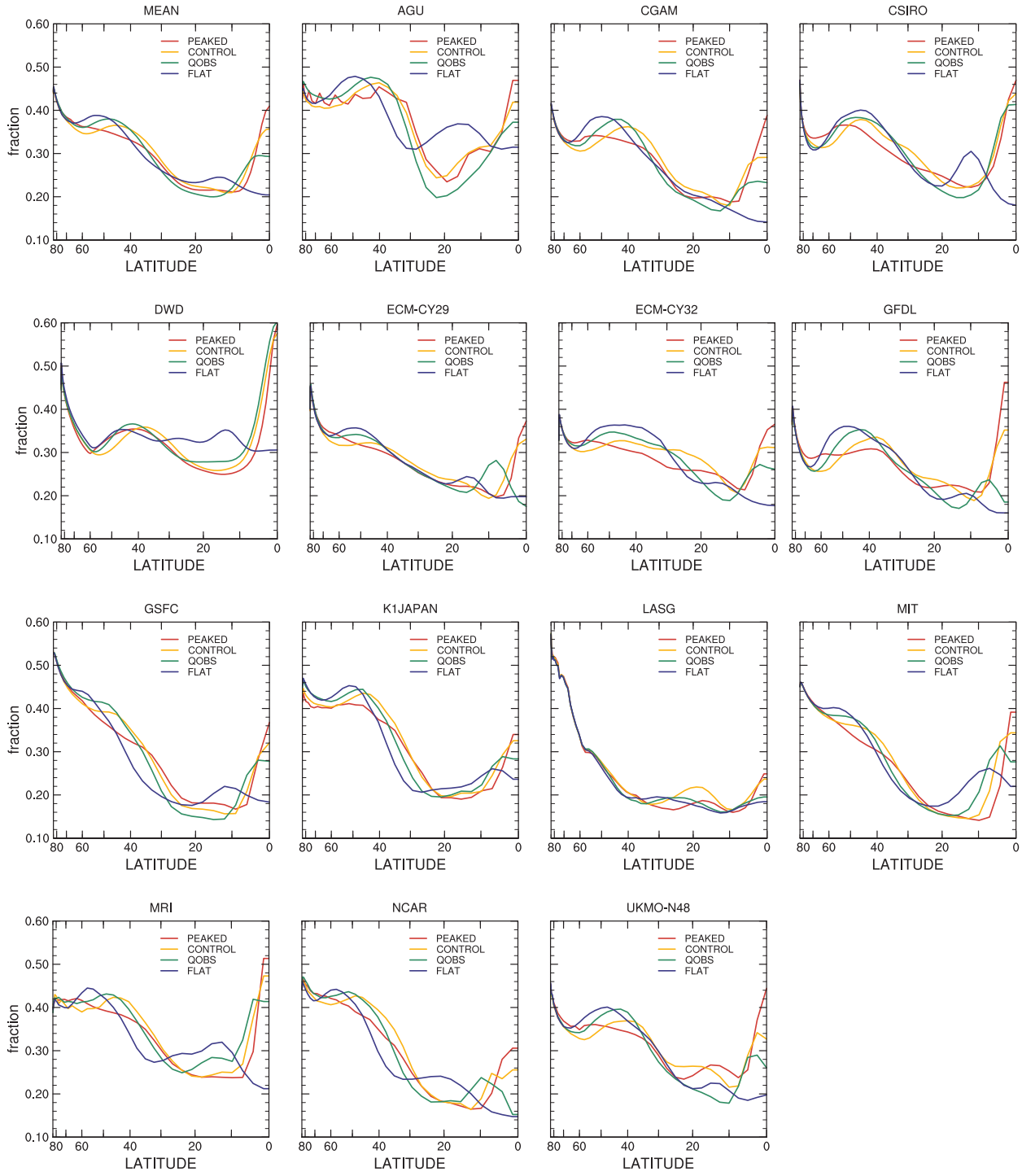

Figure 5.34: Zonal-time average albedo (albedo) for individual models from PEAKED, CONTROL, QOBS and FLAT SST distributions, fraction.

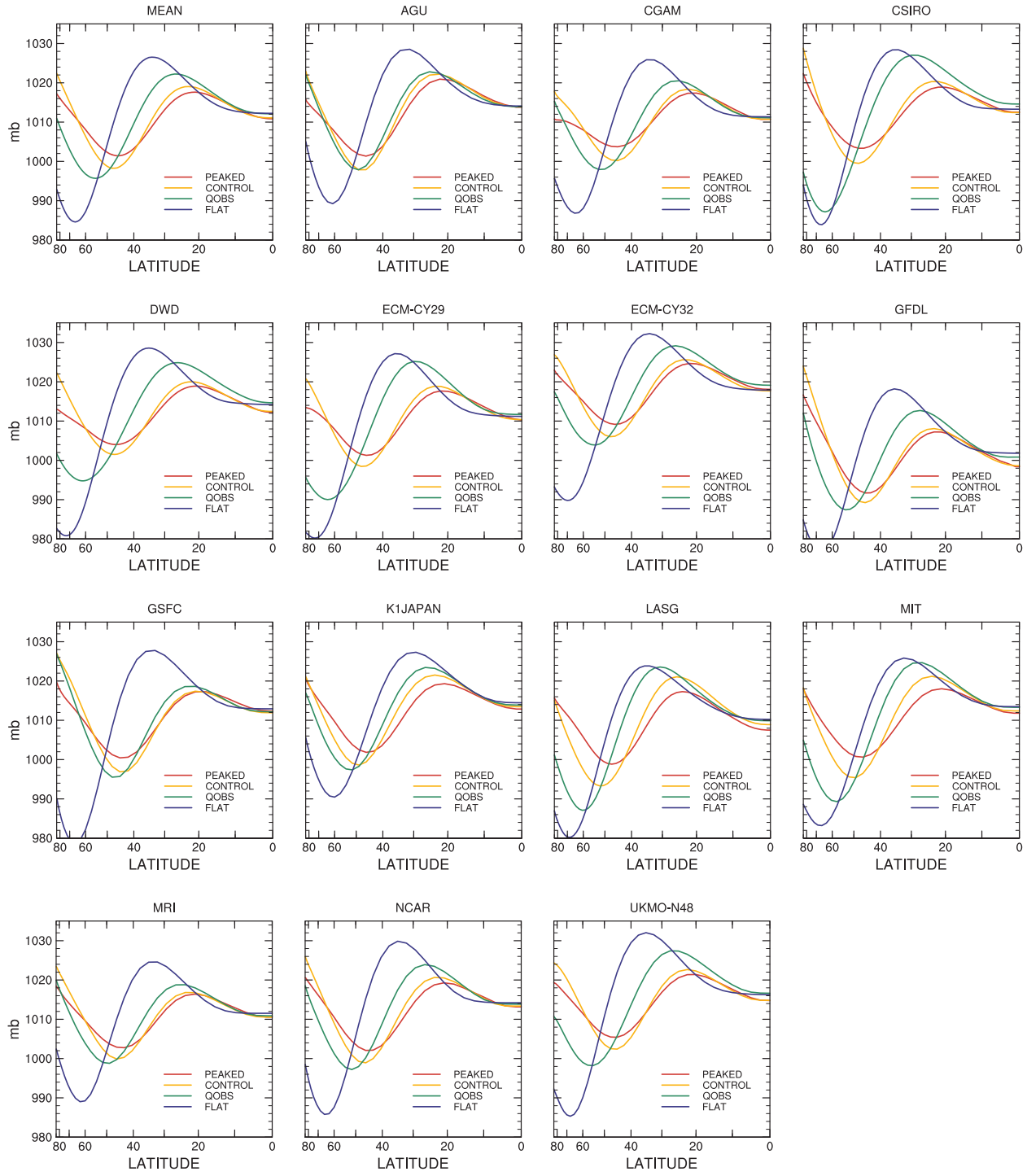

Figure 5.35: Zonal-time average surface pressure (ps) for individual models from PEAKED, CONTROL, QOBS and FLAT SST distributions, mb.

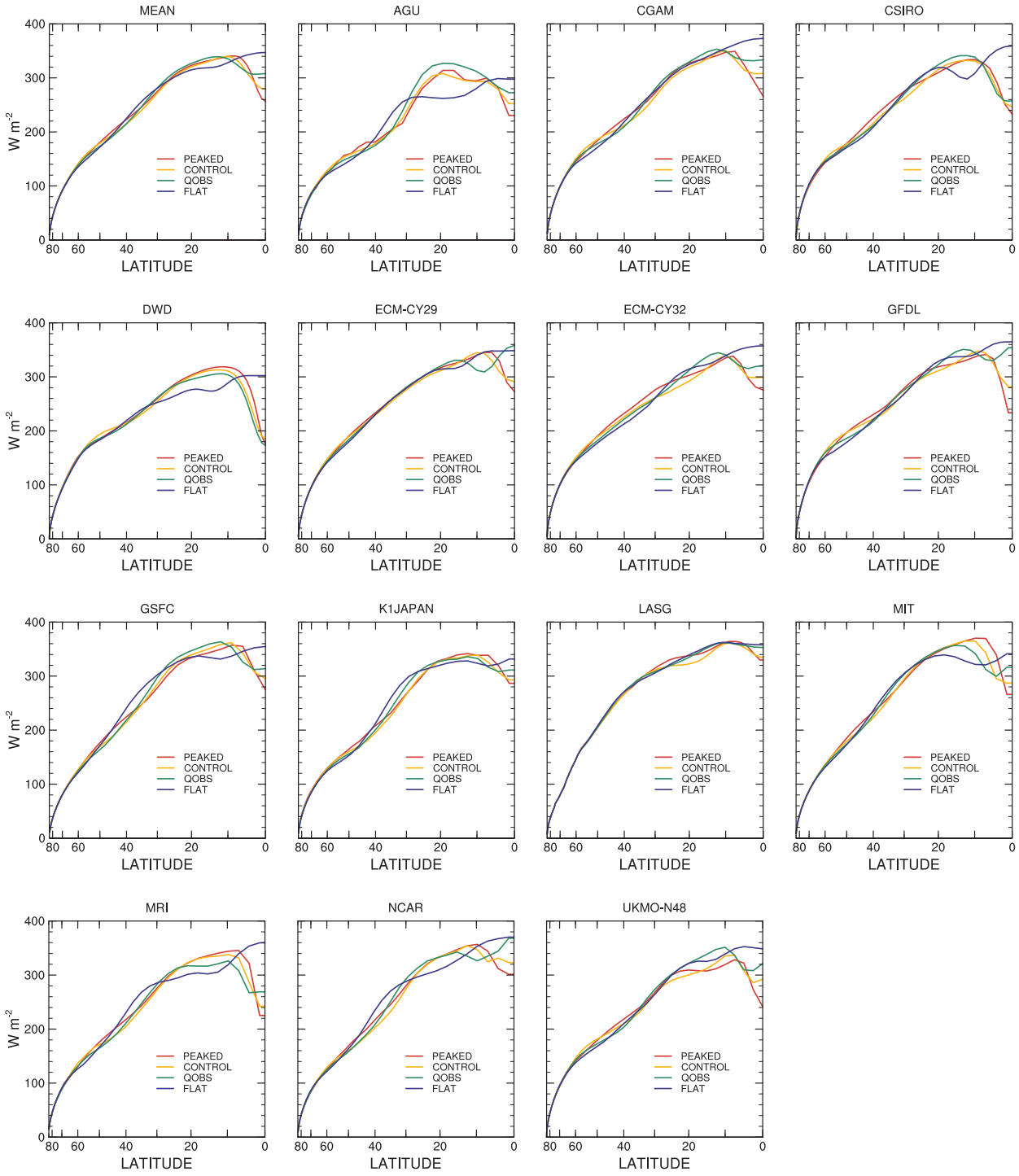

Figure 5.36: Zonal-time average TOA net shortwave radiation (sw_toa) for individual models from PEAKED, CONTROL, QOBS and FLAT SST distributions, W m^{-2}, +ve downward.

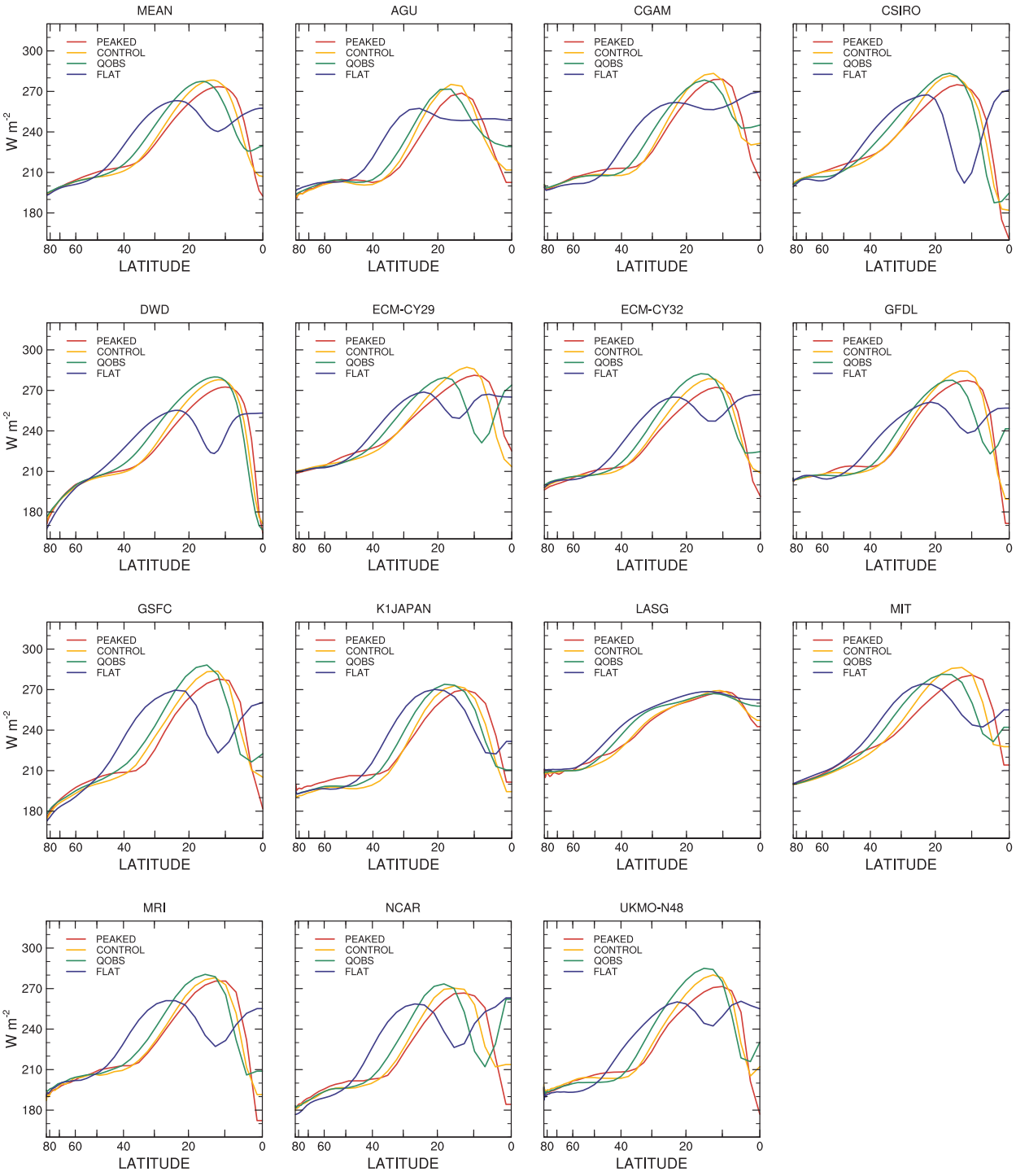

Figure 5.37: Zonal-time average TOA net longwave radiation (lw_toa) for individual models from PEAKED, CONTROL, QOBS and FLAT SST distributions, W m^{-2}, +ve upward.

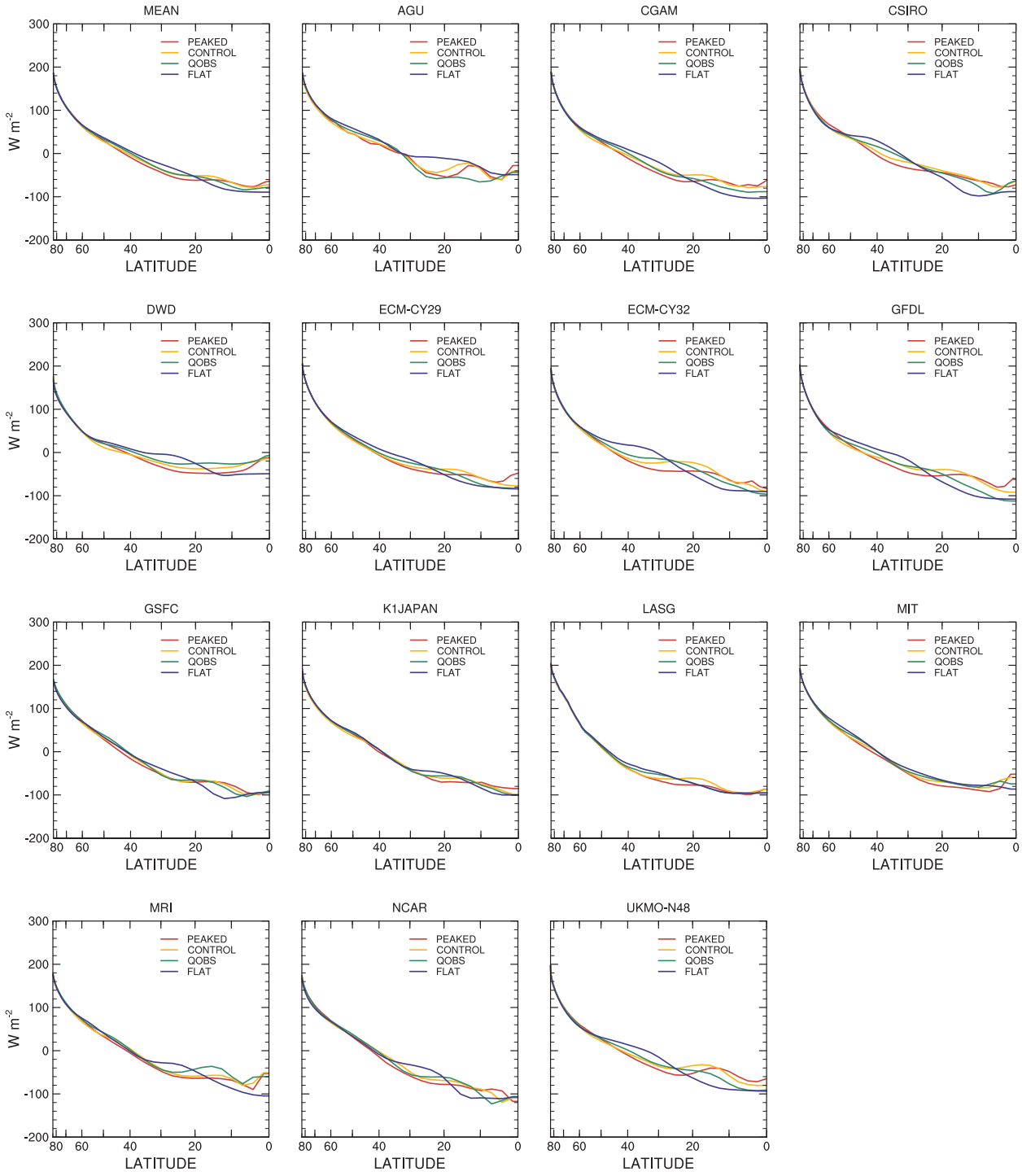

Figure 5.38: Zonal-time average TOA net radiation flux (rflux_toa) for individual models from PEAKED, CONTROL, QOBS and FLAT SST distributions, W m^{-2}, +ve upward.

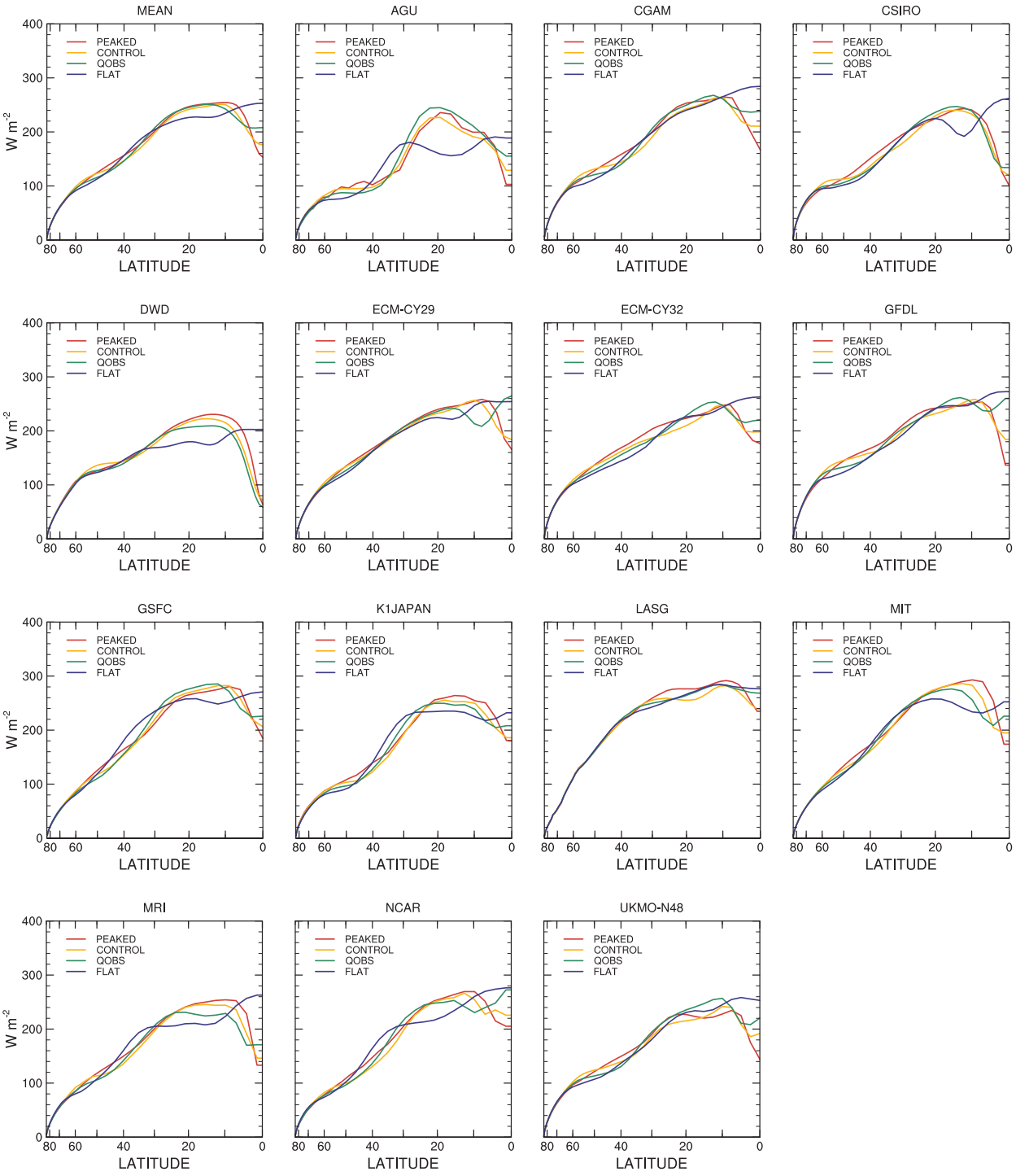

Figure 5.39: Zonal-time average surface net shortwave radiation (ssw) for individual models from PEAKED, CONTROL, QOBS and FLAT SST distributions, W m^{-2}, +ve downward.

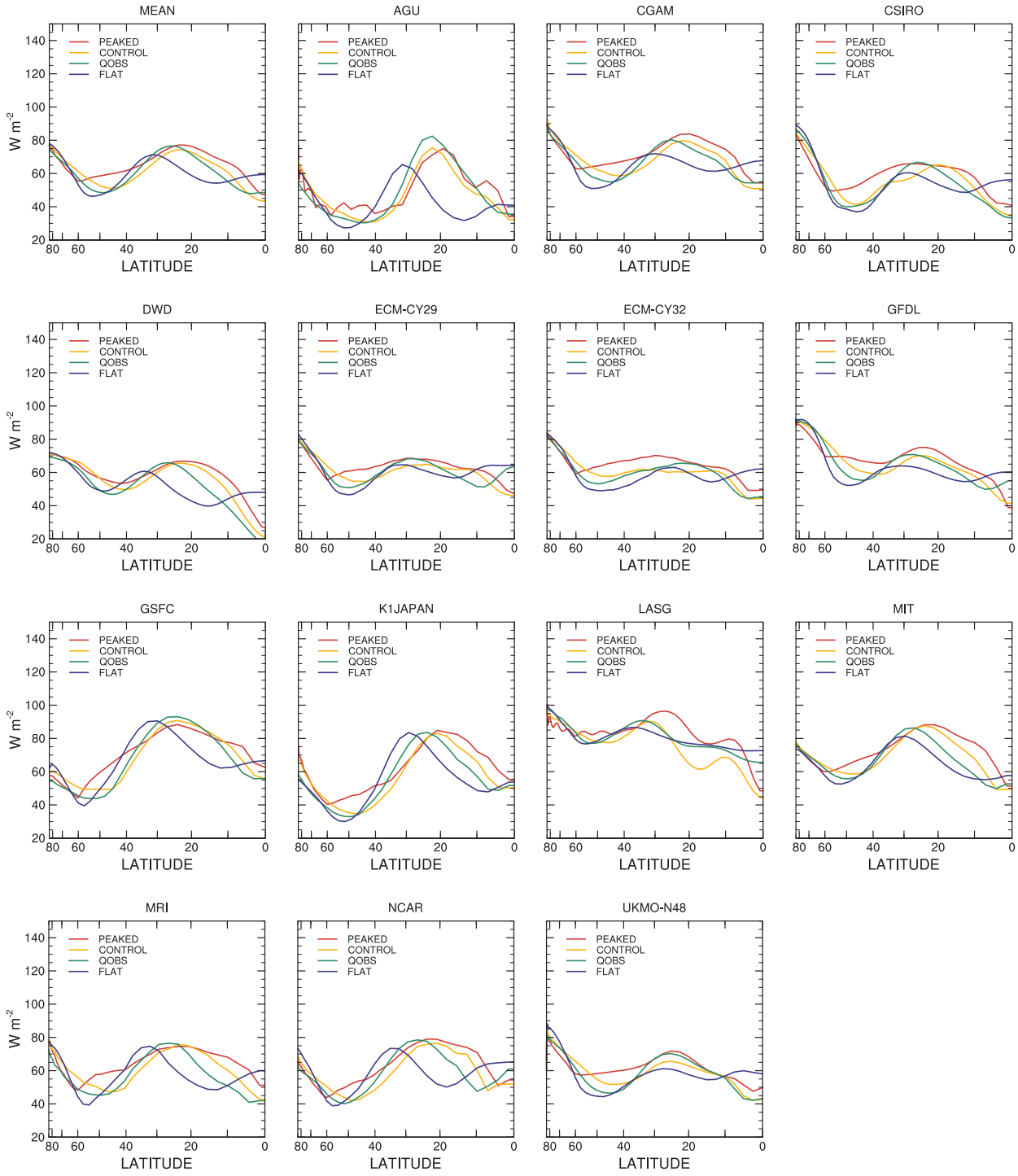

Figure 5.40: Zonal-time average surface net longwave radiation (slw) for individual models from PEAKED, CONTROL, QOBS and FLAT SST distributions, W m^{-2}, +ve upward.

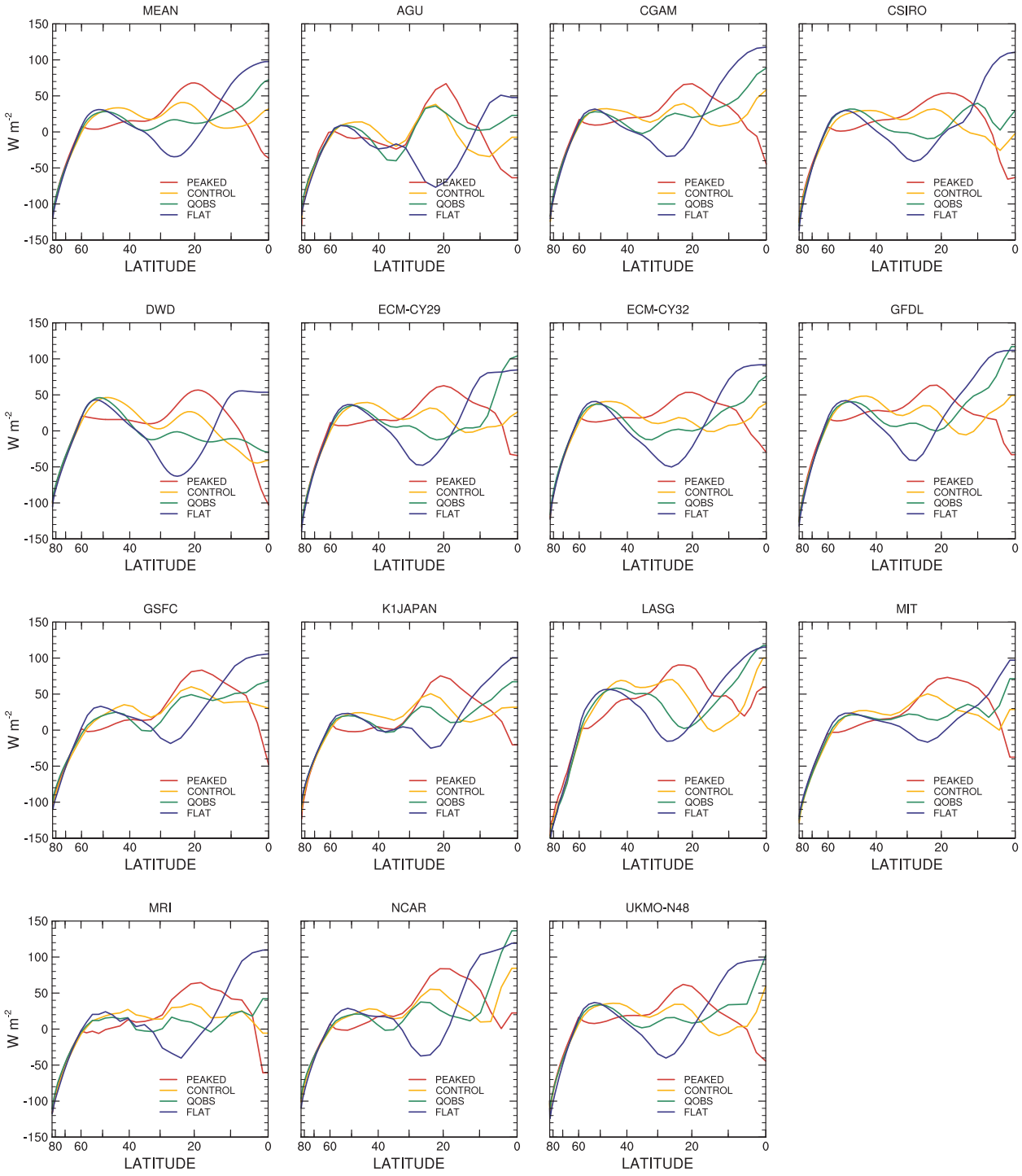

Figure 5.41: Zonal-time average surface net flux (rflux_sfce) for individual models from PEAKED, CONTROL, QOBS and FLAT SST distributions, W m^{-2}, +ve downward.

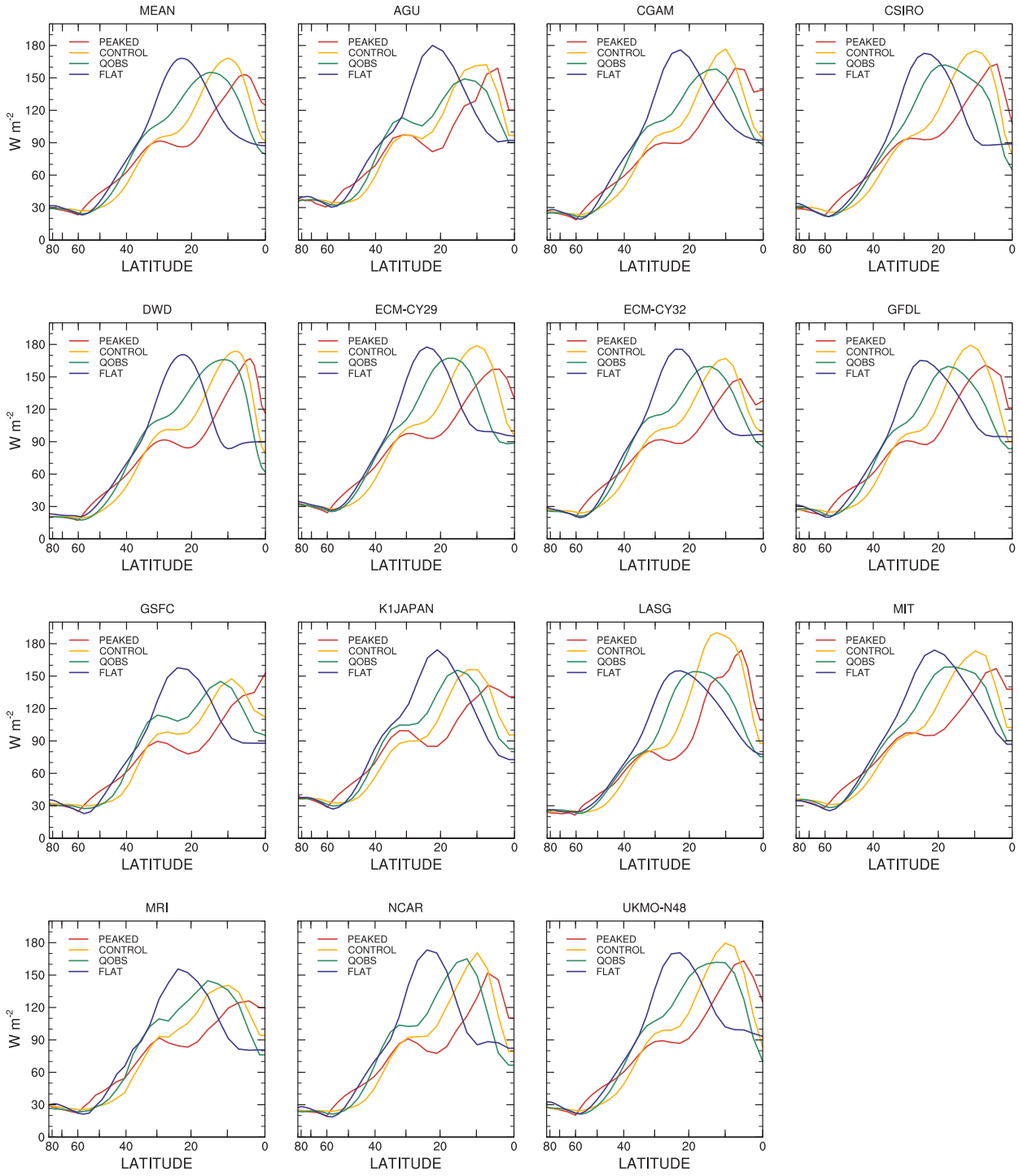

Figure 5.42: Zonal-time average surface latent heat flux (slh) for individual models from PEAKED, CONTROL, QOBS and FLAT SST distributions, W m^{-2}.

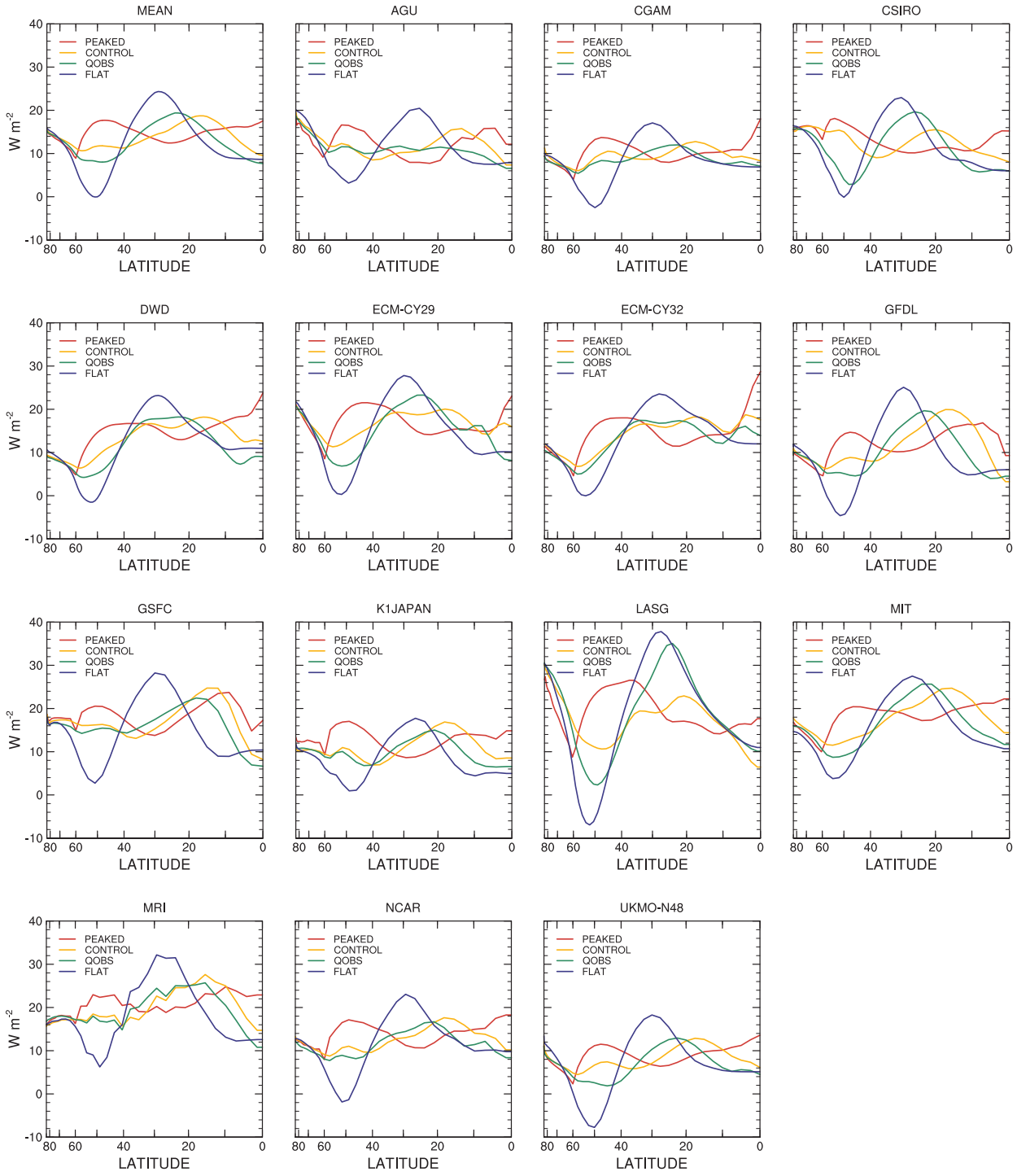

Figure 5.43: Zonal-time average surface sensible heat flux (ssh) for individual models from PEAKED, CONTROL, QOBS and FLAT SST distributions, W m^{-2}.

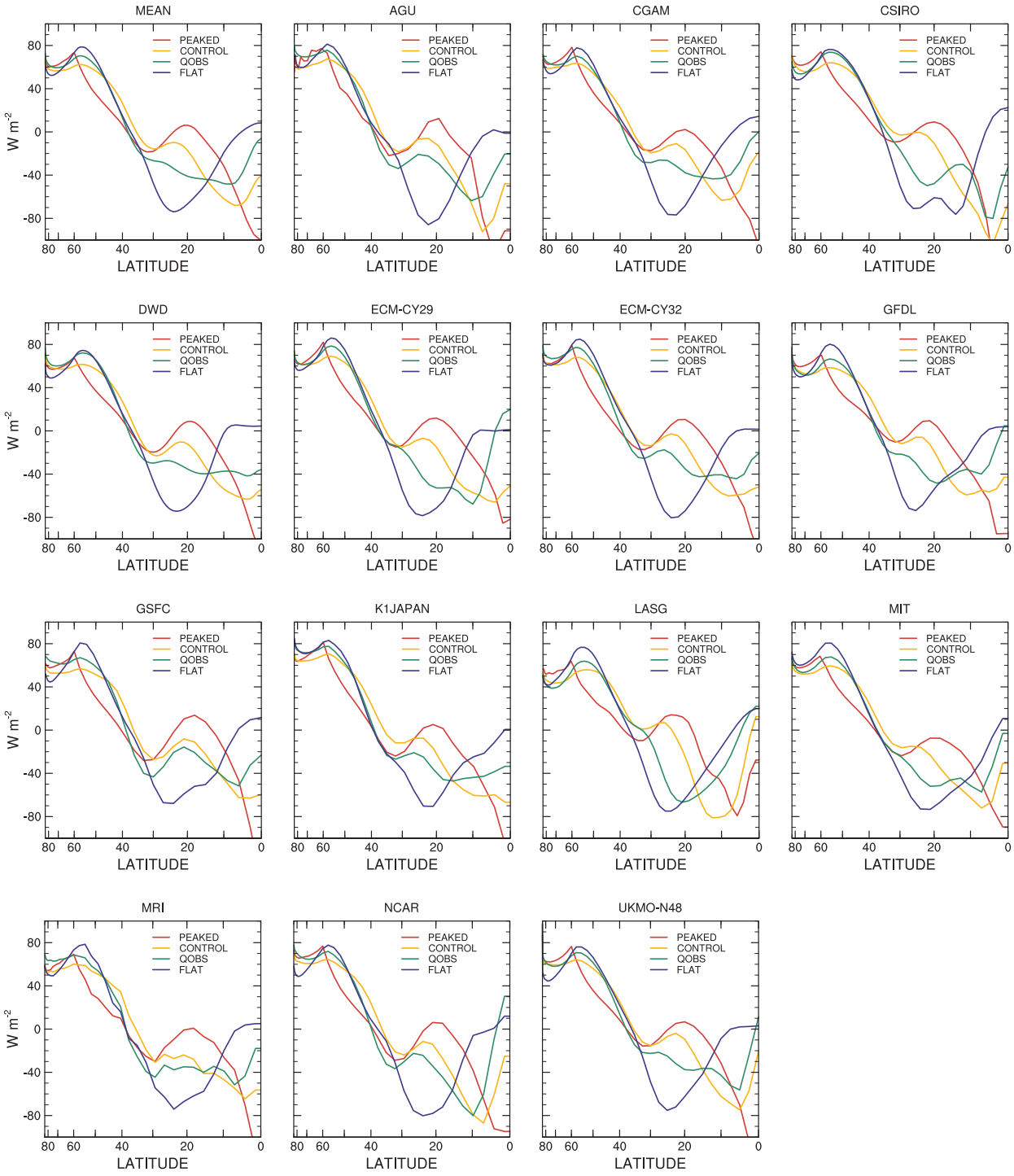

Figure 5.44: Zonal-time average net flux (rflux) for individual models from PEAKED, CONTROL, QOBS and FLAT SST distributions, W m^{-2}, +ve out of atmosphere.

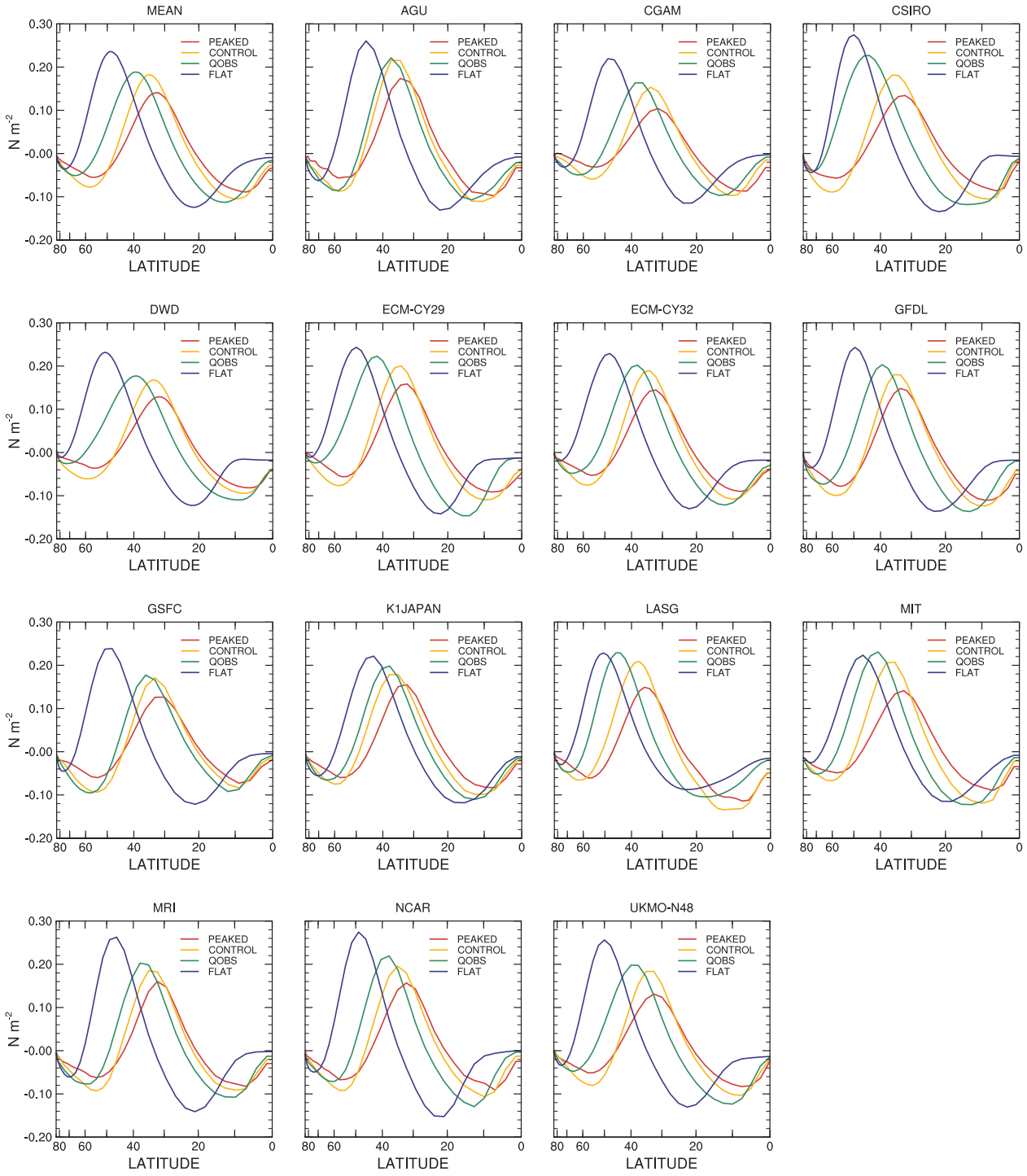

Figure 5.45: Zonal-time average zonal surface stress (tauu) for individual models from PEAKED, CONTROL, QOBS and FLAT SST distributions, N m^{-2}.

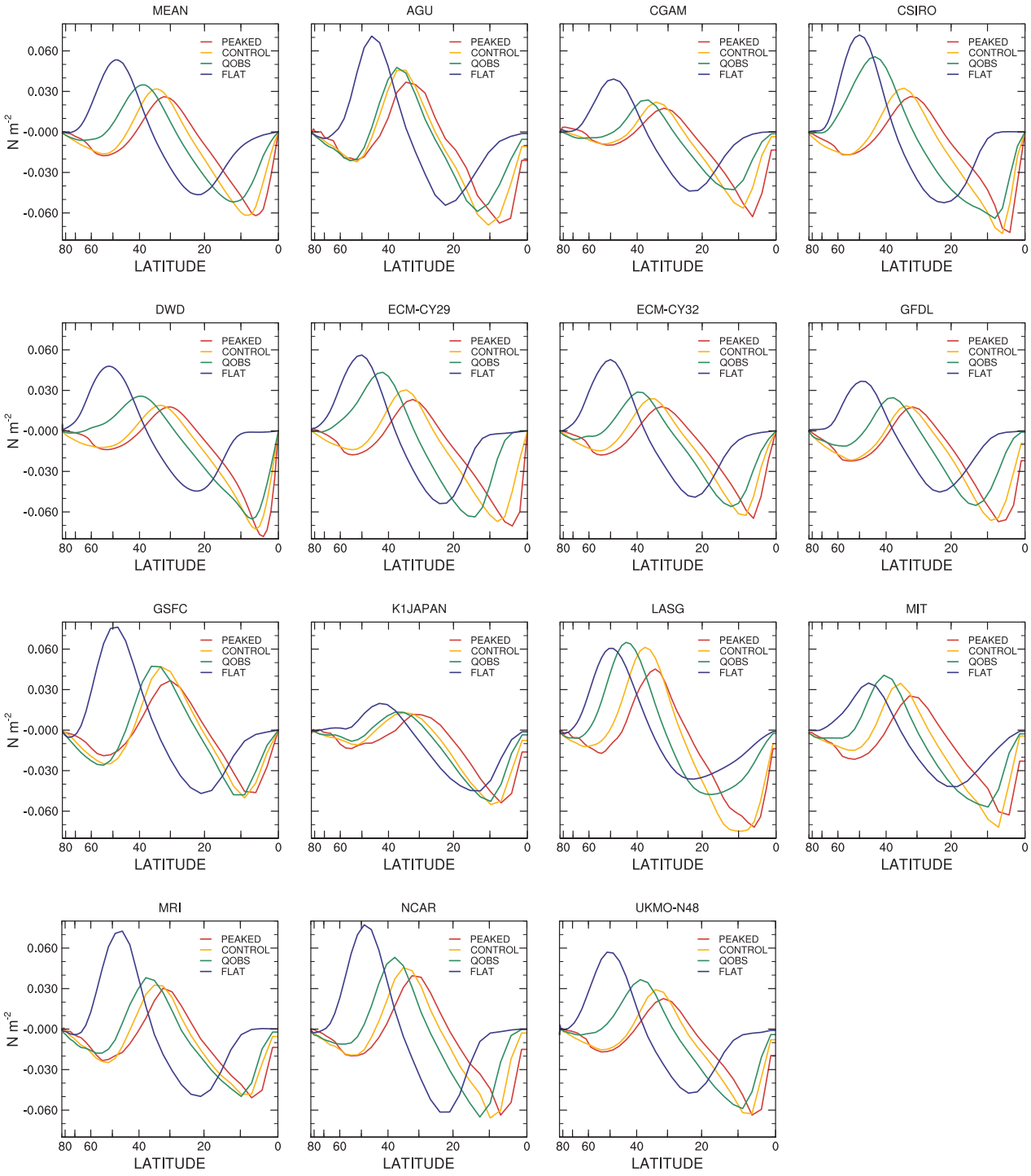

Figure 5.46: Zonal-time average meridional surface stress (tauv) for individual models from PEAKED, CONTROL, QOBS and FLAT SST distributions, N m^{-2}.

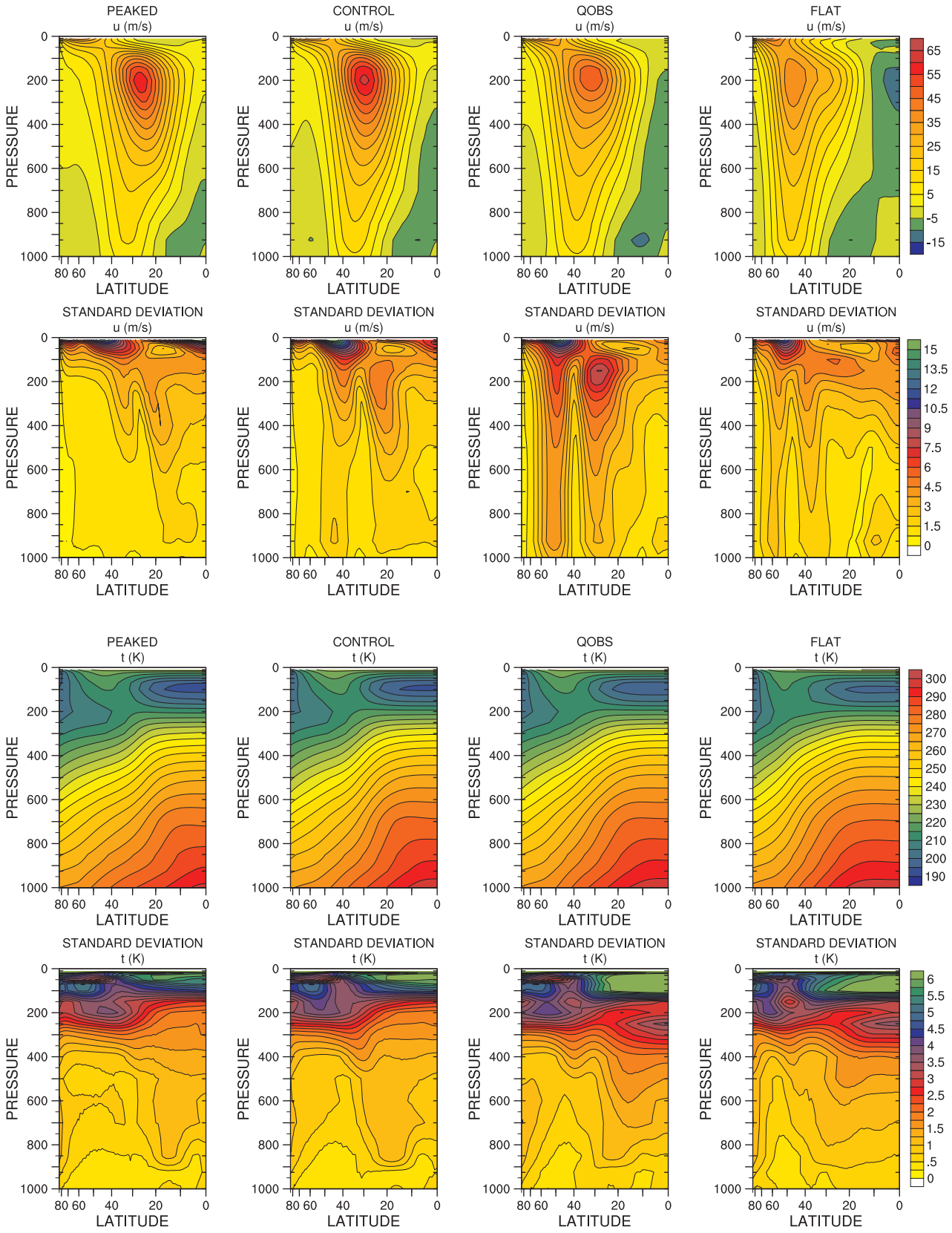

Figure 5.47: Zonal-time average multi-model mean and standard deviation zonal wind (u) and temperature (t) for PEAKED, CONTROL, QOBS and FLAT.

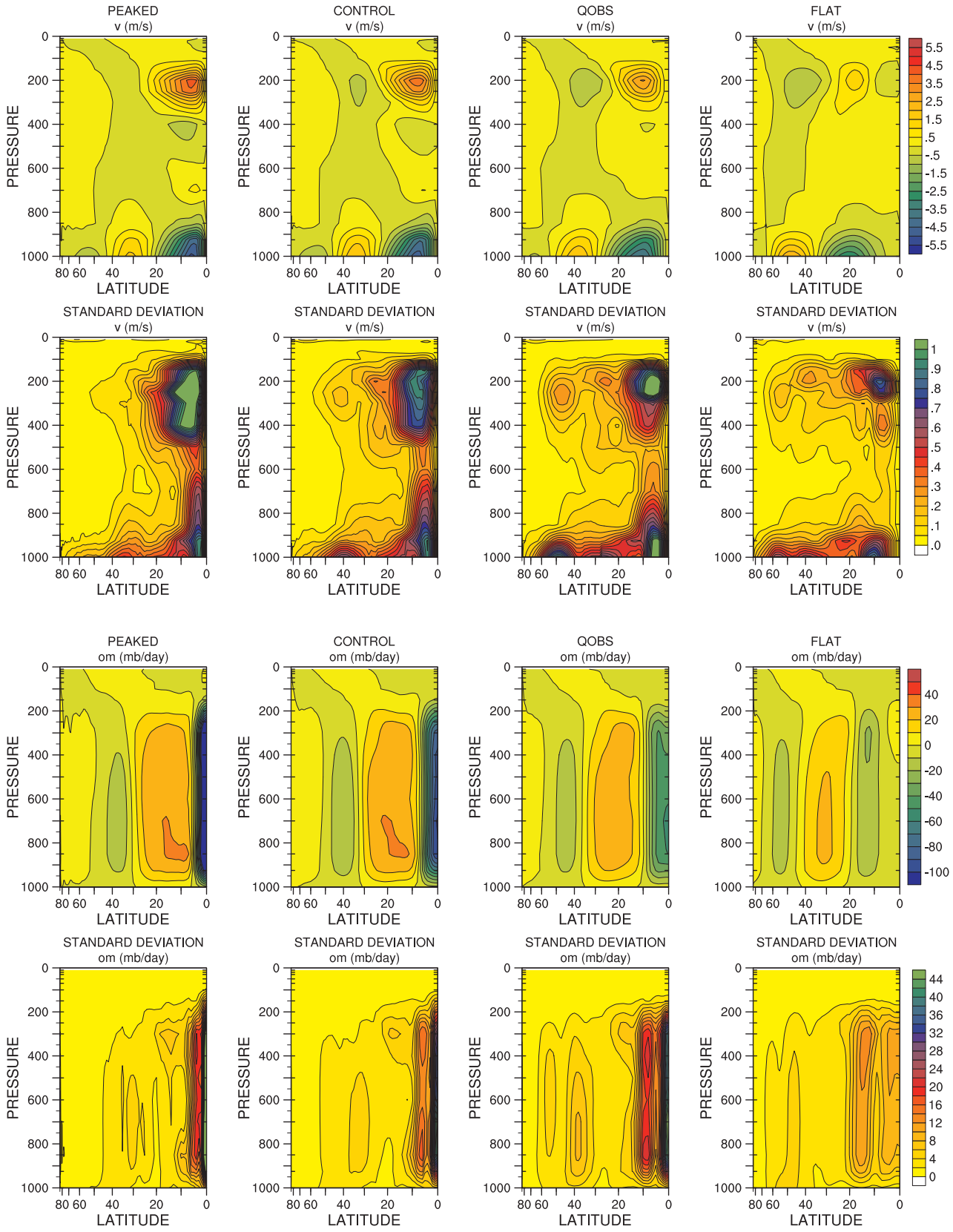

Figure 5.48: Zonal-time average multi-model mean and standard deviation meridional wind (v) and vertical wind (om) for PEAKED, CONTROL, QOBS and FLAT.

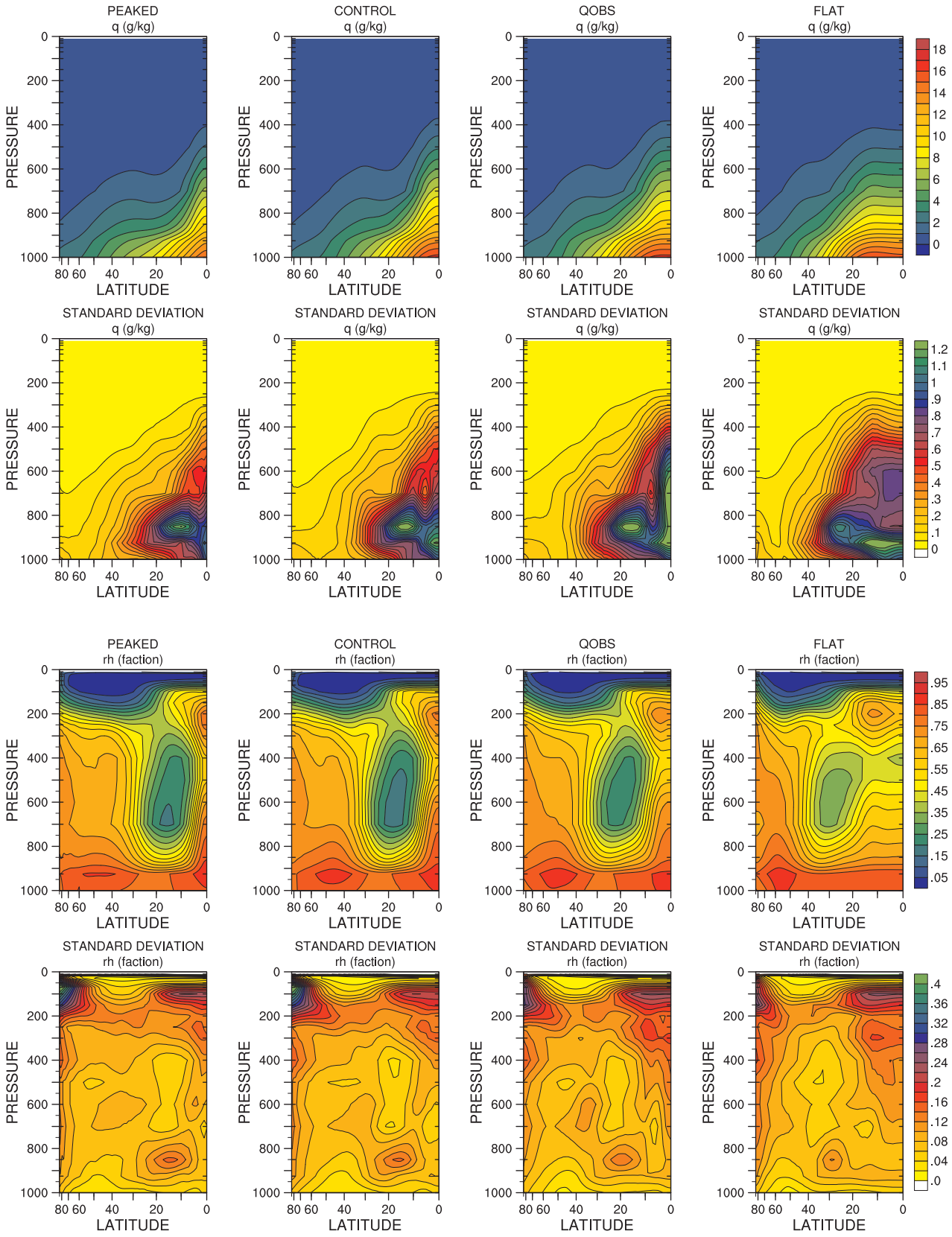

Figure 5.49: Zonal-time average multi-model mean and standard deviation specific humidity (q) and relative humidity (rh) for PEAKED, CONTROL, QOBS and FLAT.

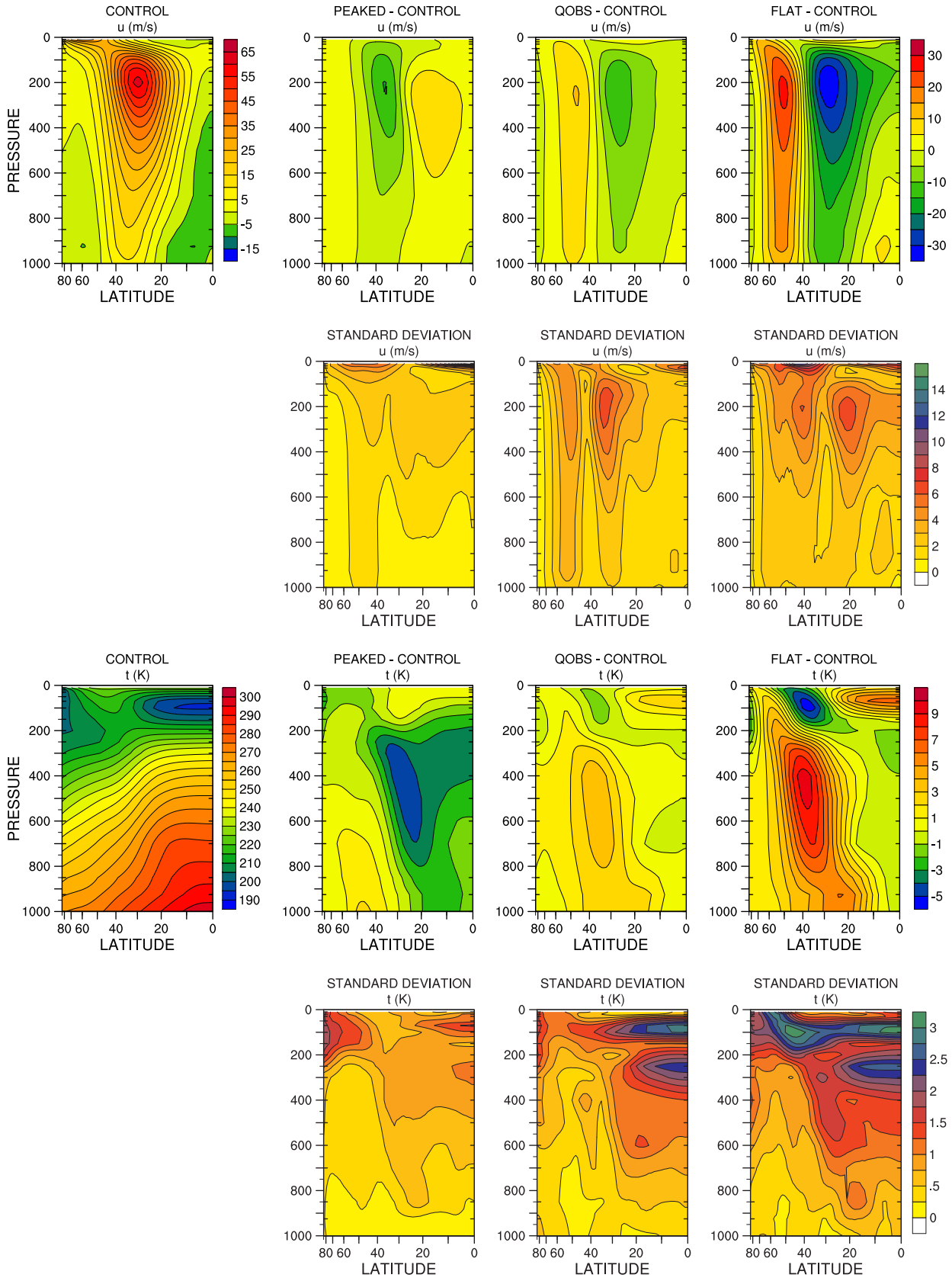

Figure 5.50: Zonal-time average multi-model mean and standard deviation, CONTROL, PEAKED−CONTROL, QOBS−CONTROL and FLAT−CONTROL, zonal wind (u) and temperature (t).

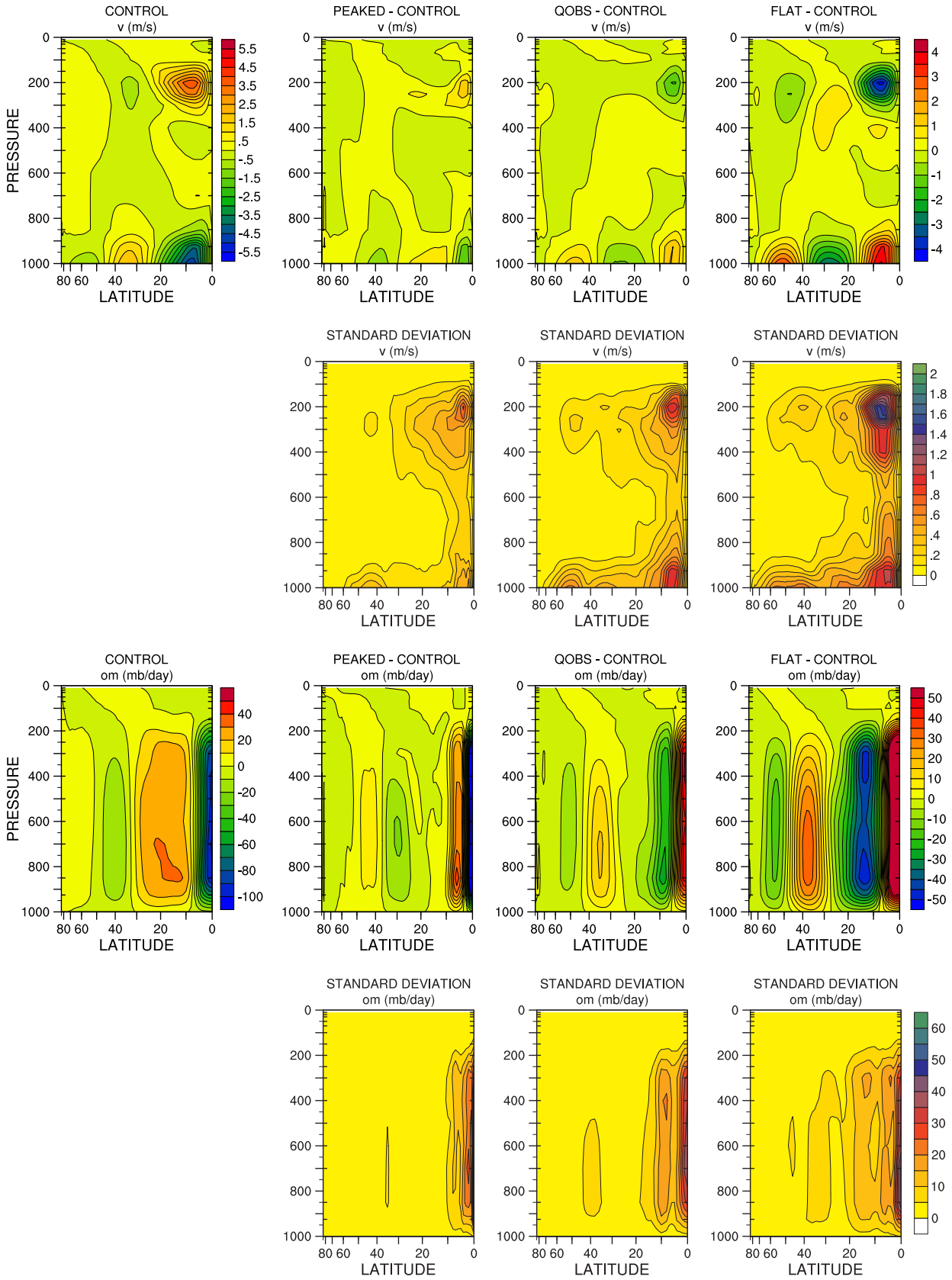

Figure 5.51: Zonal-time average multi-model mean and standard deviation, CONTROL, PEAKED−CONTROL, QOBS−CONTROL and FLAT−CONTROL, meridional wind (v) and vertical wind (om).

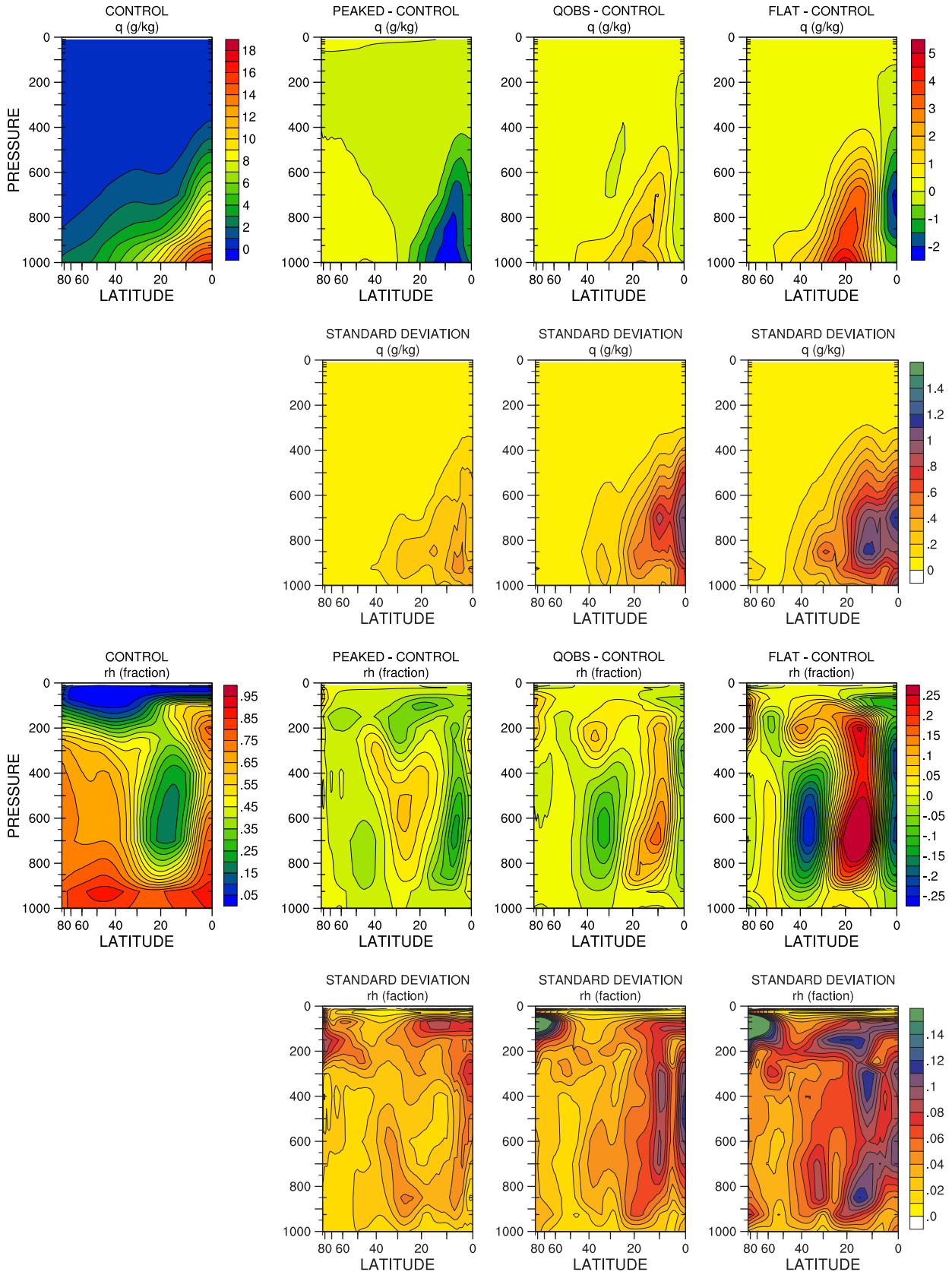

Figure 5.52: Zonal-time average multi-model mean and standard deviation, CONTROL, PEAKED−CONTROL, QOBS−CONTROL and FLAT−CONTROL, specific humidity (q) and relative humidity (rh).

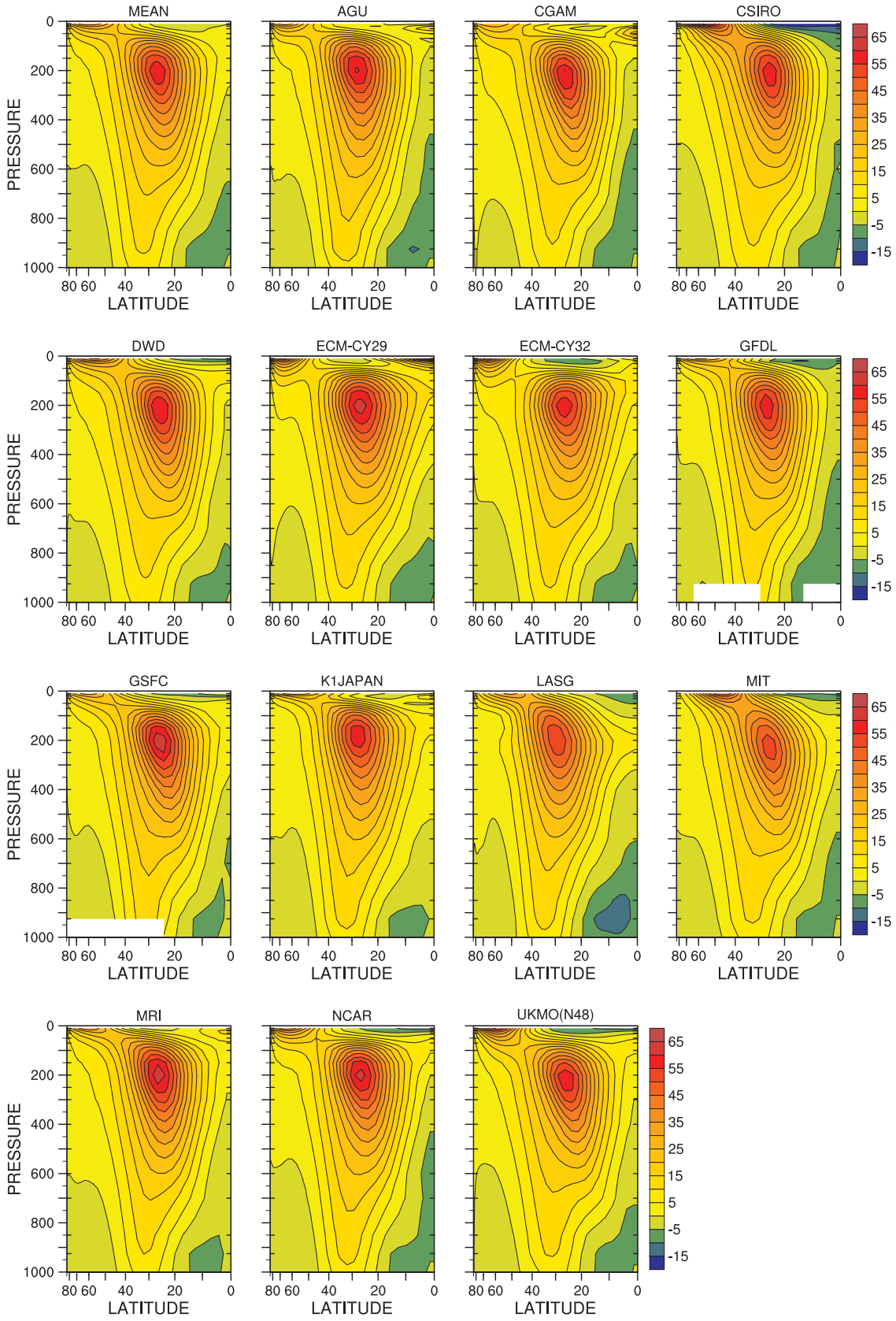

Figure 5.53: Zonal-time average zonal wind (u), PEAKED, individual models, m s^{-1}.

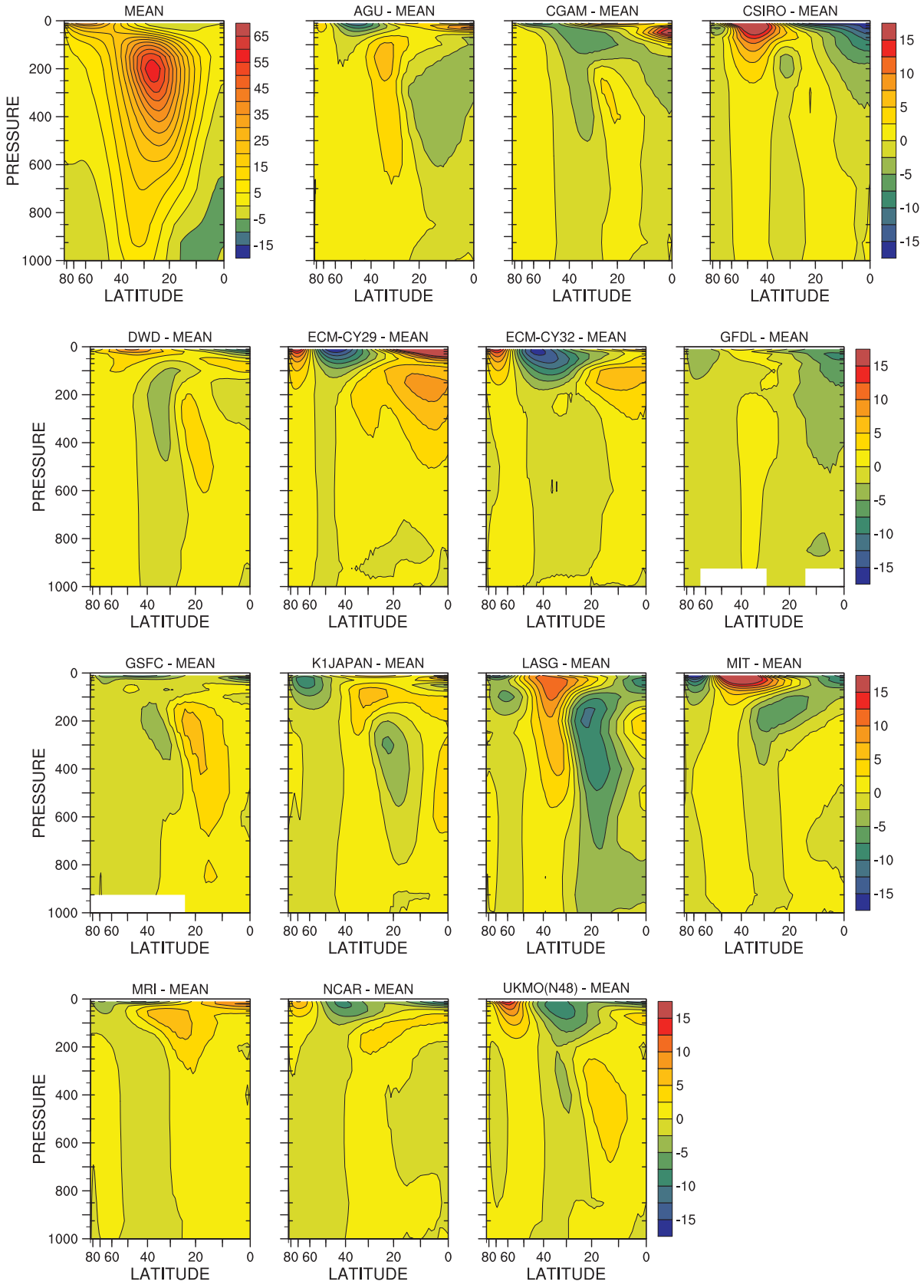

Figure 5.54: Zonal-time average zonal wind (u), PEAKED, individual models minus multi-model mean, m s^{-1}.

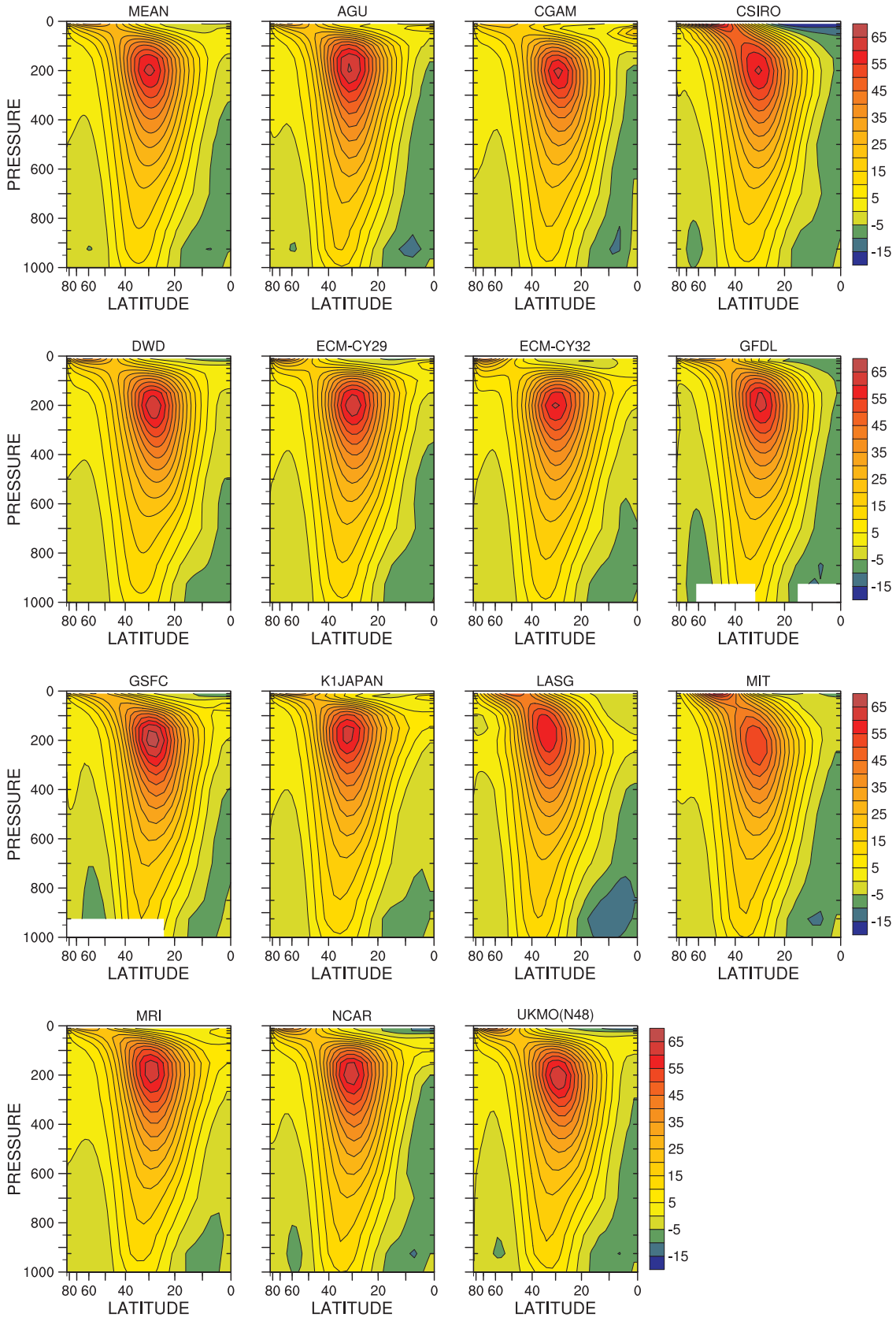

Figure 5.55: Zonal-time average zonal wind (u), CONTROL, individual models, m s^{-1}.

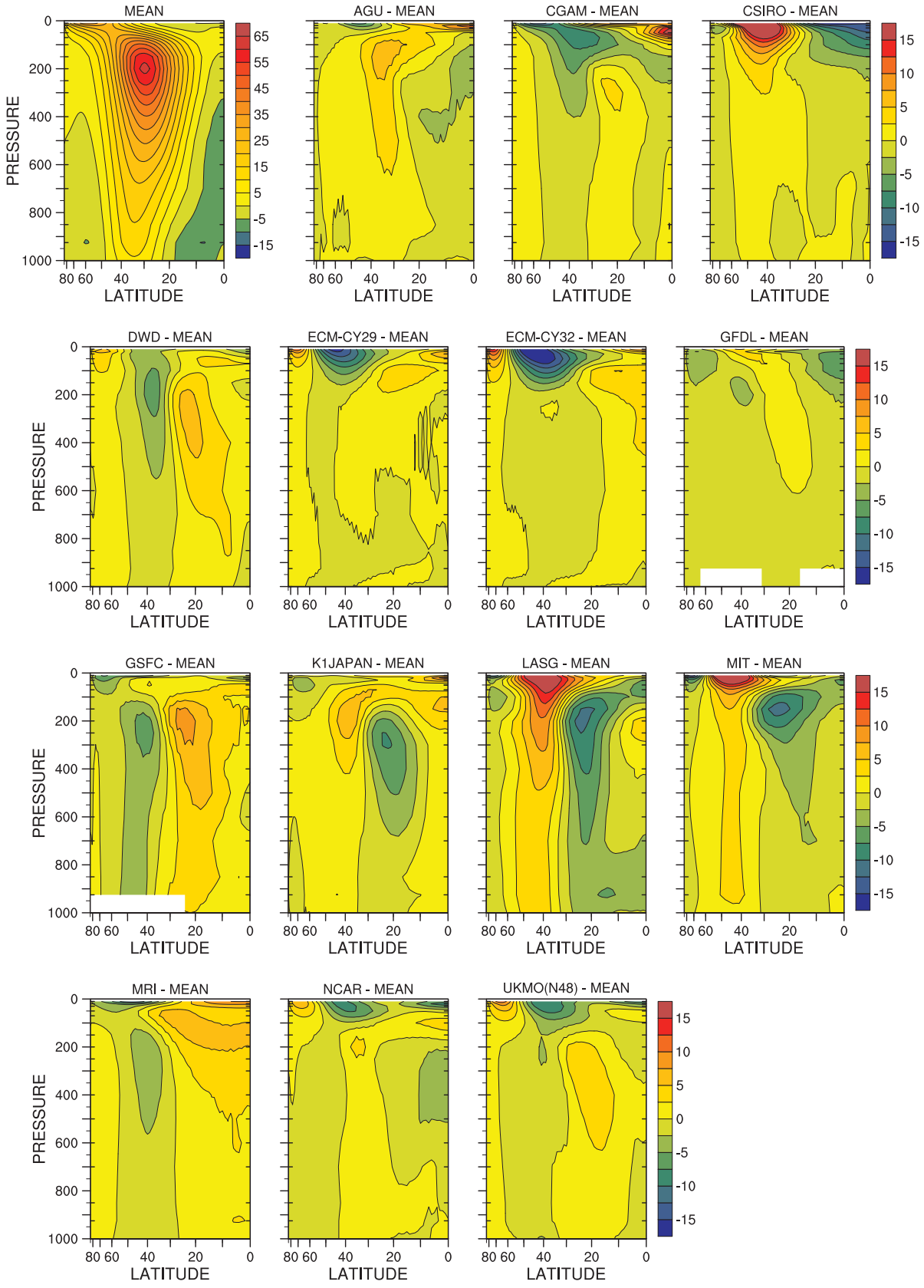

Figure 5.56: Zonal-time average zonal wind (u), CONTROL, individual models minus multi-model mean, m s^{-1}.

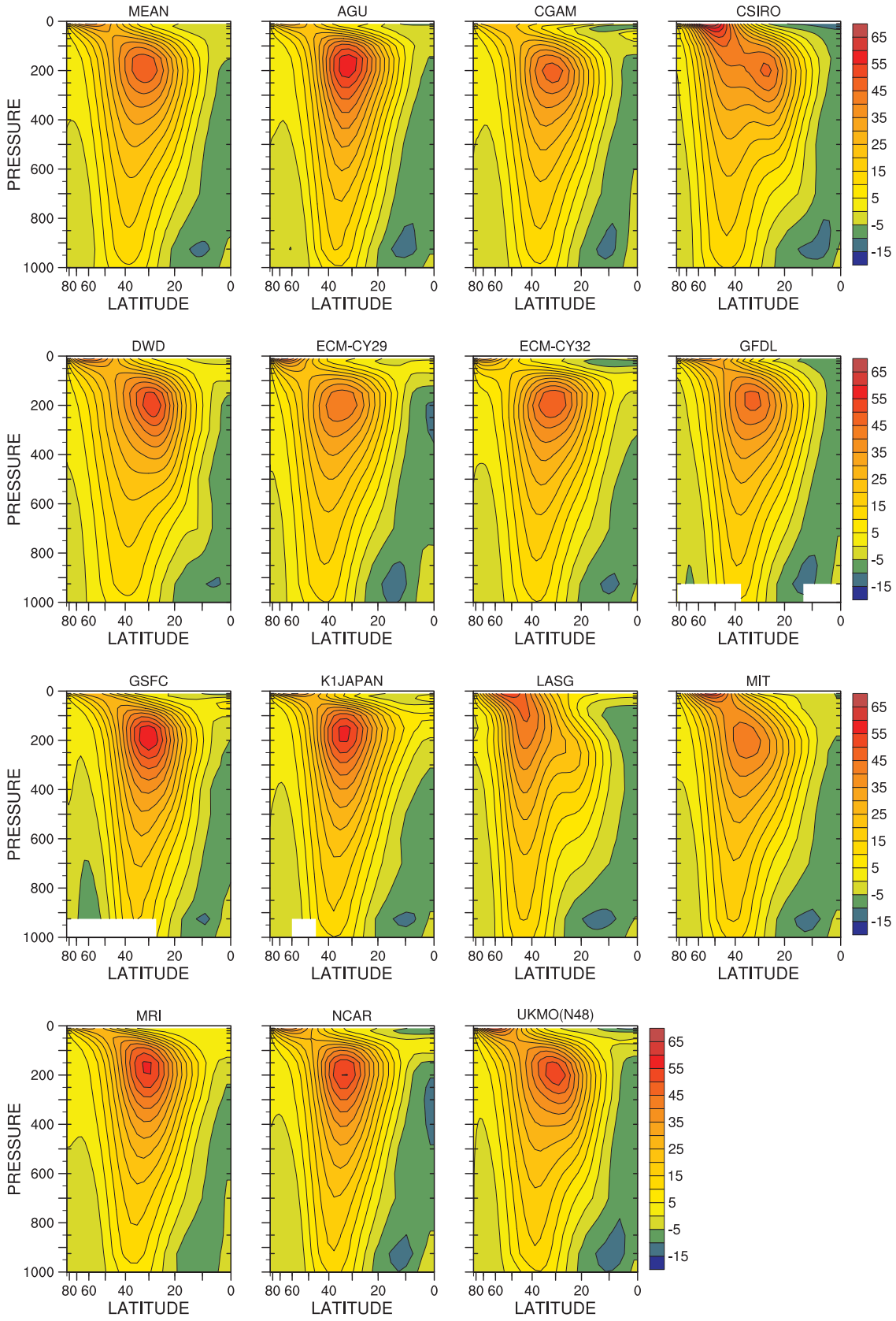

Figure 5.57: Zonal-time average zonal wind (u), QOBS, individual models, m s^{-1}.

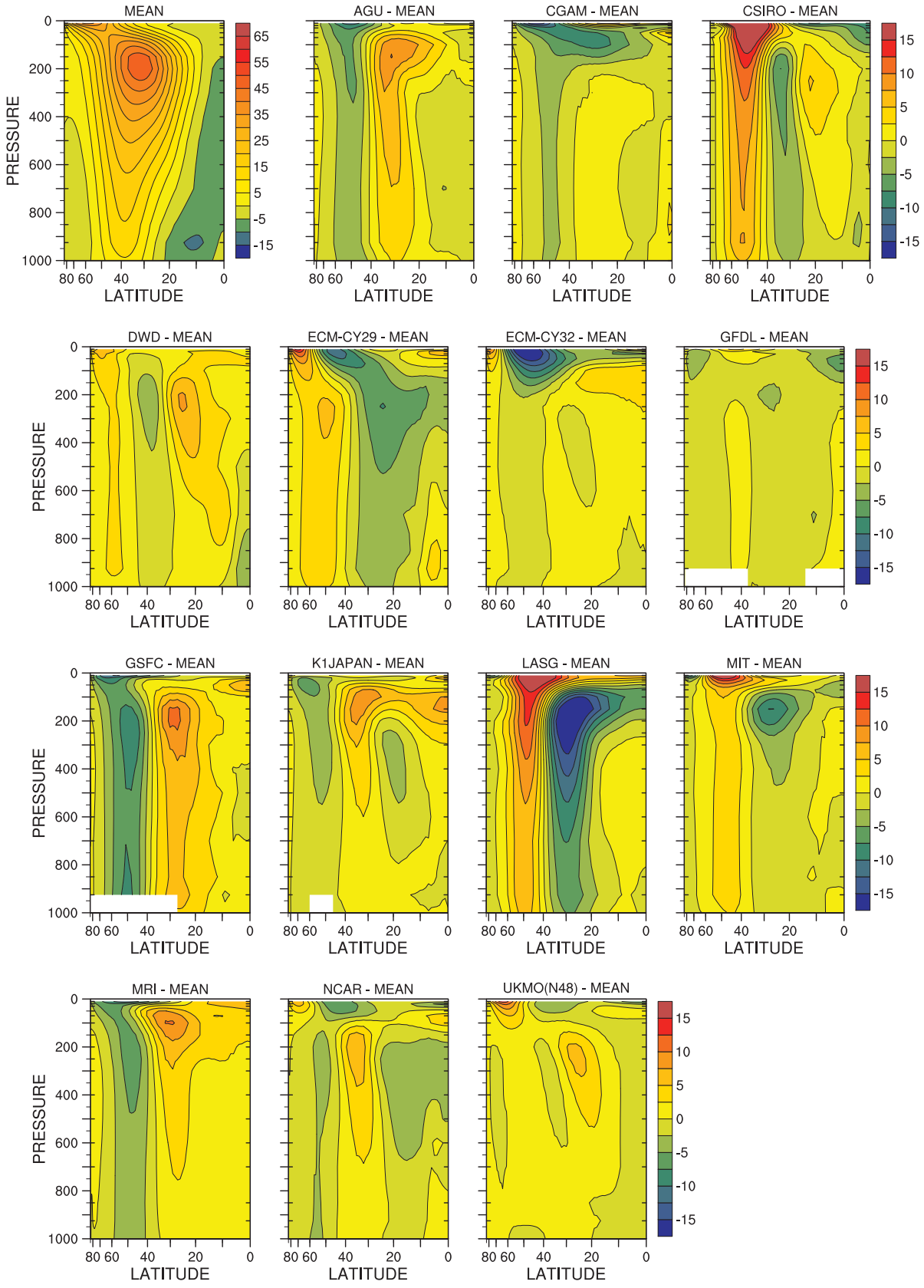

Figure 5.58: Zonal-time average zonal wind (u), QOBS, individual models minus multi-model mean, m s^{-1}.

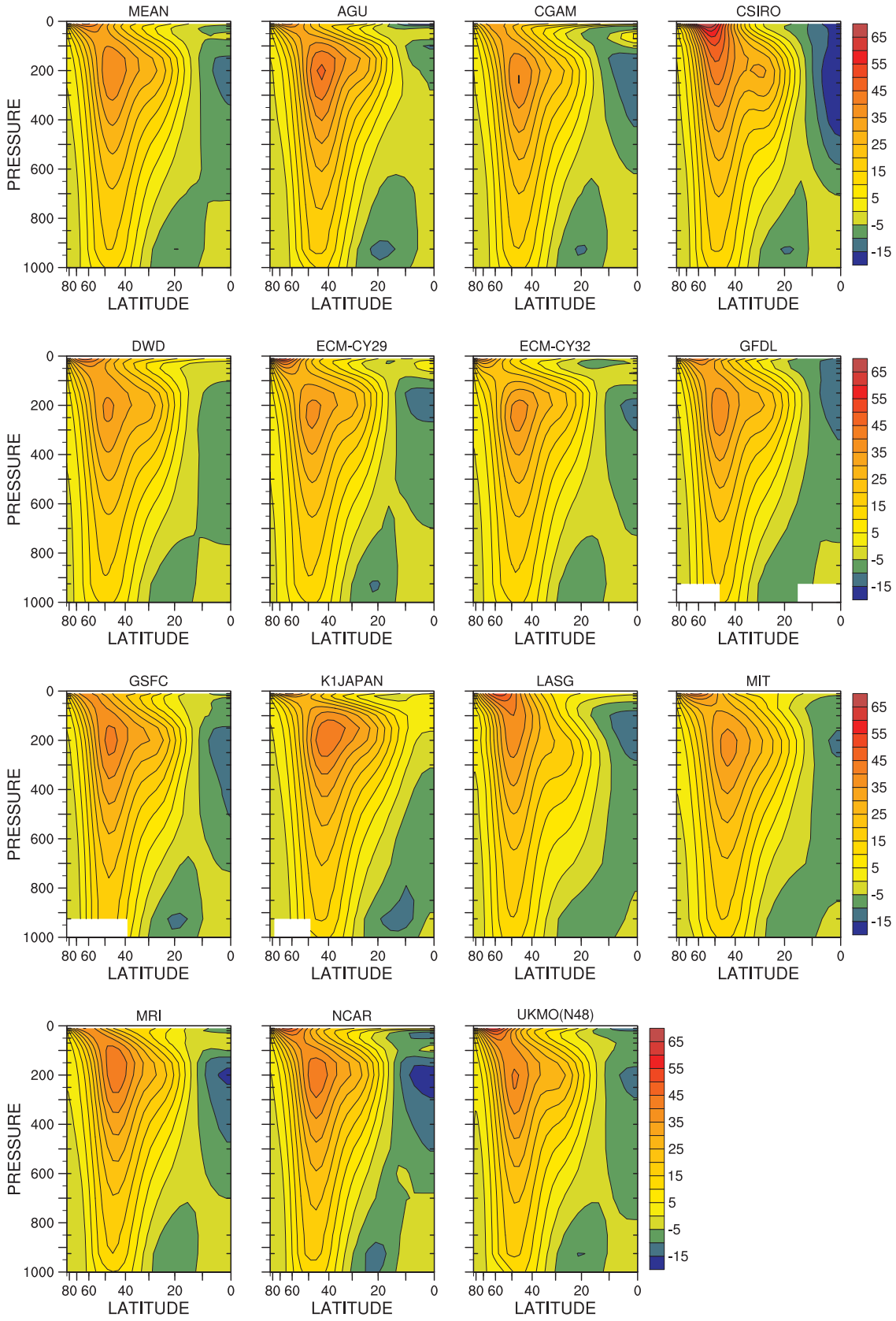

Figure 5.59: Zonal-time average zonal wind (u), FLAT, individual models, m s^{-1}.

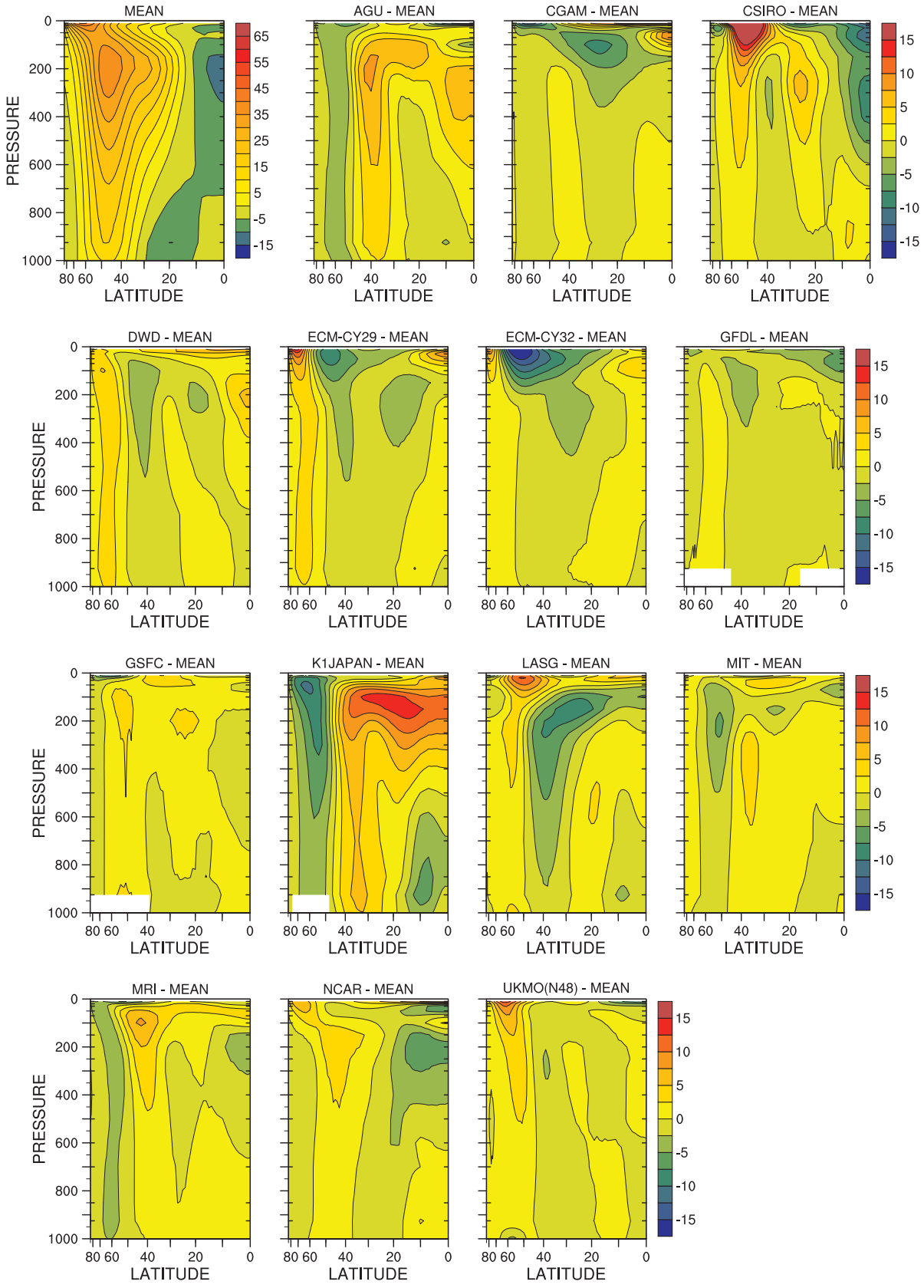

Figure 5.60: Zonal-time average zonal wind (u), FLAT, individual models minus multi-model mean, m s^{-1}.

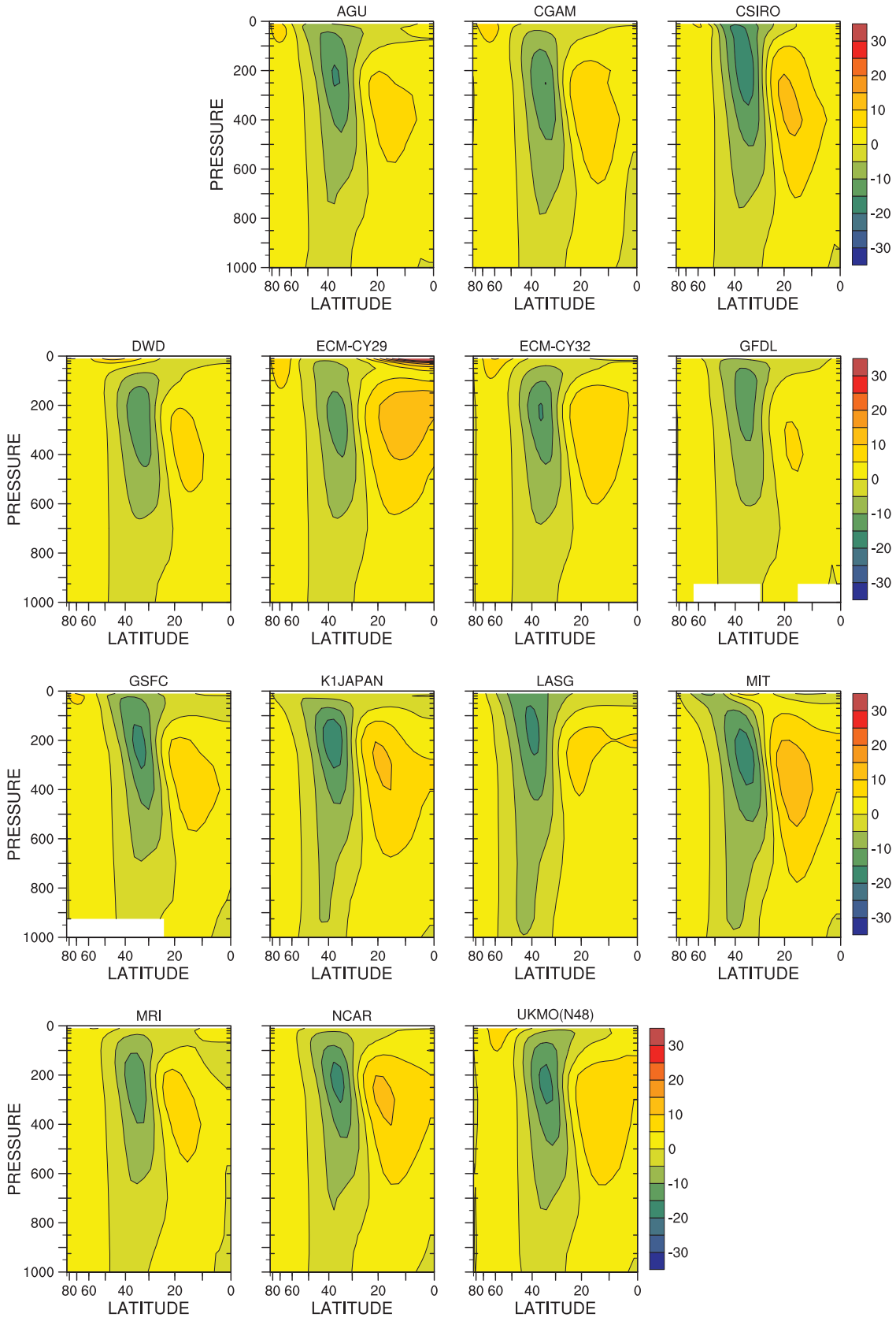

Figure 5.61: Zonal-time average zonal wind (u), PEAKED−CONTROL, individual models, m s^{-1}.

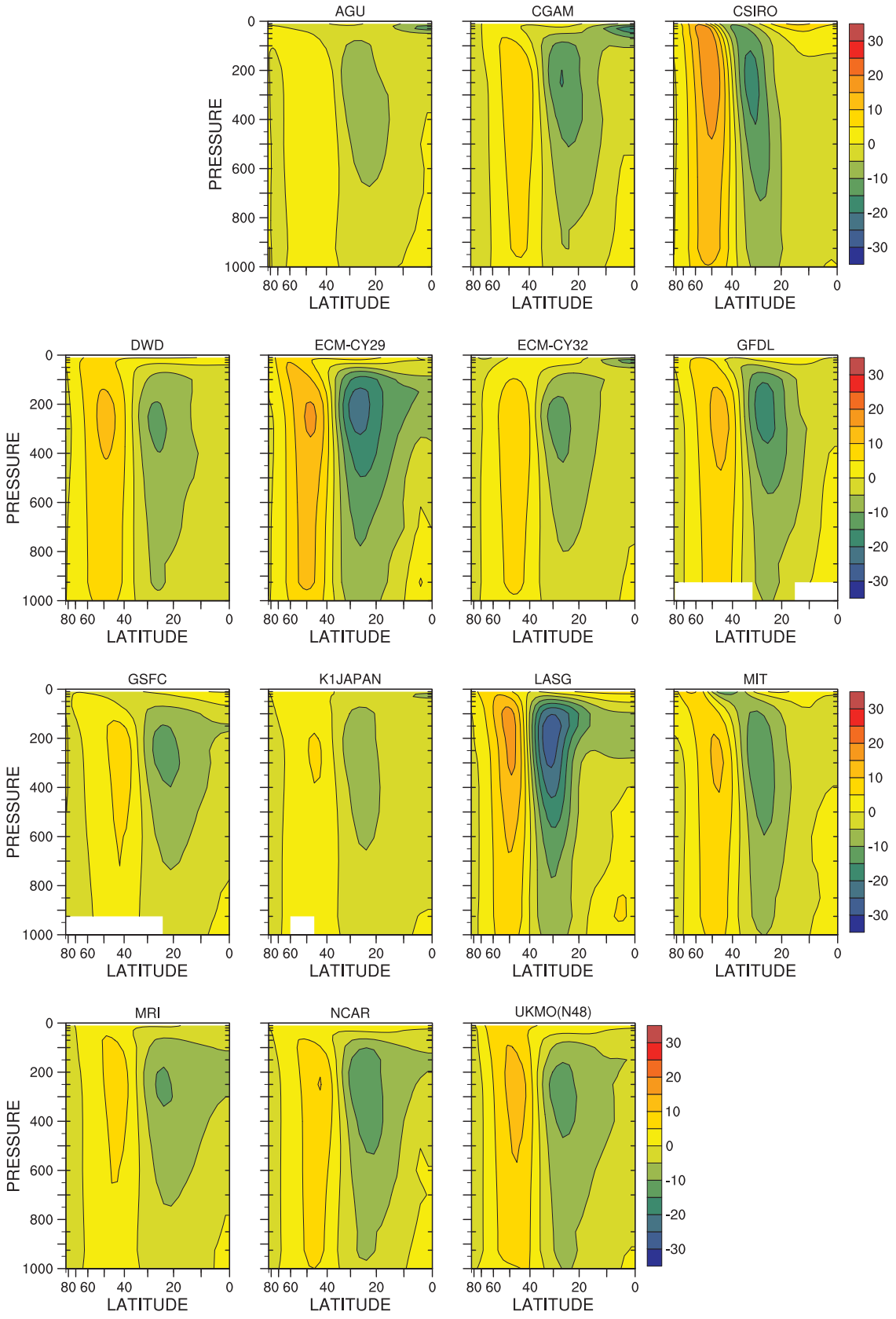

Figure 5.62: Zonal-time average zonal wind (u), QOBS−CONTROL, individual models, m s^{-1}.

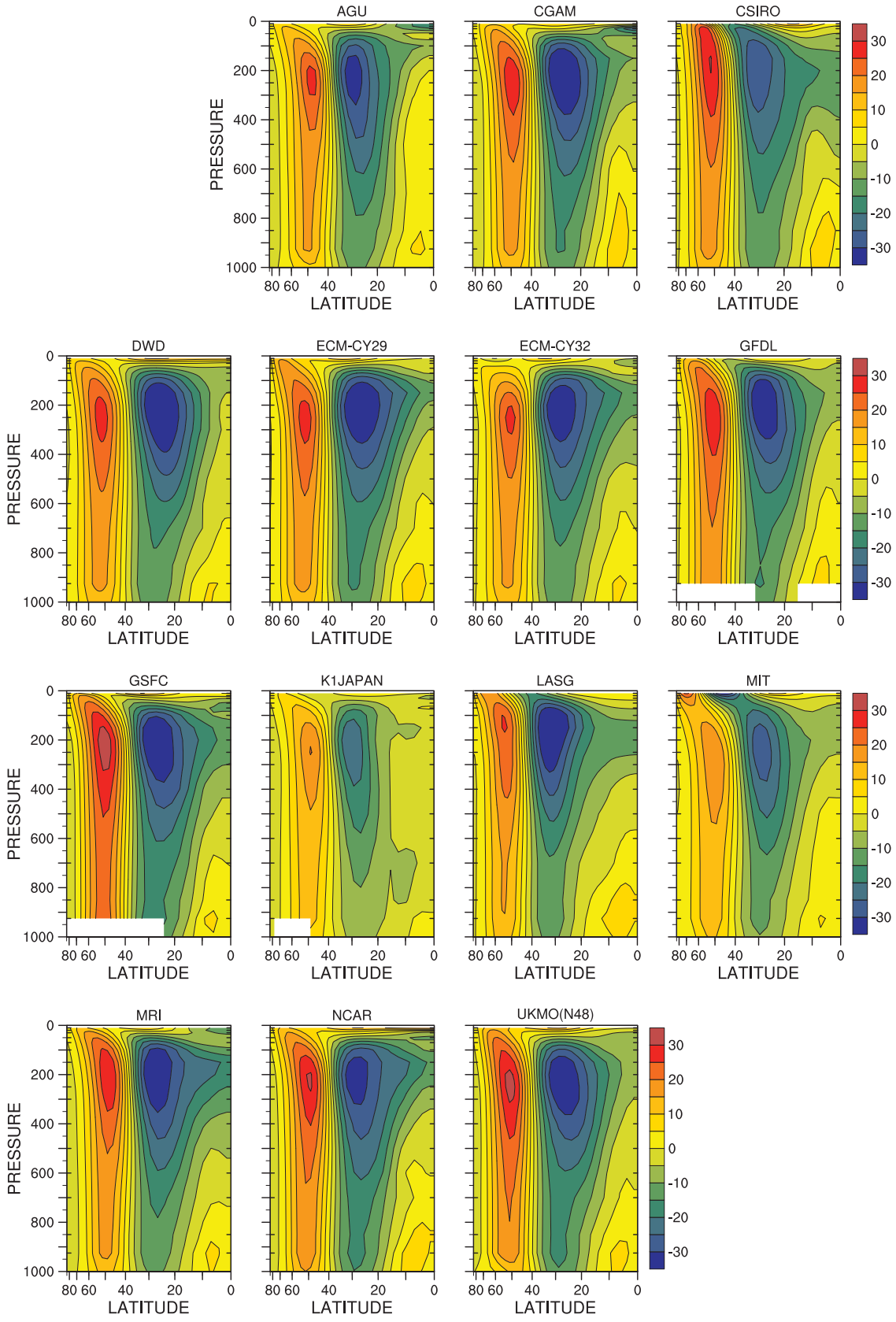

Figure 5.63: Zonal-time average zonal wind (u), FLAT−CONTROL, individual models, m s^{-1}.

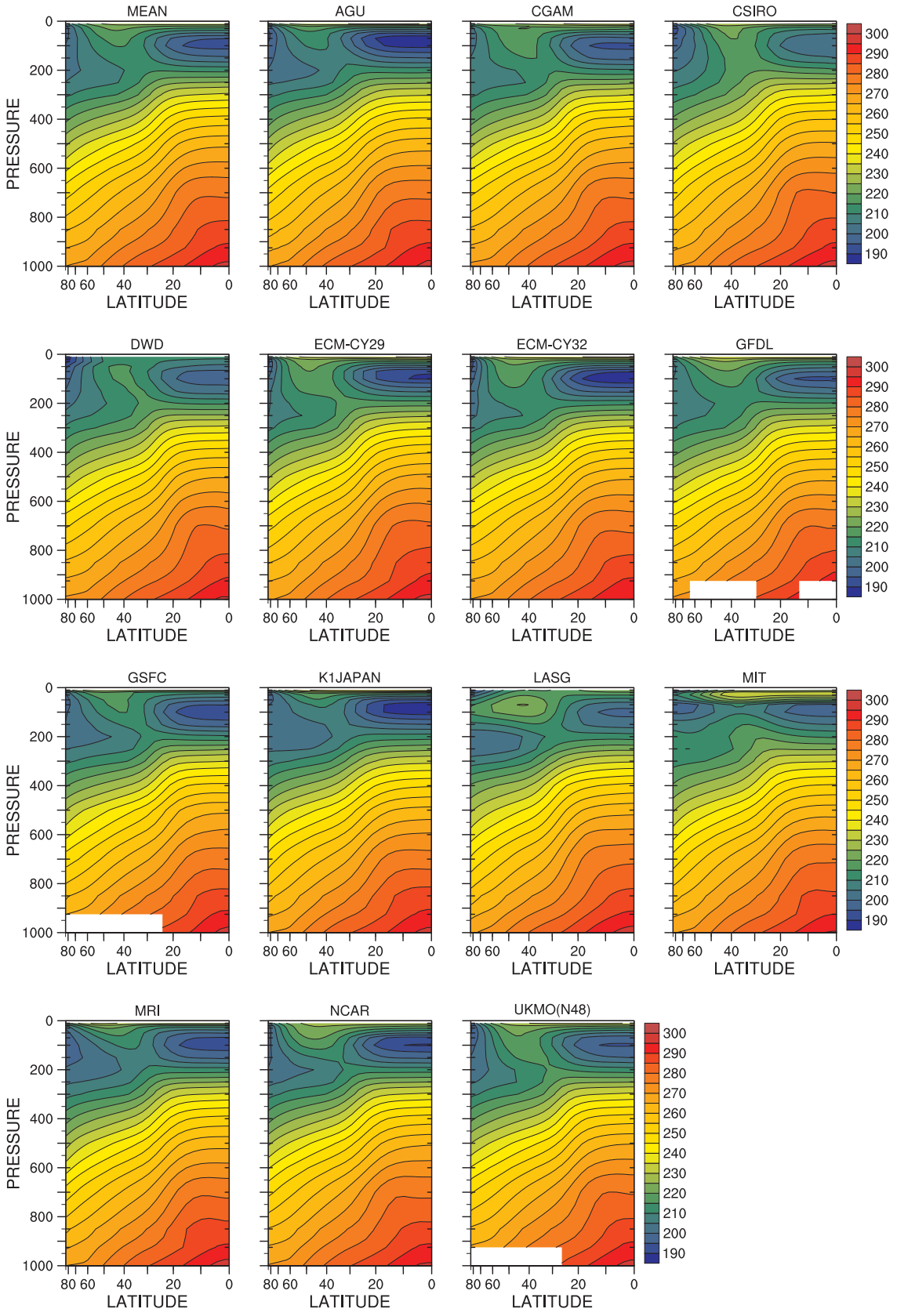

Figure 5.64: Zonal-time average temperature (t), PEAKED, individual models, K.

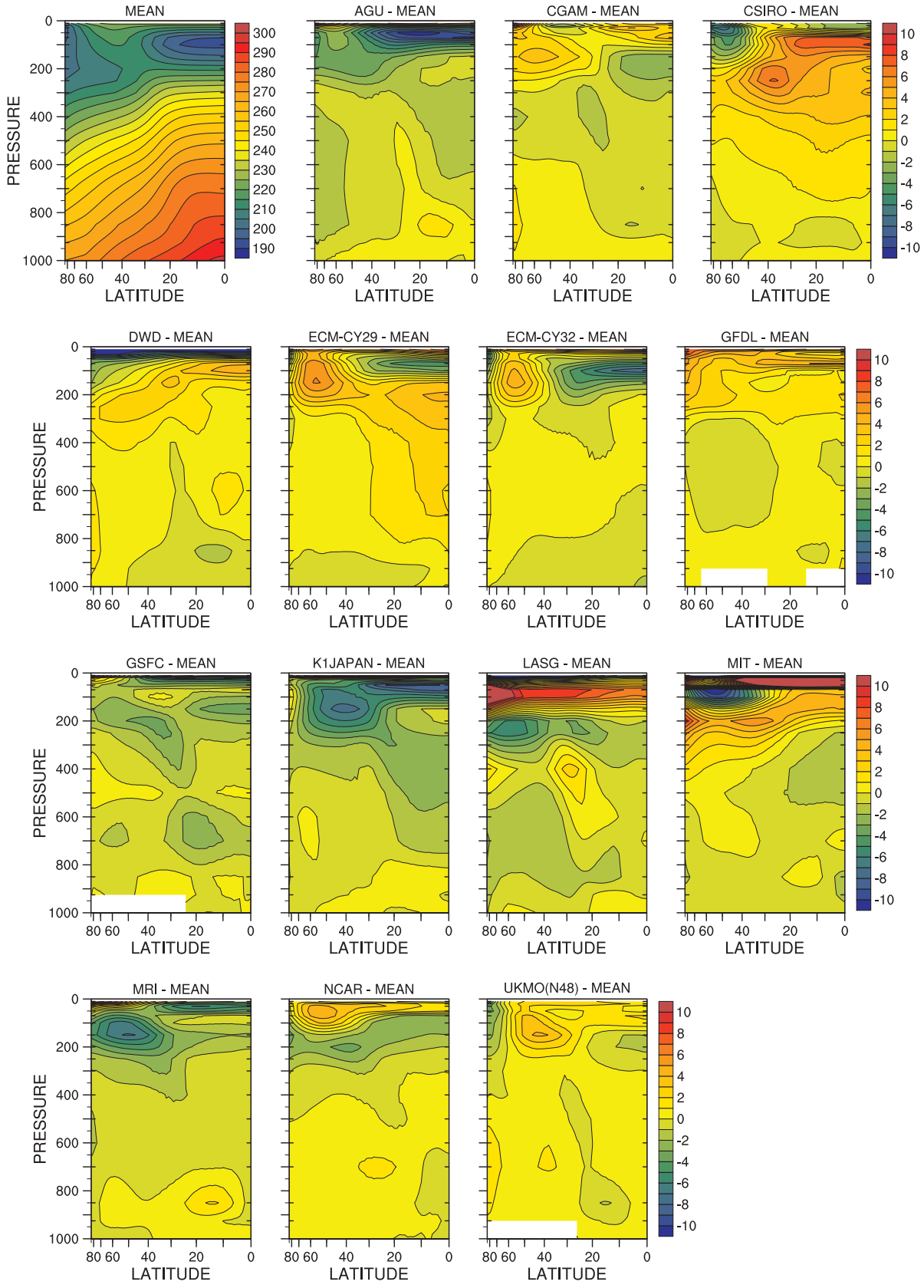

Figure 5.65: Zonal-time average temperature (t), PEAKED, individual models minus multi-model mean, K.

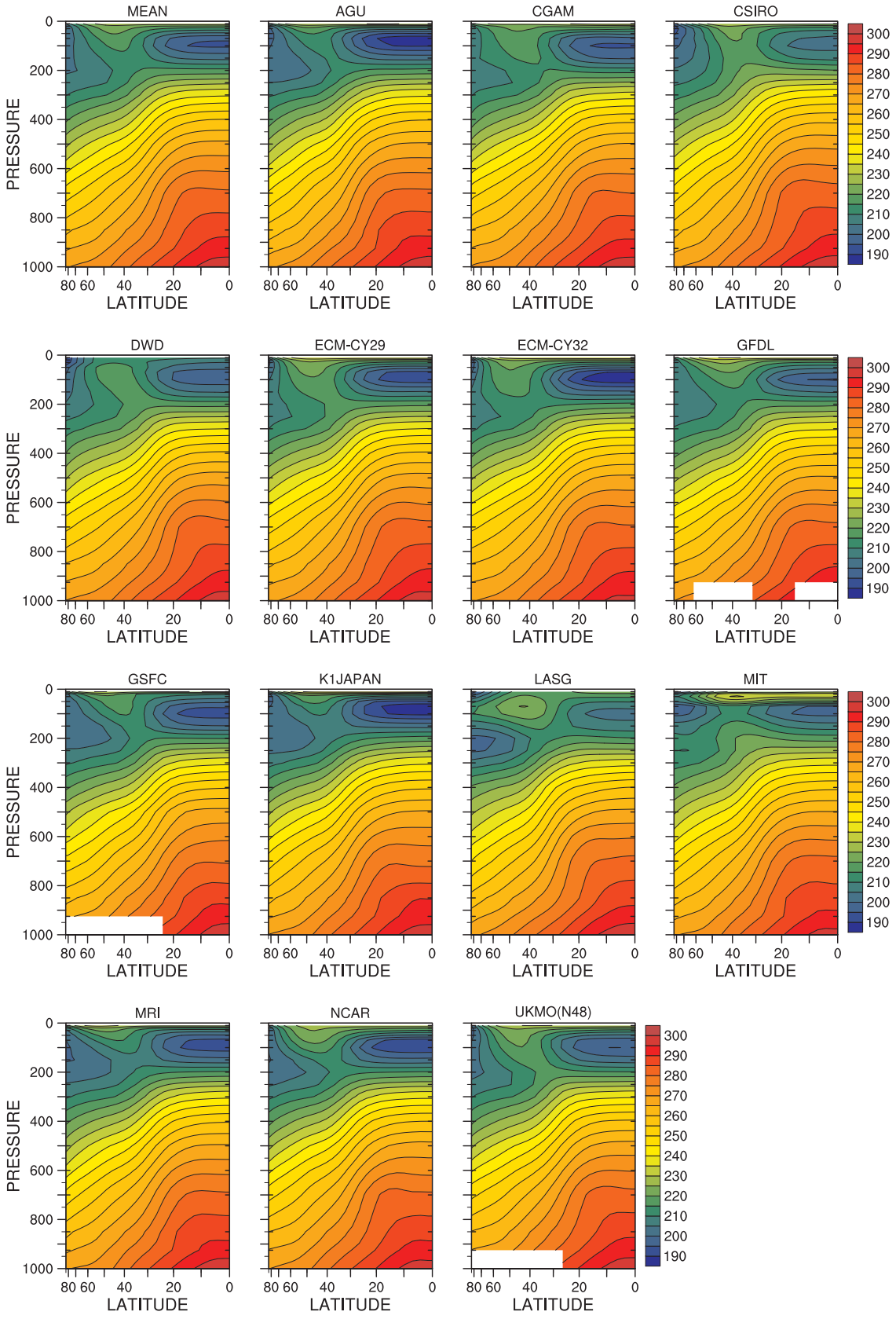

Figure 5.66: Zonal-time average temperature (t), CONTROL, individual models, K.

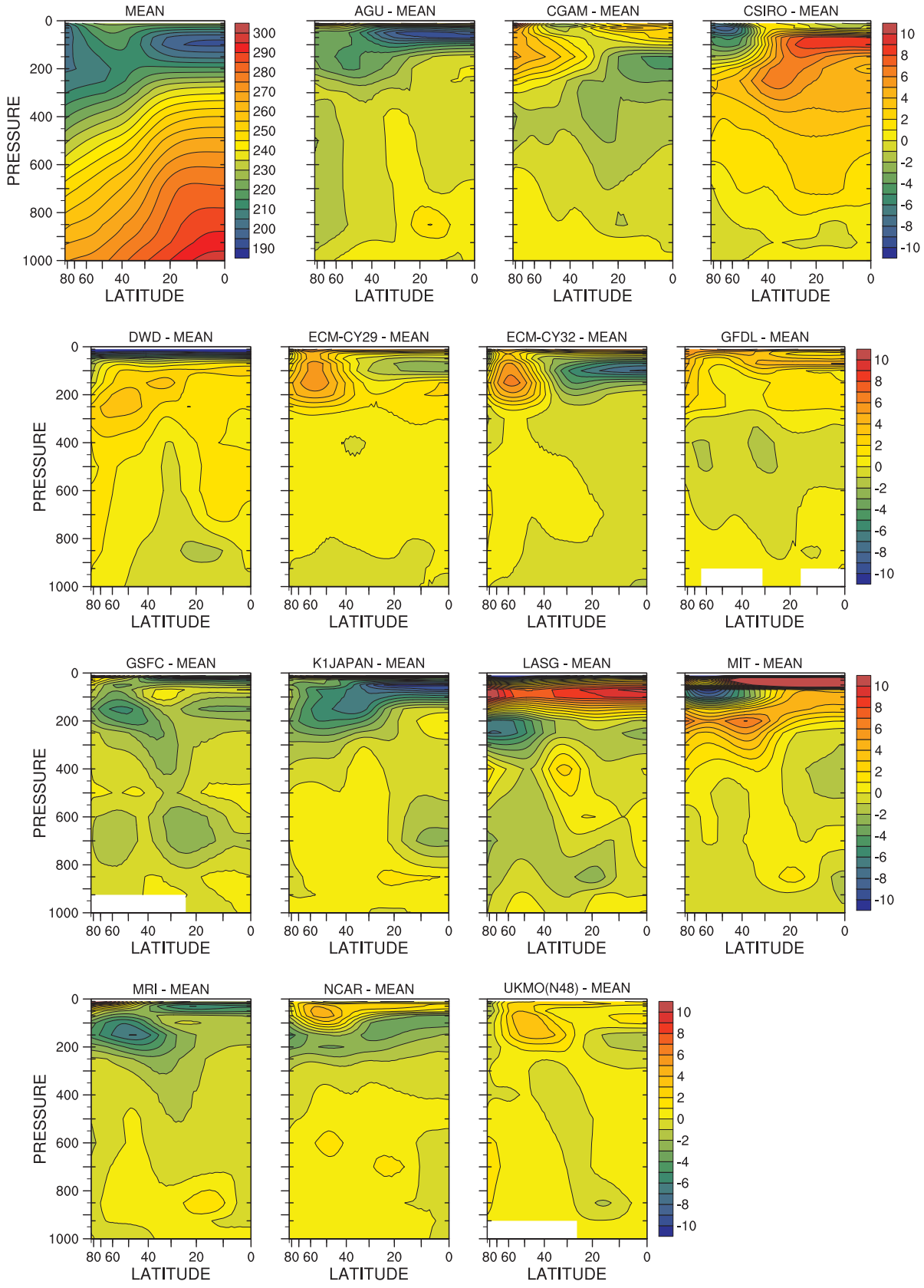

Figure 5.67: Zonal-time average temperature (t), CONTROL, individual models minus multi-model mean, K.

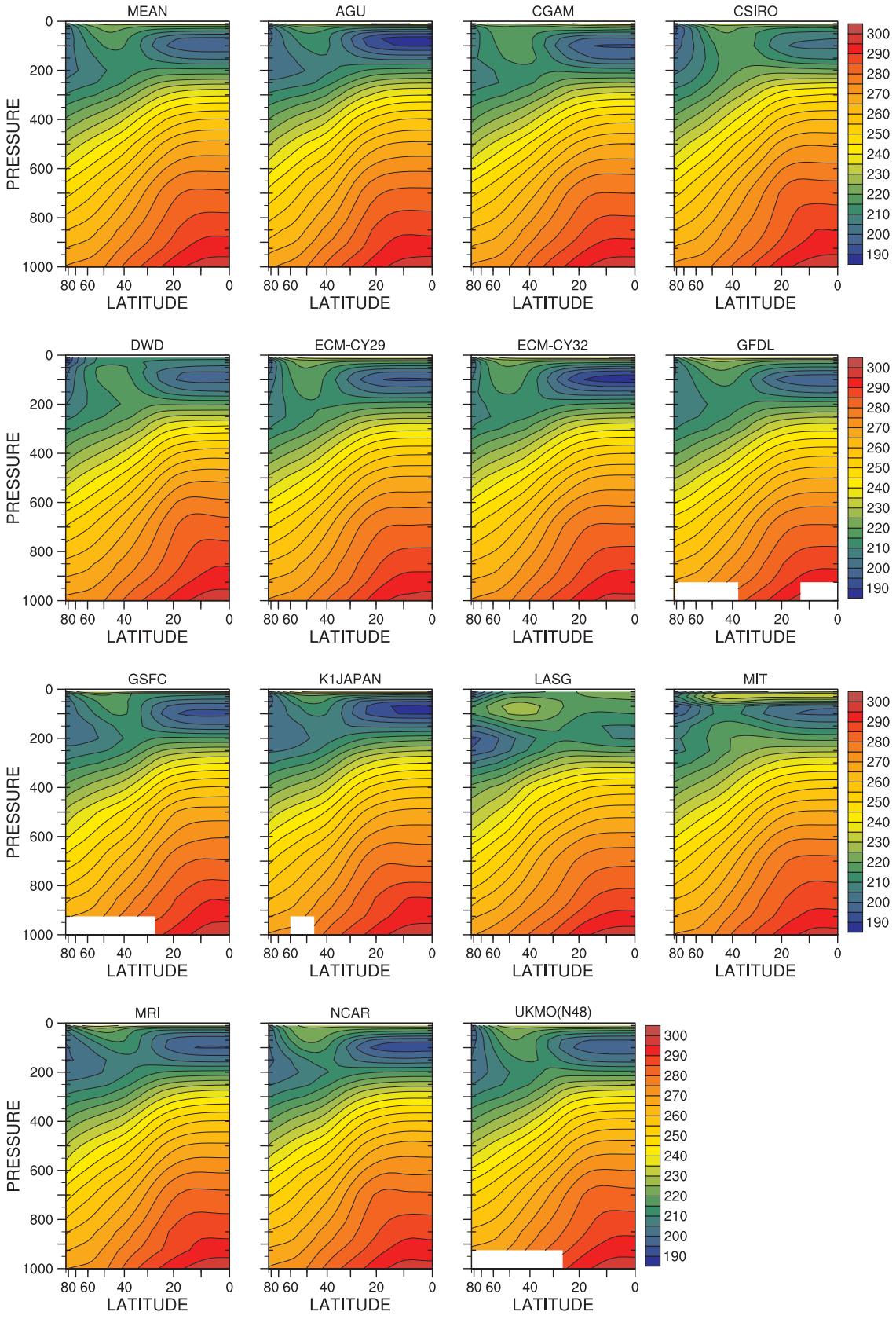

Figure 5.68: Zonal-time average temperature (t), QOBS, individual models, K.

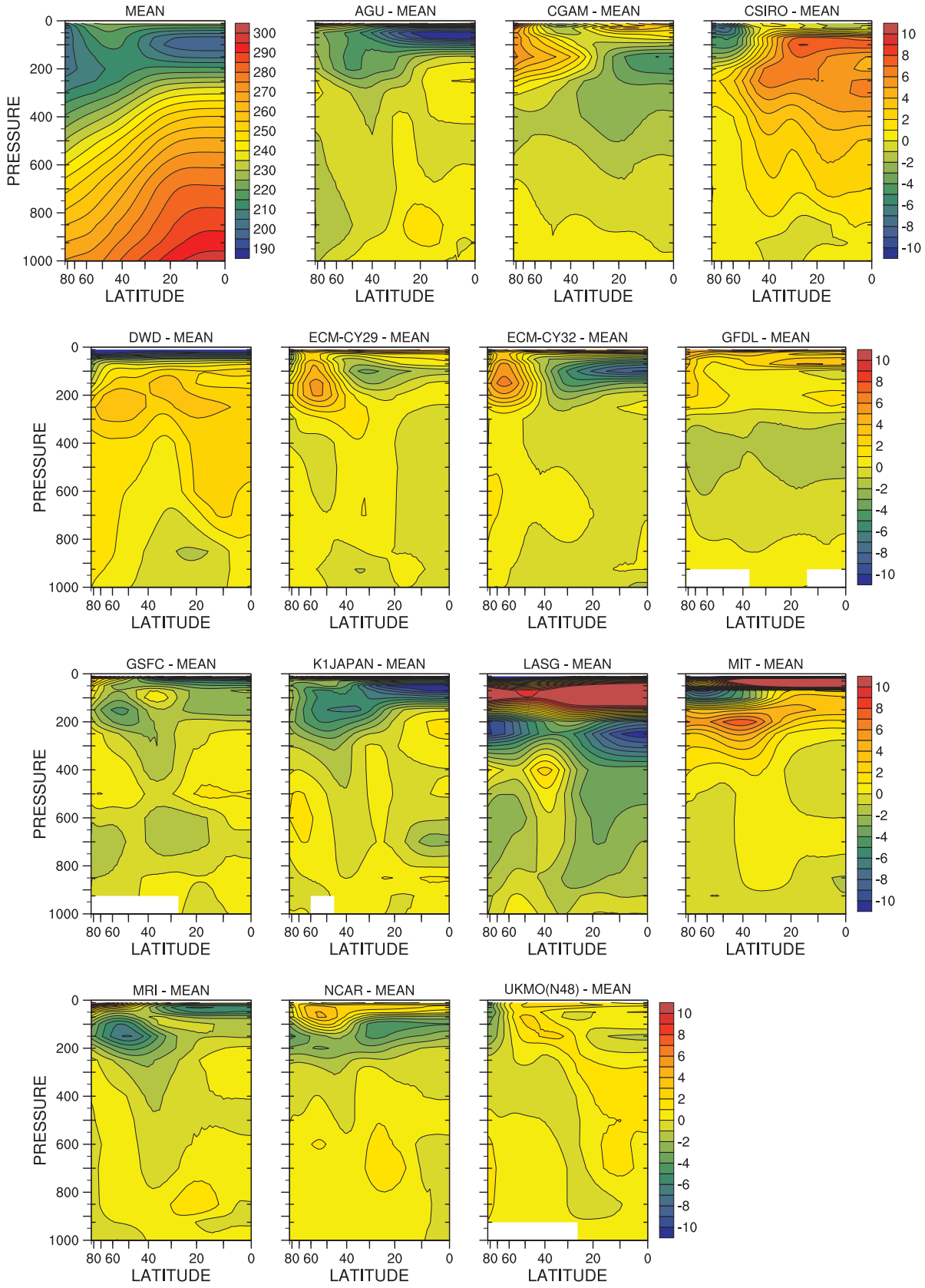

Figure 5.69: Zonal-time average temperature (t), QOBS, individual models minus multi-model mean, K.

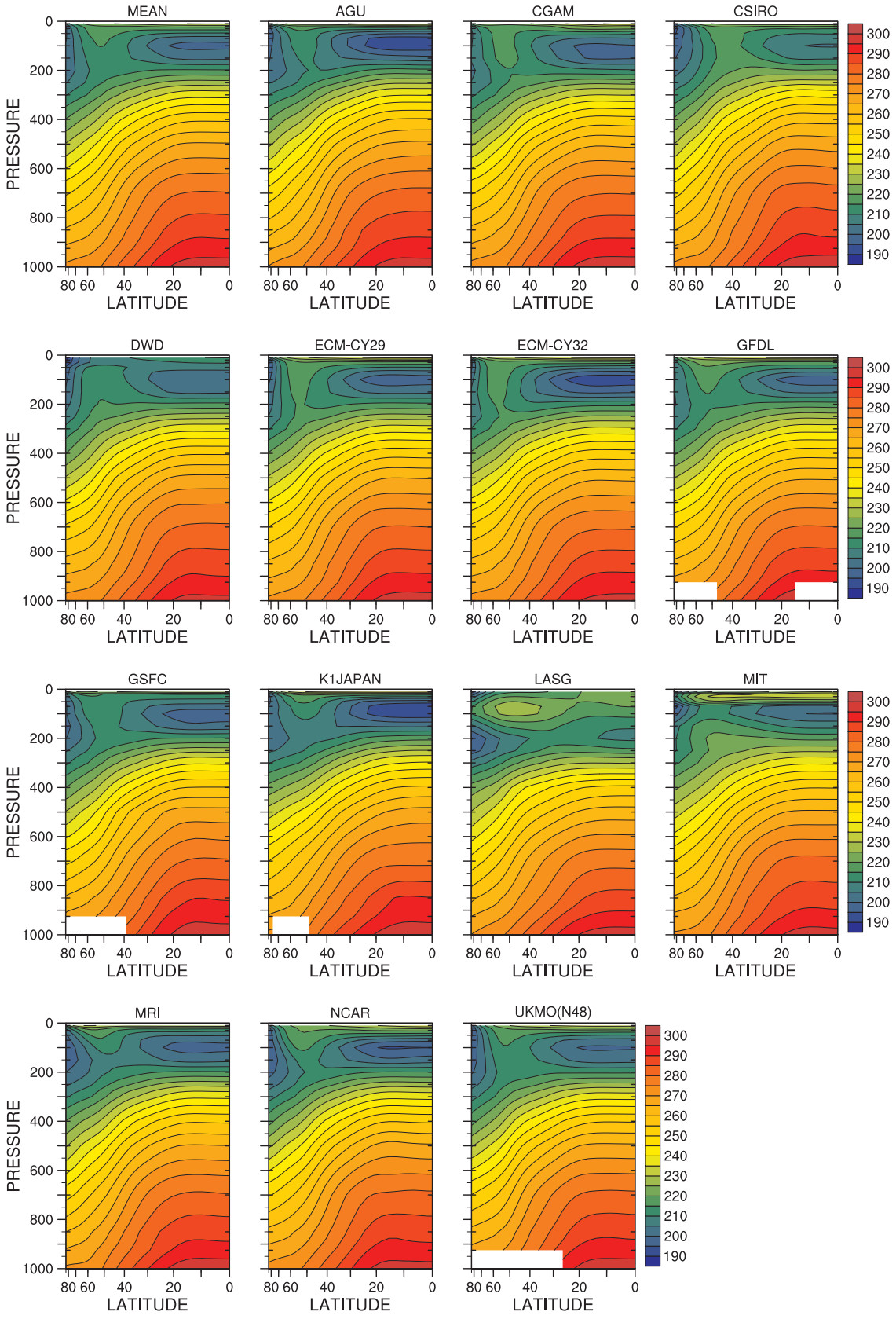

Figure 5.70: Zonal-time average temperature (t), FLAT, individual models, K.

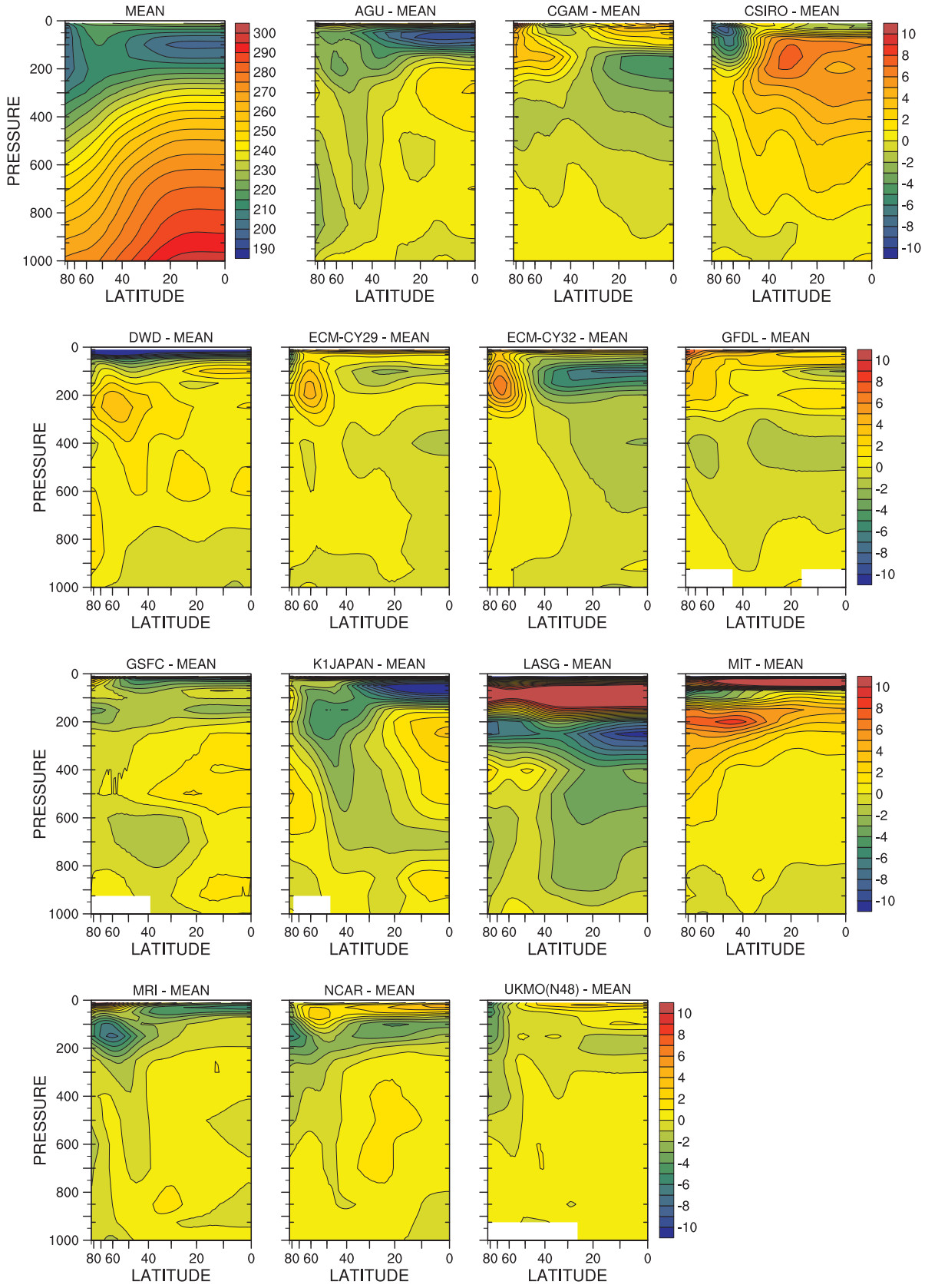

Figure 5.71: Zonal-time average temperature (t), FLAT, individual models minus multi-model mean, K.

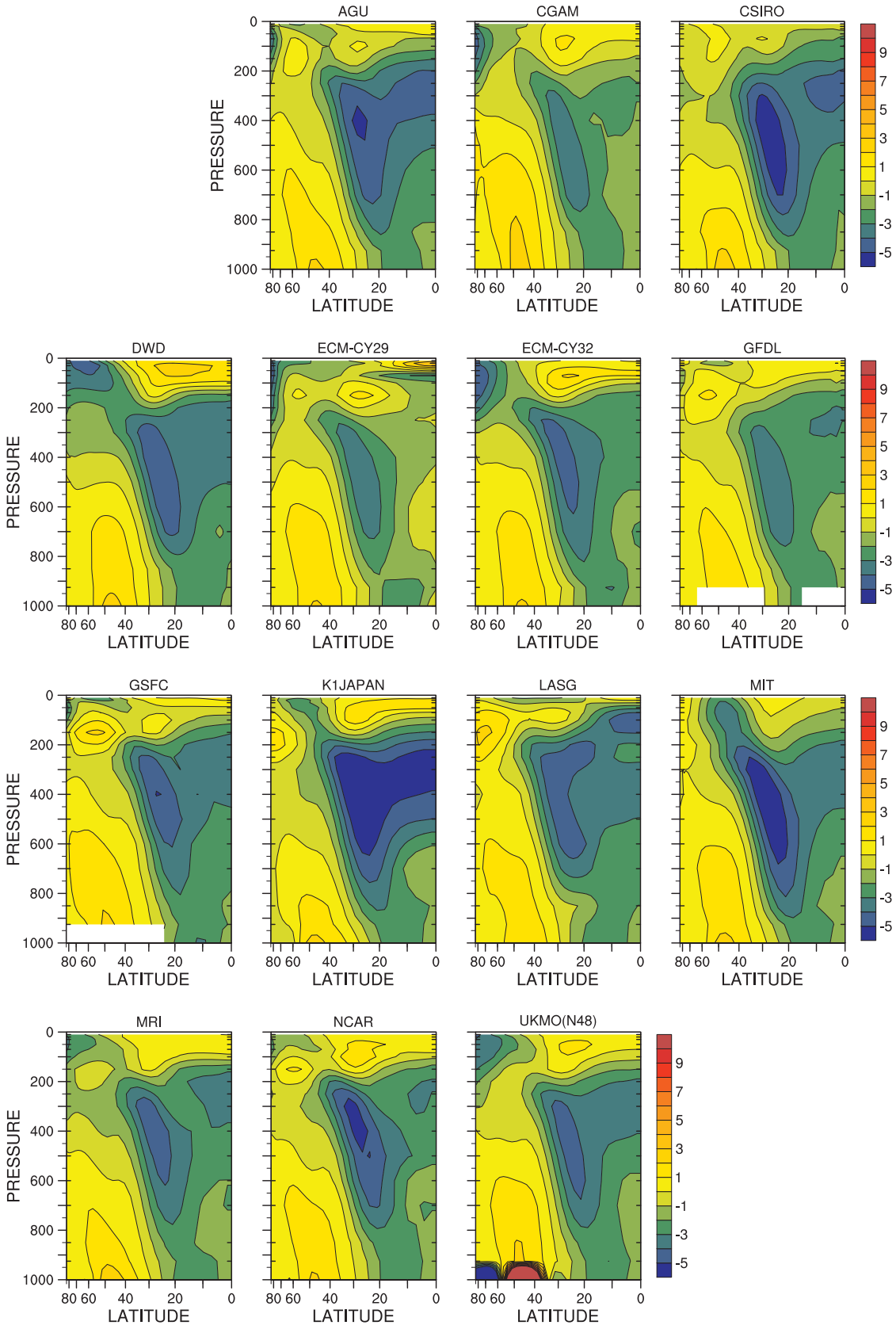

Figure 5.72: Zonal-time average temperature (t), PEAKED−CONTROL, individual models, K.

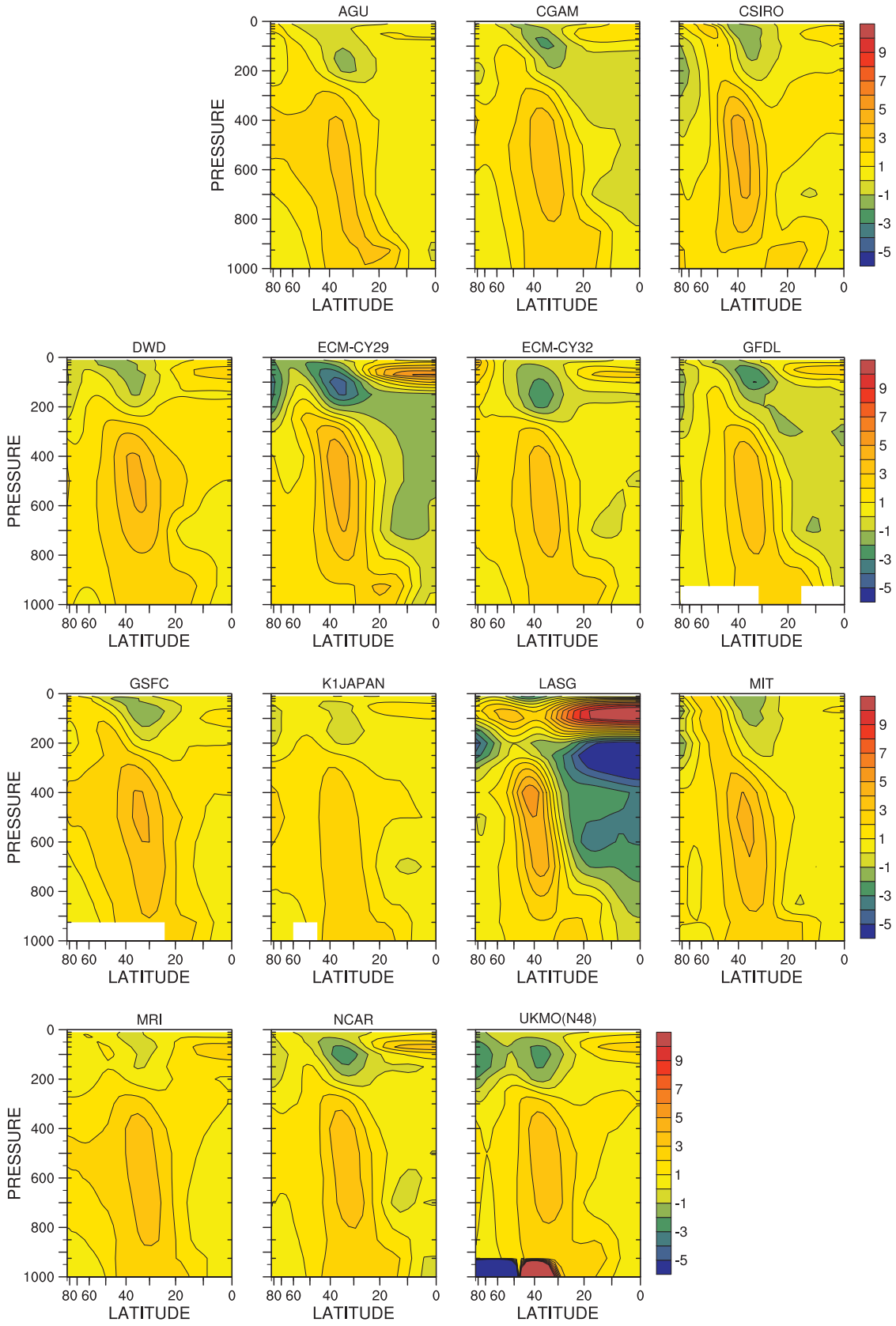

Figure 5.73: Zonal-time average temperature (t), QOBS−CONTROL, individual models, K.

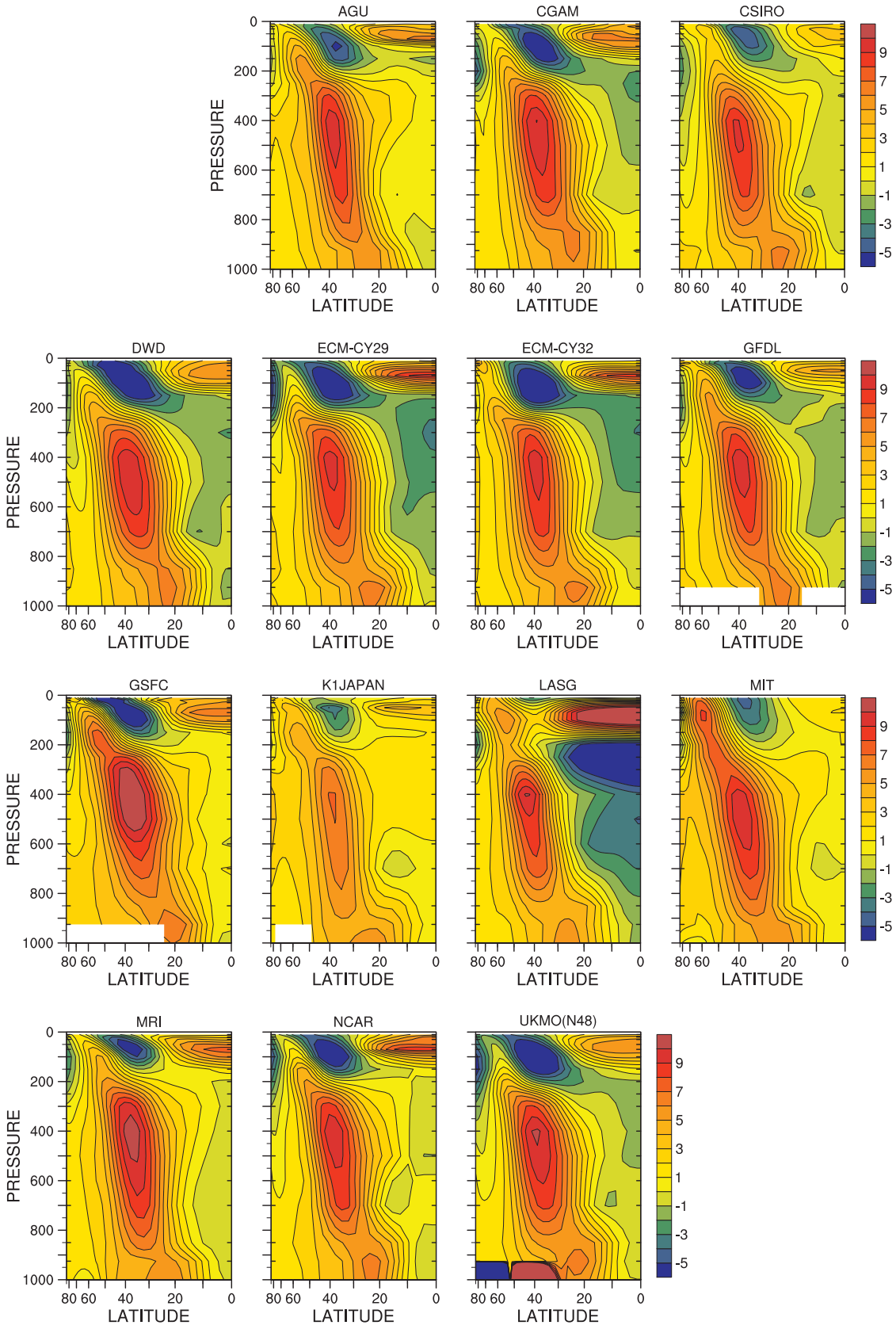

Figure 5.74: Zonal-time average temperature (t), FLAT−CONTROL, individual models, K.

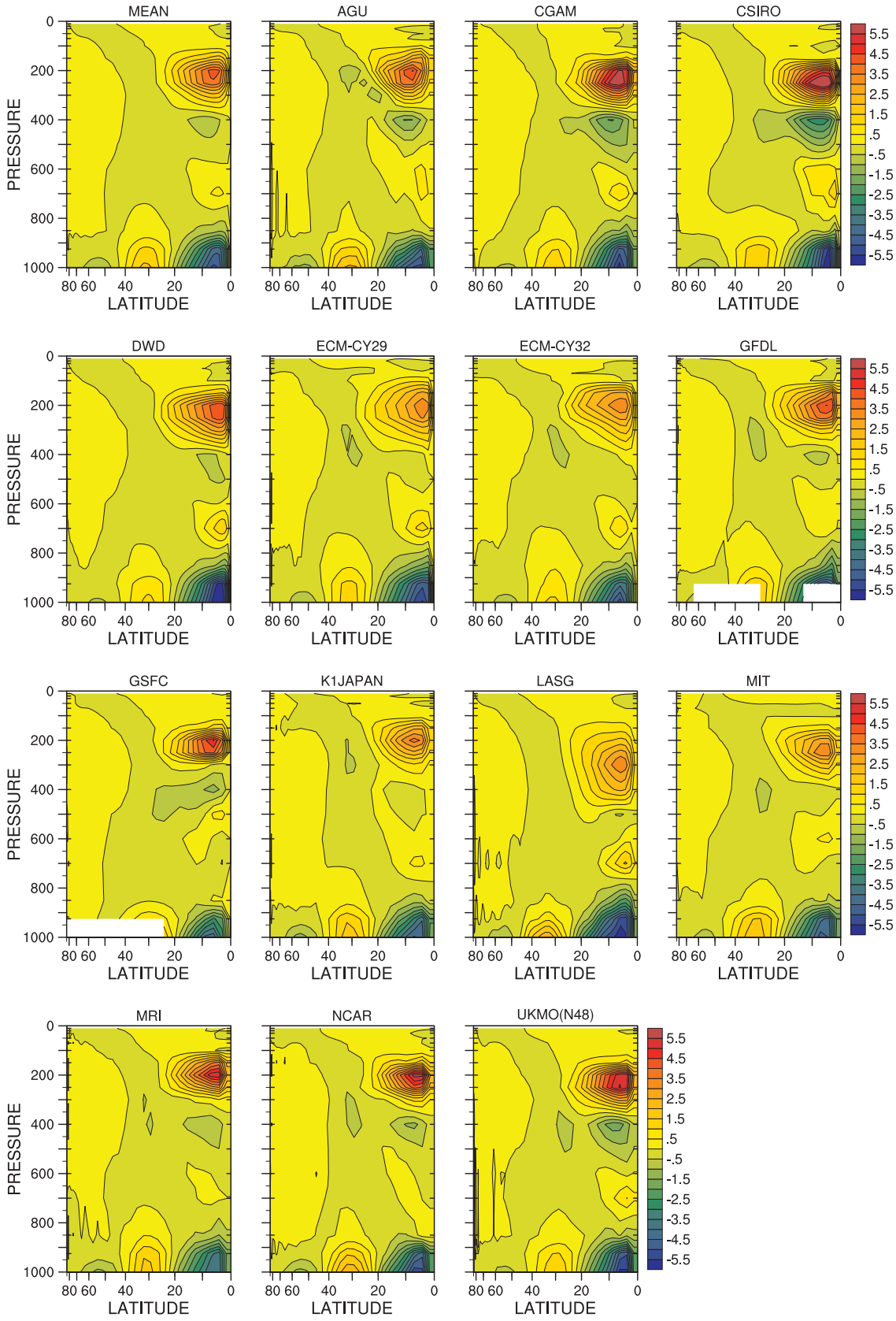

Figure 5.75: Zonal-time average meridional wind (v), PEAKED, individual models, m s^{-1}.

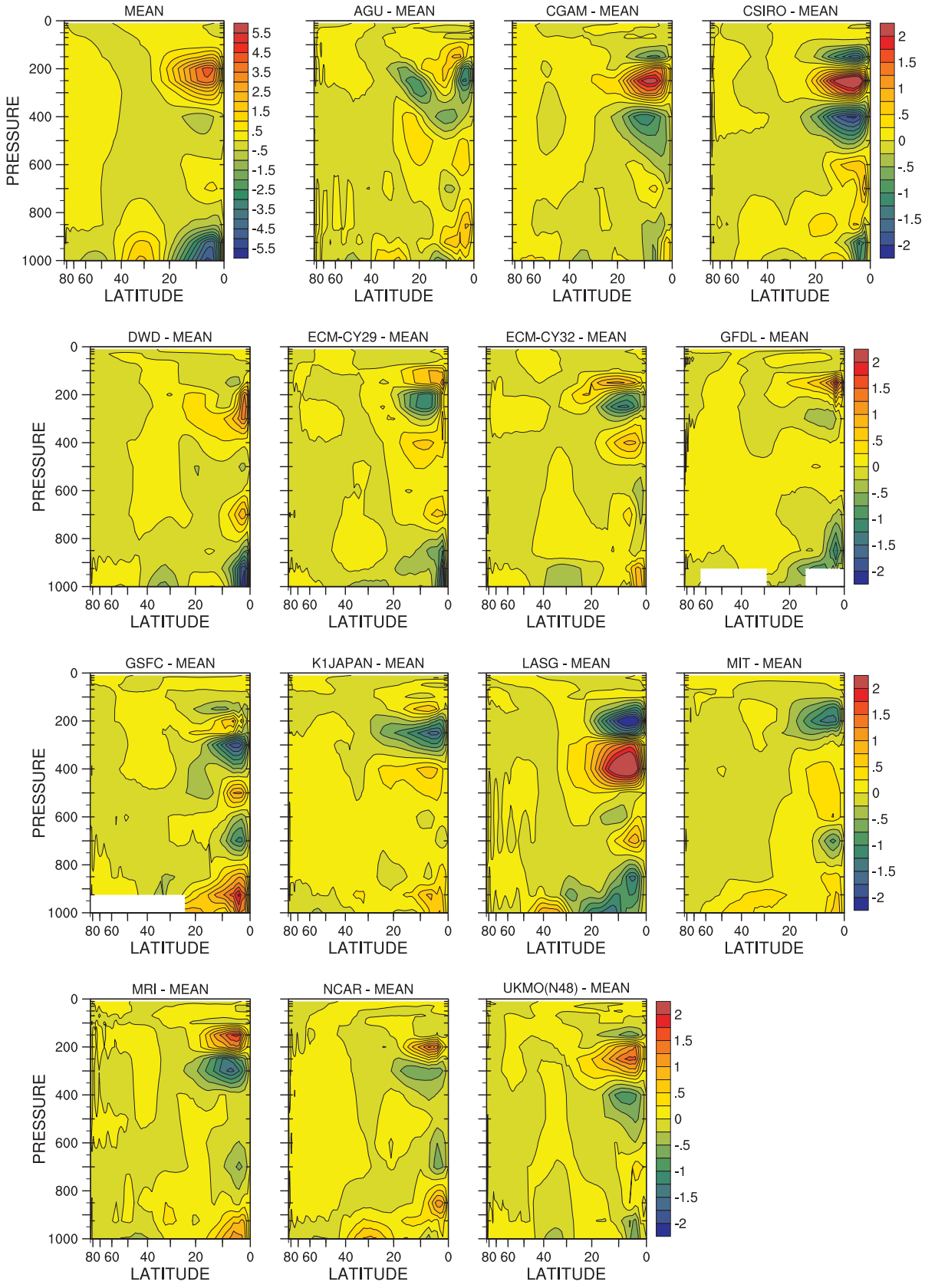

Figure 5.76: Zonal-time average meridional wind (v), PEAKED, individual models minus multi-model mean, m s^{-1}.

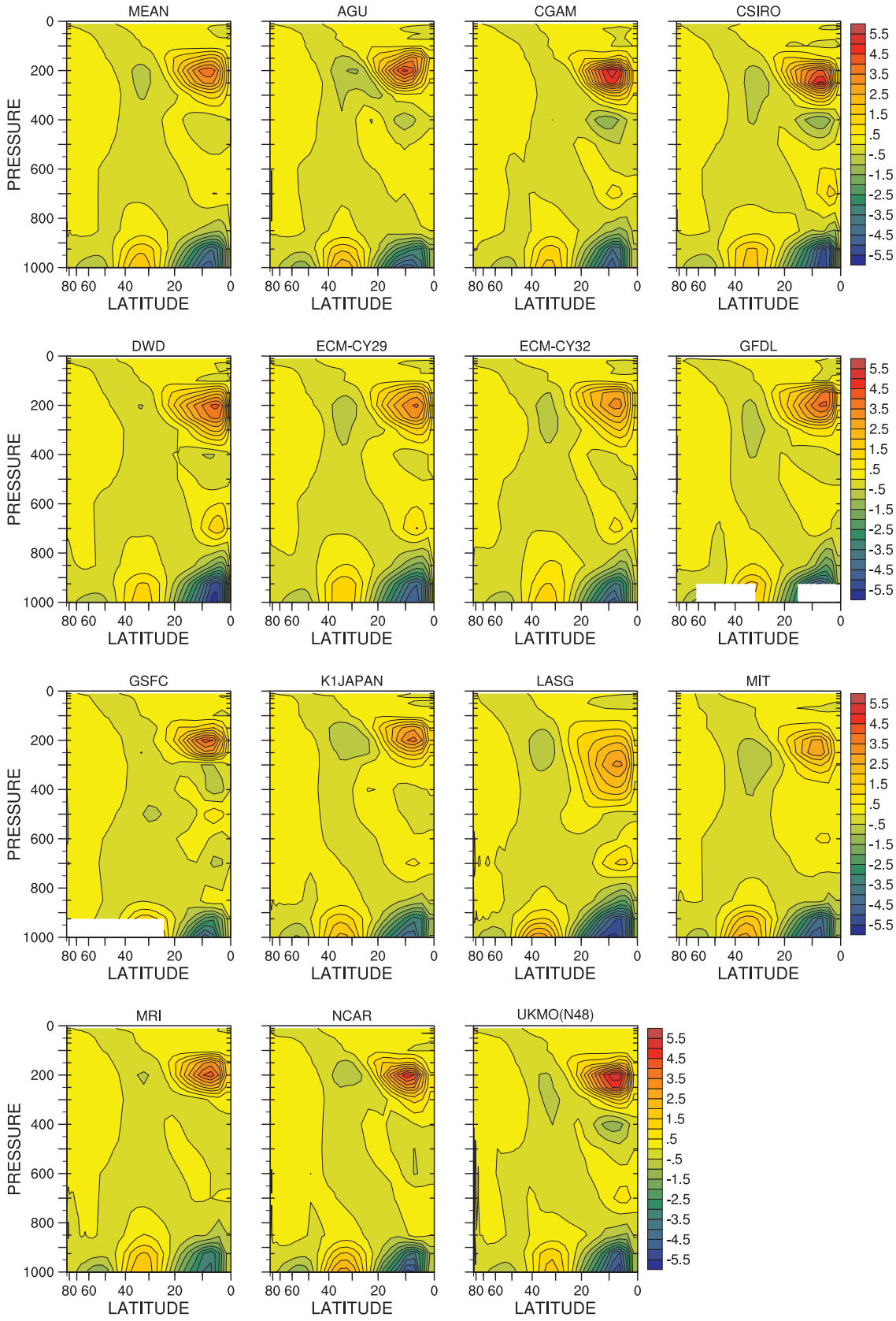

Figure 5.77: Zonal-time average meridional wind (v), CONTROL, individual models, m s^{-1}.

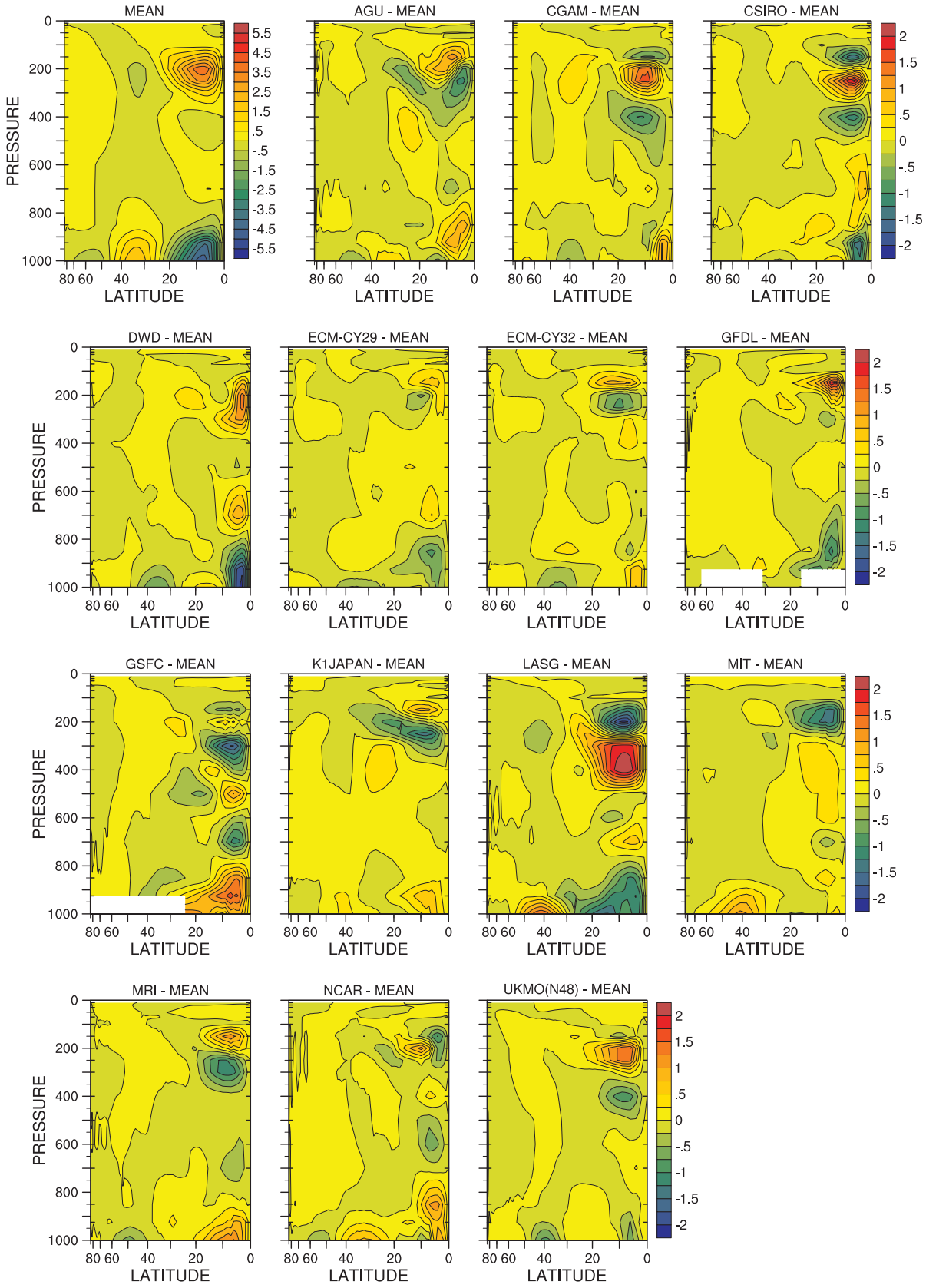

Figure 5.78: Zonal-time average meridional wind (v), CONTROL, individual models minus multi-model mean, m s^{-1}.

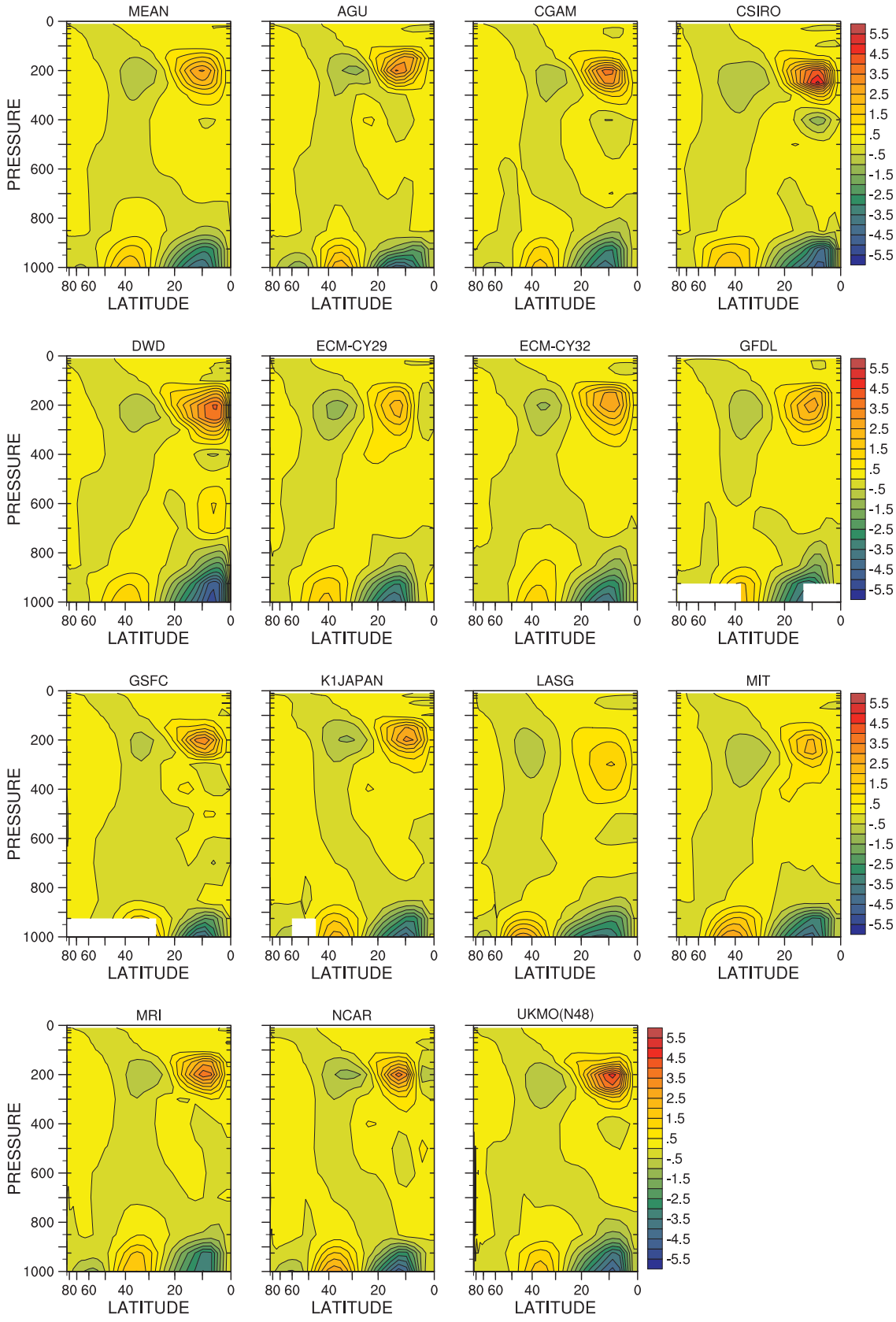

Figure 5.79: Zonal-time average meridional wind (v), QOBS, individual models, m s^{-1}.

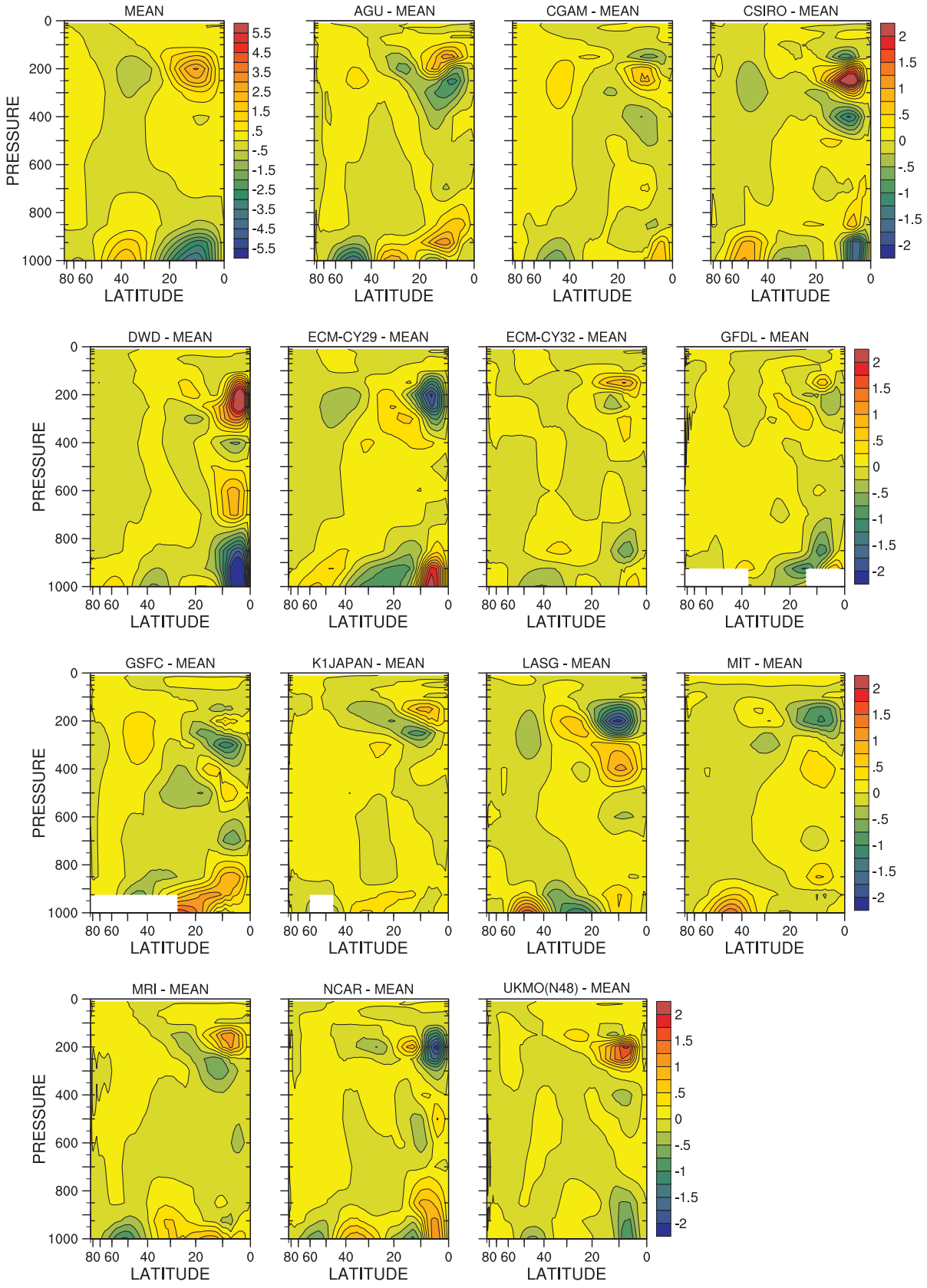

Figure 5.80: Zonal-time average meridional wind (v), QOBS, individual models minus multi-model mean, m s^{-1}.

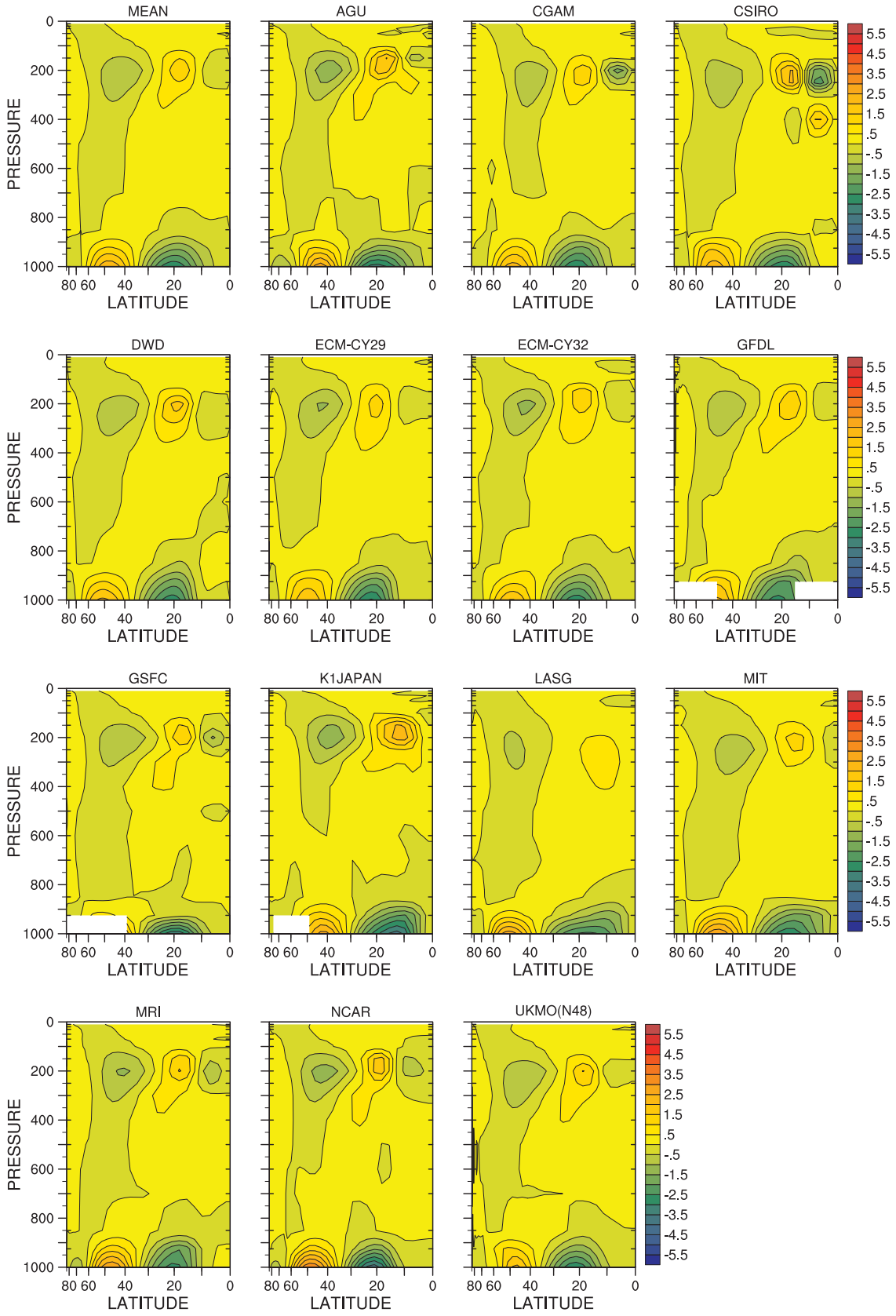

Figure 5.81: Zonal-time average meridional wind (v), FLAT, individual models, m s^{-1}.

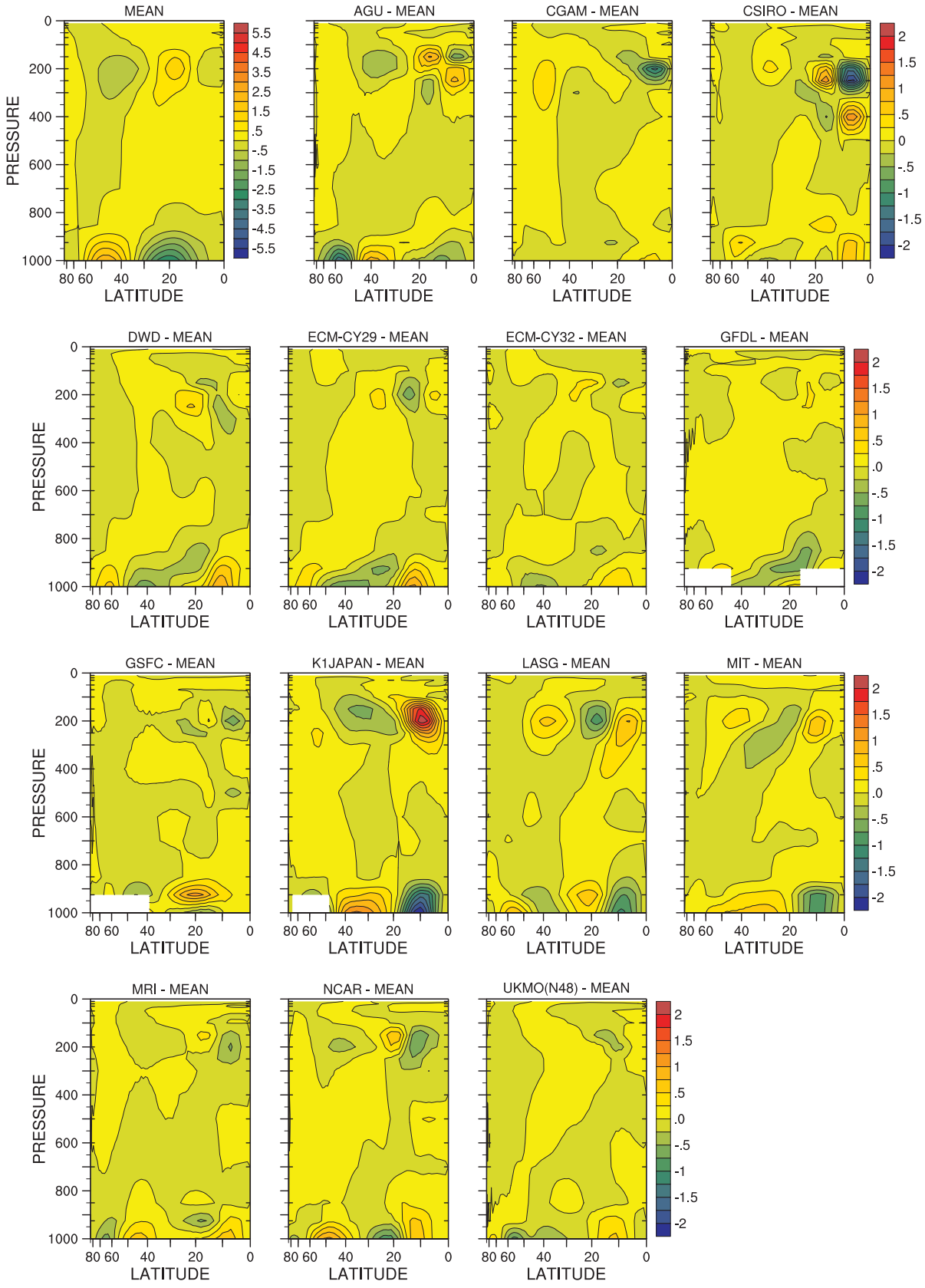

Figure 5.82: Zonal-time average meridional wind (v), FLAT, individual models minus multi-model mean, m s^{-1}.

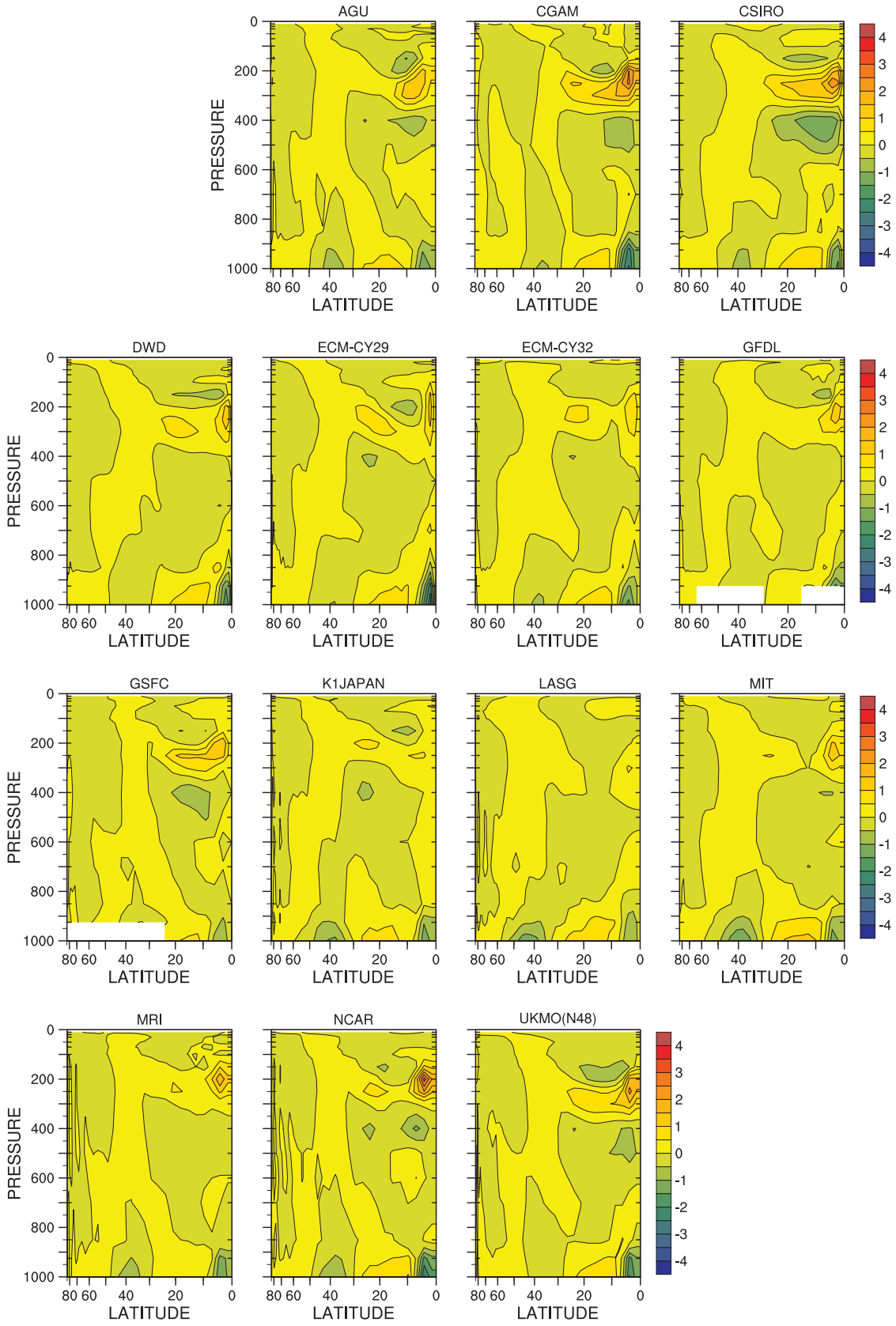

Figure 5.83: Zonal-time average meridional wind (v), PEAKED−CONTROL, individual models, m s^{-1}.

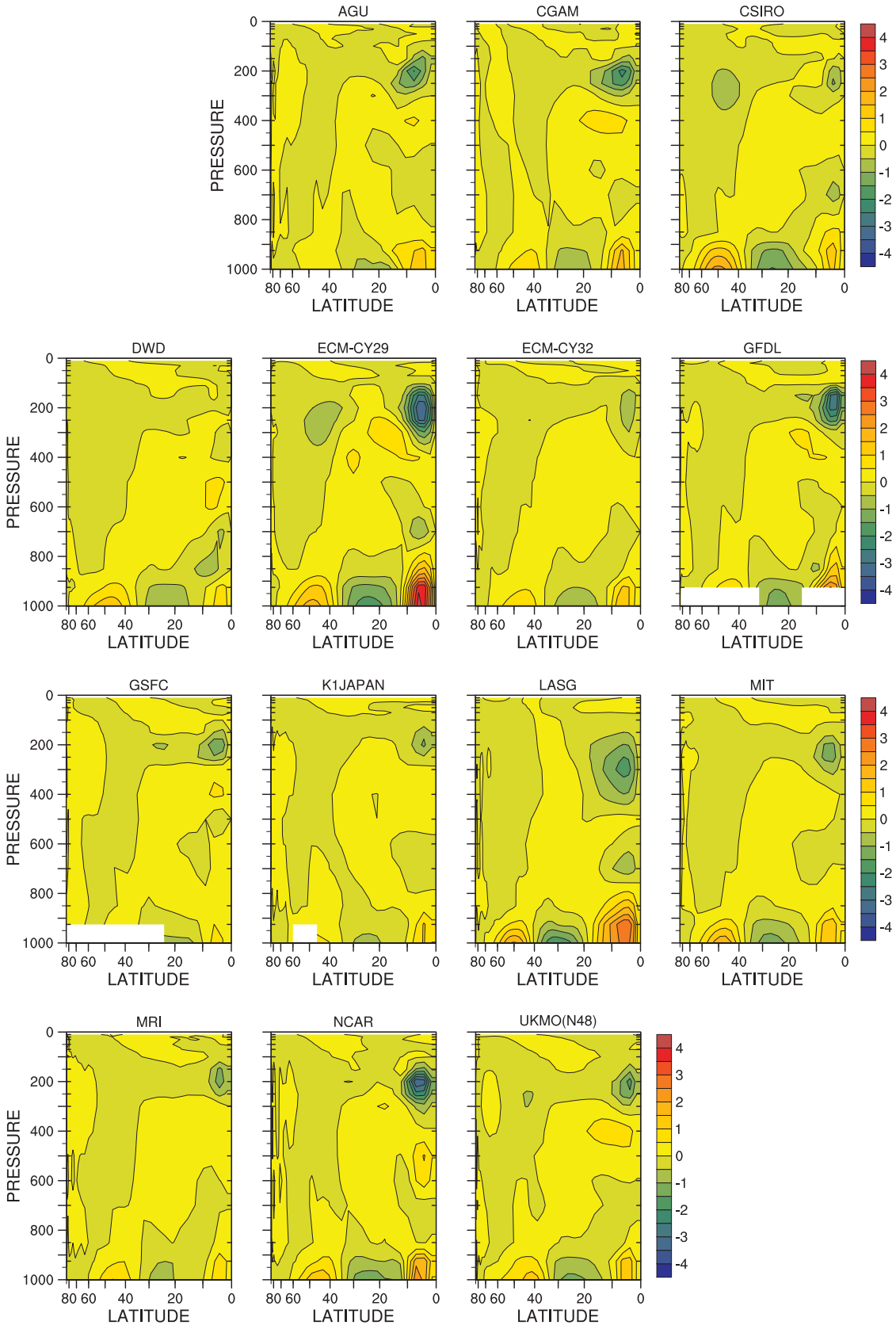

Figure 5.84: Zonal-time average meridional wind (v), QOBS−CONTROL, individual models, m s^{-1}.

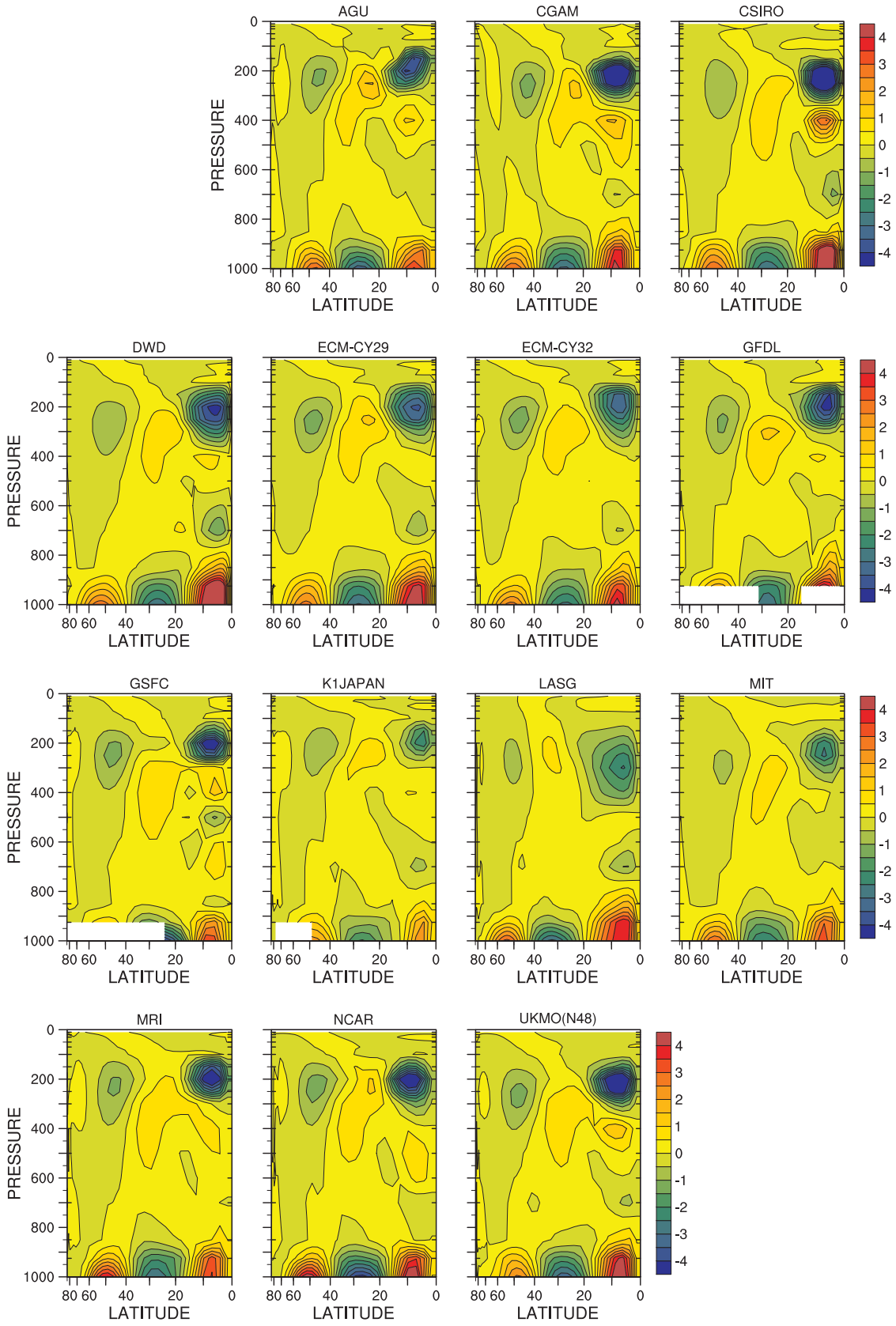

Figure 5.85: Zonal-time average meridional wind (v), FLAT−CONTROL, individual models, m s^{-1}.

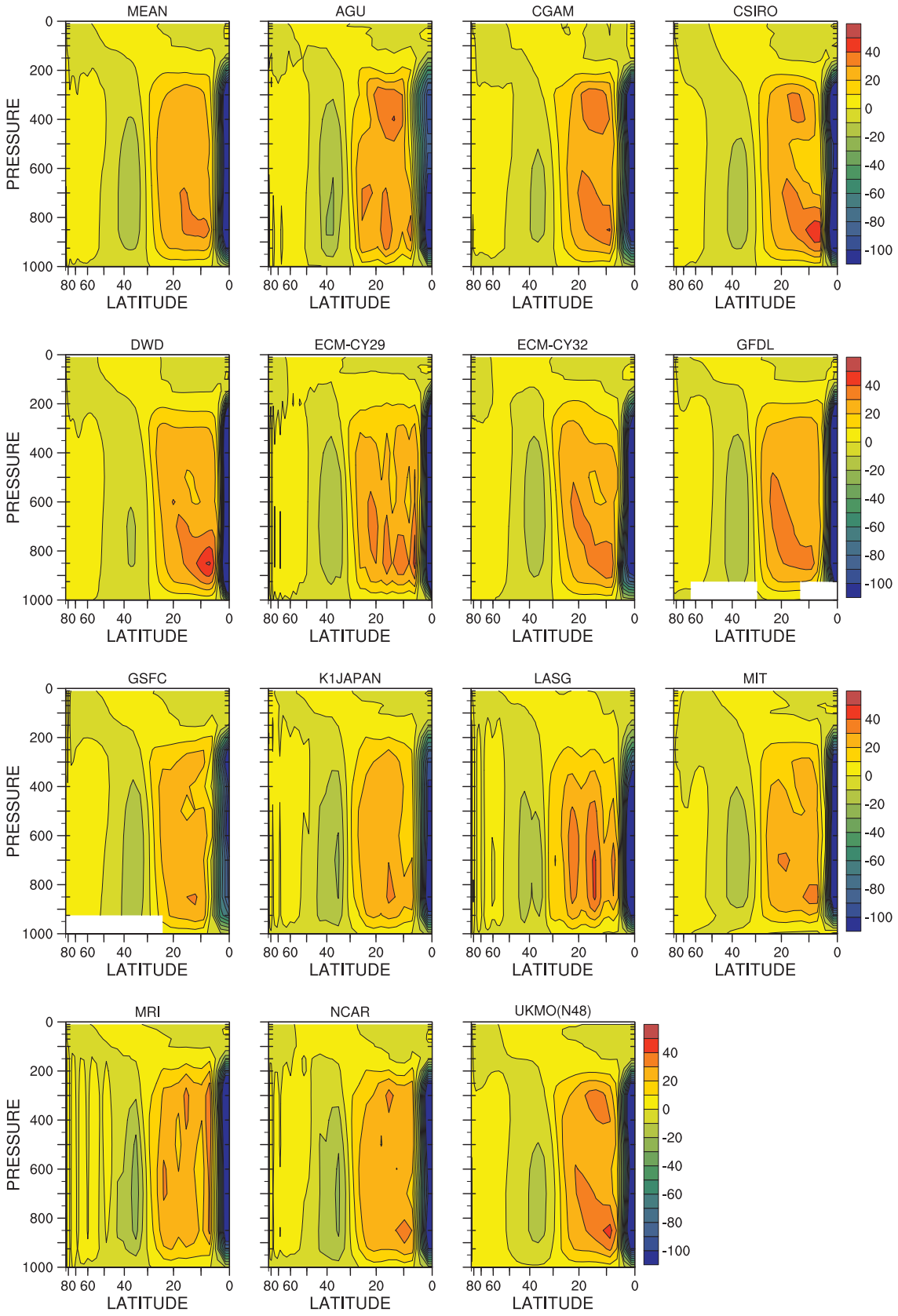

Figure 5.86: Zonal-time average vertical velocity (om), PEAKED, individual models, mb day^{-1}.

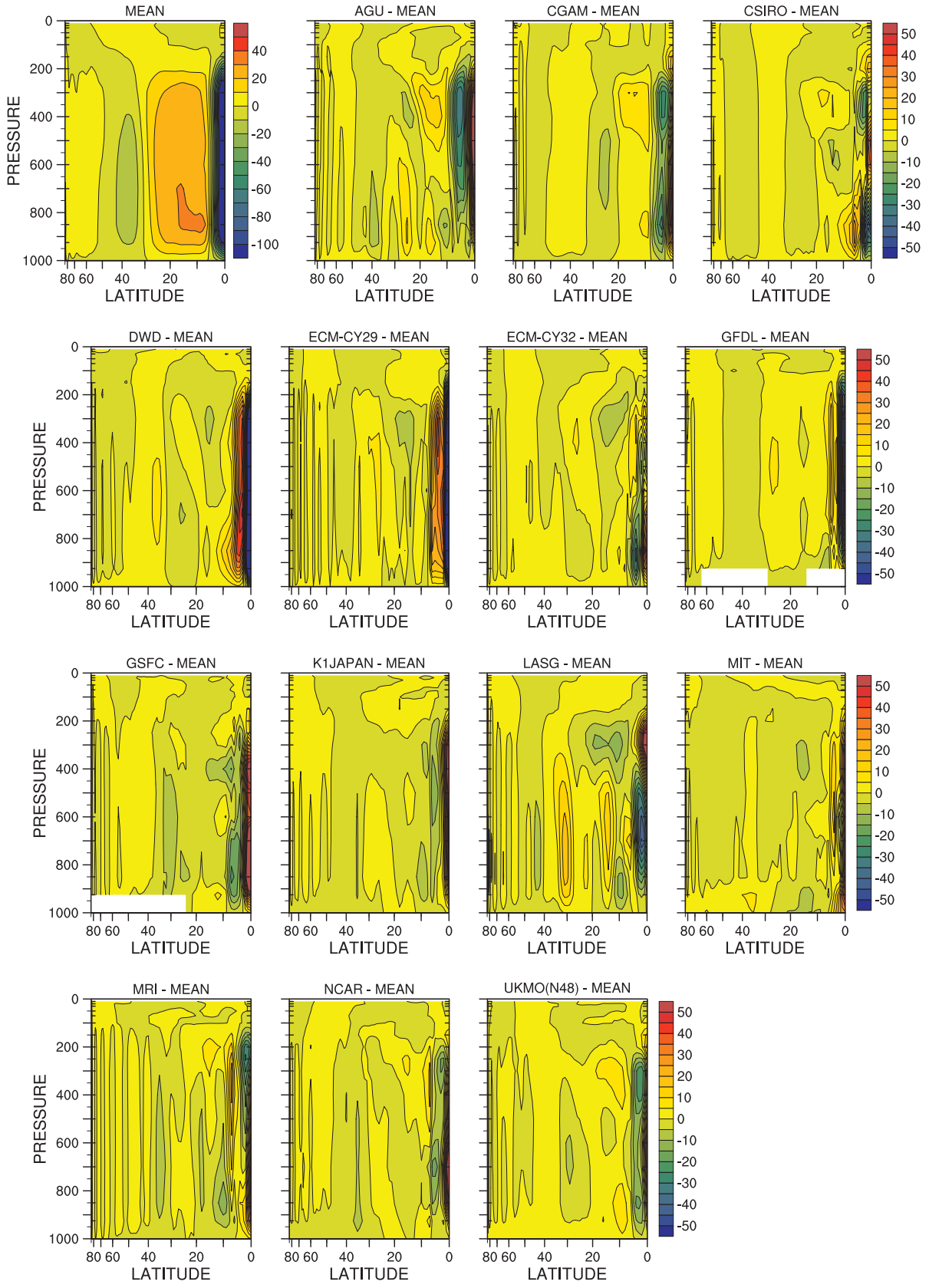

Figure 5.87: Zonal-time average vertical velocity (om), PEAKED, individual models minus multi-model mean, mb day^{-1}.

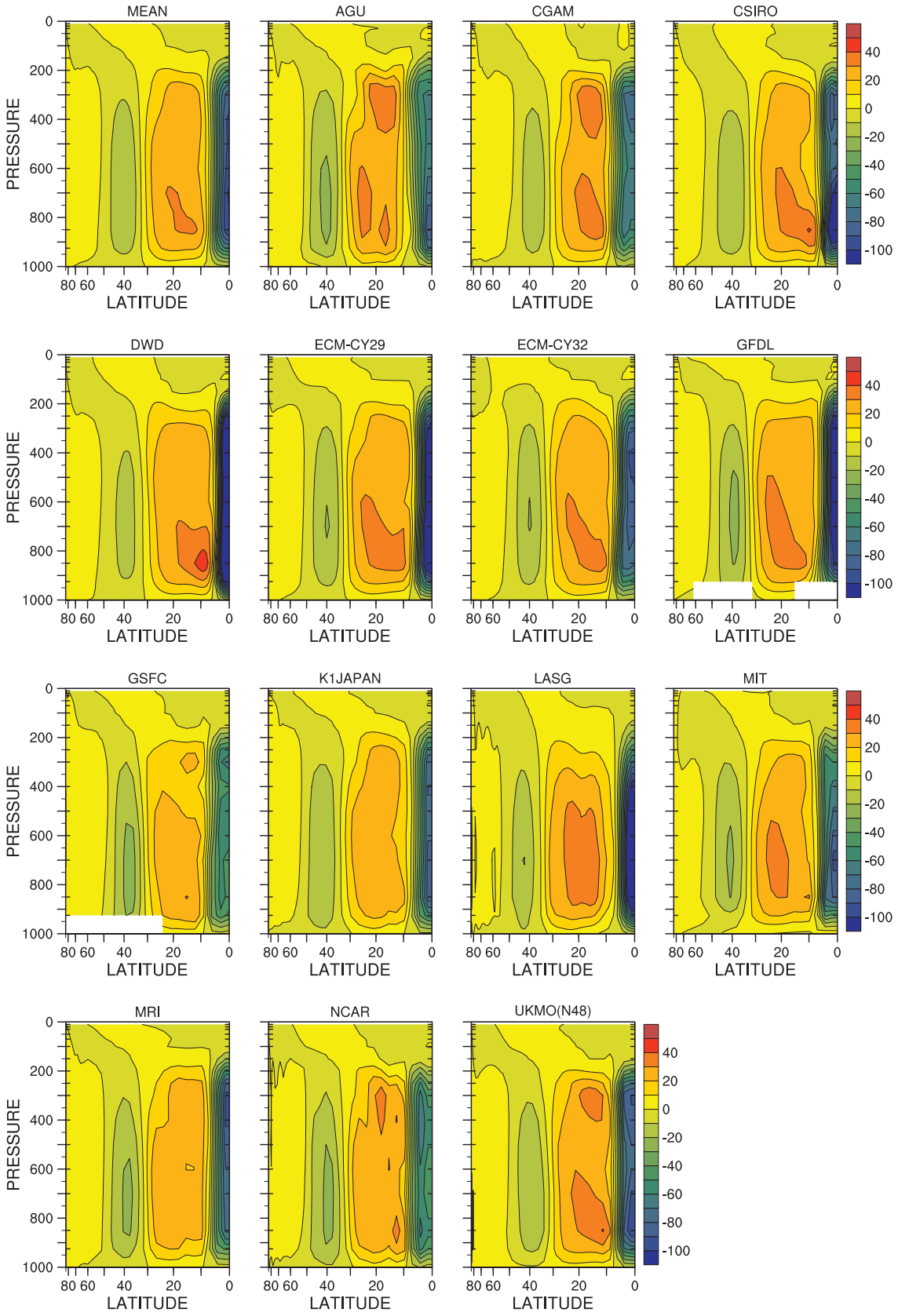

Figure 5.88: Zonal-time average vertical velocity (om), CONTROL, individual models, mb day^{-1}.

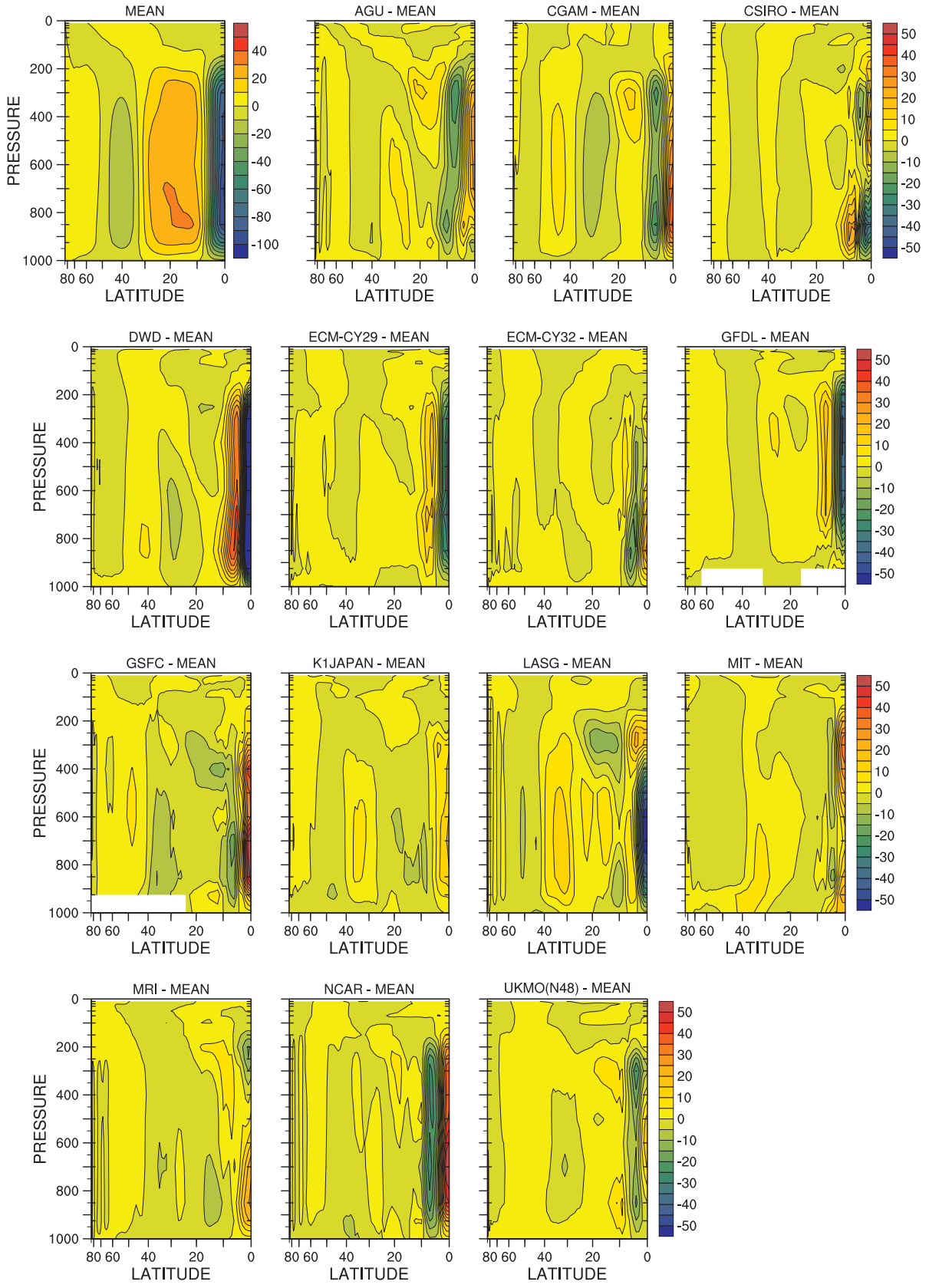

Figure 5.89: Zonal-time average vertical velocity (om), CONTROL, individual models minus multi-model mean, mb day^{-1}.

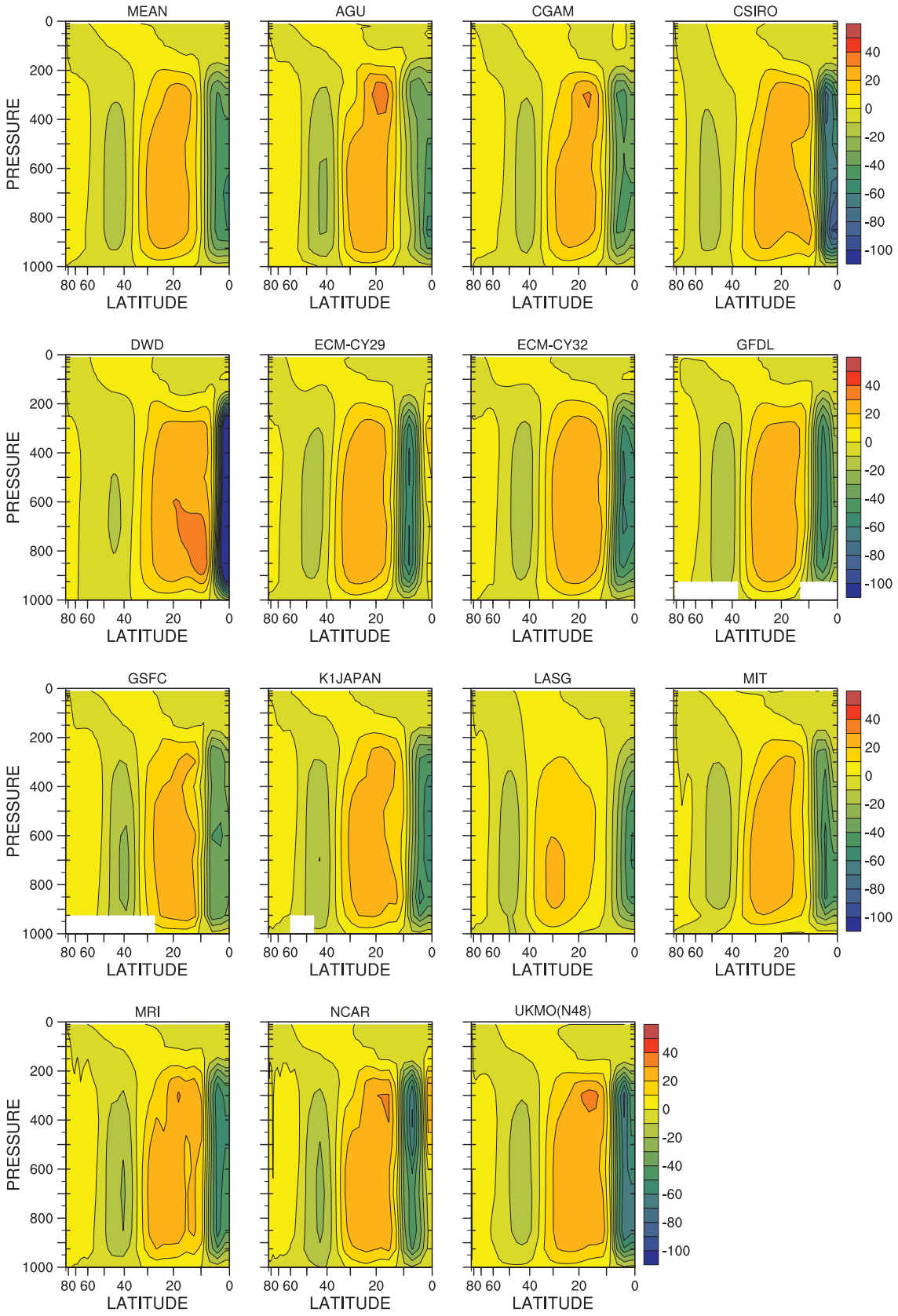

Figure 5.90: Zonal-time average vertical velocity (om), QOBS, individual models, mb day^{-1}.

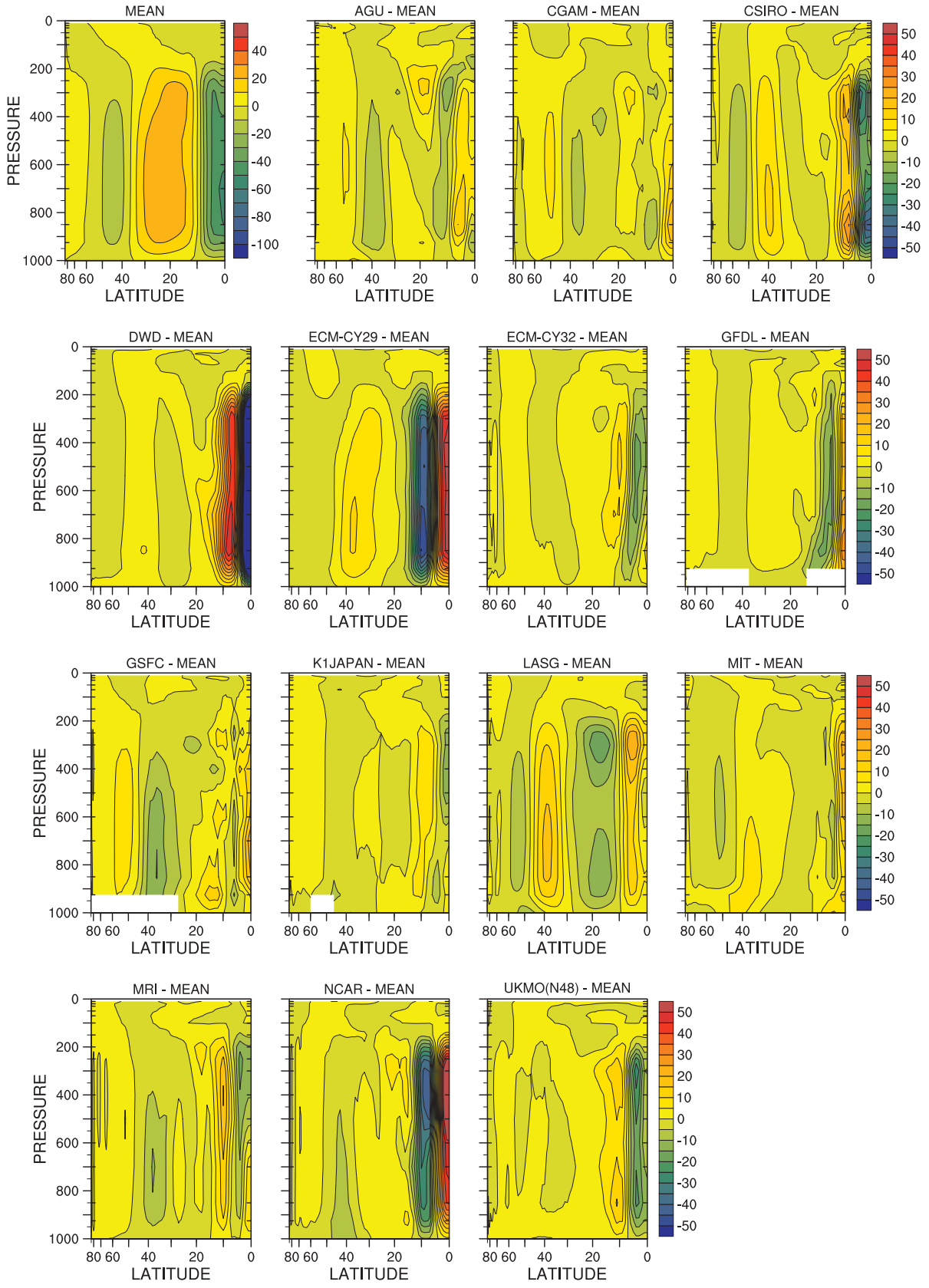

Figure 5.91: Zonal-time average vertical velocity (om), QOBS, individual models minus multi-model mean, mb day^{-1}.

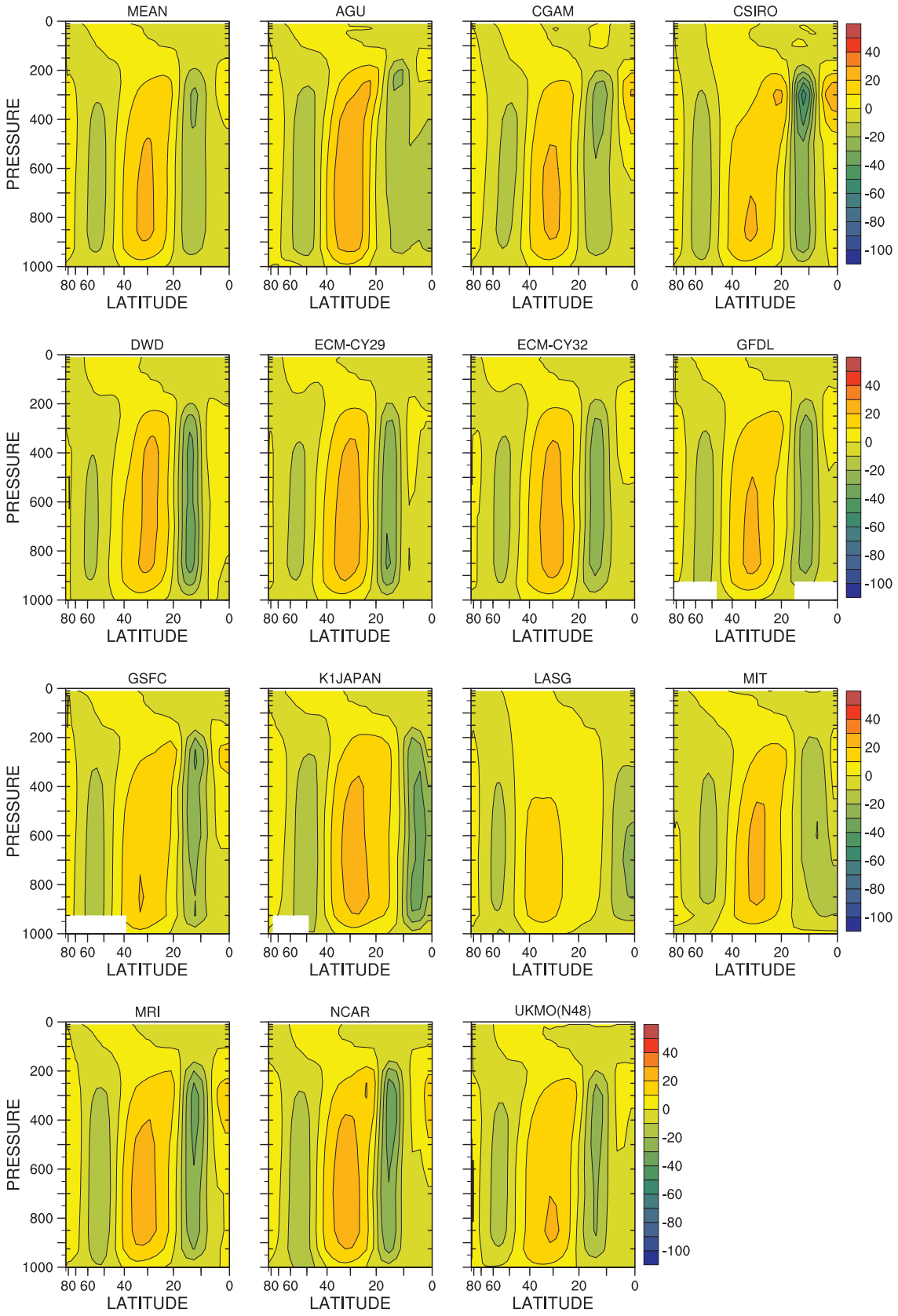

Figure 5.92: Zonal-time average vertical velocity (om), FLAT, individual models, mb day^{-1}.

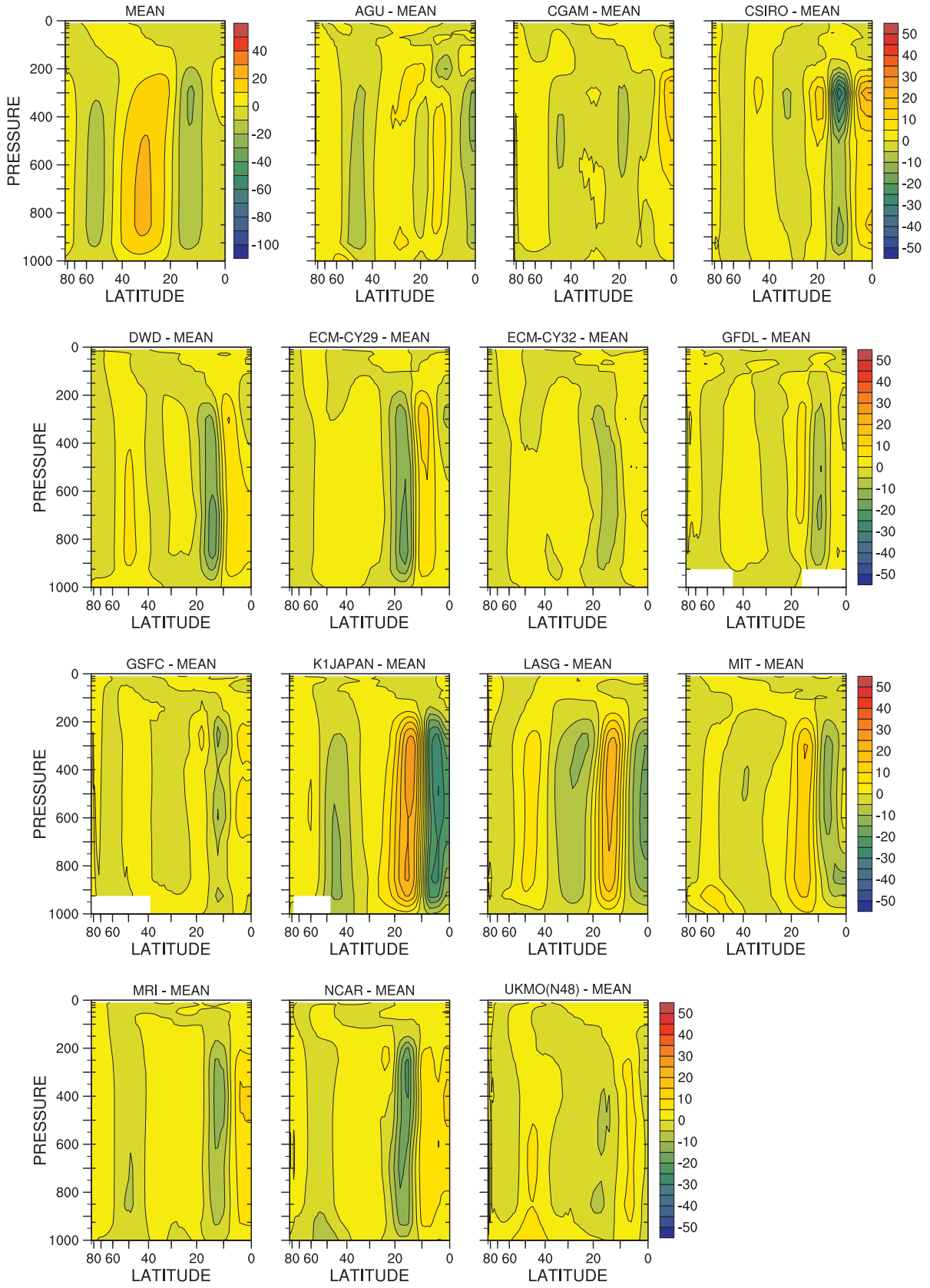

Figure 5.93: Zonal-time average vertical velocity (om), FLAT, individual models minus multi-model mean, mb day^{-1}.

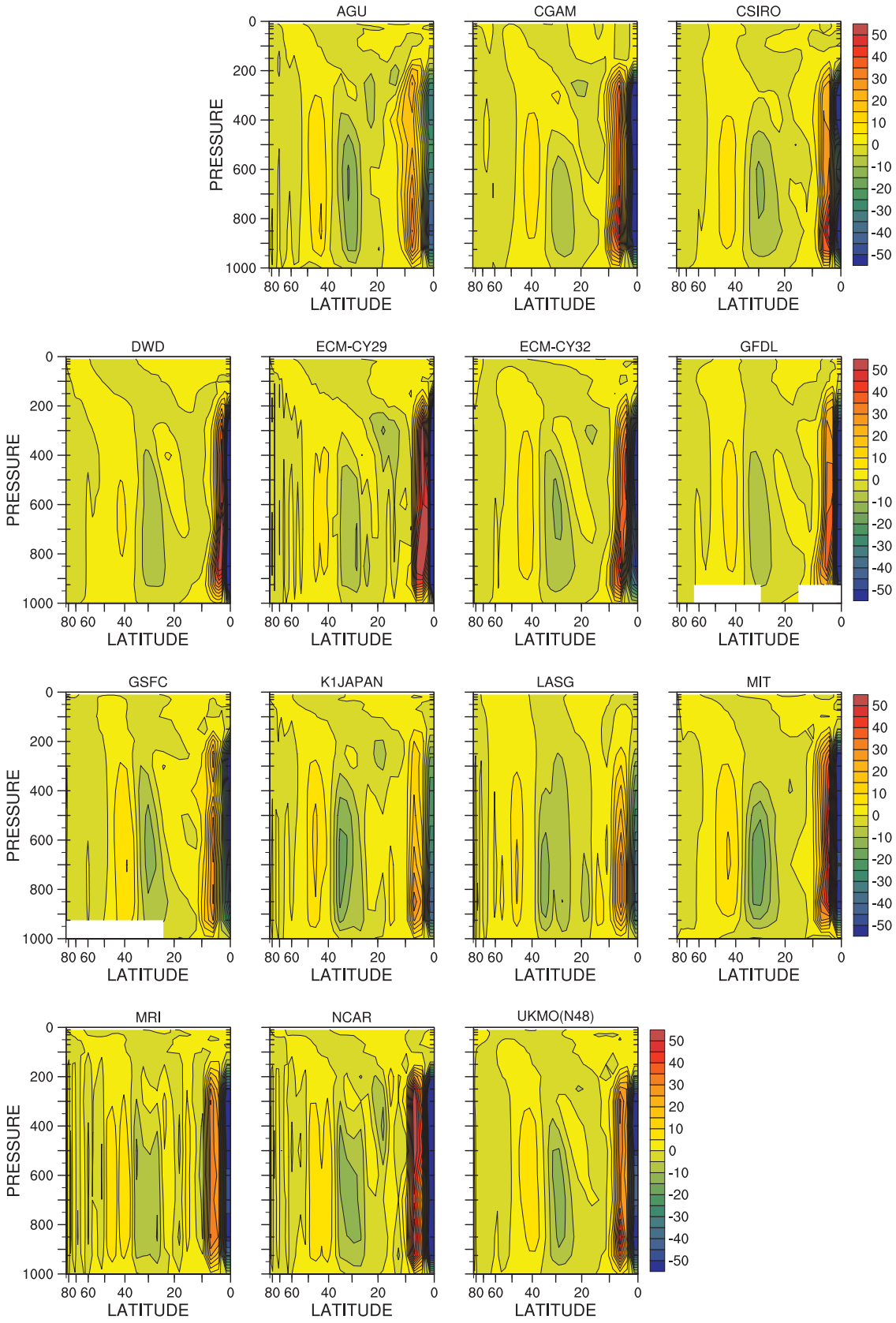

Figure 5.94: Zonal-time average vertical velocity (om), PEAKED−CONTROL, individual models, mb day^{-1}.

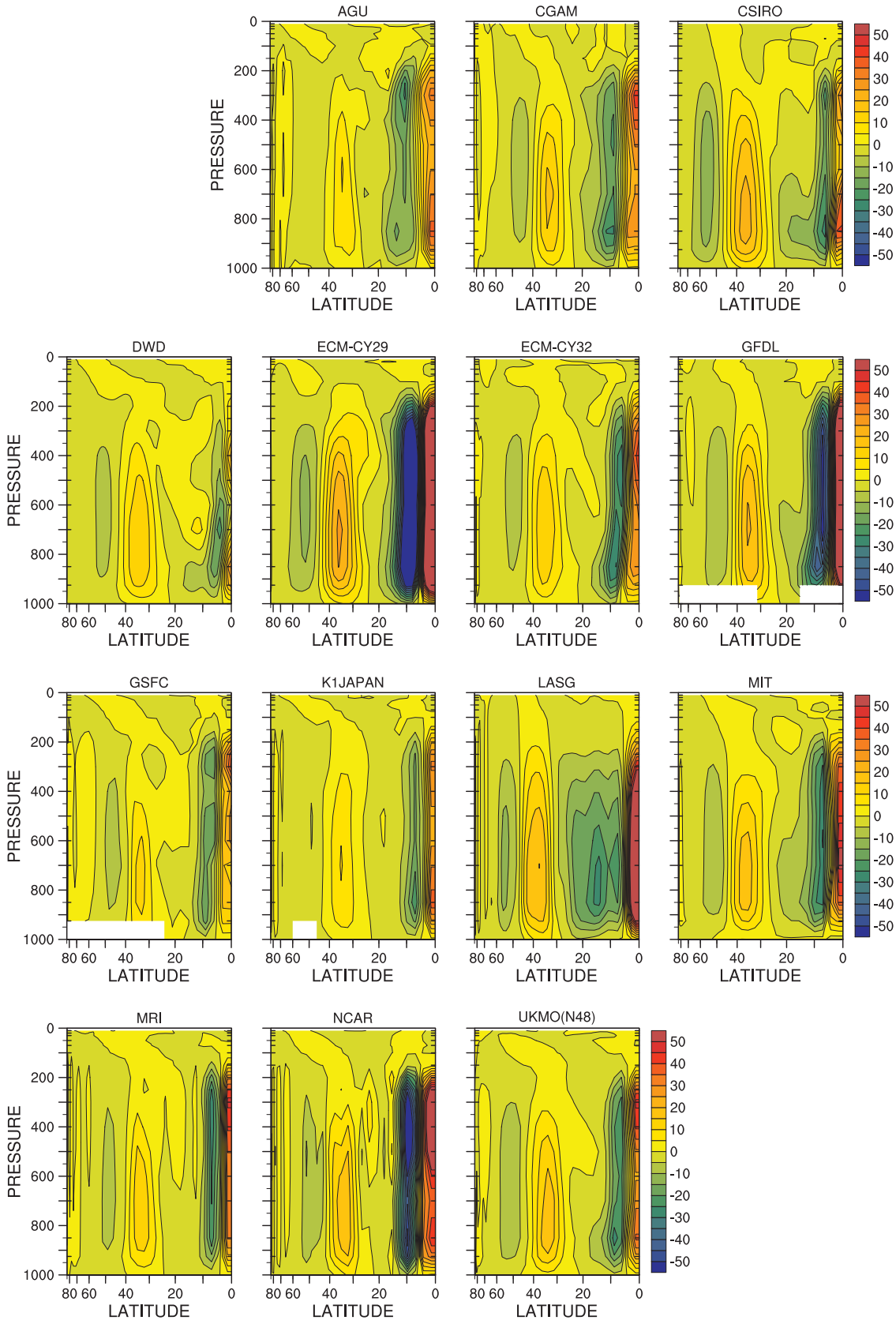

Figure 5.95: Zonal-time average vertical velocity (om), QOBS−CONTROL, individual models, mb day^{-1}.

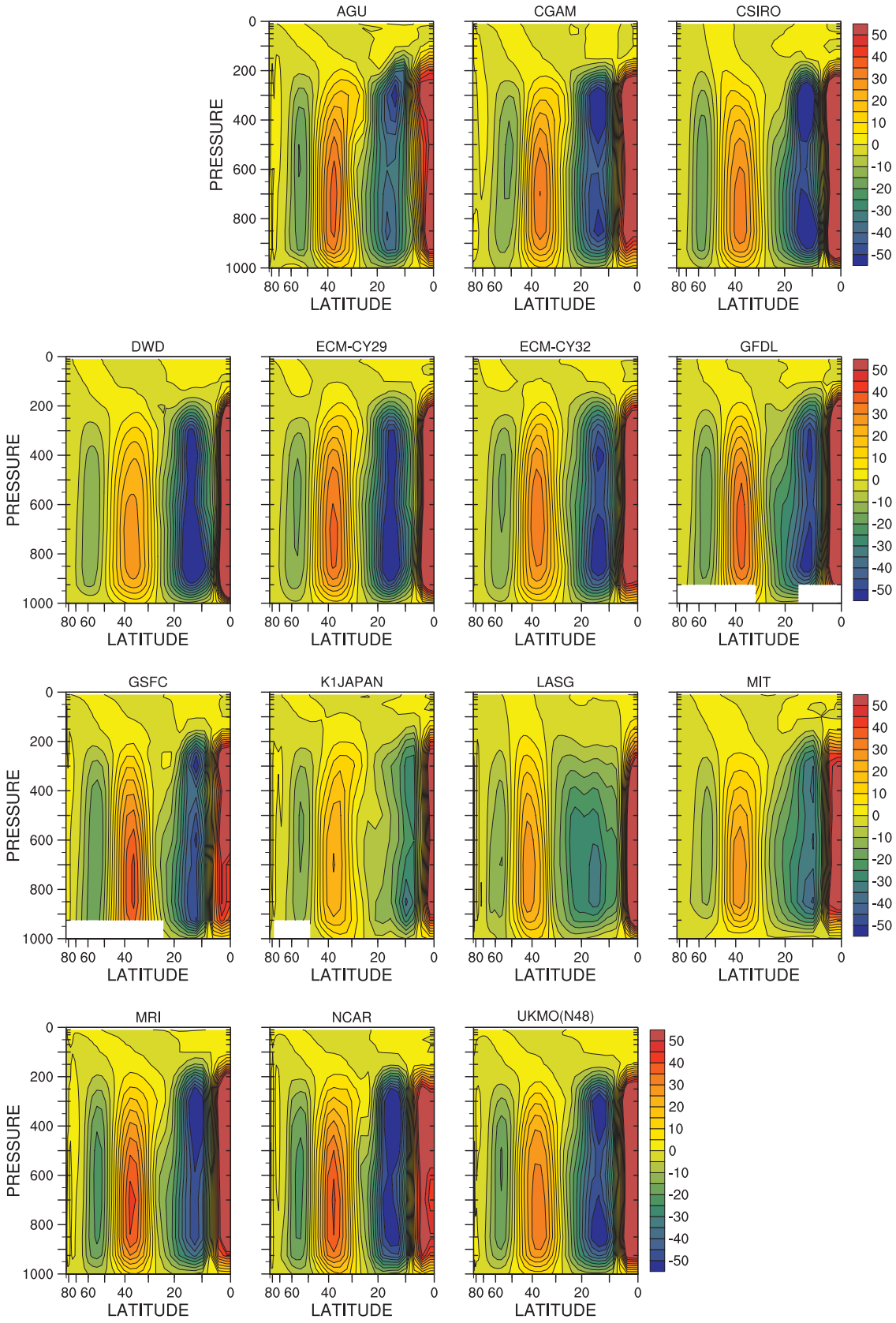

Figure 5.96: Zonal-time average vertical velocity (om), FLAT−CONTROL, individual models, mb day^{-1}.

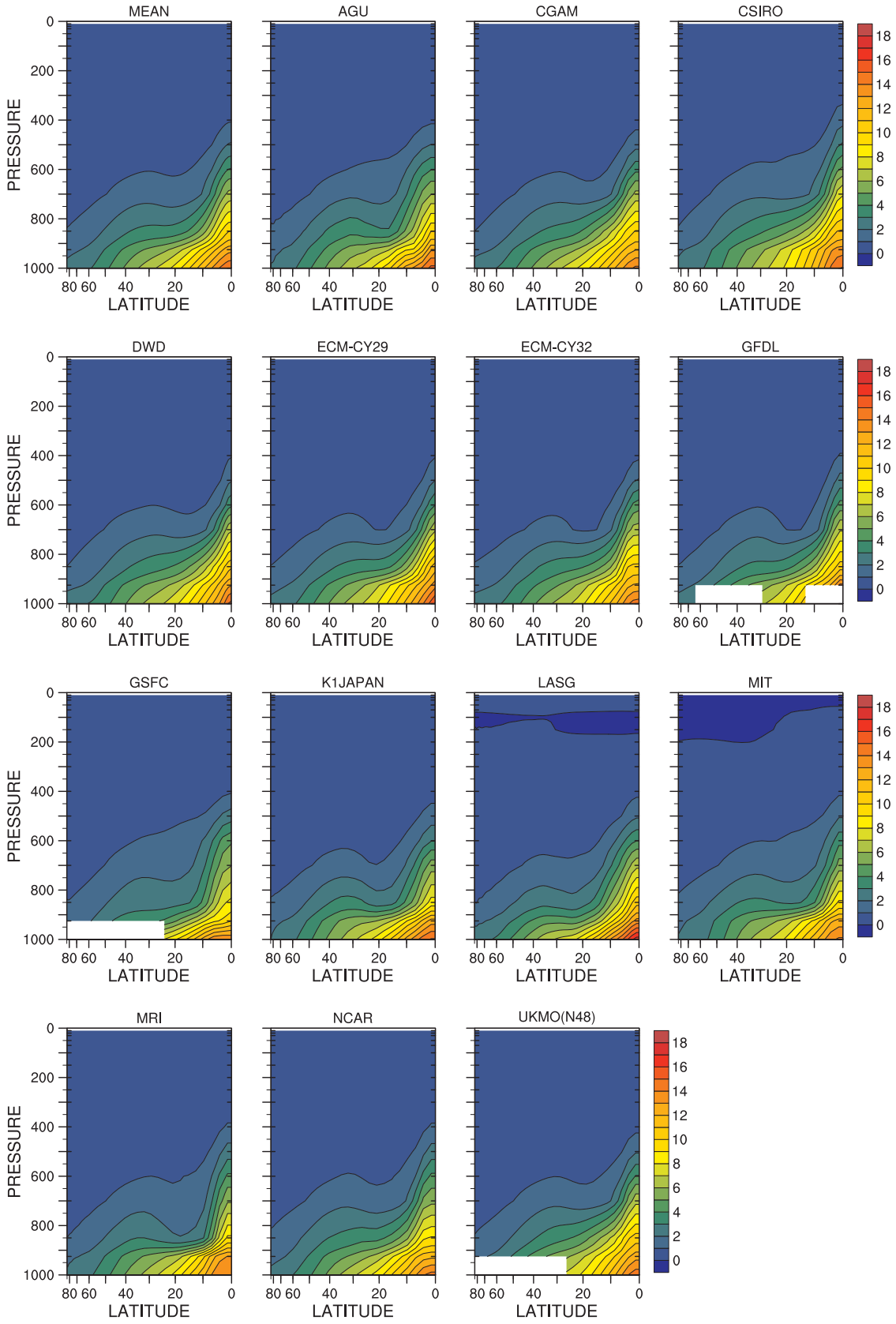

Figure 5.97: Zonal-time average specific humidity (q), PEAKED, individual models, g kg^{-1}.

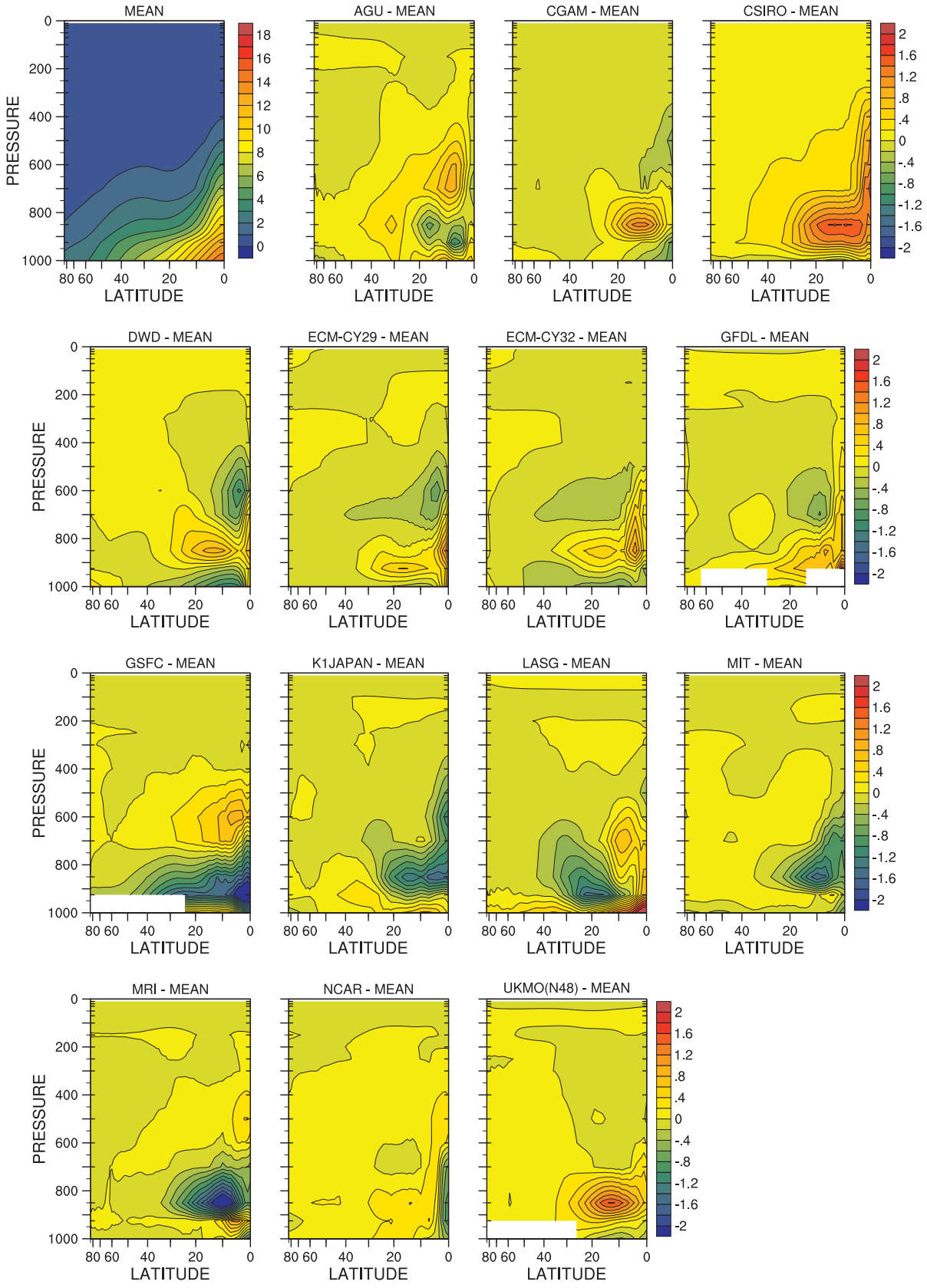

Figure 5.98: Zonal-time average specific humidity (q), PEAKED, individual models minus multi-model mean, g kg^{-1}.

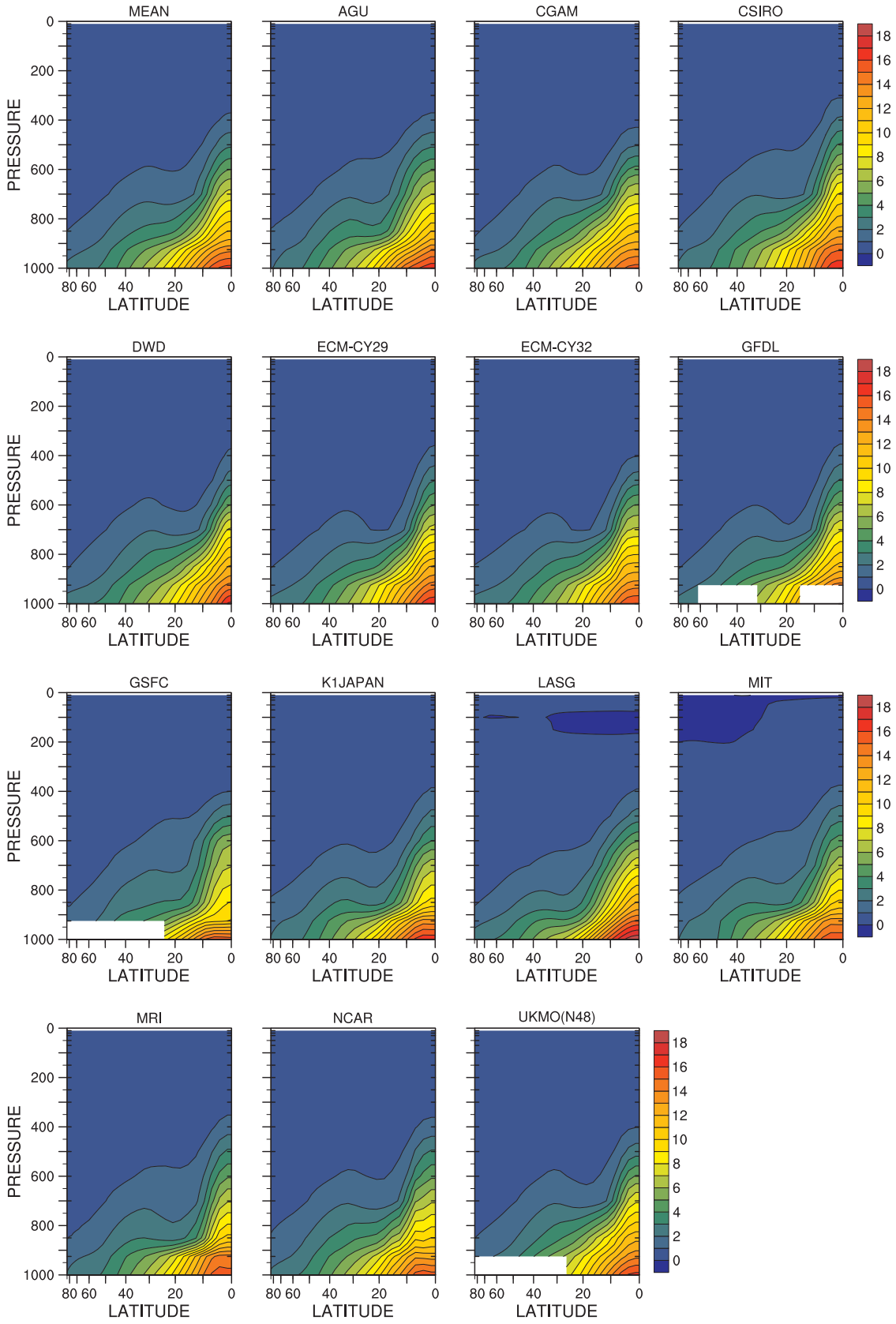

Figure 5.99: Zonal-time average specific humidity (q), CONTROL, individual models, g kg^{-1}.

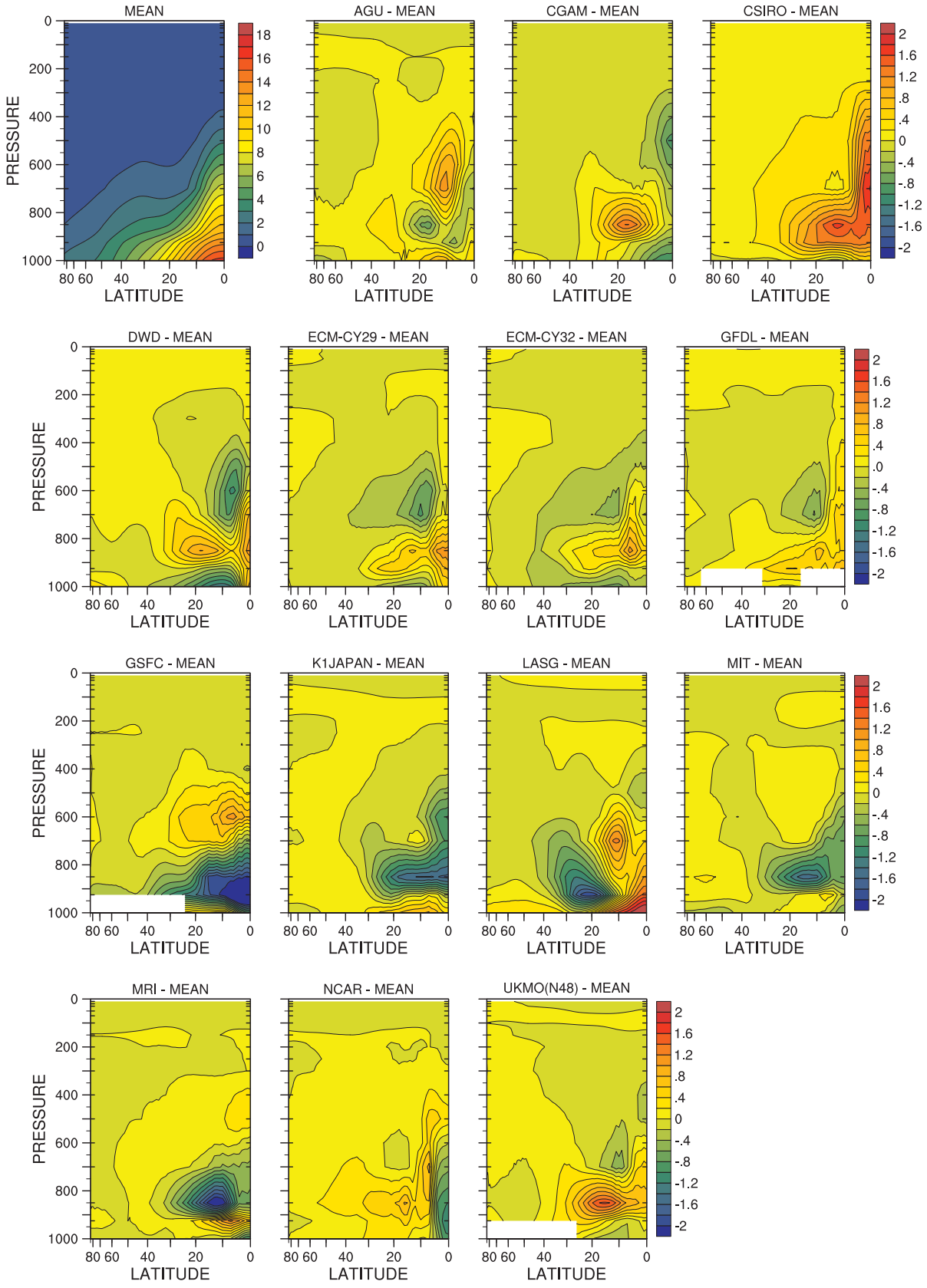

Figure 5.100: Zonal-time average specific humidity (q), CONTROL, individual models minus multi-model mean, g kg^{-1}.

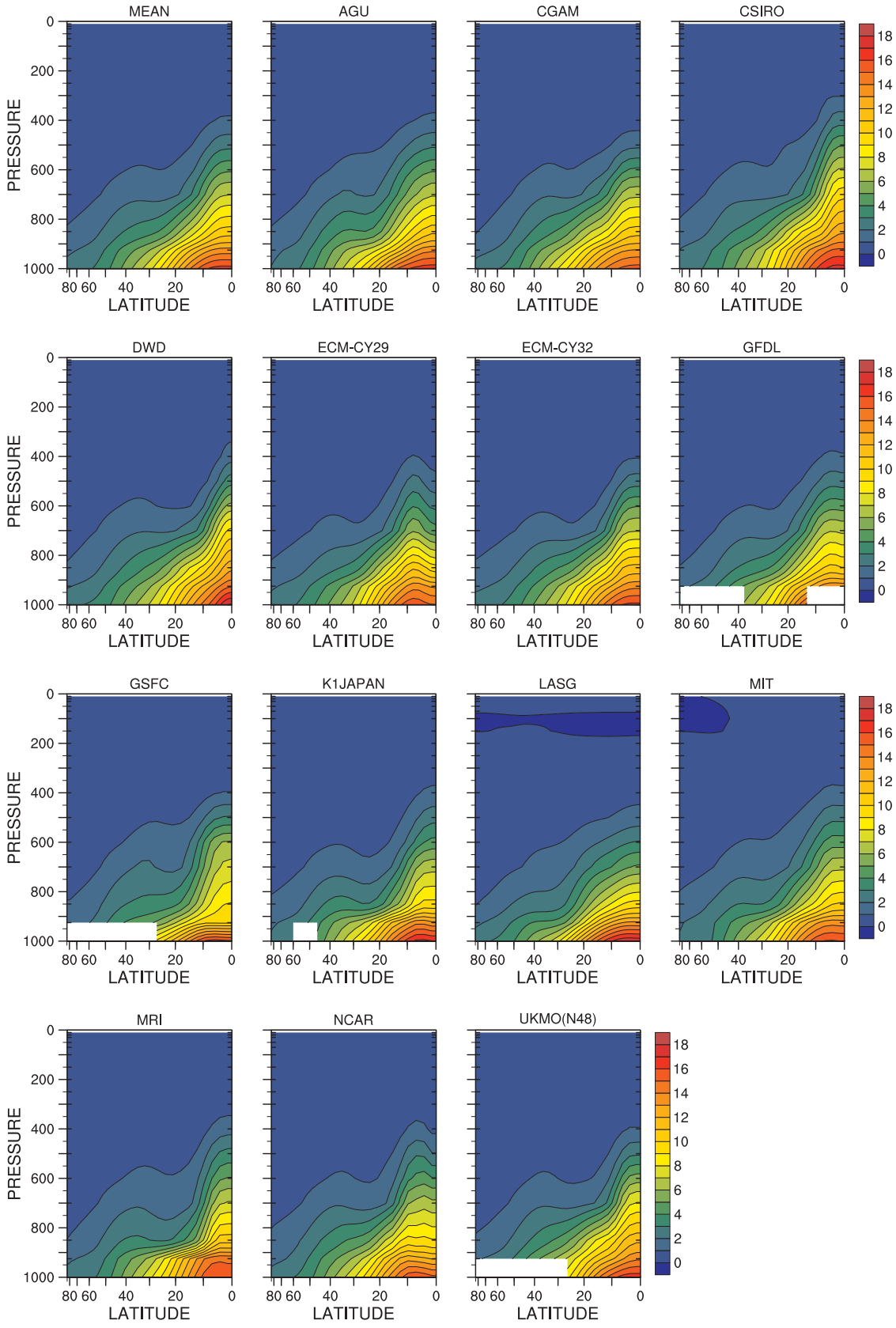

Figure 5.101: Zonal-time average specific humidity (q), QOBS, individual models, g kg^{-1}.

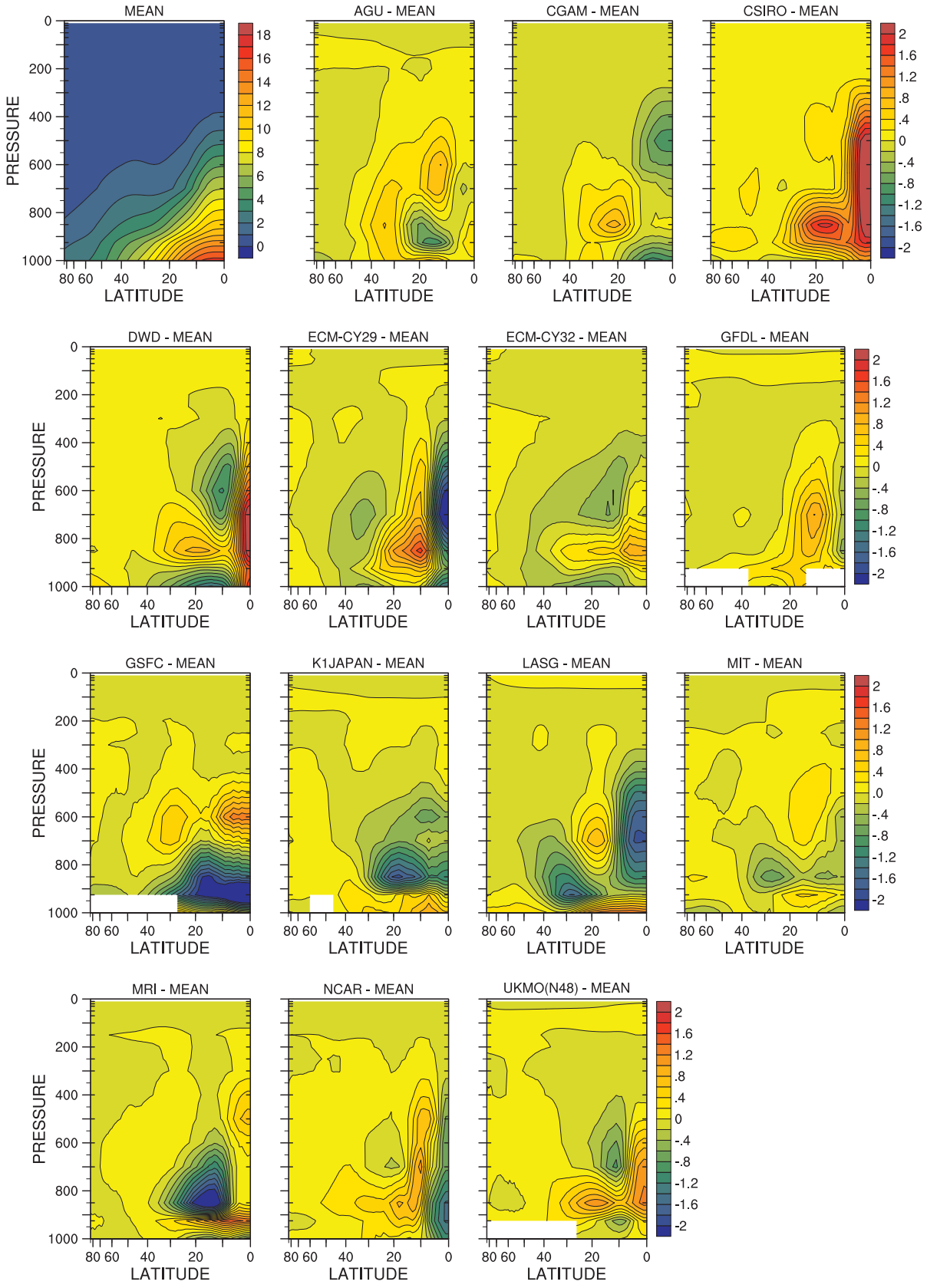

Figure 5.102: Zonal-time average specific humidity (q), QOBS, individual models minus multi-model mean, g kg^{-1}.

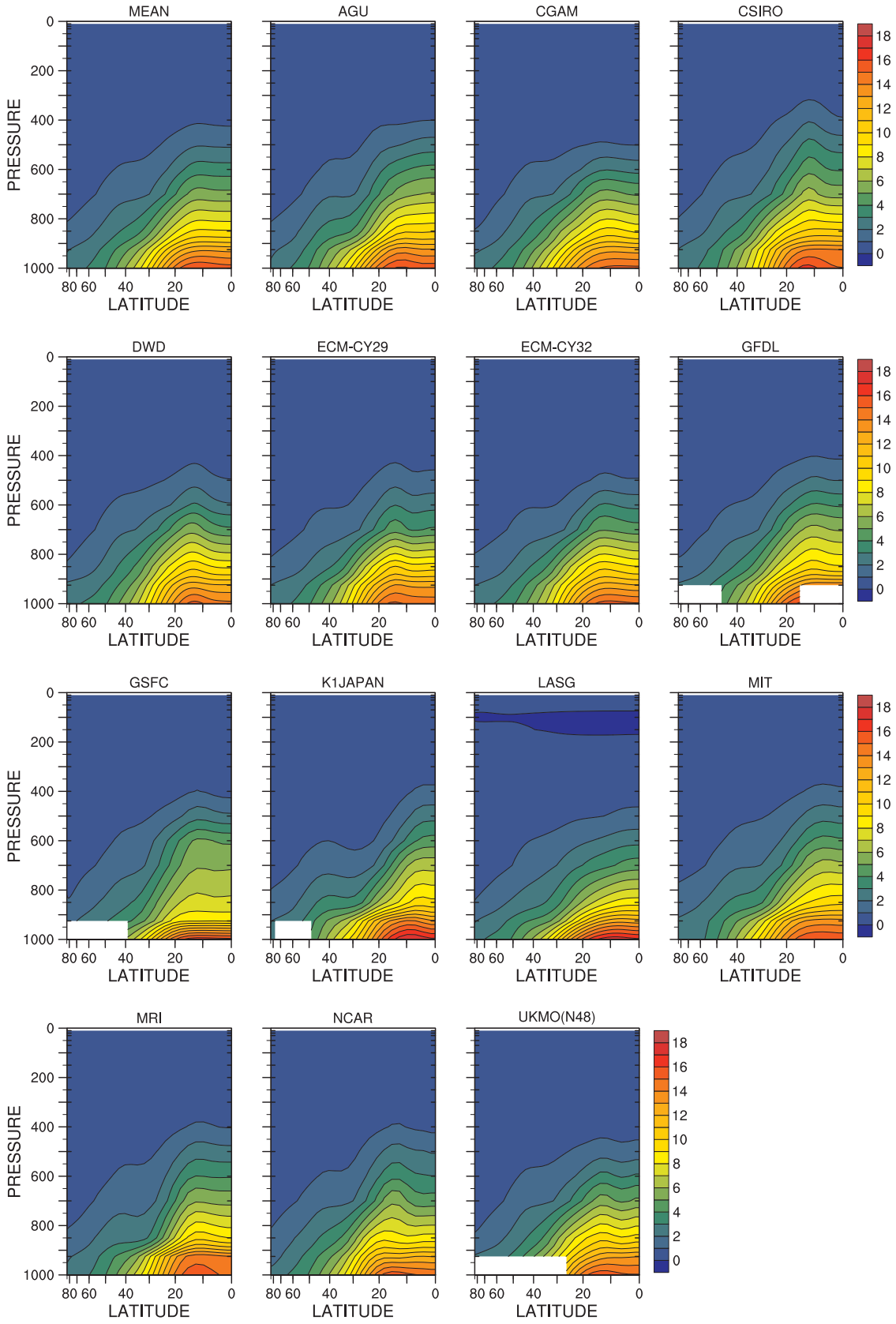

Figure 5.103: Zonal-time average specific humidity (q), FLAT, individual models, g kg^{-1}.

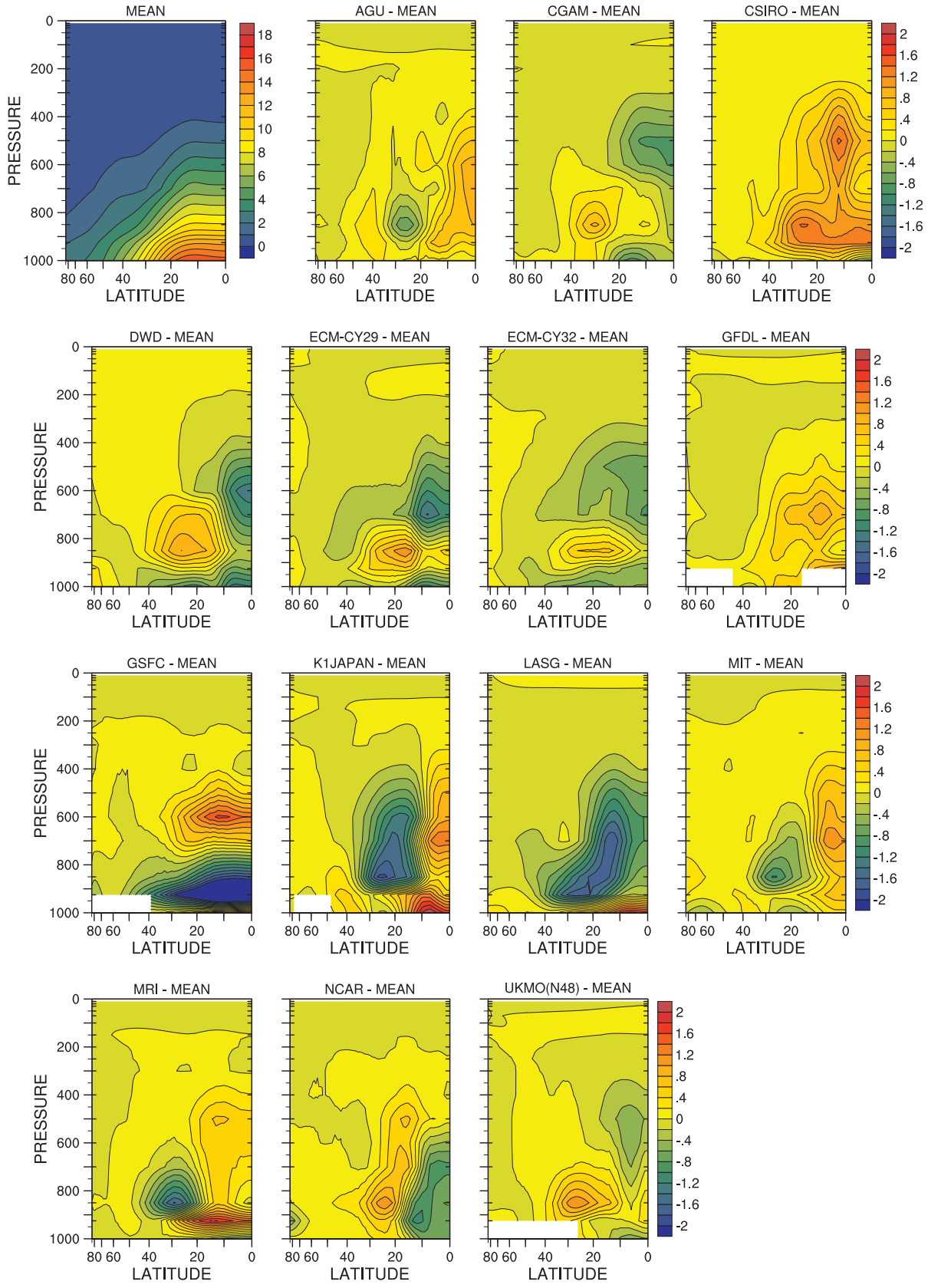

Figure 5.104: Zonal-time average specific humidity (q), FLAT, individual models minus multi-model mean, g kg^{-1}.

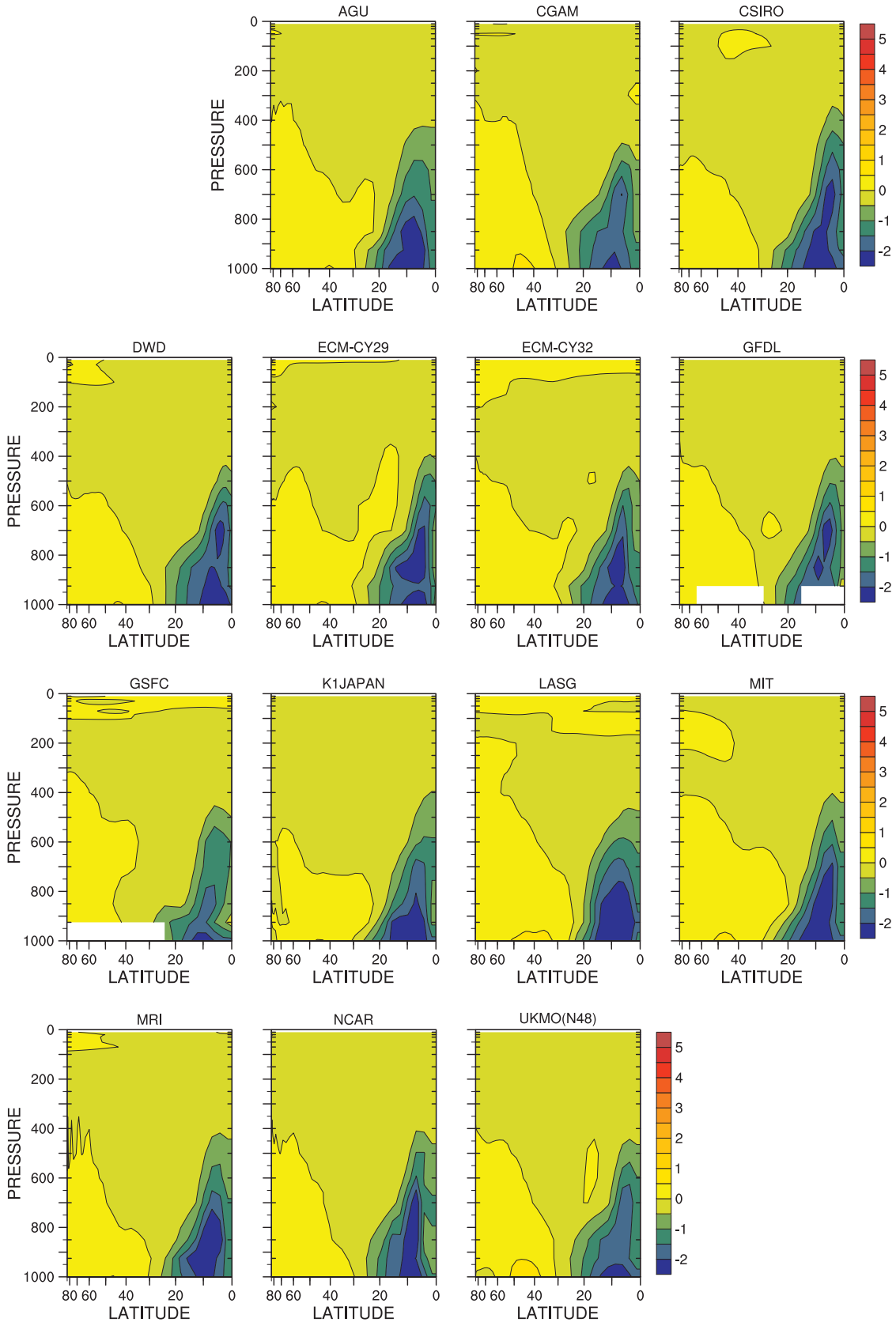

Figure 5.105: Zonal-time average specific humidity (q), PEAKED−CONTROL, individual models, g kg^{-1}.

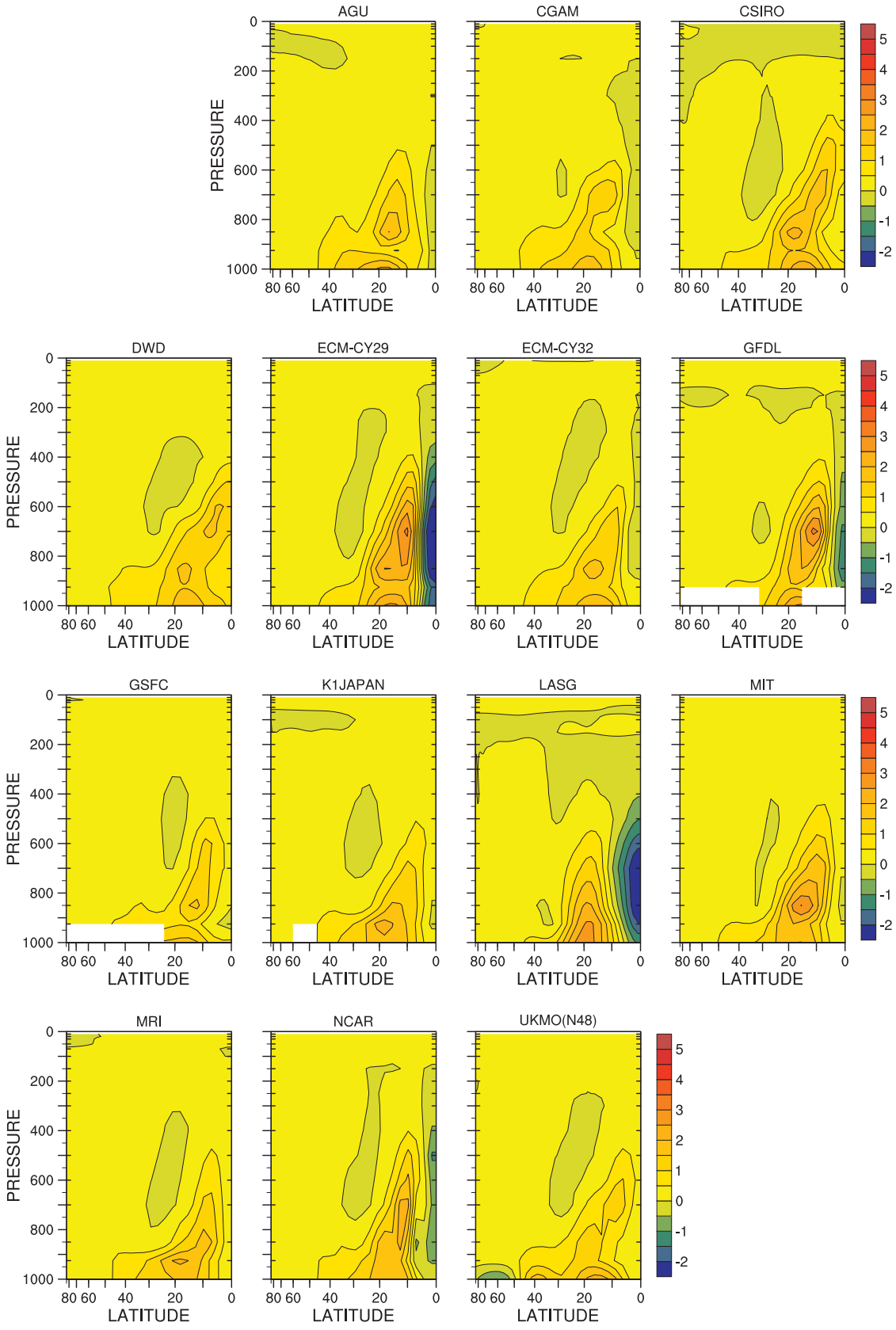

Figure 5.106: Zonal-time average specific humidity (q), QOBS−CONTROL, individual models, g kg^{-1}.

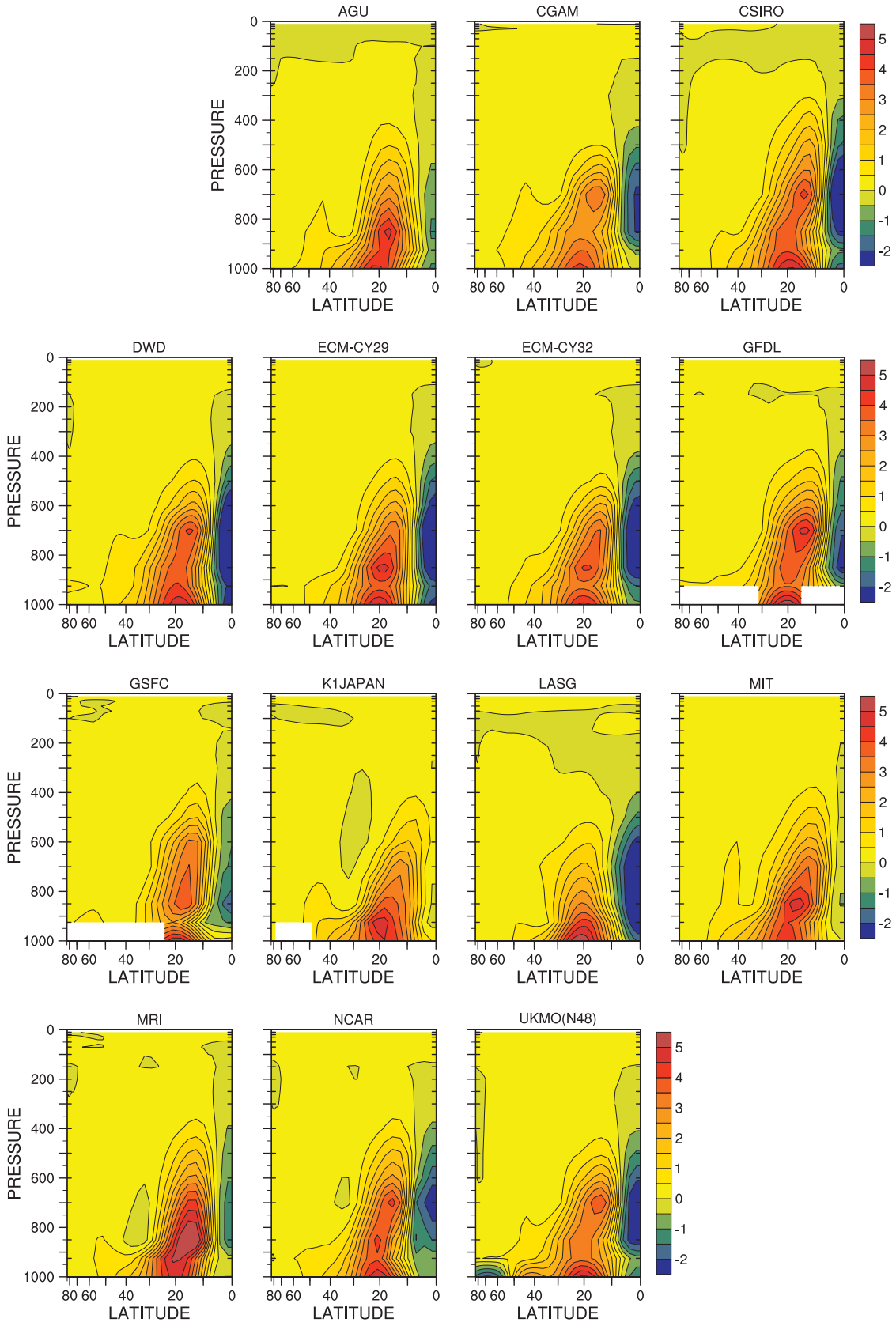

Figure 5.107: Zonal-time average specific humidity (q), FLAT−CONTROL, individual models, g kg^{-1}.

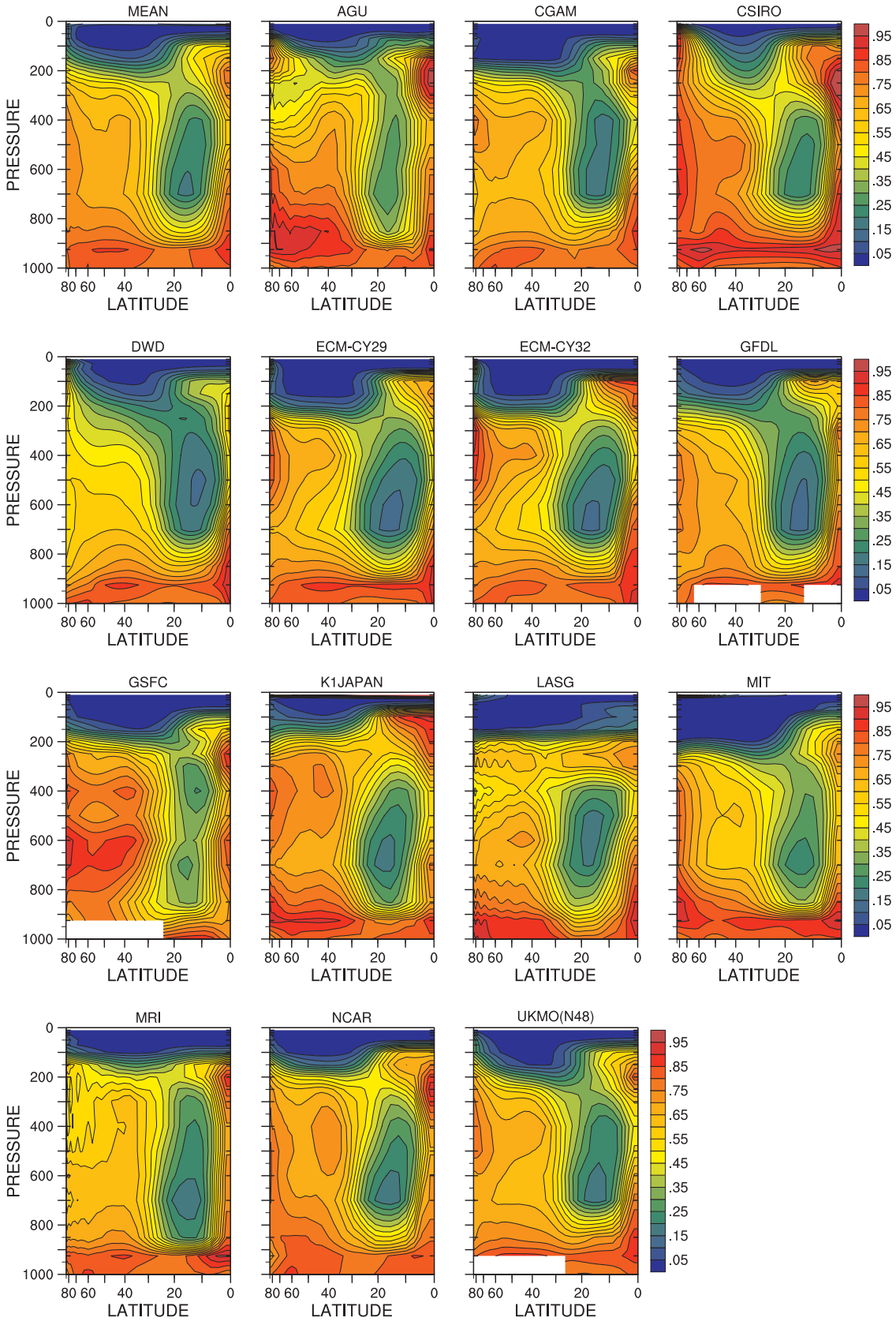

Figure 5.108: Zonal-time average relative humidity (rh), PEAKED, individual models, fraction.

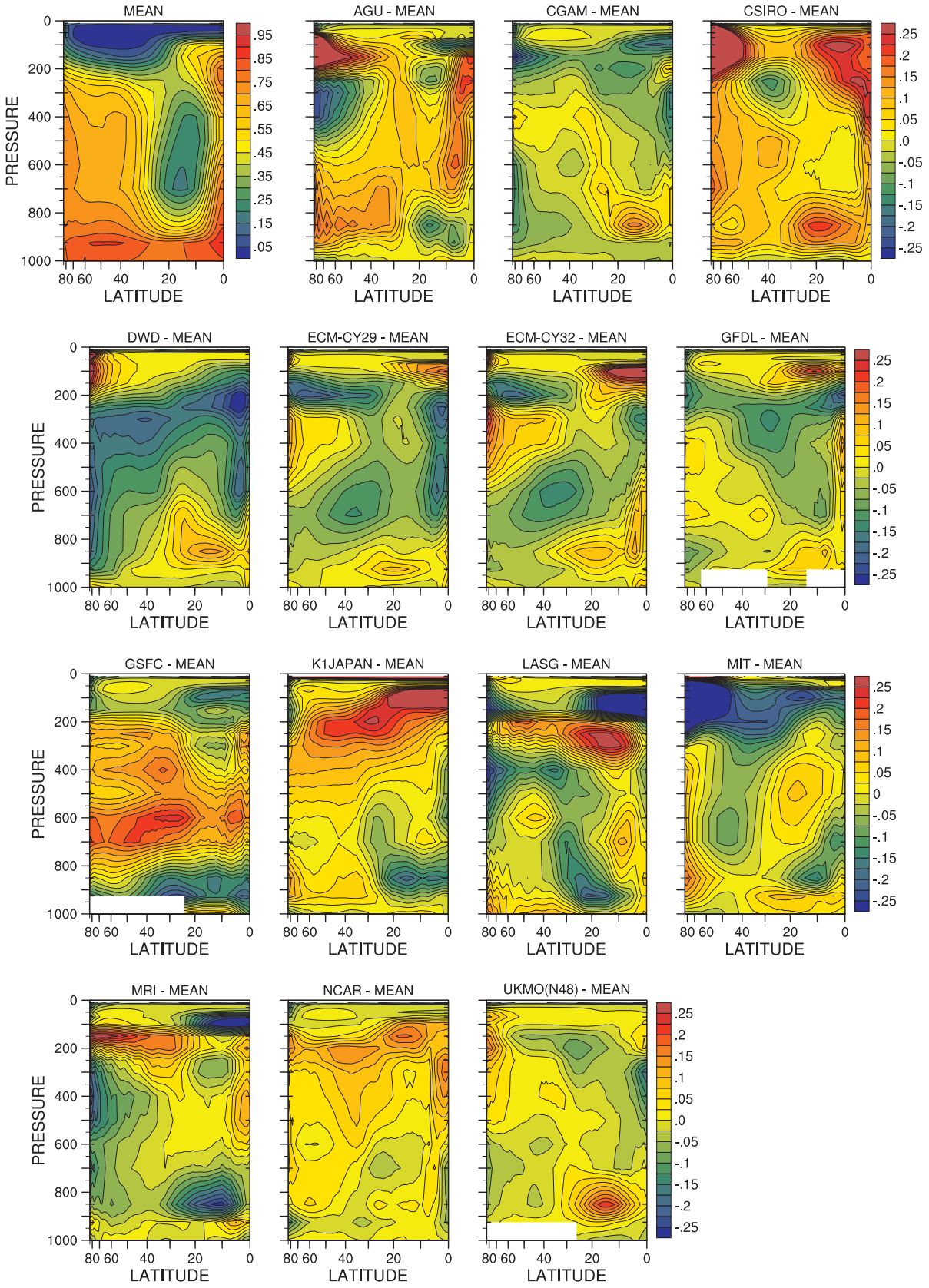

Figure 5.109: Zonal-time average relative humidity (rh), PEAKED, individual models minus multi-model mean, fraction.

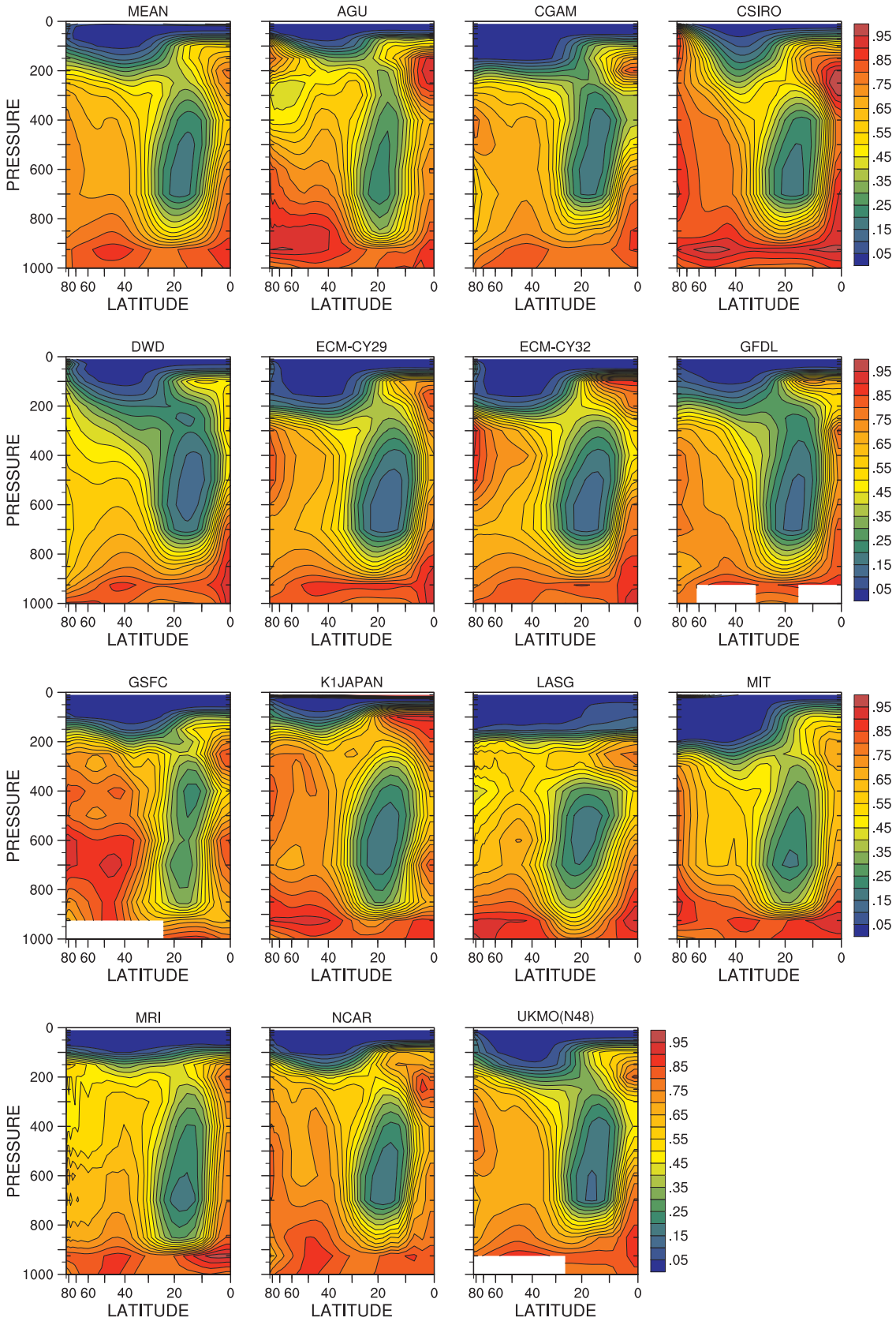

Figure 5.110: Zonal-time average relative humidity (rh), CONTROL, individual models, fraction.

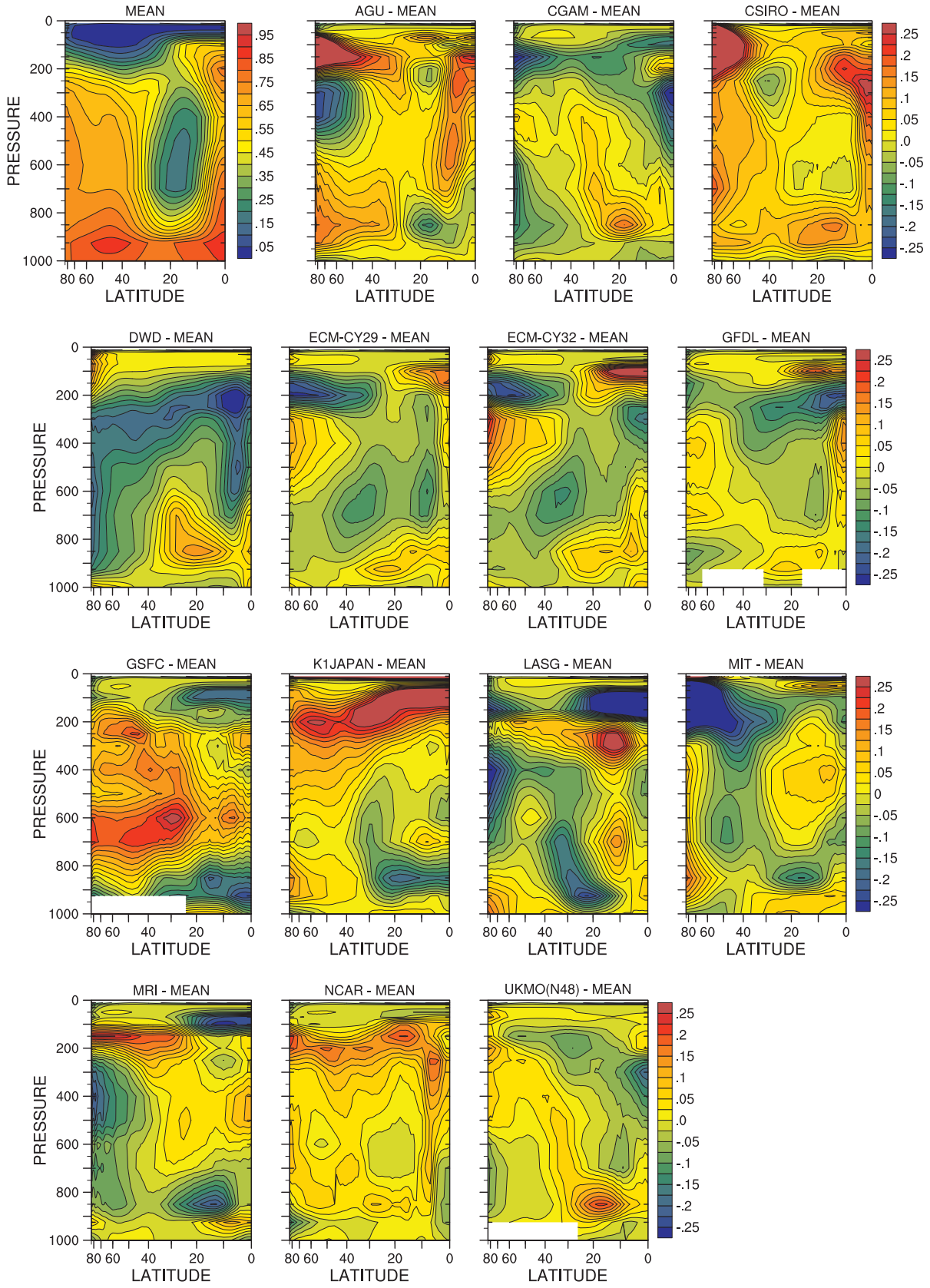

Figure 5.111: Zonal-time average relative humidity (rh), CONTROL, individual models minus multi-model mean, fraction.

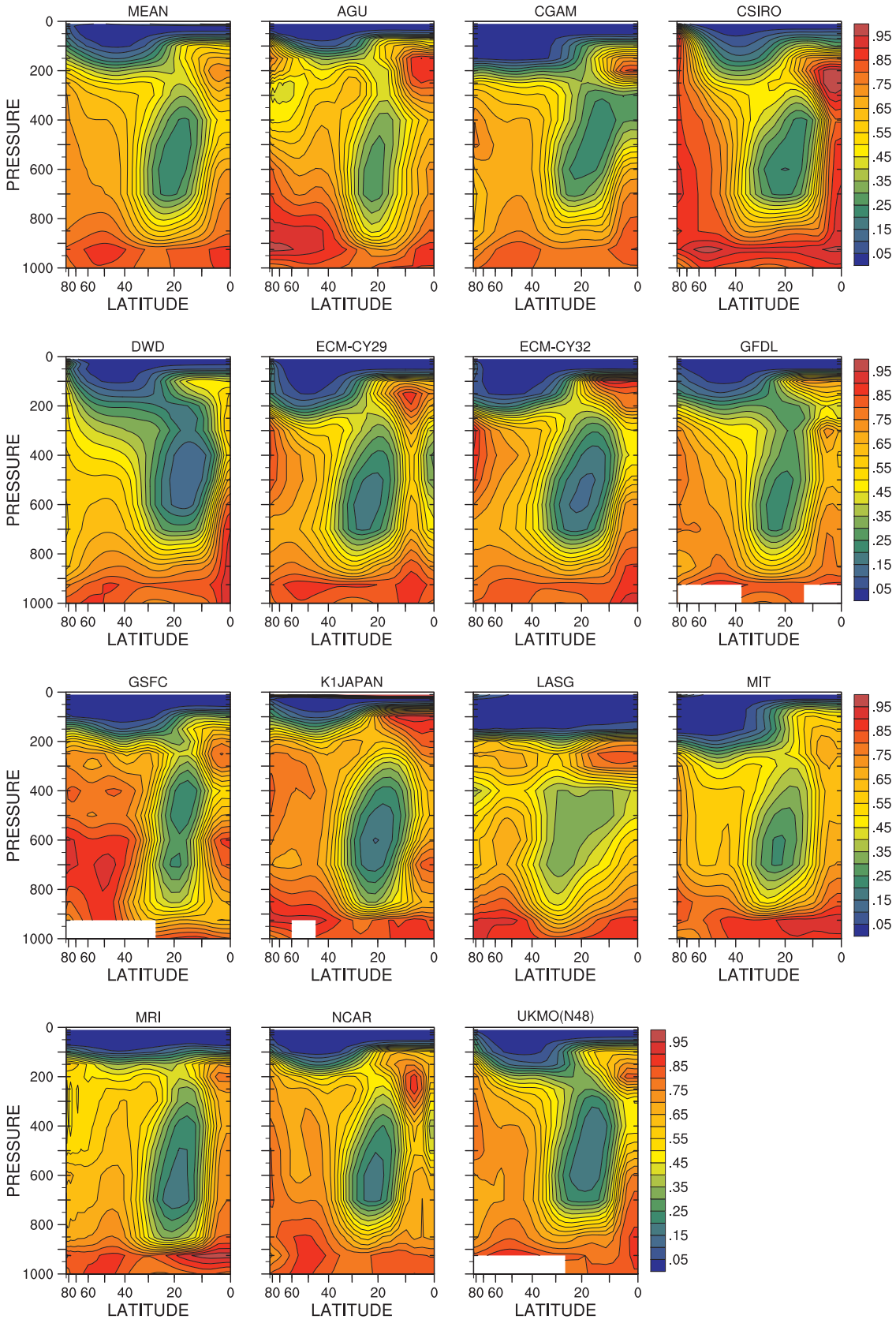

Figure 5.112: Zonal-time average relative humidity (rh), QOBS, individual models, fraction.

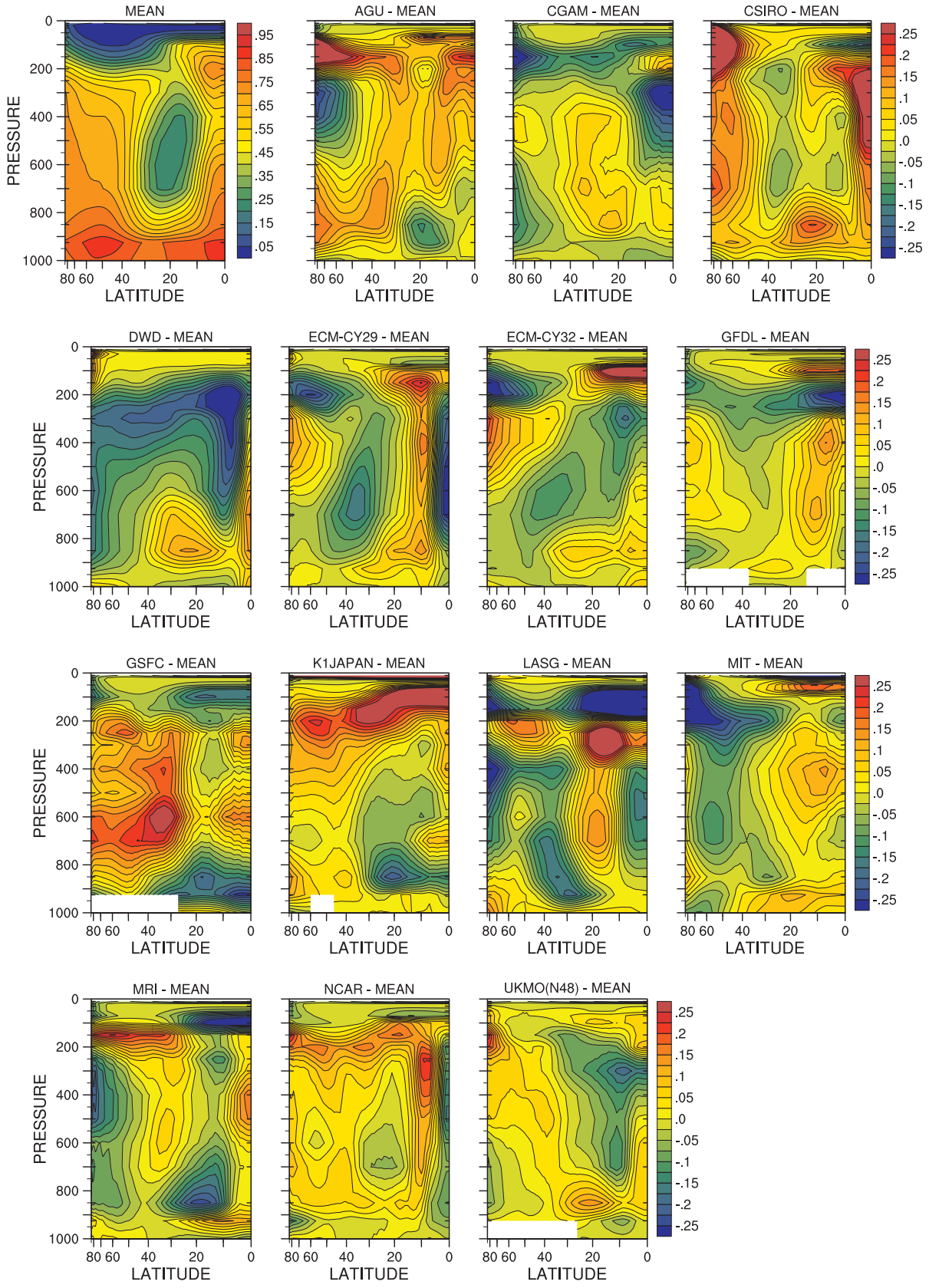

Figure 5.113: Zonal-time average relative humidity (rh), QOBS, individual models minus multi-model mean, fraction.

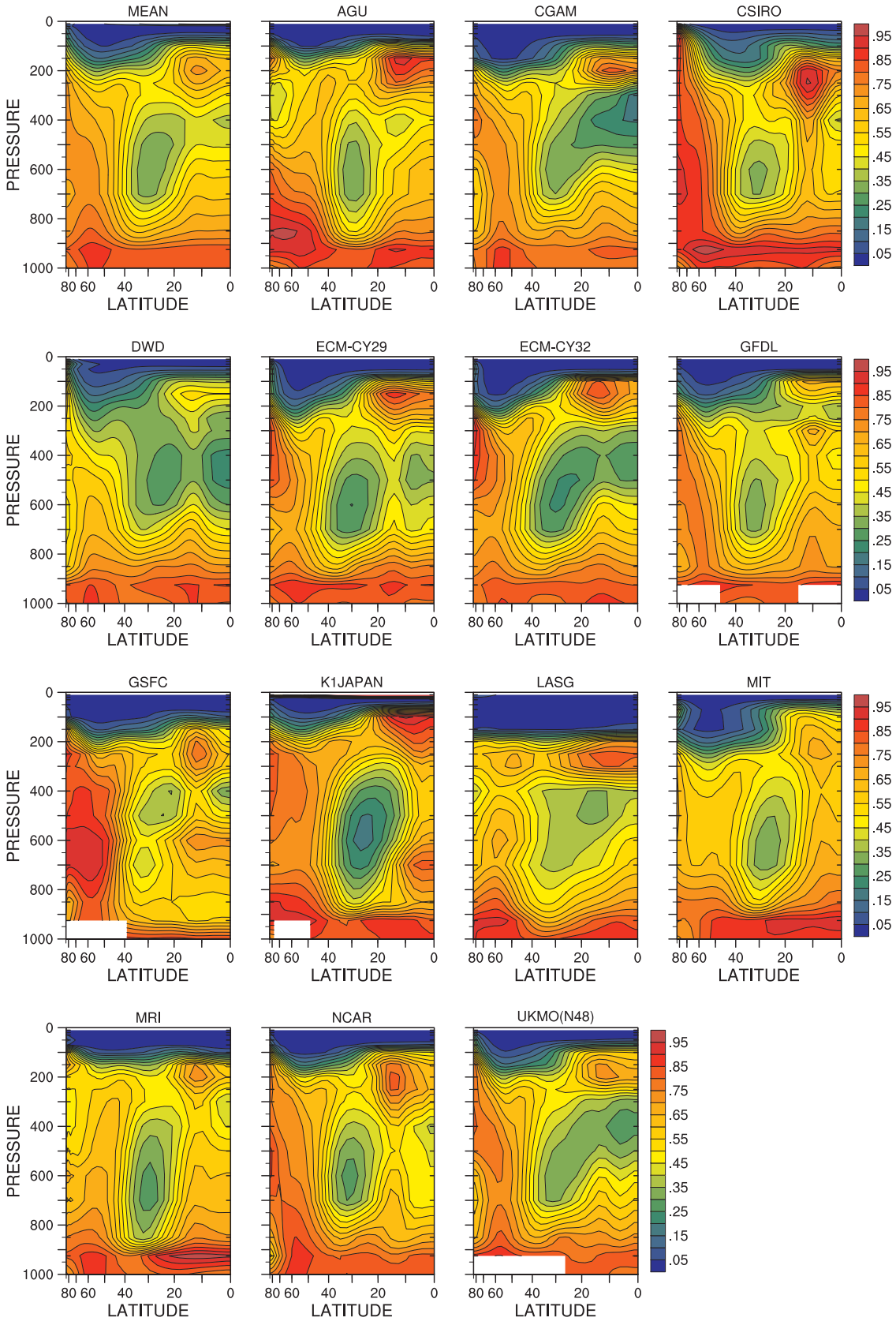

Figure 5.114: Zonal-time average relative humidity (rh), FLAT, individual models, fraction.

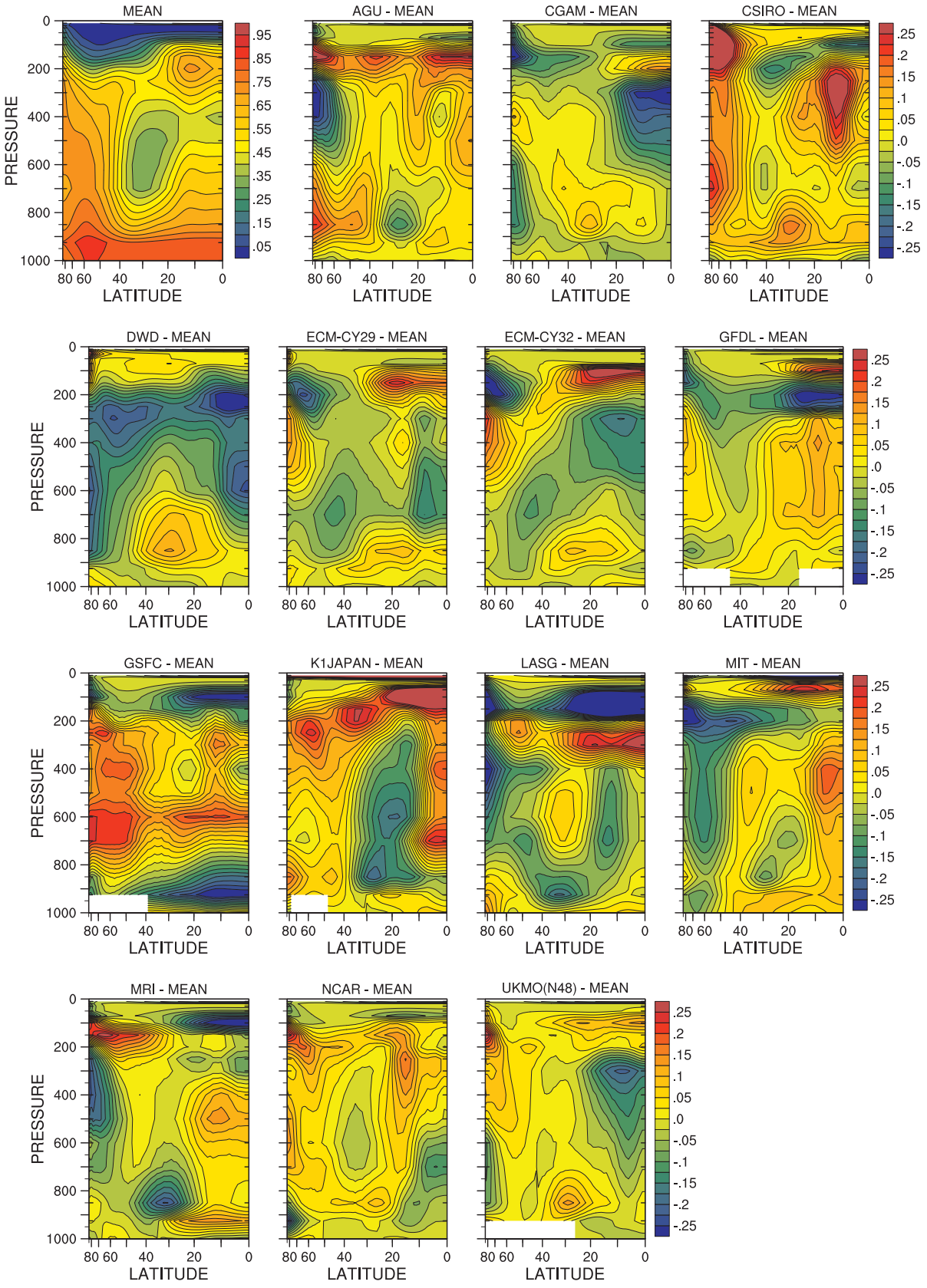

Figure 5.115: Zonal-time average relative humidity (rh), FLAT, individual models minus multi-model mean, fraction.

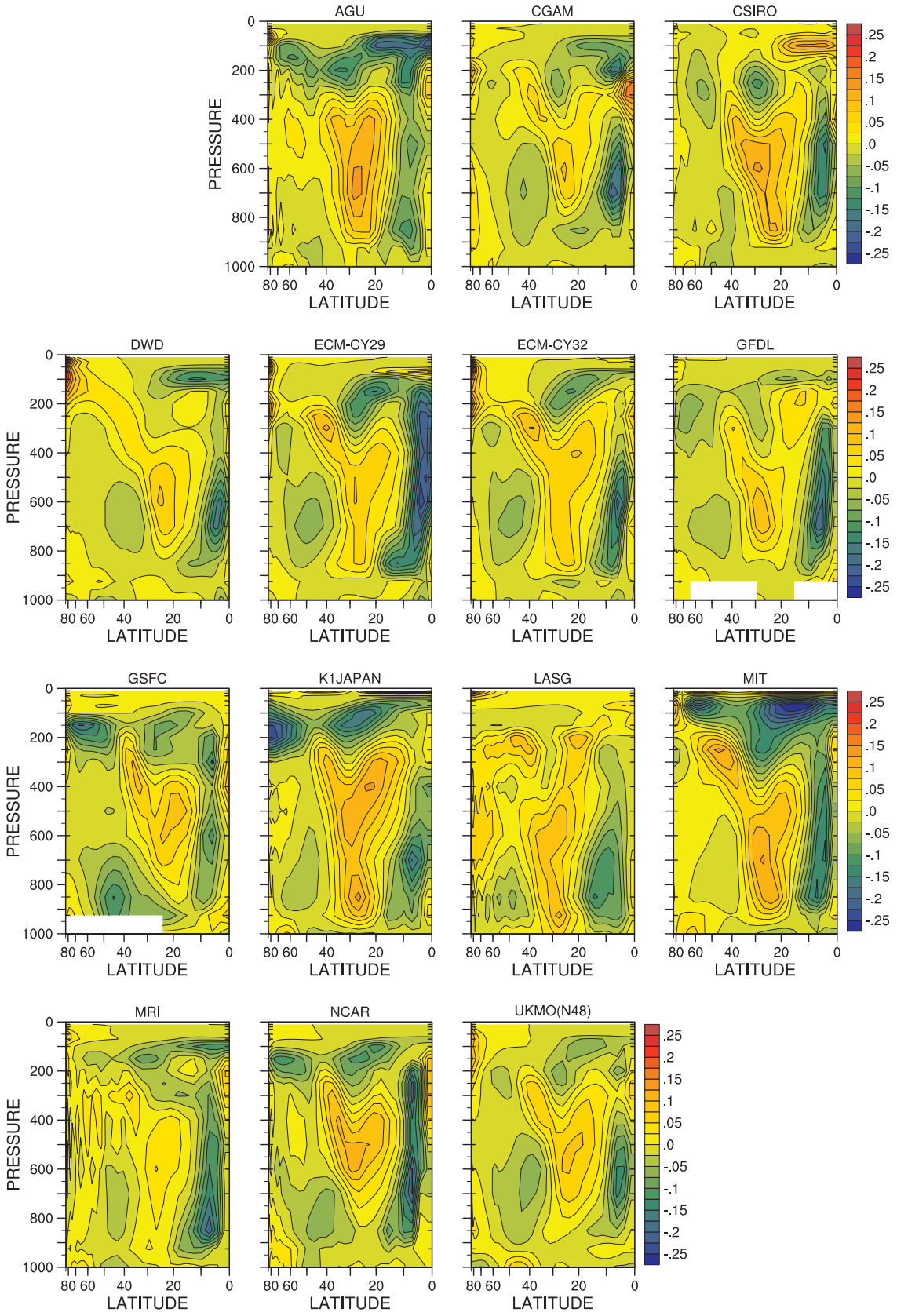

Figure 5.116: Zonal-time average relative humidity (rh), PEAKED−CONTROL, individual models, fraction.

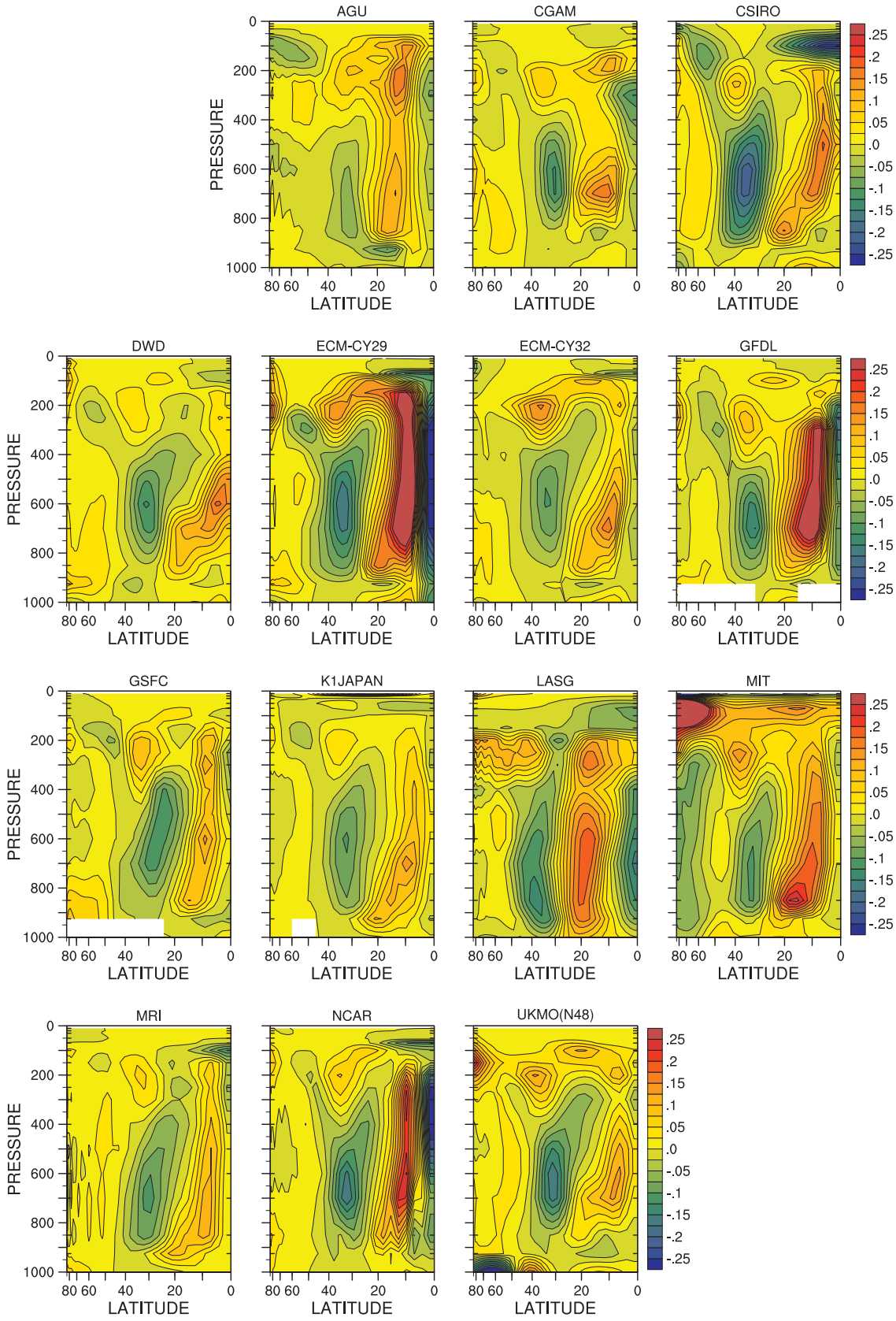

Figure 5.117: Zonal-time average relative humidity (rh), QOBS−CONTROL, individual models, fraction.

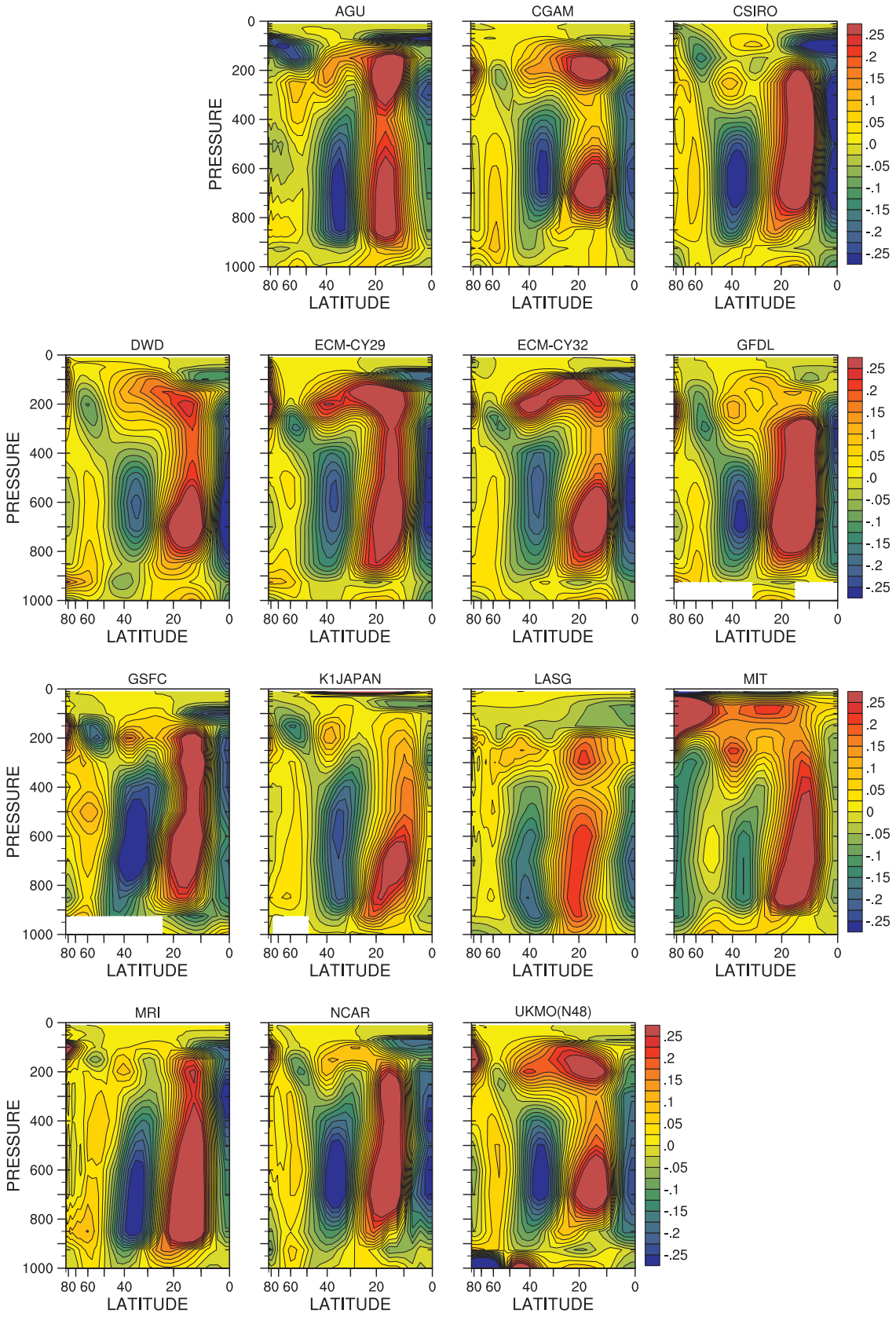

Figure 5.118: Zonal-time average relative humidity (rh), FLAT−CONTROL, individual models, fraction.

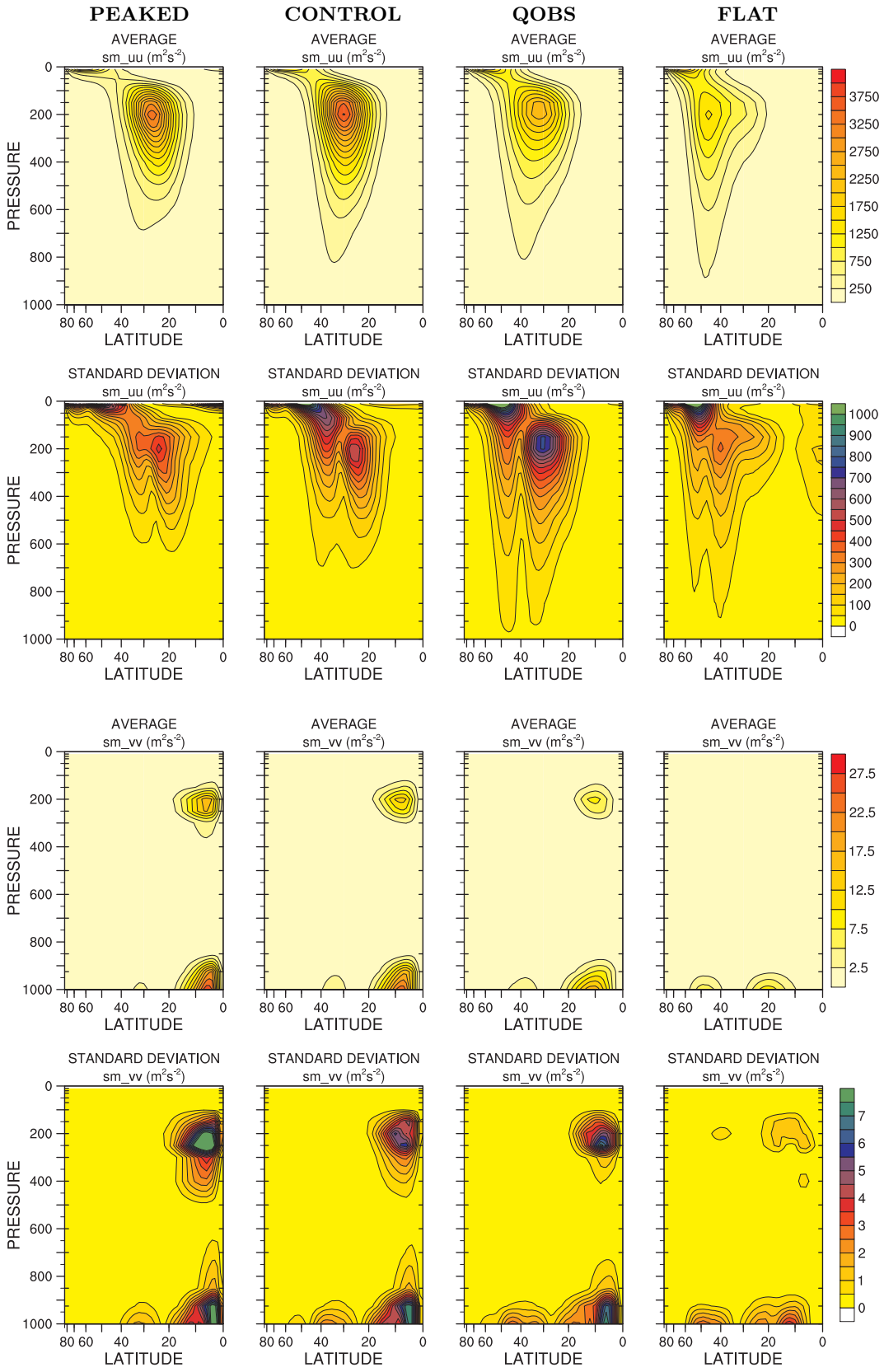

Figure 5.119: Multi-model mean and standard deviation, stationary mean, sm_uu, $[\overline{u}]^2$ and sm_vv, $[\overline{v}]^2$ for PEAKED, CONTROL, QOBS and FLAT.

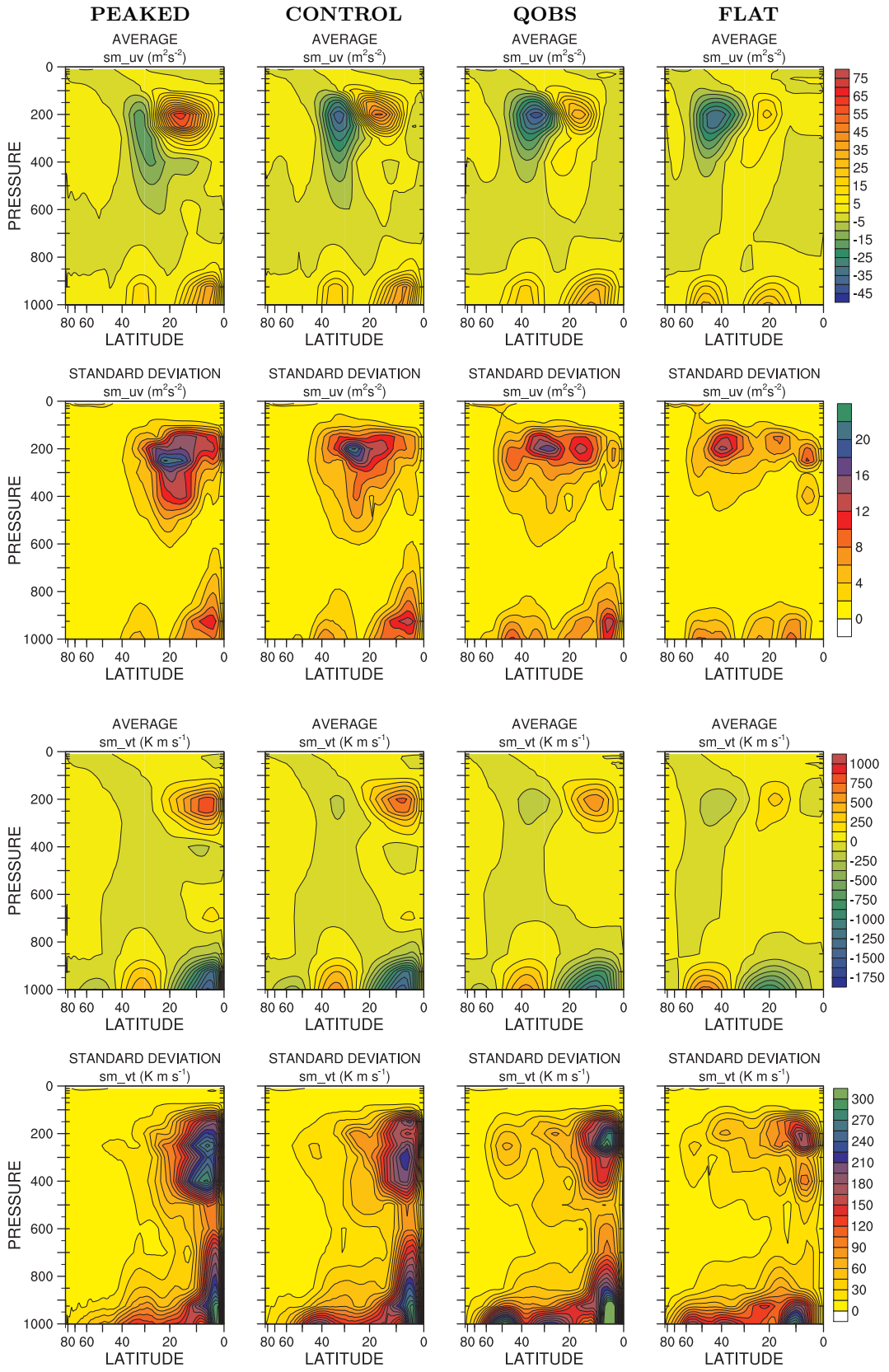

Figure 5.120: Multi-model mean and standard deviation, stationary mean, sm_uv, $[\overline{u}]\,[\overline{v}]$ and sm_vt, $[\overline{v}]\left[\overline{T}\right]$ for PEAKED, CONTROL, QOBS and FLAT.

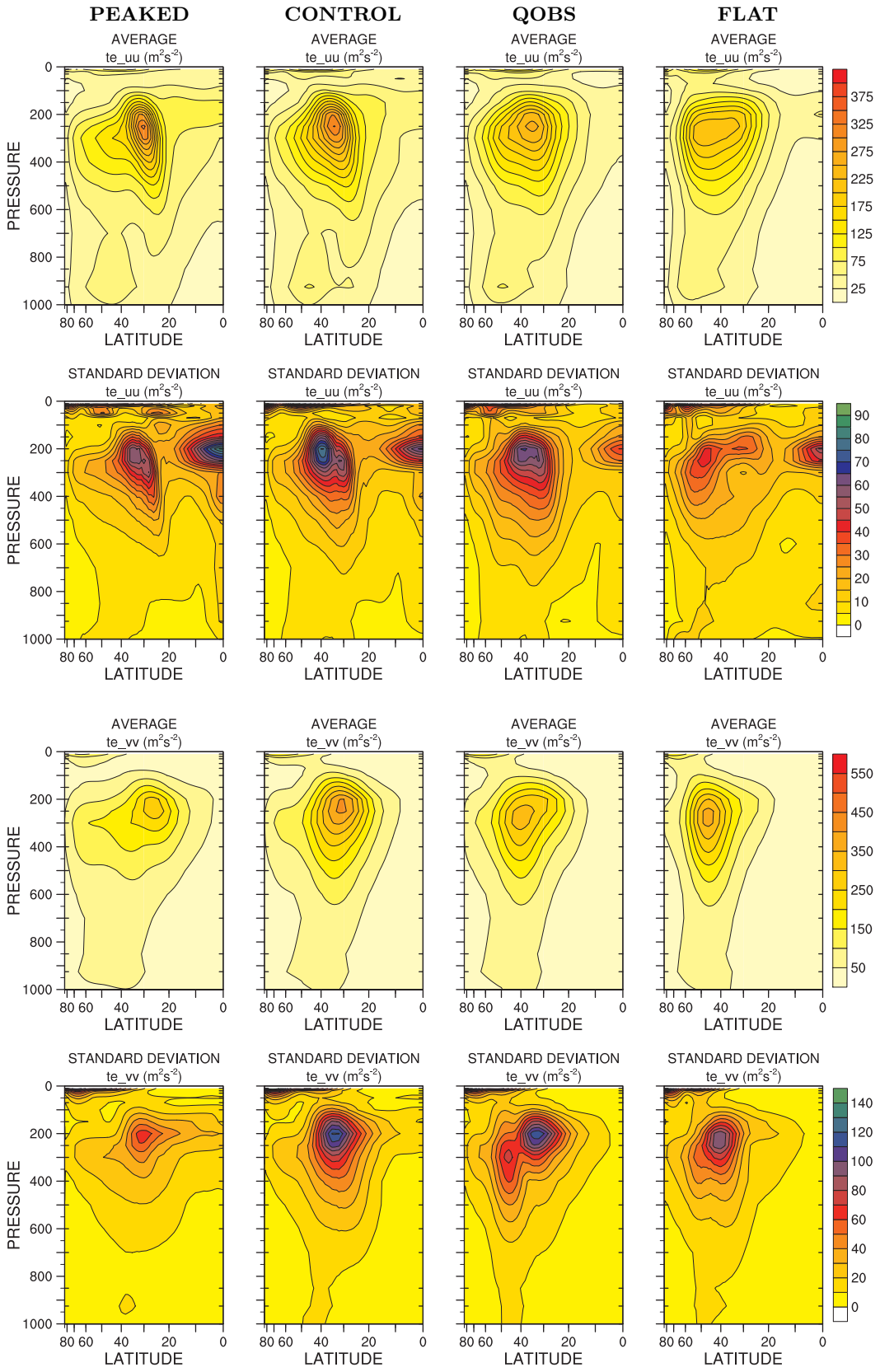

Figure 5.121: Multi-model mean and standard deviation, transient eddy, te_uu, $\overline{\left[(u'^*)^2\right]}$ and te_vv, $\overline{\left[(v'^*)^2\right]}$ for PEAKED, CONTROL, QOBS and FLAT.

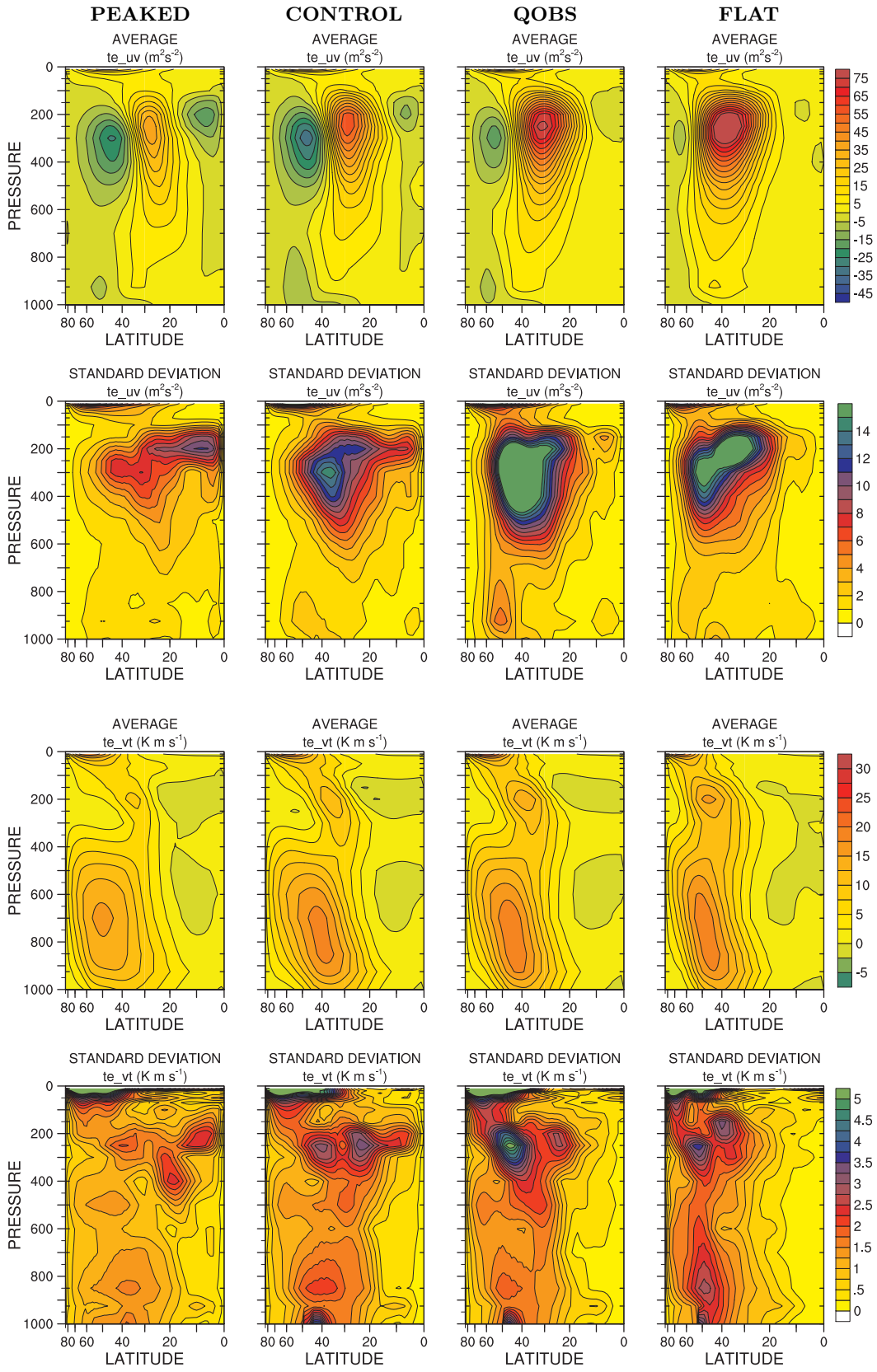

Figure 5.122: Multi-model mean and standard deviation, transient eddy, te_uv, $\overline{[u'^* v'^*]}$ and te_vt, $\overline{[v'^* T'^*]}$ for PEAKED, CONTROL, QOBS and FLAT.

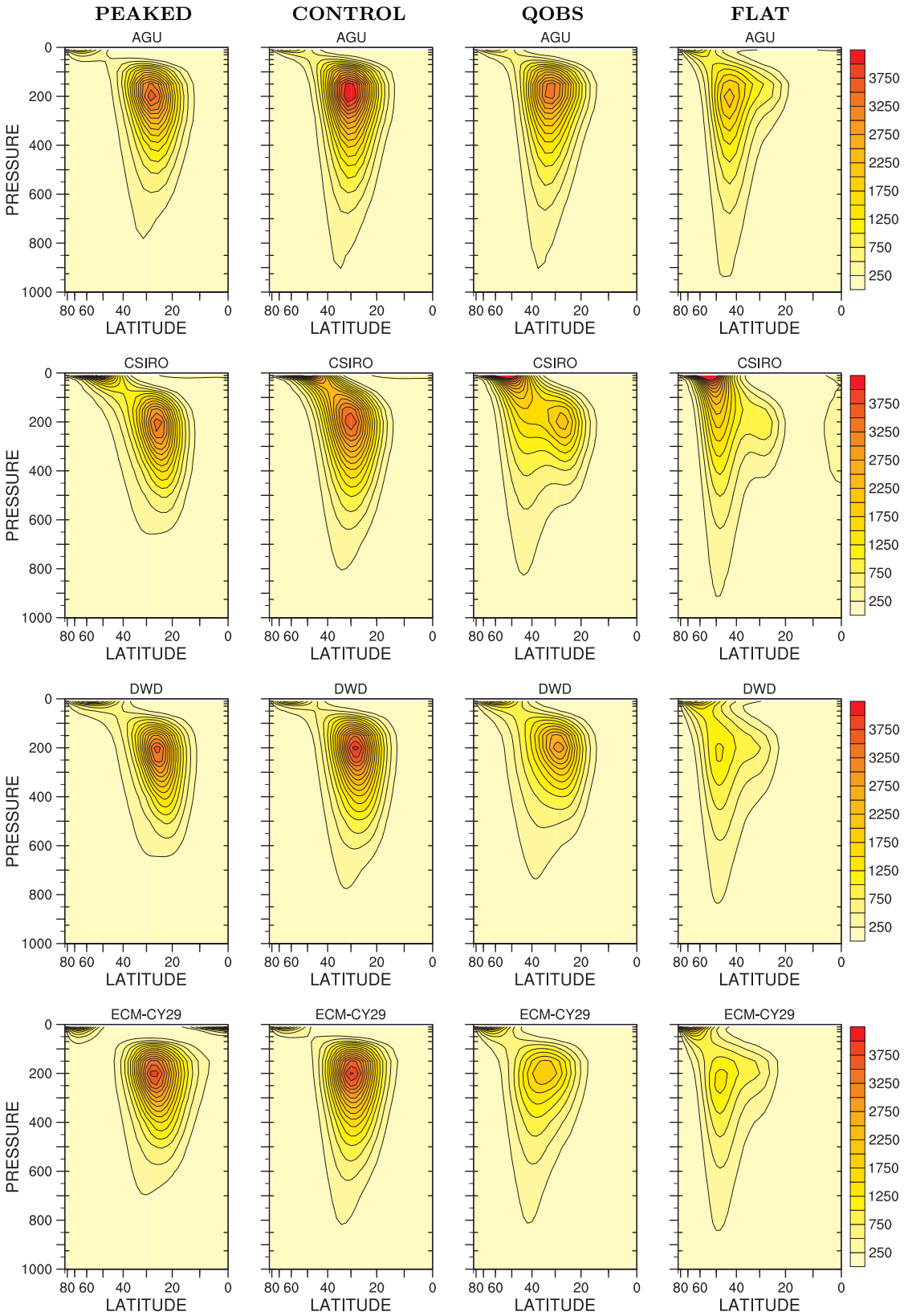

Figure 5.123: Individual model u variance, stationary mean, sm_uu, $[\overline{u}]^2$, $m^2\ s^{-2}$.

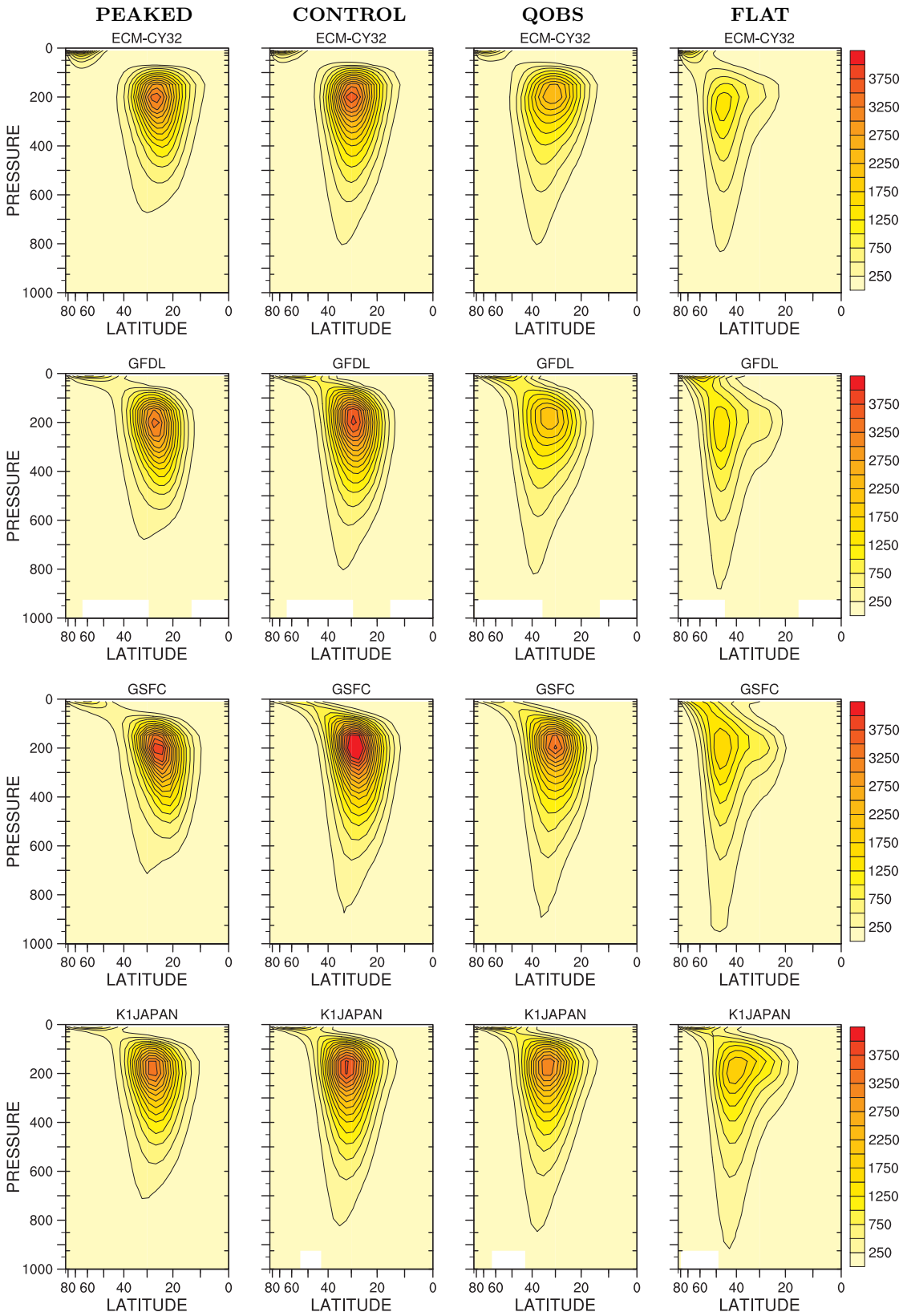

Figure 5.123 (continued): Individual model u variance, stationary mean, sm_uu, $[\overline{u}]^2$, $m^2\ s^{-2}$.

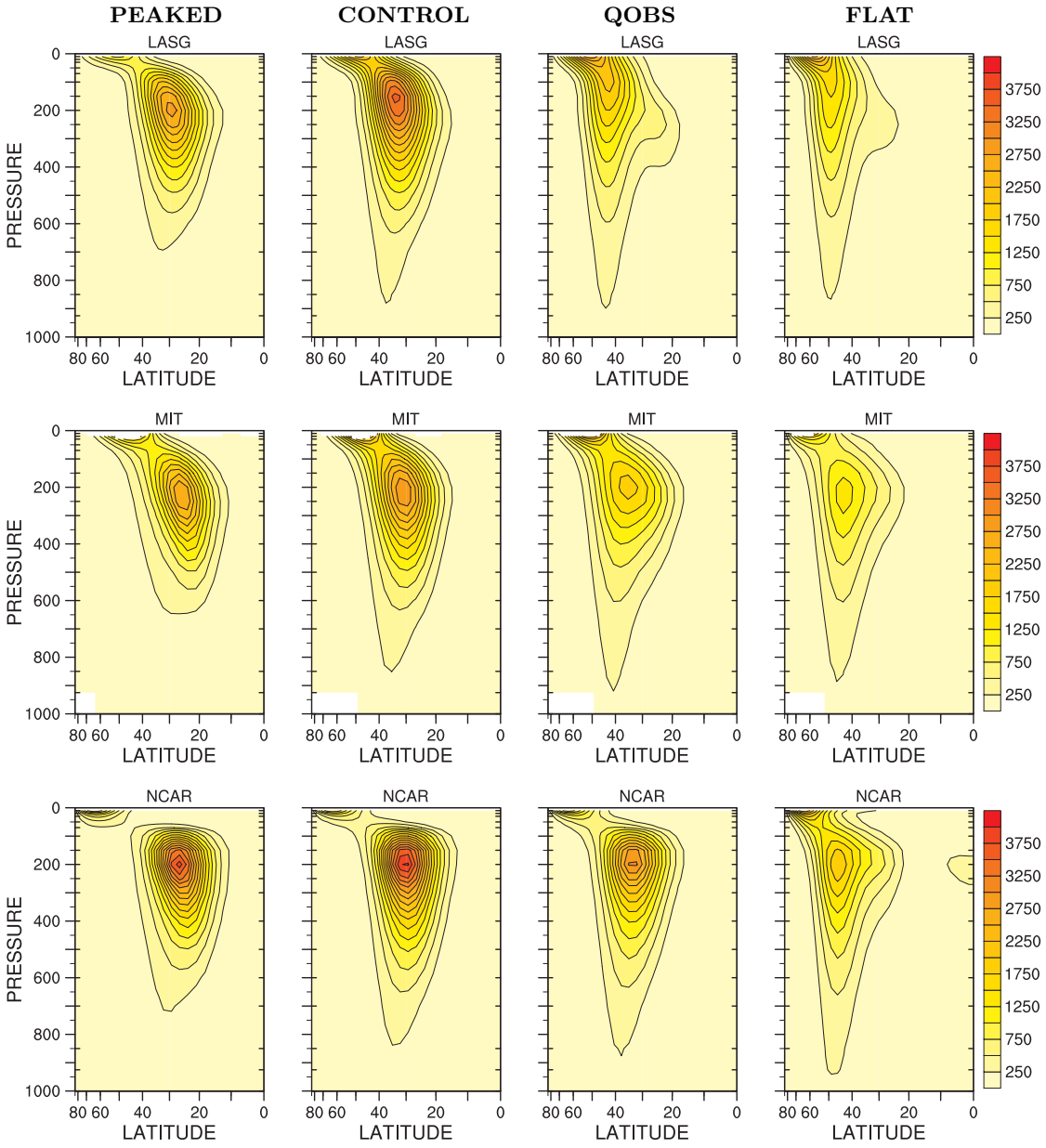

Figure 5.123 (continued): Individual model u variance, stationary mean, sm_uu, $[\overline{u}]^2$, $m^2\ s^{-2}$.

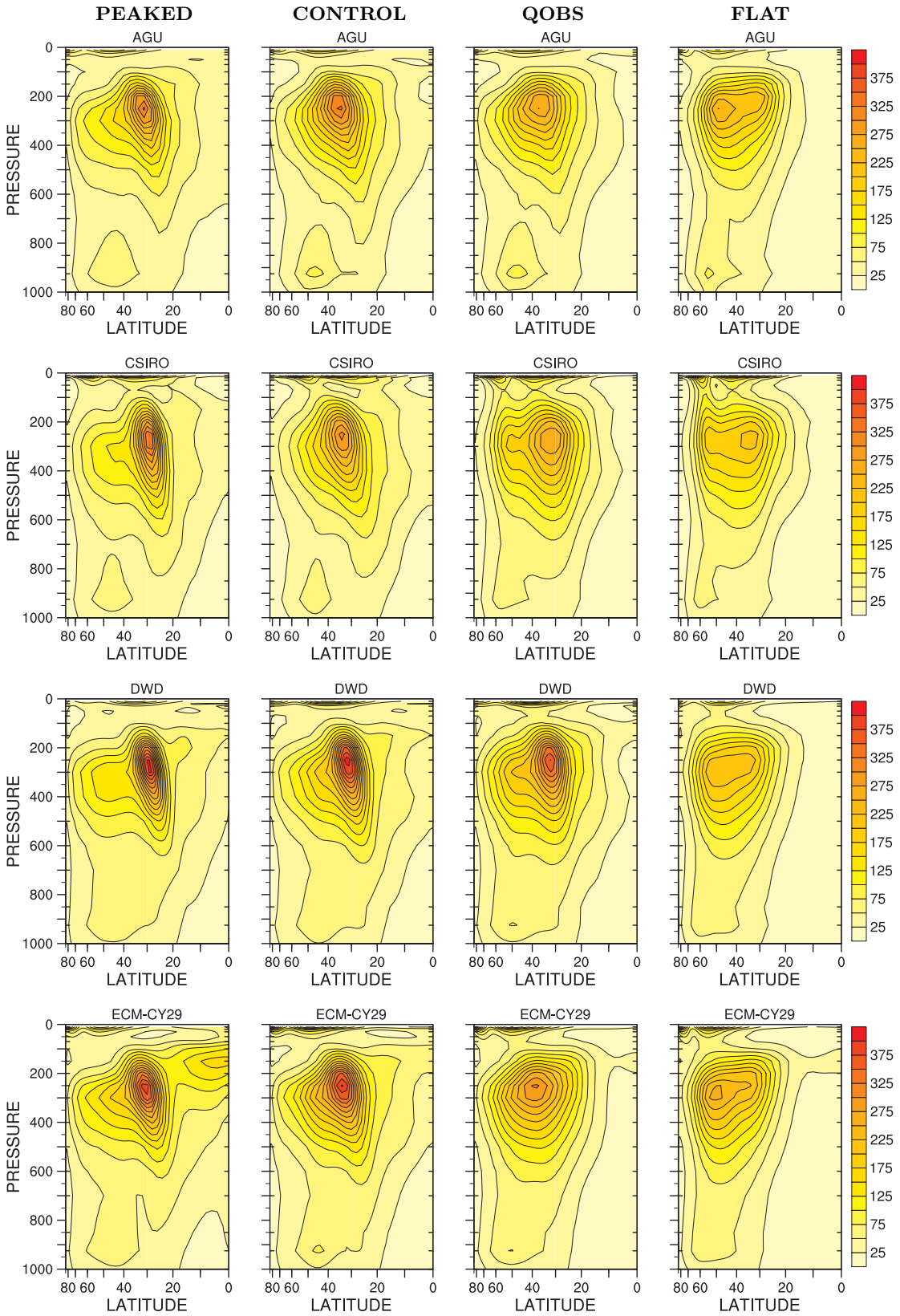

Figure 5.124: Individual model u variance, transient eddy, te_uu, $\overline{\left[(u'^*)^2\right]}$, $m^2\ s^{-2}$.

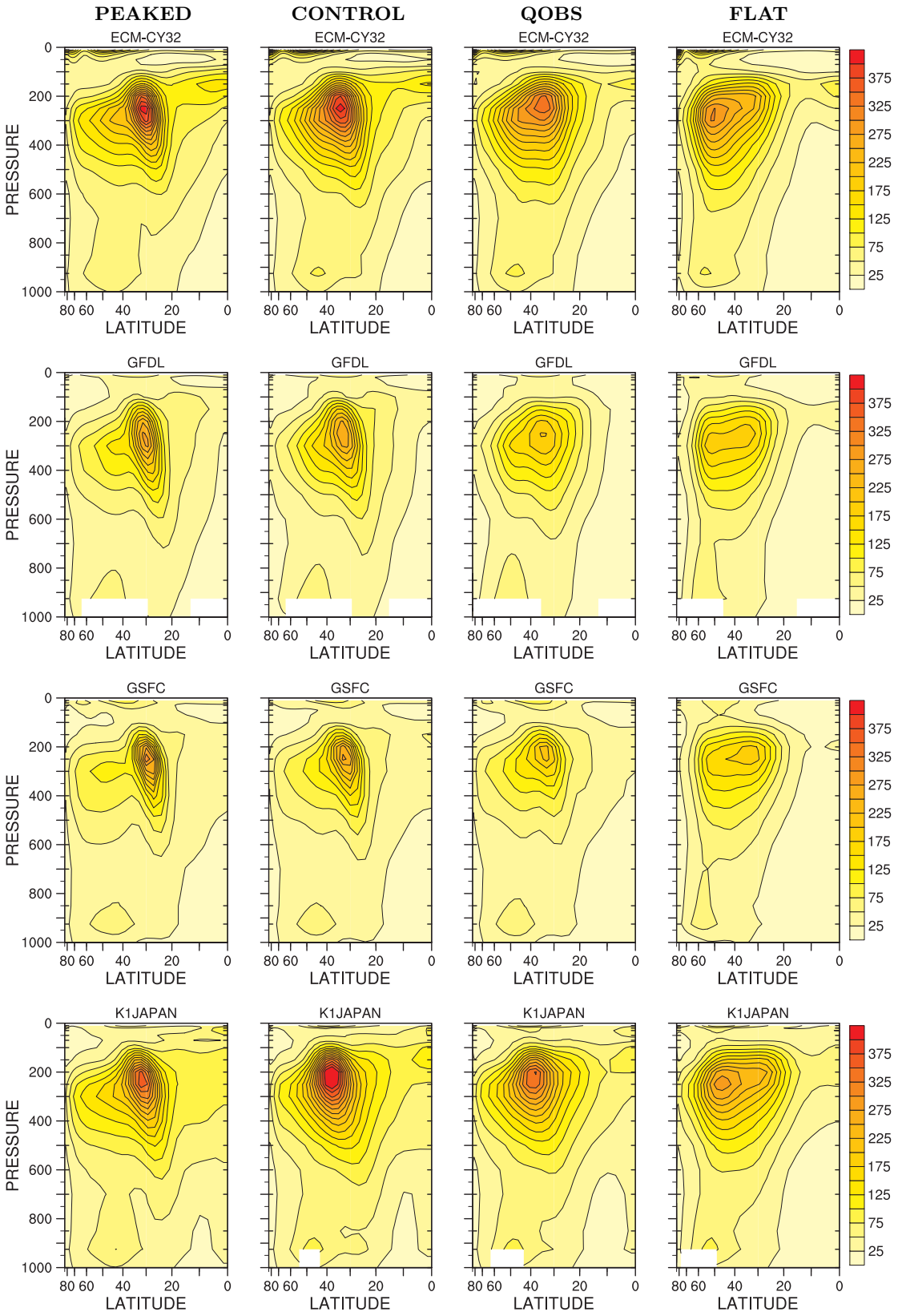

Figure 5.124 (continued): Individual model u variance, transient eddy, te_uu, $\overline{\left[(u'^*)^2\right]}$, $m^2\ s^{-2}$.

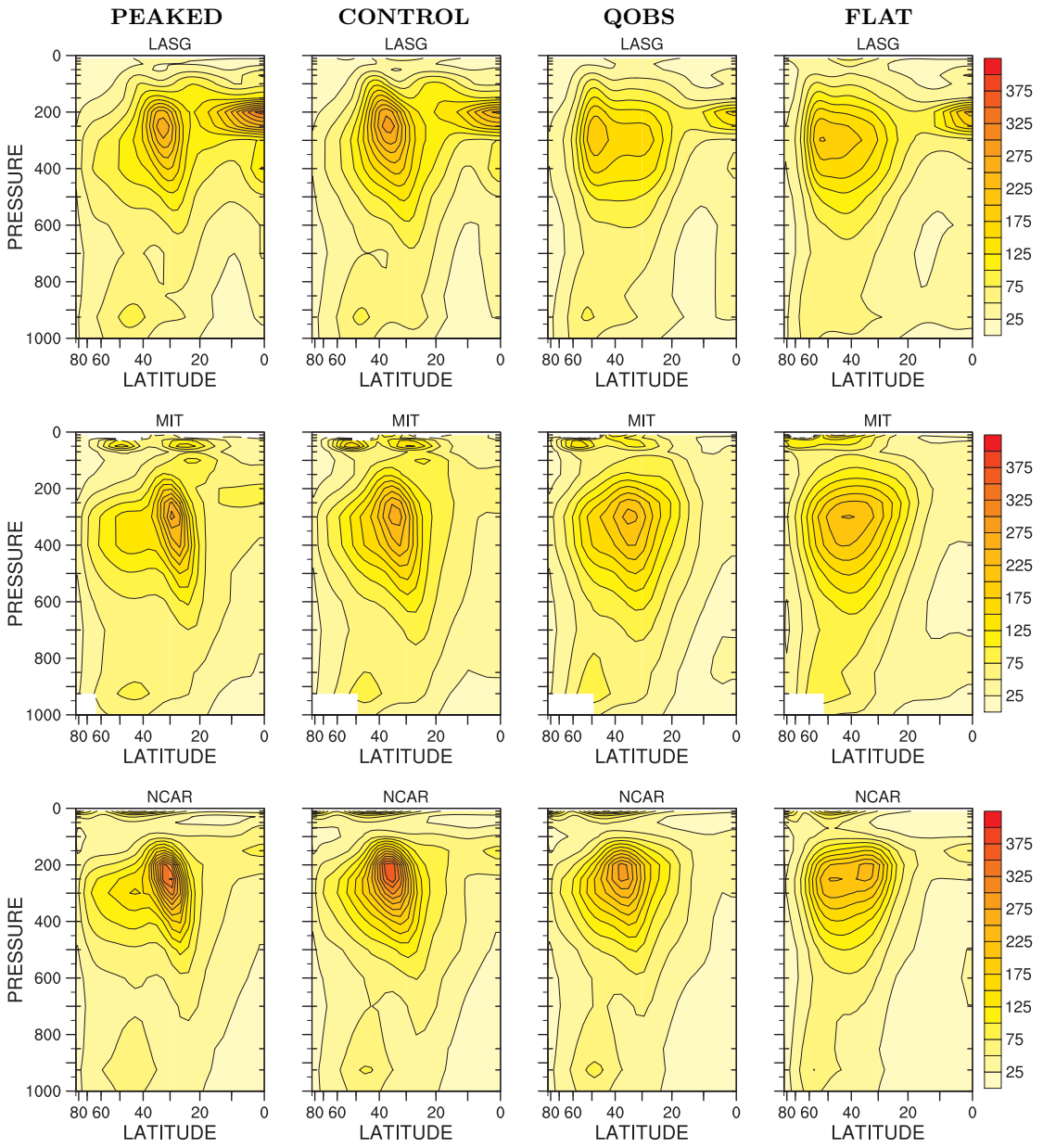

Figure 5.124 (continued): Individual model u variance, transient eddy, te_uu, $\left(\overline{\left[(u'^*)^2\right]}\right)$, $m^2\ s^{-2}$.

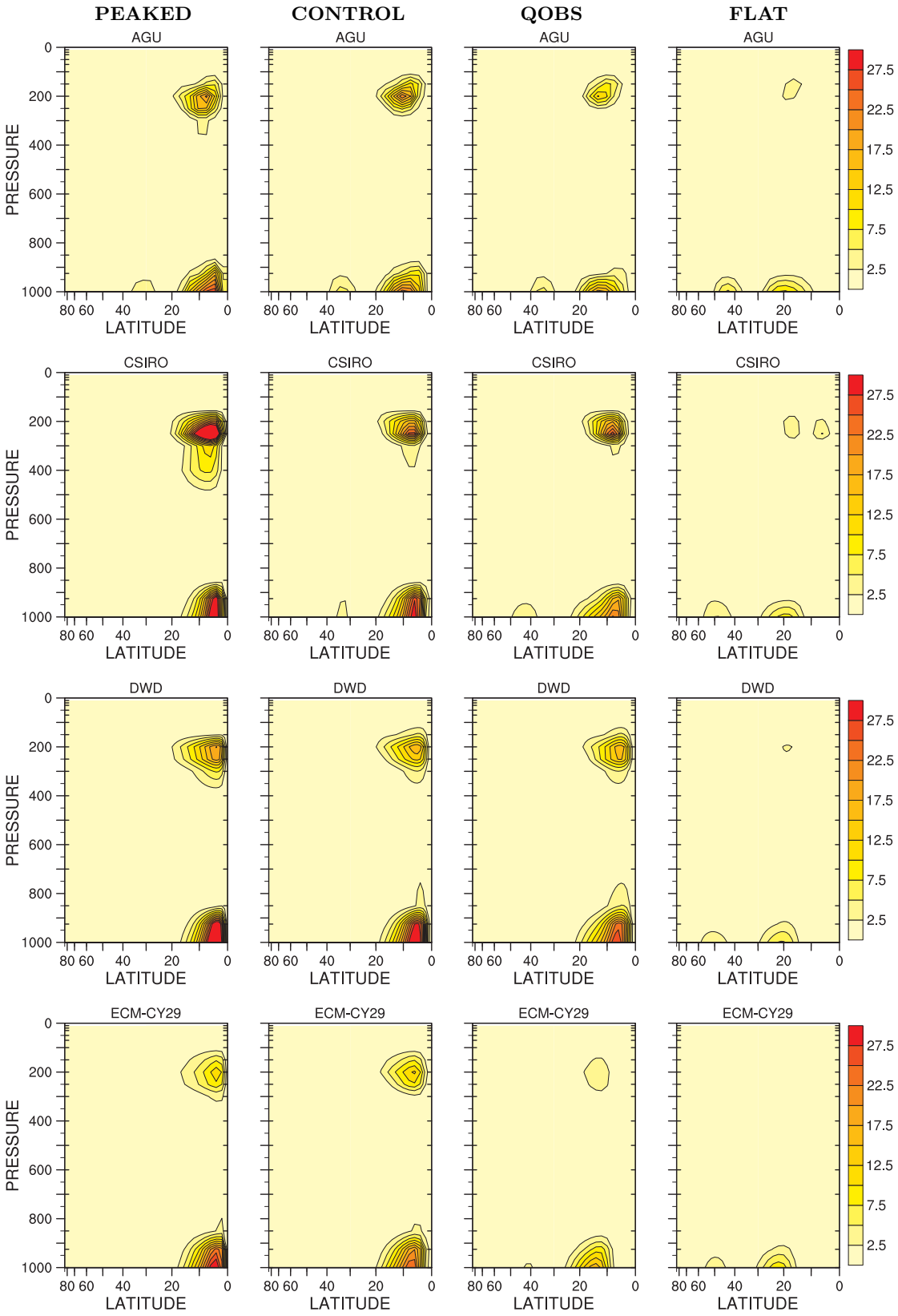

Figure 5.125: Individual model v variance, stationary mean, sm_vv, $[\overline{v}]^2$, $m^2\ s^{-2}$.

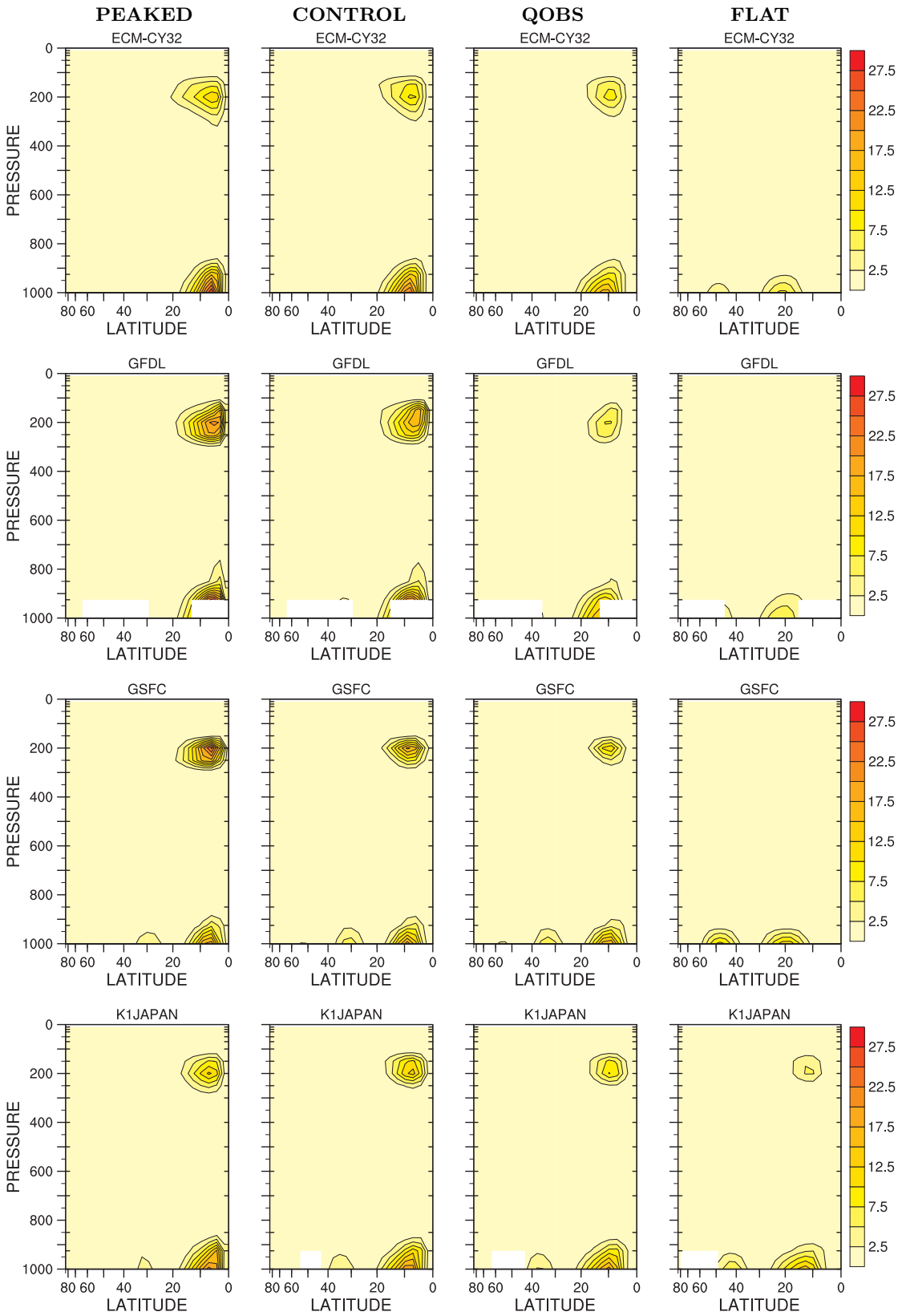

Figure 5.125 (continued): Individual model v variance, stationary mean, sm_vv, $[\overline{v}]^2$, $m^2\ s^{-2}$.

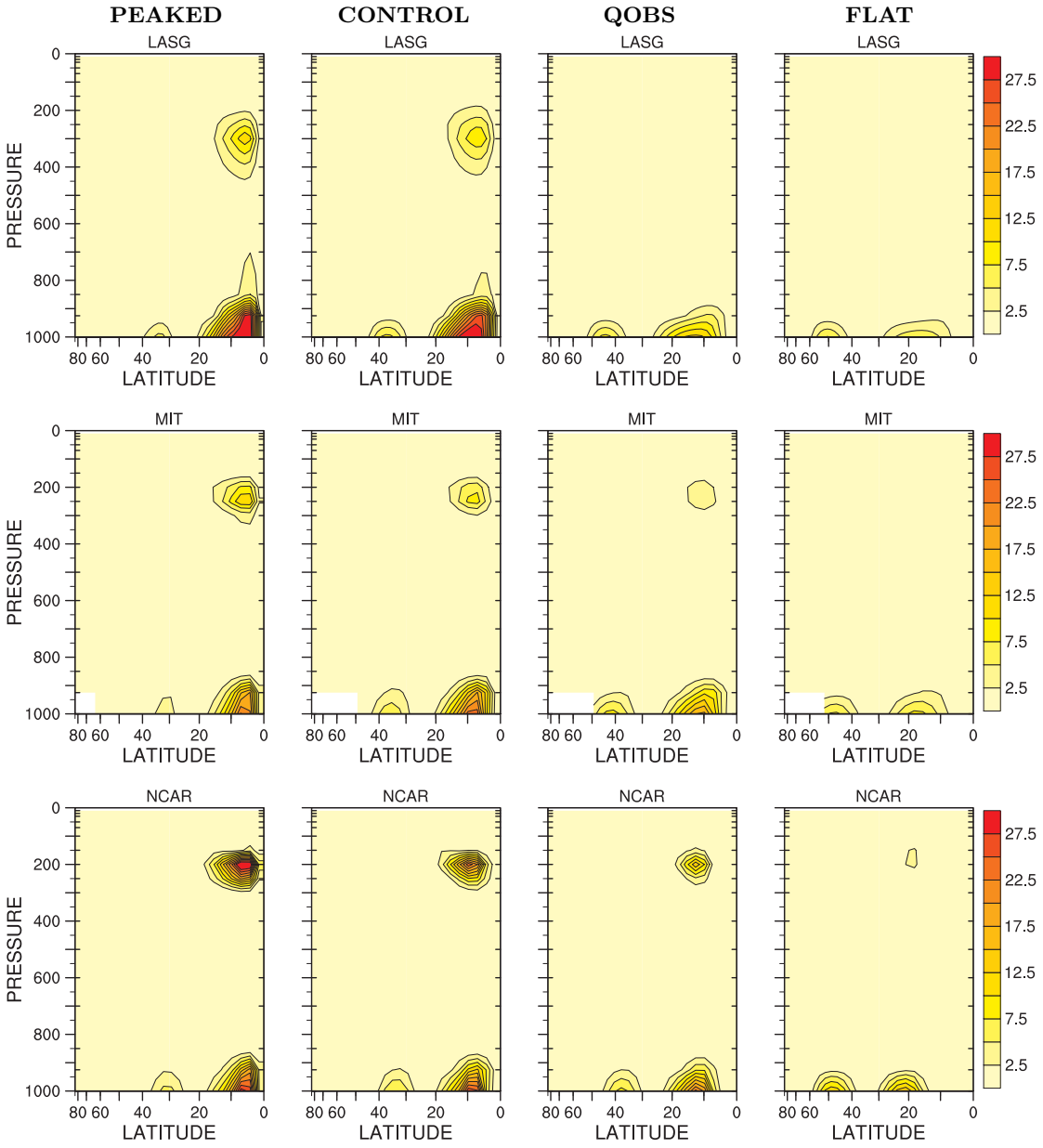

Figure 5.125 (continued): Individual model v variance, stationary mean, sm_vv, $[\overline{v}]^2$, m^2 s^{-2}.

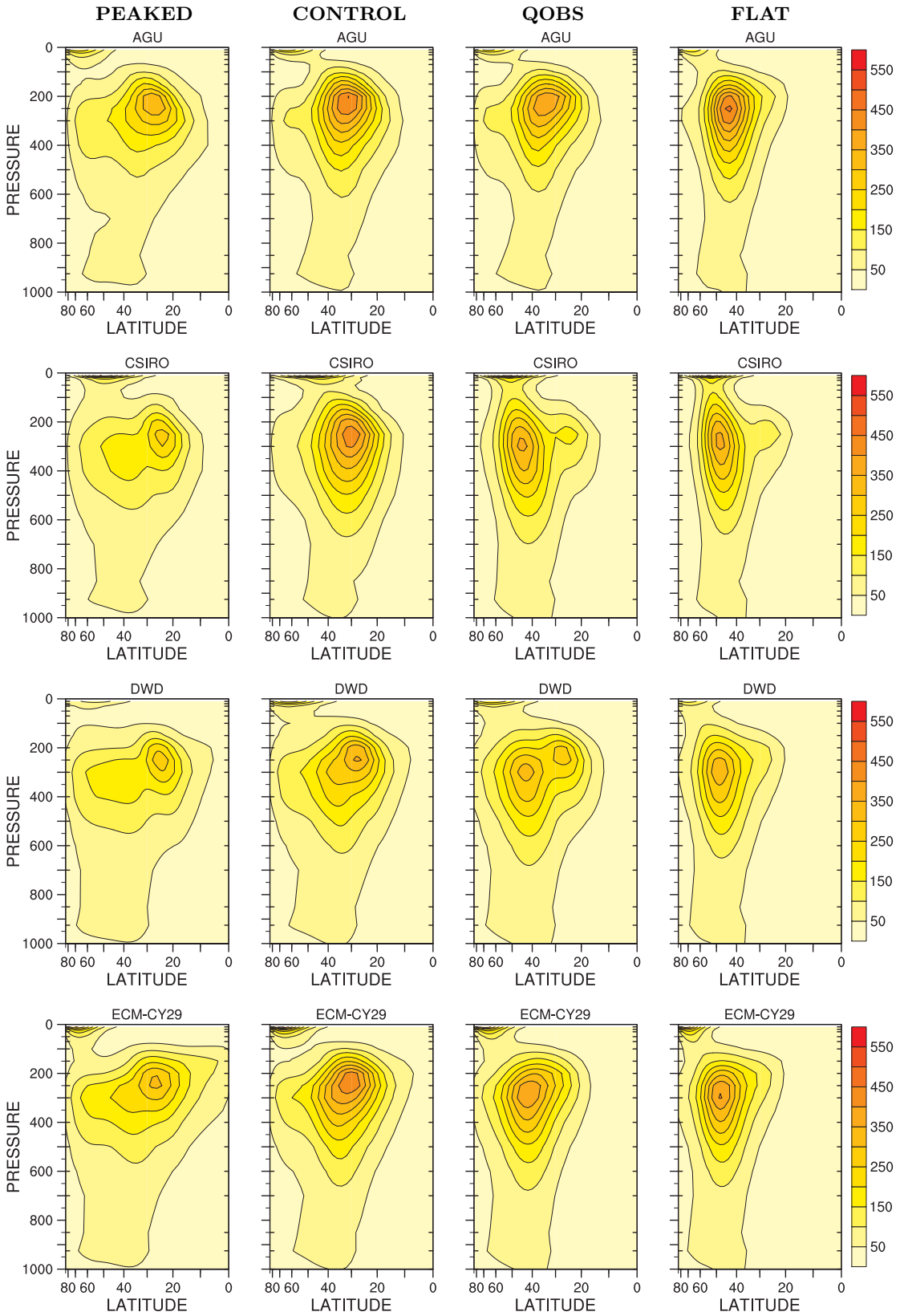

Figure 5.126: Individual model v variance, transient eddy, te_vv, $\overline{\left[(v'^*)^2\right]}$, m^2 s^{-2}.

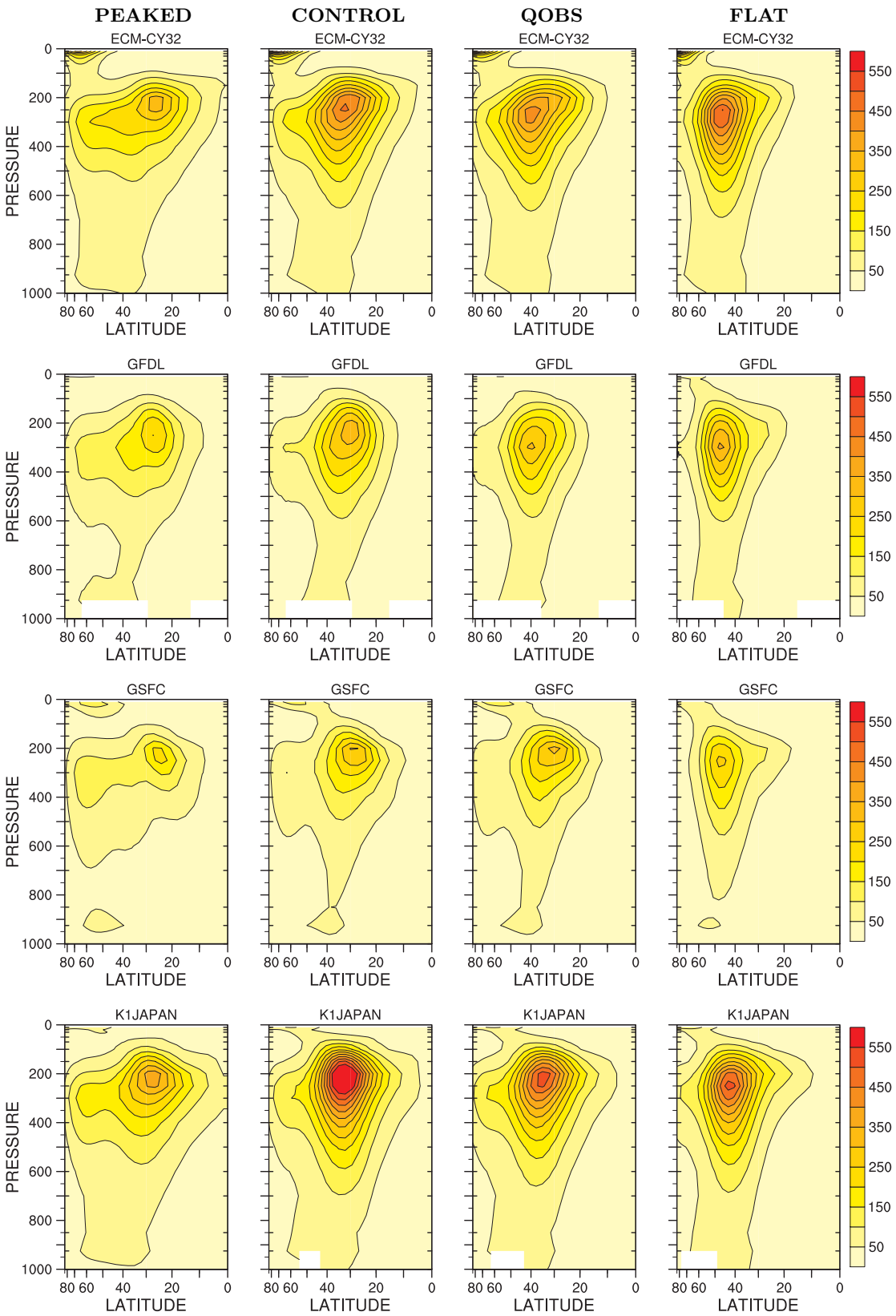

Figure 5.126 (continued): Individual model v variance, transient eddy, te_vv, $\overline{\left[(v'^{*})^{2}\right]}$, m^2 s^{-2}.

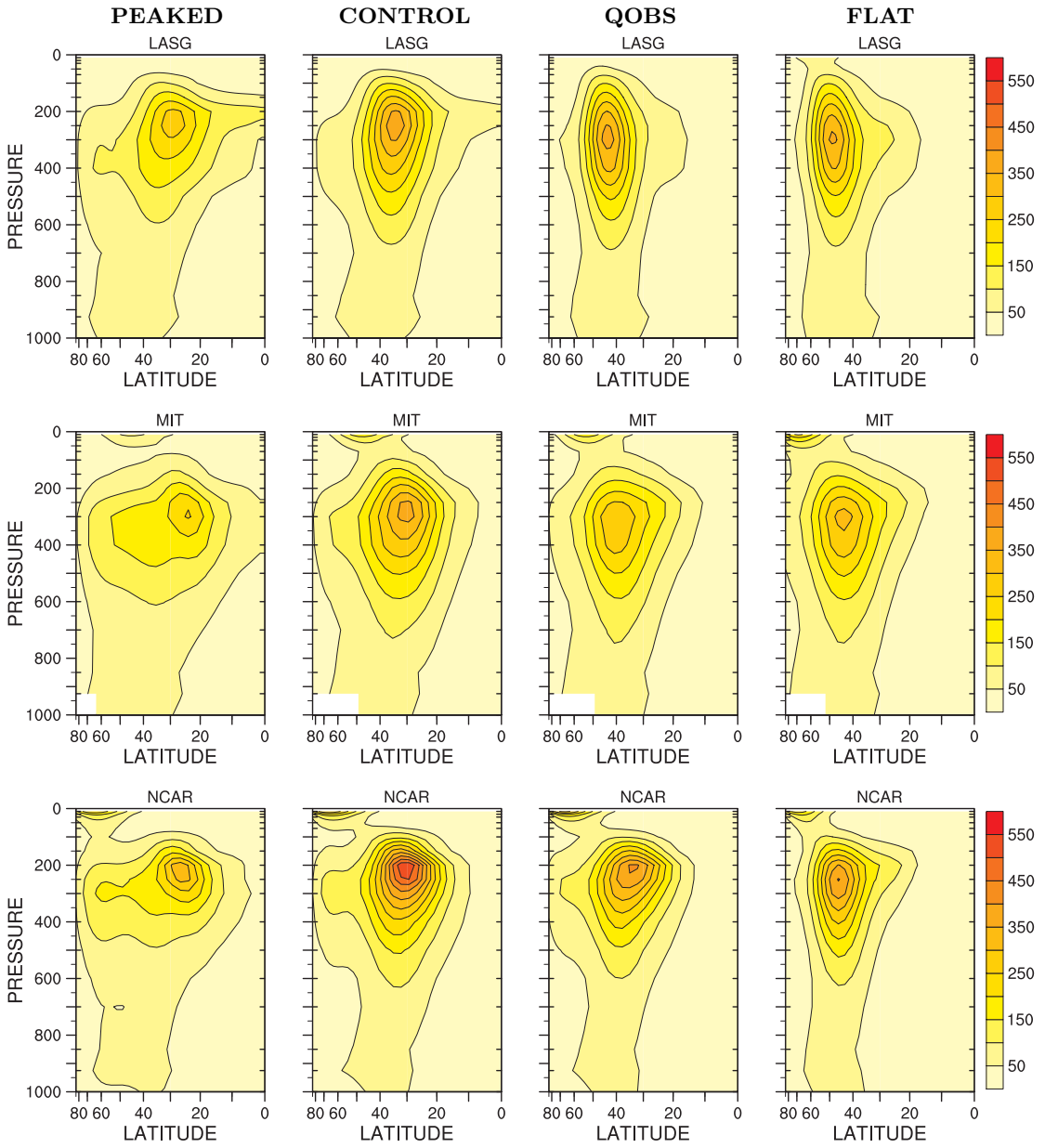

Figure 5.126 (continued): Individual model v variance, transient eddy, te_vv, $\overline{\left[(v'^*)^2\right]}$, m^2 s^{-2}.

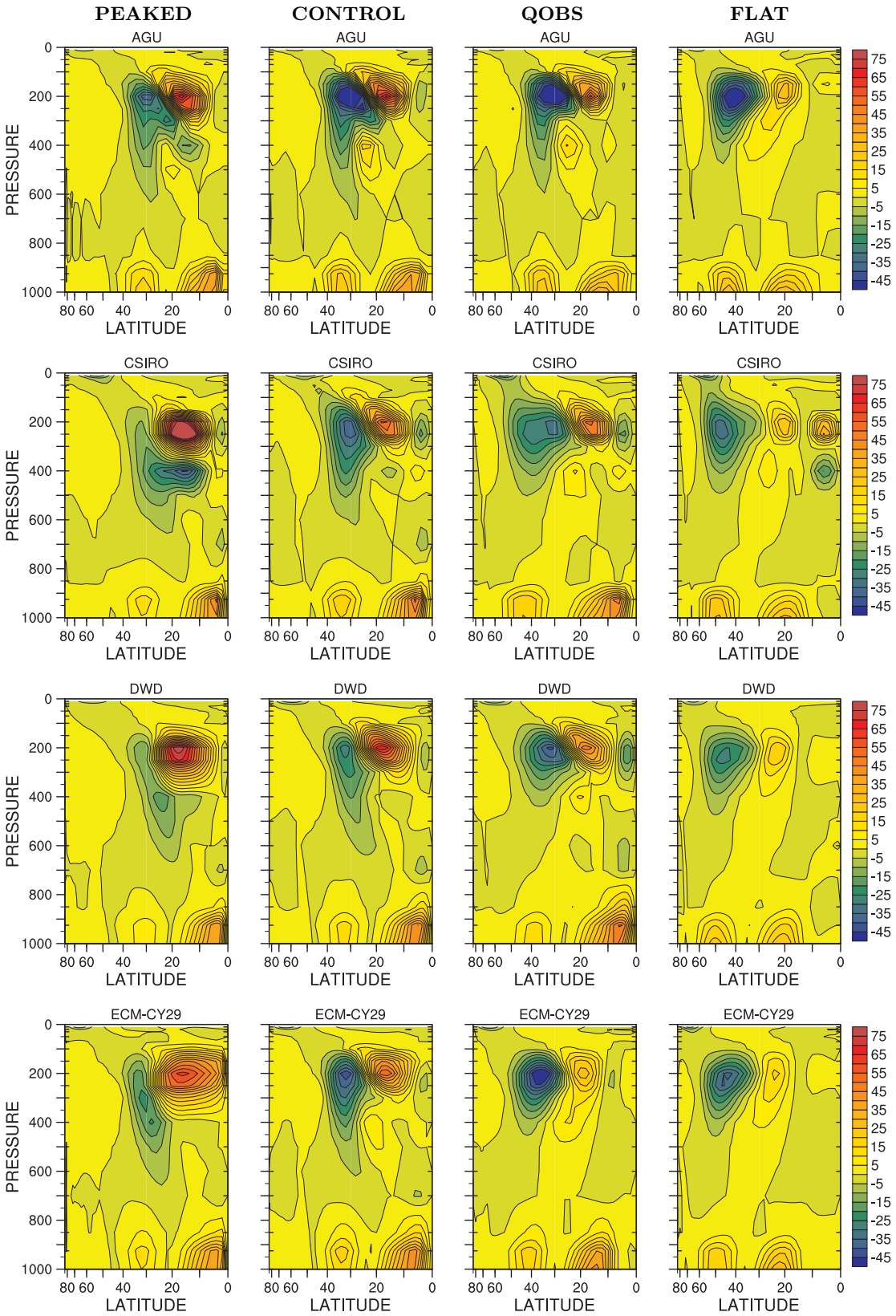

Figure 5.127: Individual model uv co-variance, stationary mean, sm_uv, $[\overline{u}]\,[\overline{v}]$, $\mathrm{m}^2\ \mathrm{s}^{-2}$.

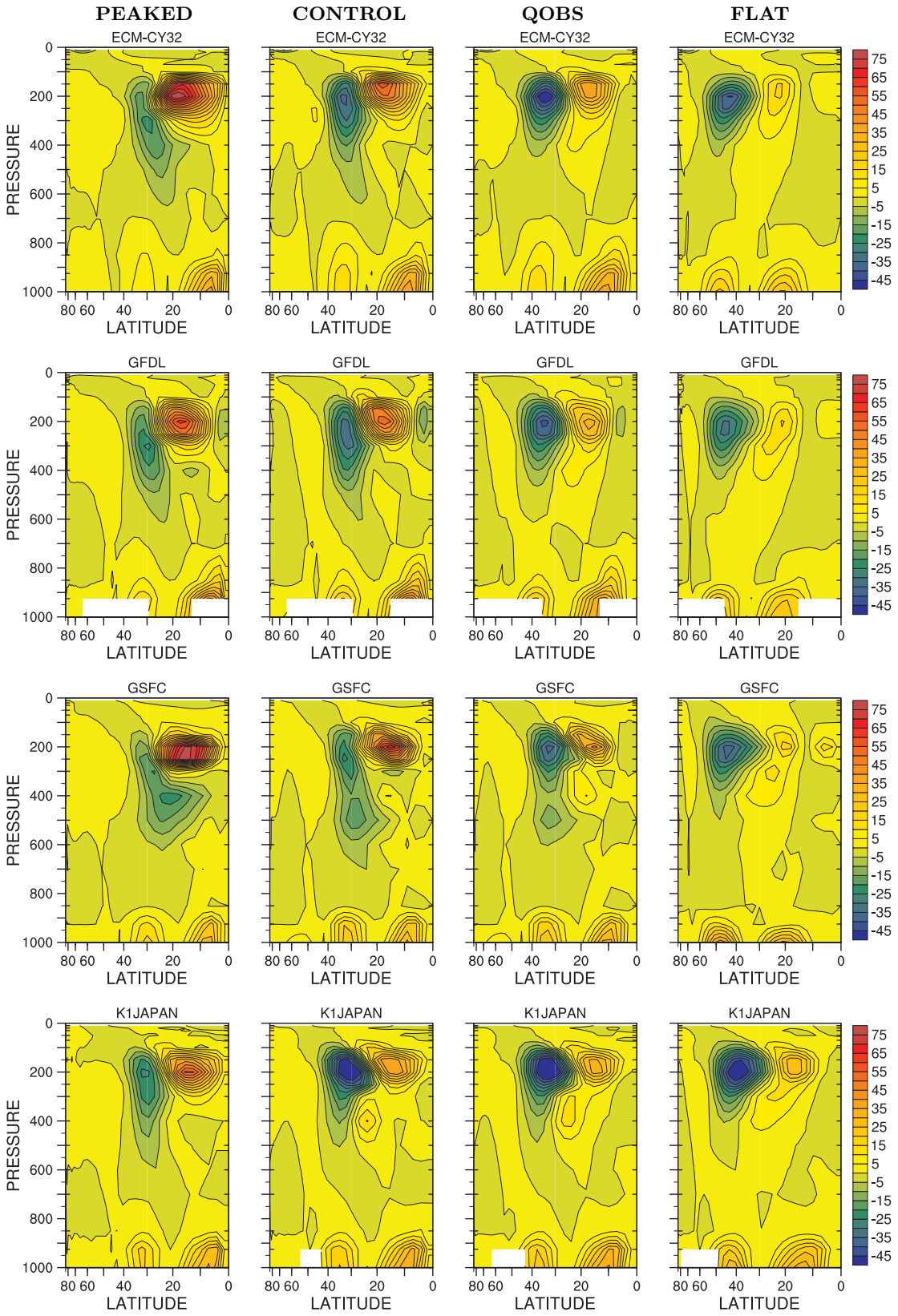

Figure 5.127 (continued): Individual model uv co-variance, stationary mean, sm_uv, $[\overline{u}]\,[\overline{v}]$, $m^2\ s^{-2}$.

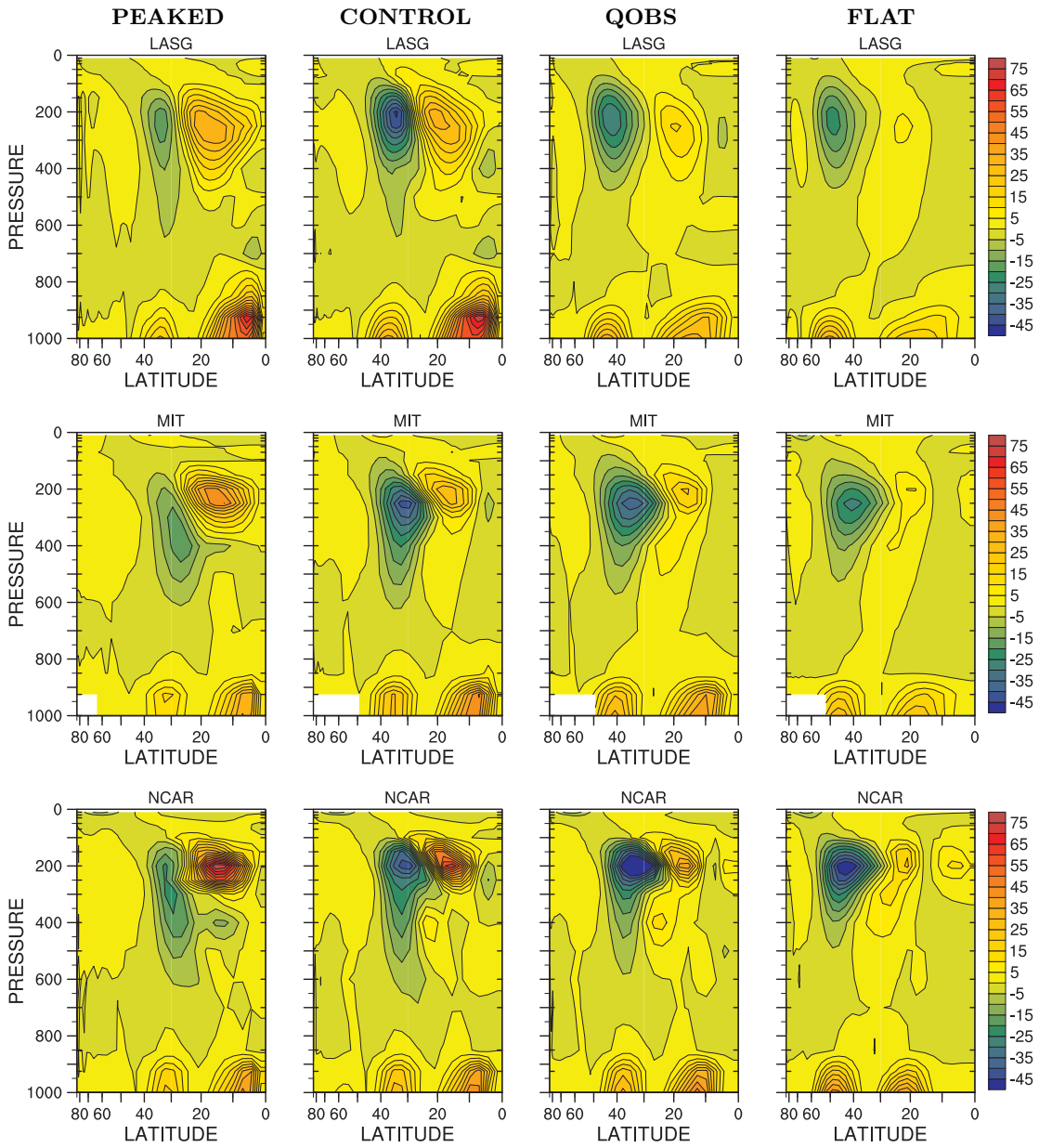

Figure 5.127 (continued): Individual model uv co-variance, stationary mean, sm_uv, $[\overline{u}]\,[\overline{v}]$, $m^2\ s^{-2}$.

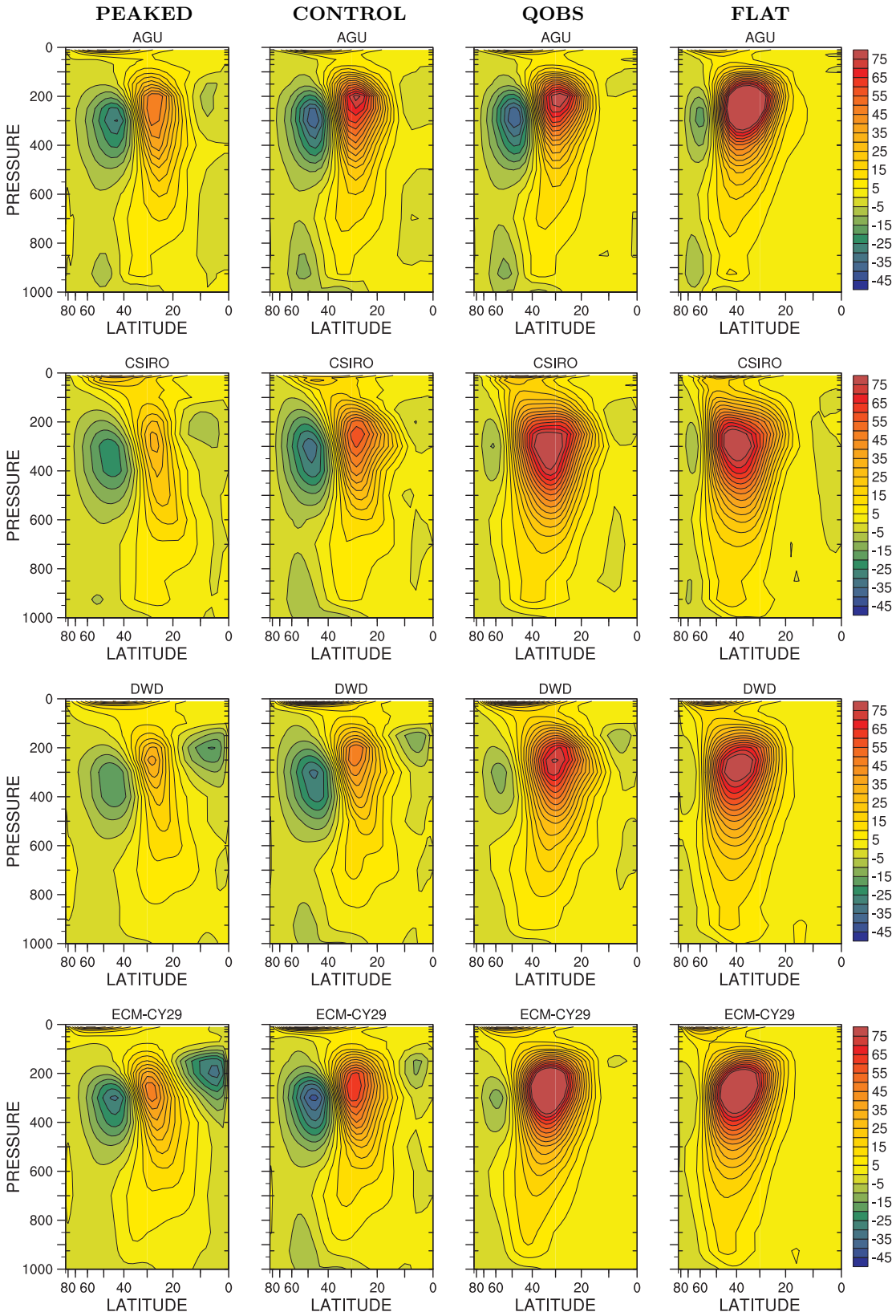

Figure 5.128: Individual model uv co-variance, transient eddy, te_uv, $\overline{[u'^* v'^*]}$, m^2 s^{-2}.

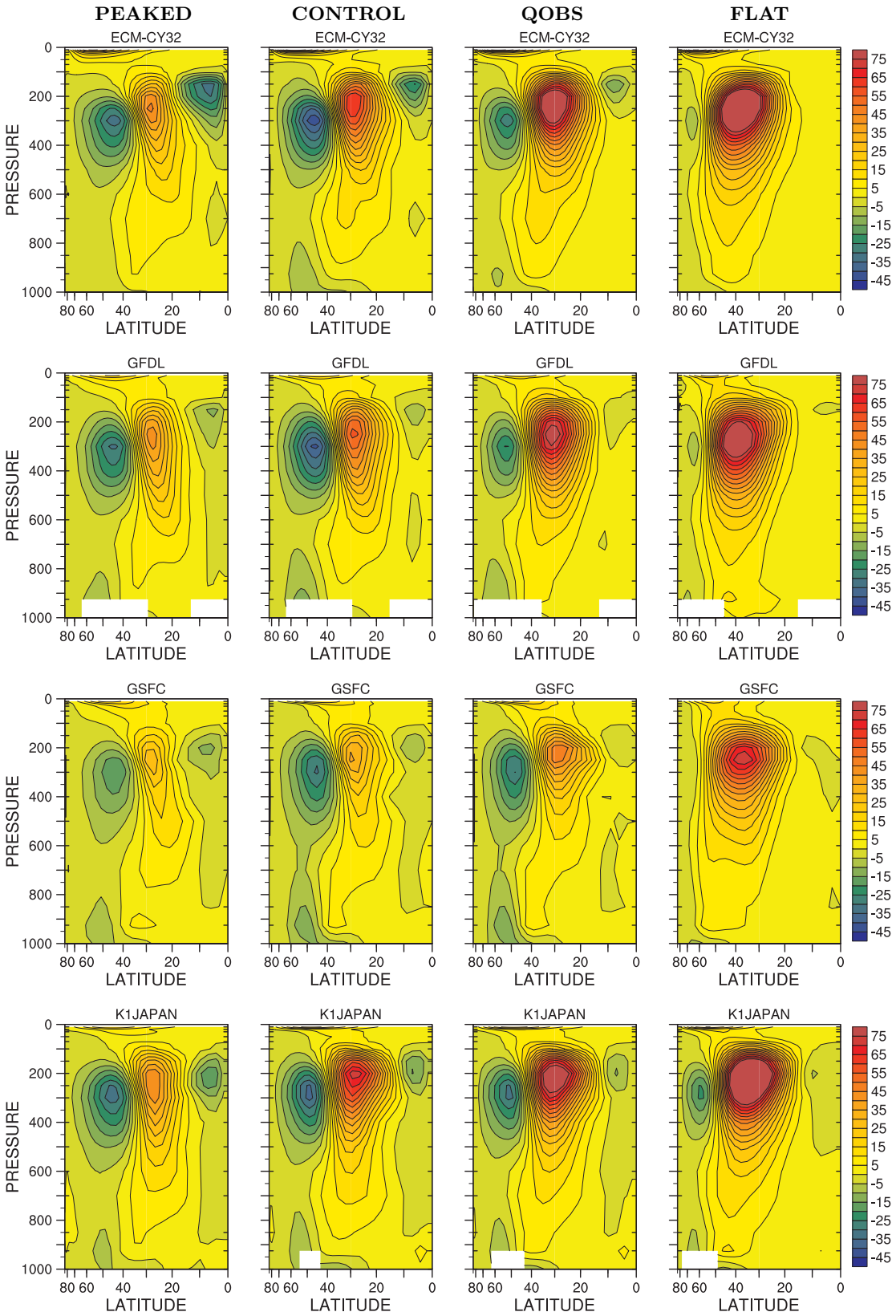

Figure 5.128 (continued): Individual model uv co-variance, transient eddy, te_uv, $\overline{[u'^* v'^*]}$, $m^2\ s^{-2}$.

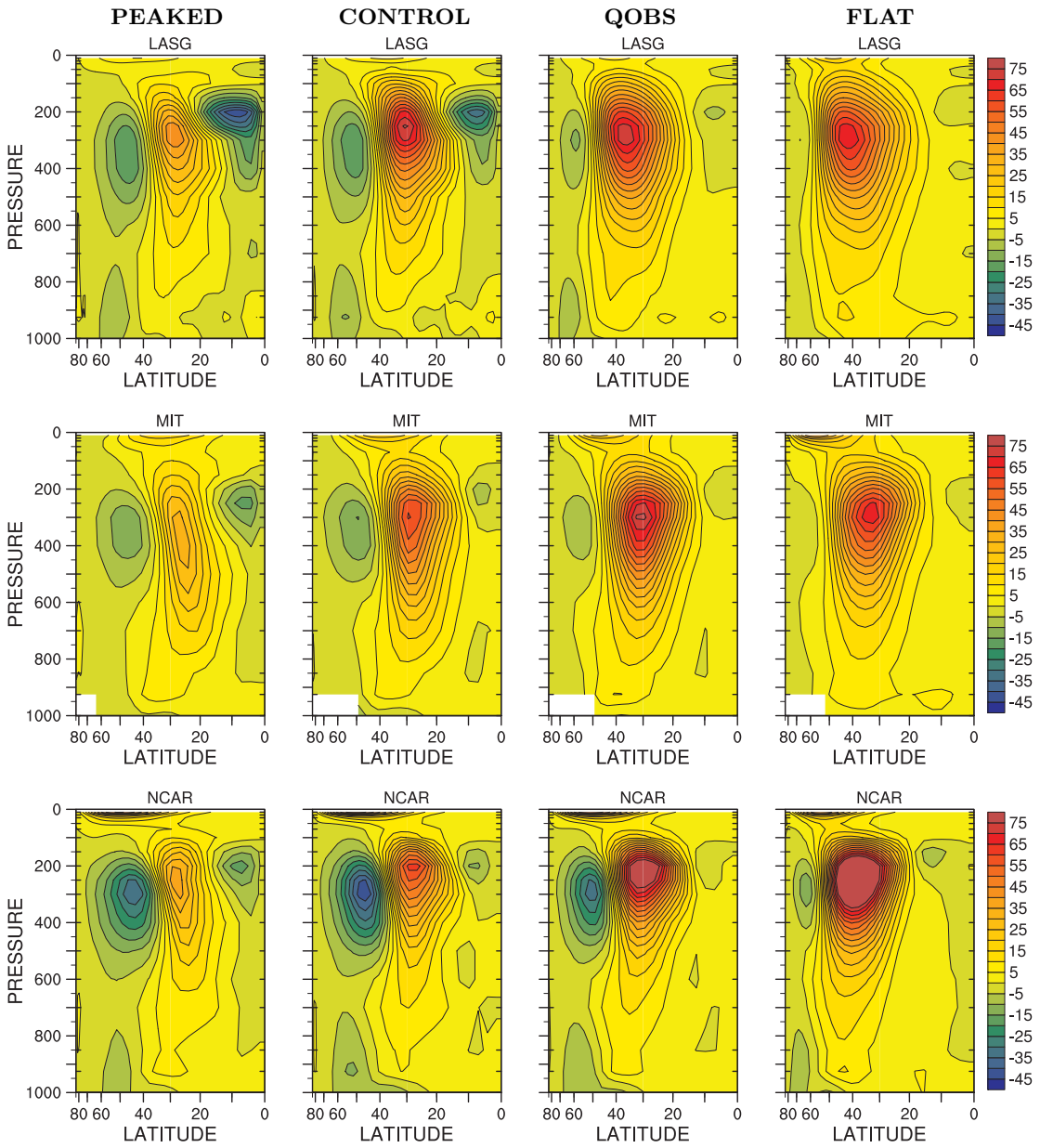

Figure 5.128 (continued): Individual model uv co-variance, transient eddy, te_uv, $\overline{[u'^* v'^*]}$, $m^2\ s^{-2}$.

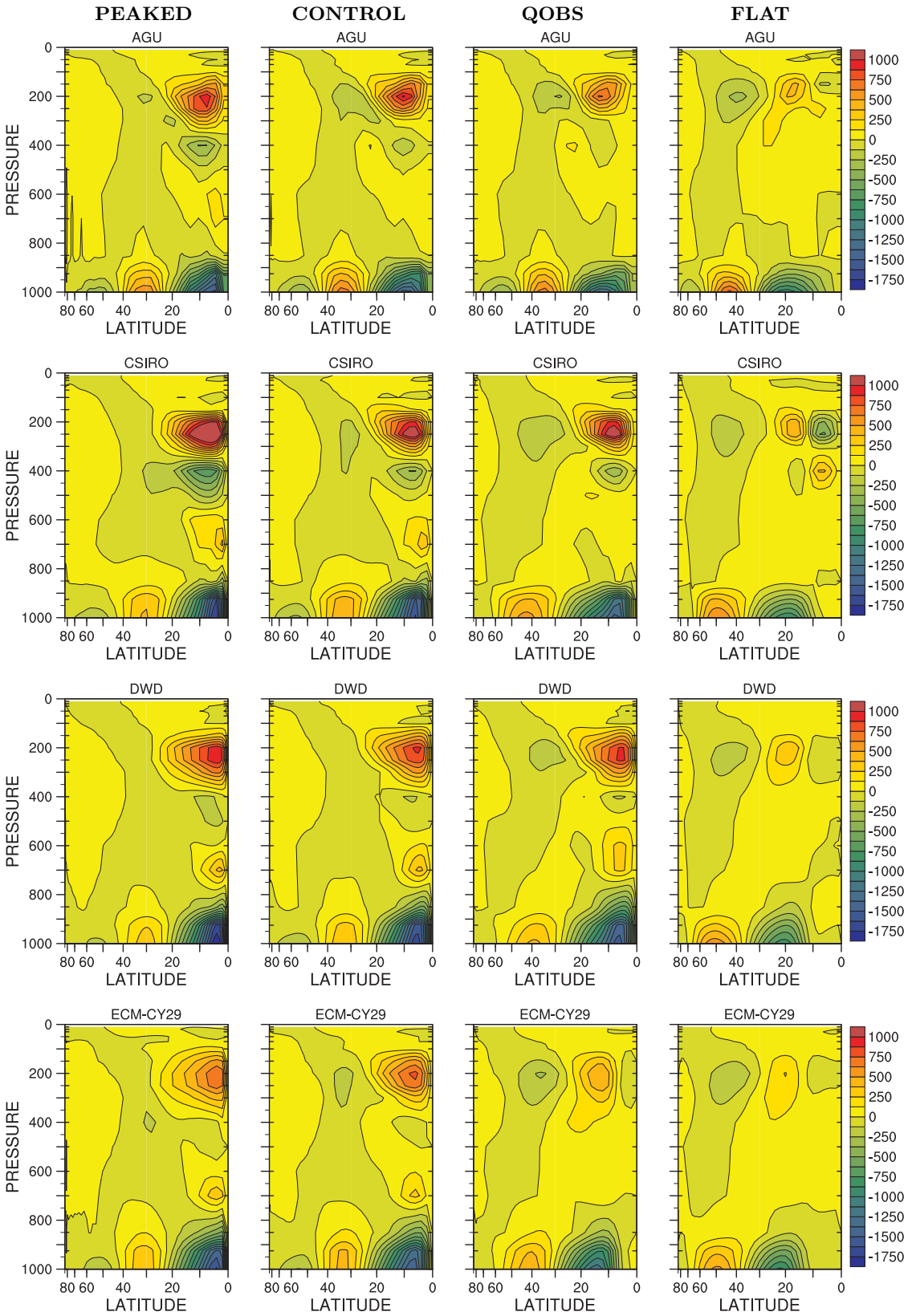

Figure 5.129: Individual model vT co-variance, stationary mean, sm_vt, $[\overline{v}]\left[\overline{T}\right]$, K m s^{-1}.

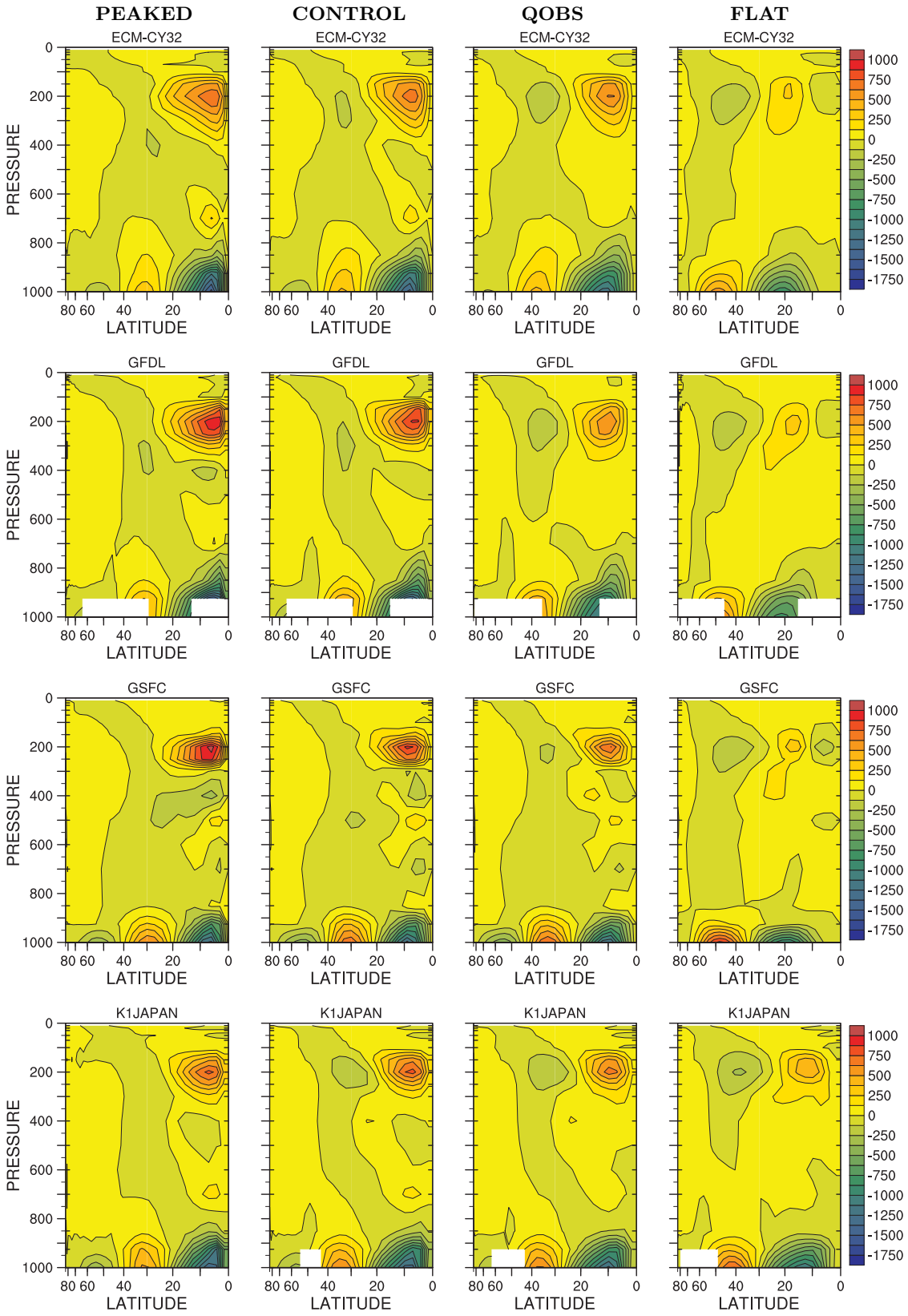

Figure 5.129 (continued): Individual model vT co-variance, stationary mean, sm_vt, $[\overline{v}]\left[\overline{T}\right]$, K m s^{-1}.

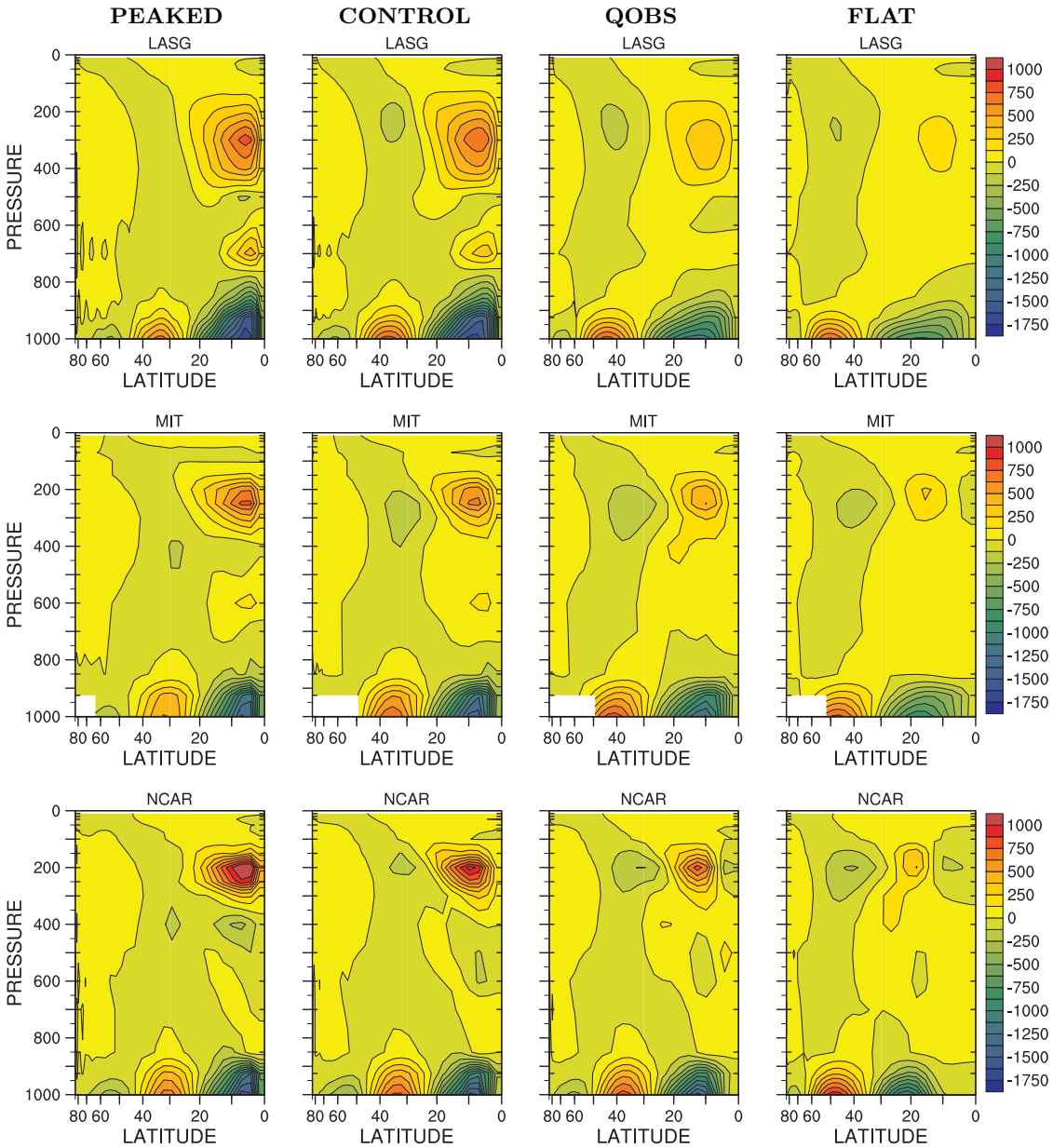

Figure 5.129 (continued): Individual model vT co-variance, stationary mean, sm_vt, $[\overline{v}]\left[\overline{T}\right]$, K m s^{-1}.

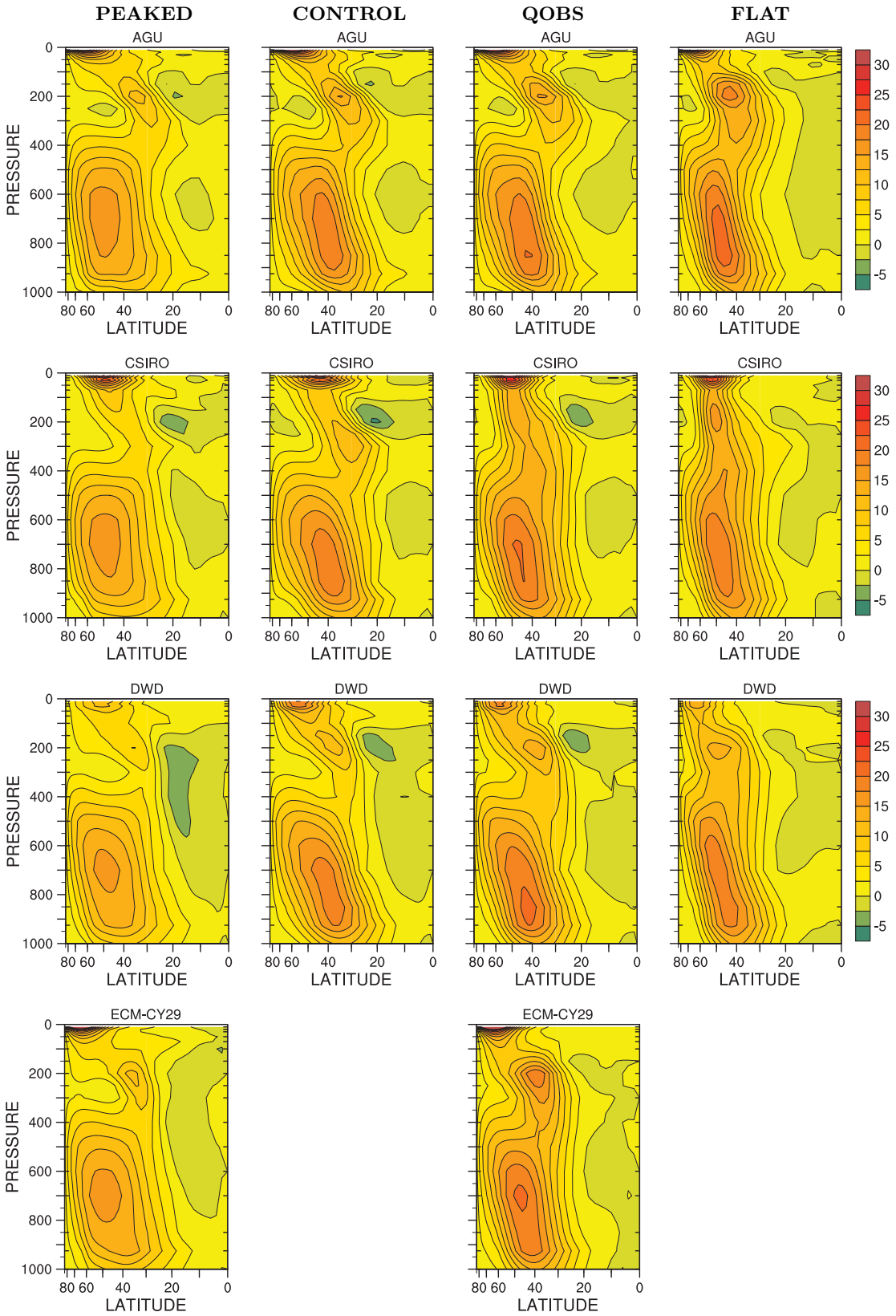

Figure 5.130: Individual model vT co-variance, transient eddy, te_vt, $\overline{[v^{*}T^{*}]}$, K m s^{-1}.

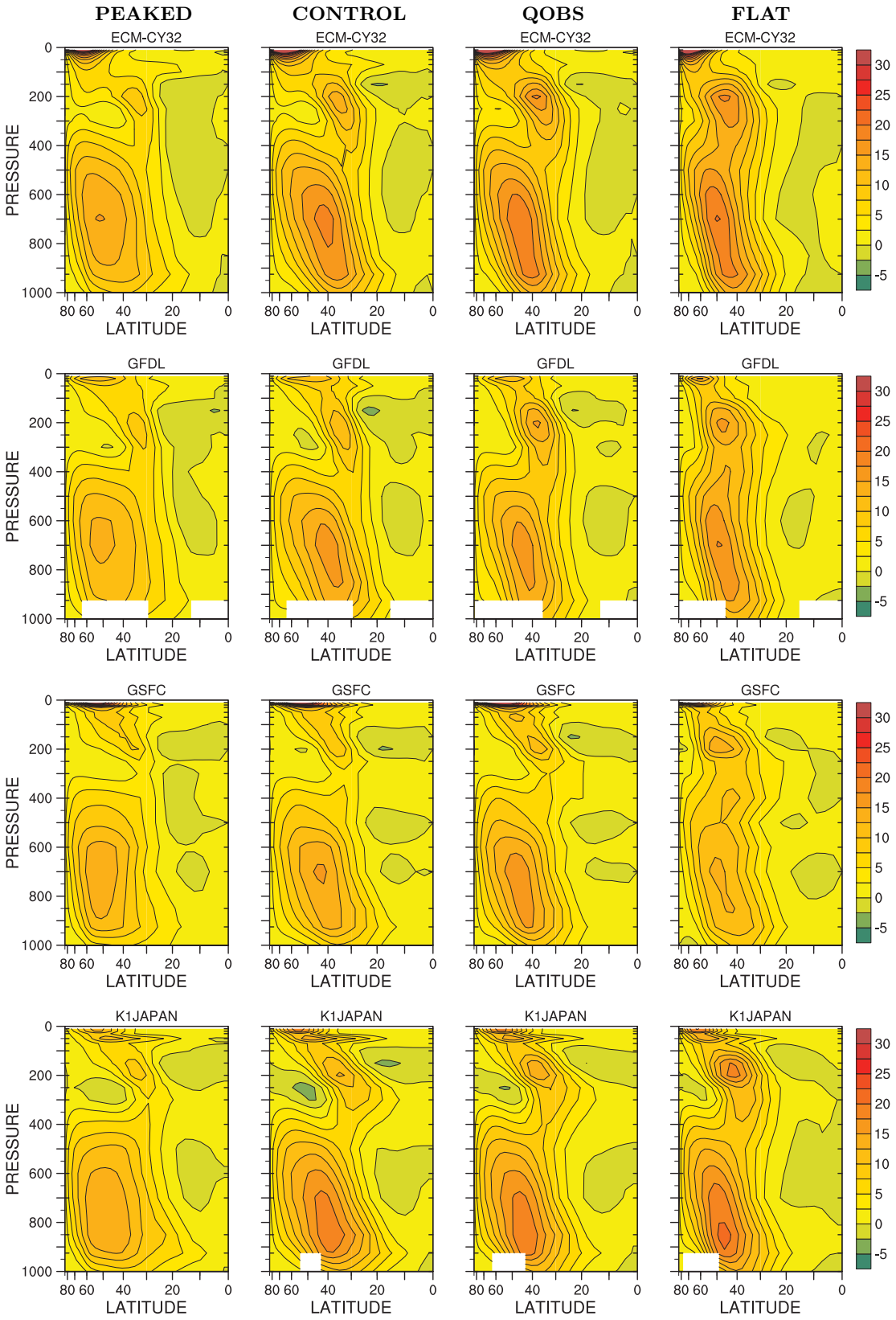

Figure 5.130 (continued): Individual model vT co-variance, transient eddy, te_vt, $\overline{[v'^* T'^*]}$, K m s^{-1}.

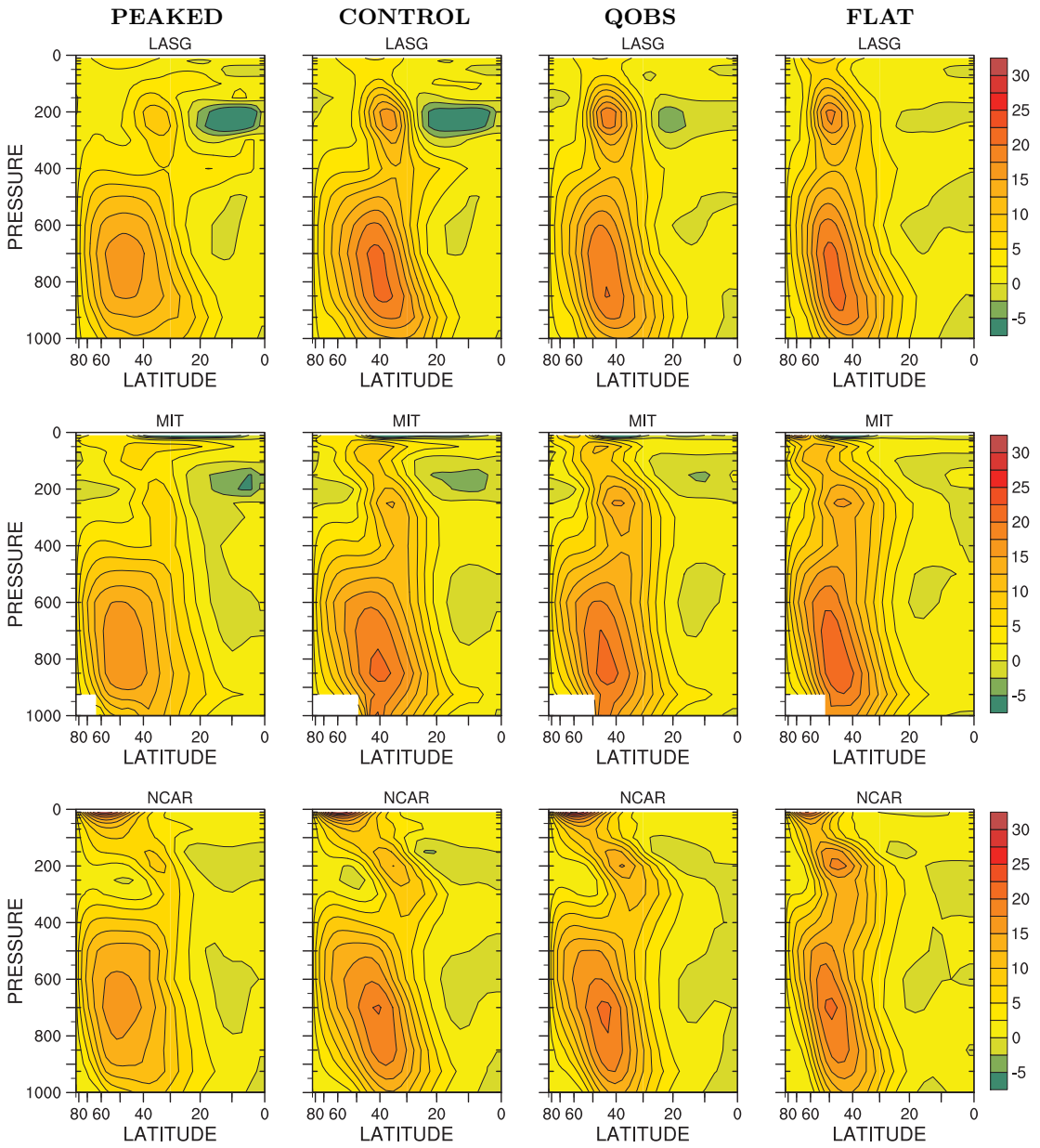

Figure 5.130 (continued): Individual model vT co-variance, transient eddy, te_vt, $\overline{[v^{*}T^{*}]}$, K m s^{-1}.

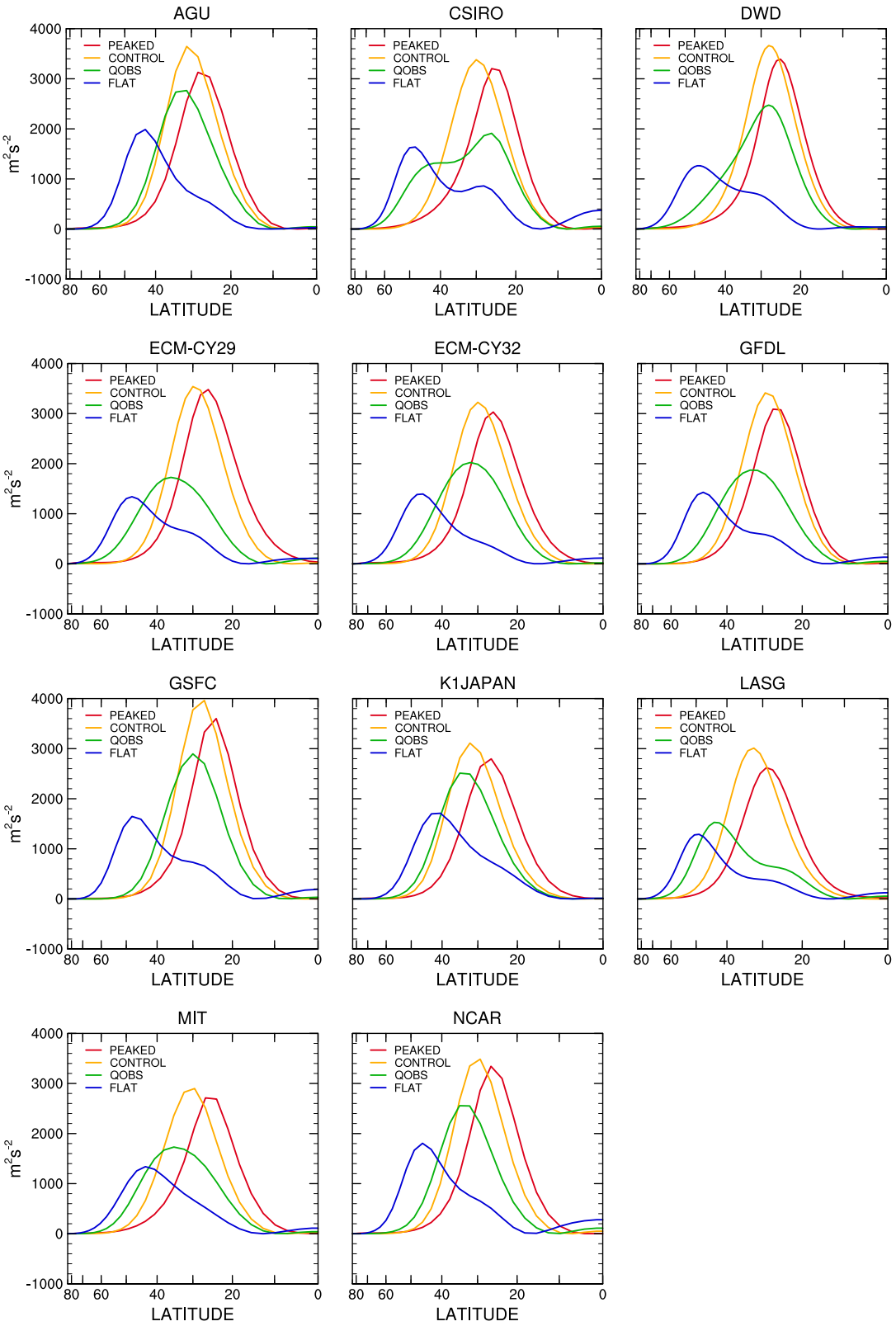

Figure 5.131: Stationary mean meridional circulation, sm_uu, $[\overline{u}]^2$, at 250 mb for individual models, PEAKED, CONTROL, QOBS and FLAT, $m^2\ s^{-2}$.

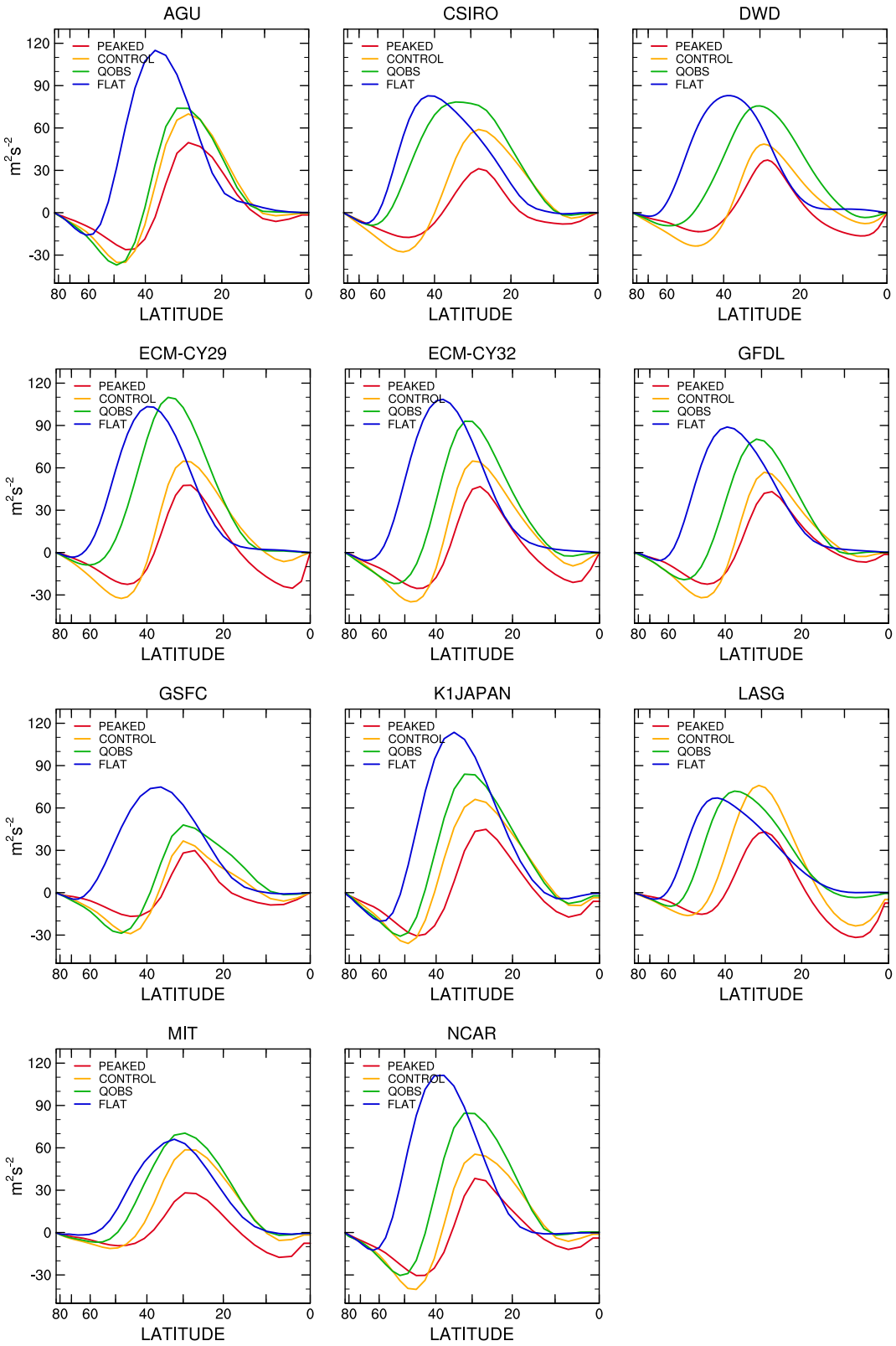

Figure 5.132: Transient eddy, te_uv, $\overline{[u^{*}v^{*}]}$, at 250 mb for individual models, PEAKED, CONTROL, QOBS and FLAT, $m^2\ s^{-2}$.

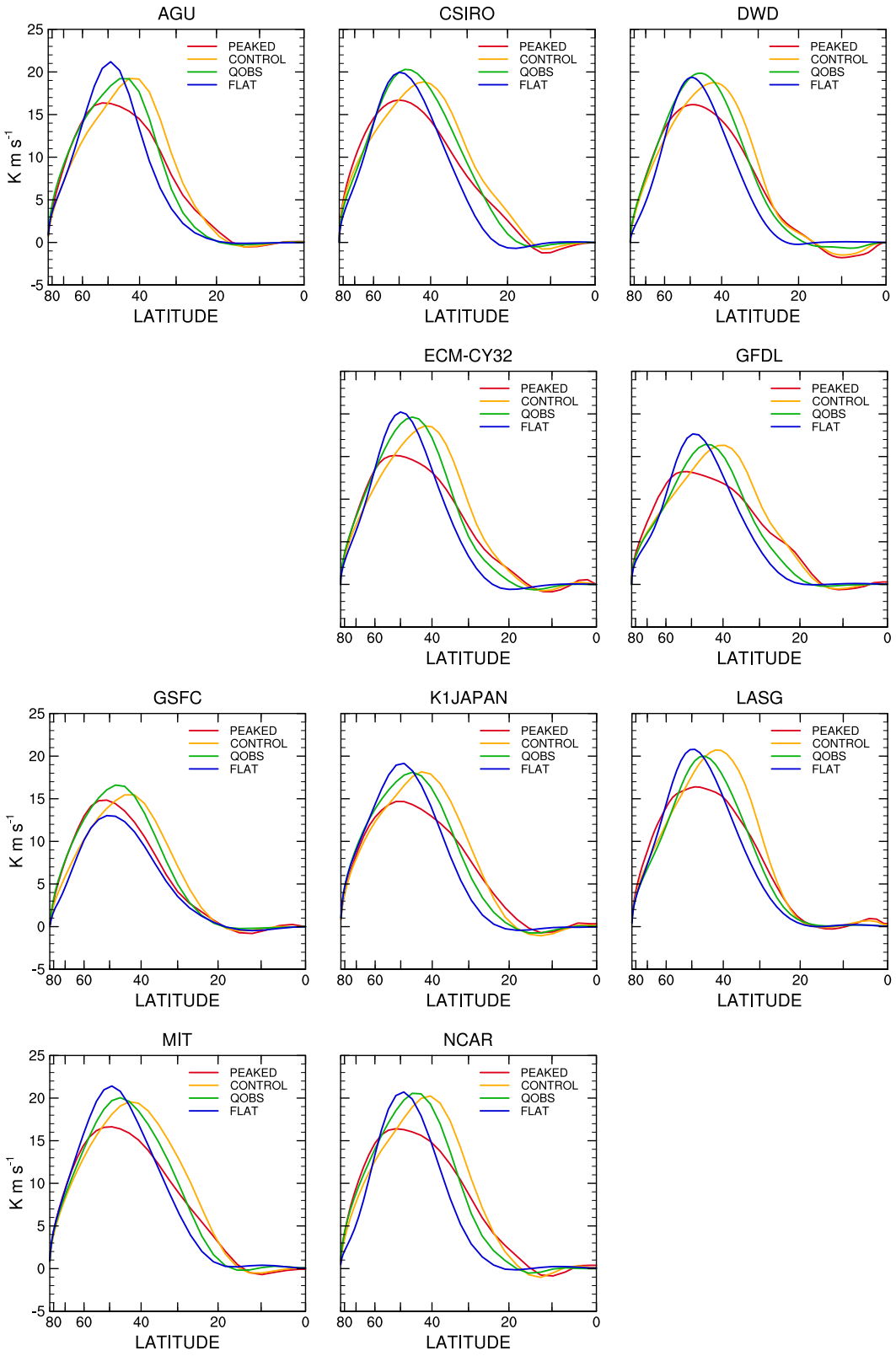

Figure 5.133: Transient eddy, te_vt, $\overline{[v^{*}T^{*}]}$, at 700 mb for individual models, PEAKED, CONTROL, QOBS and FLAT, K m s^{-1}.

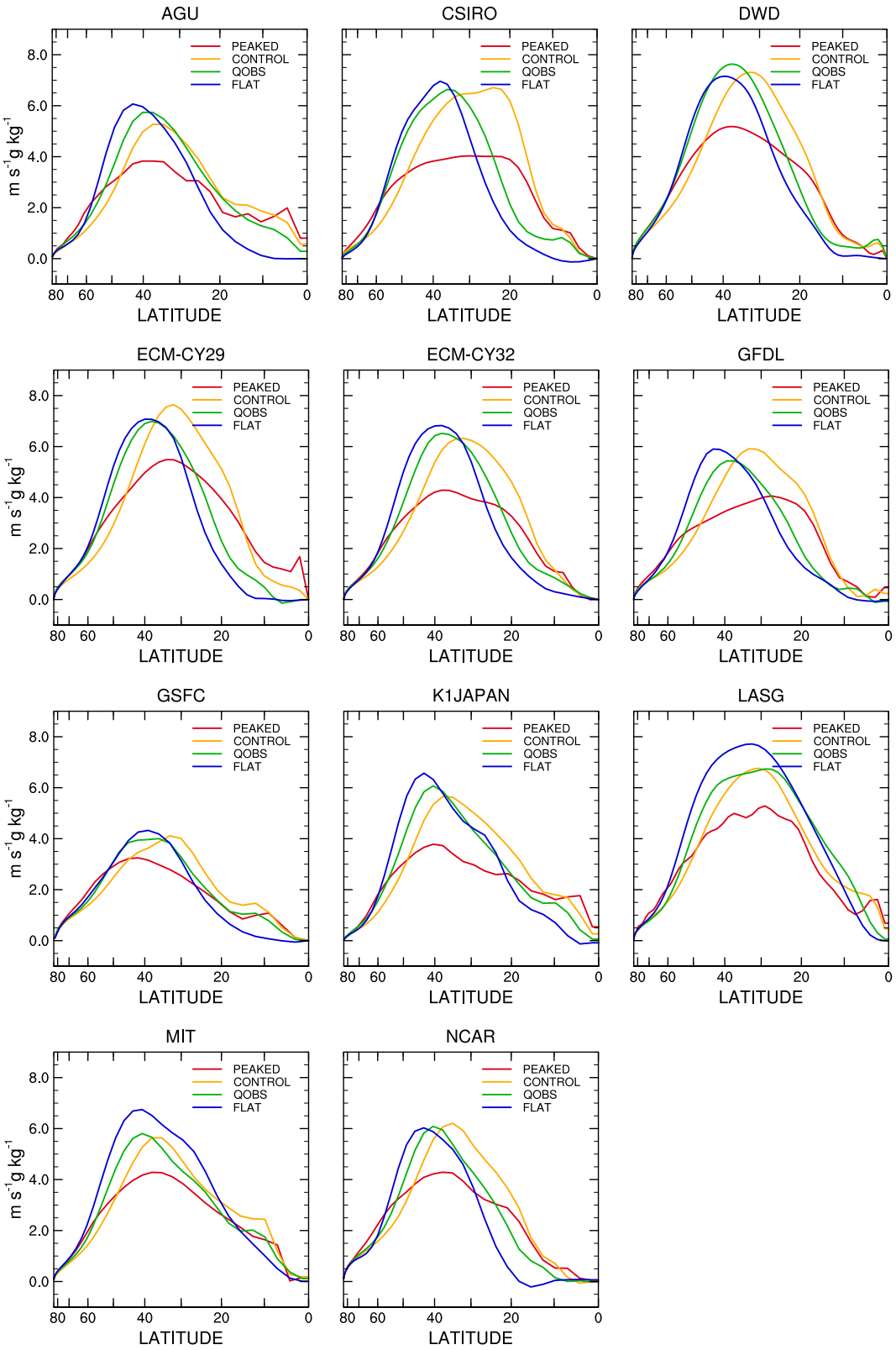

Figure 5.134: Transient eddy, te_vq, $\overline{[v'^* q'^*]}$, at 850 mb for individual models, PEAKED, CONTROL, QOBS and FLAT, m s^{-1} g kg^{-1}.

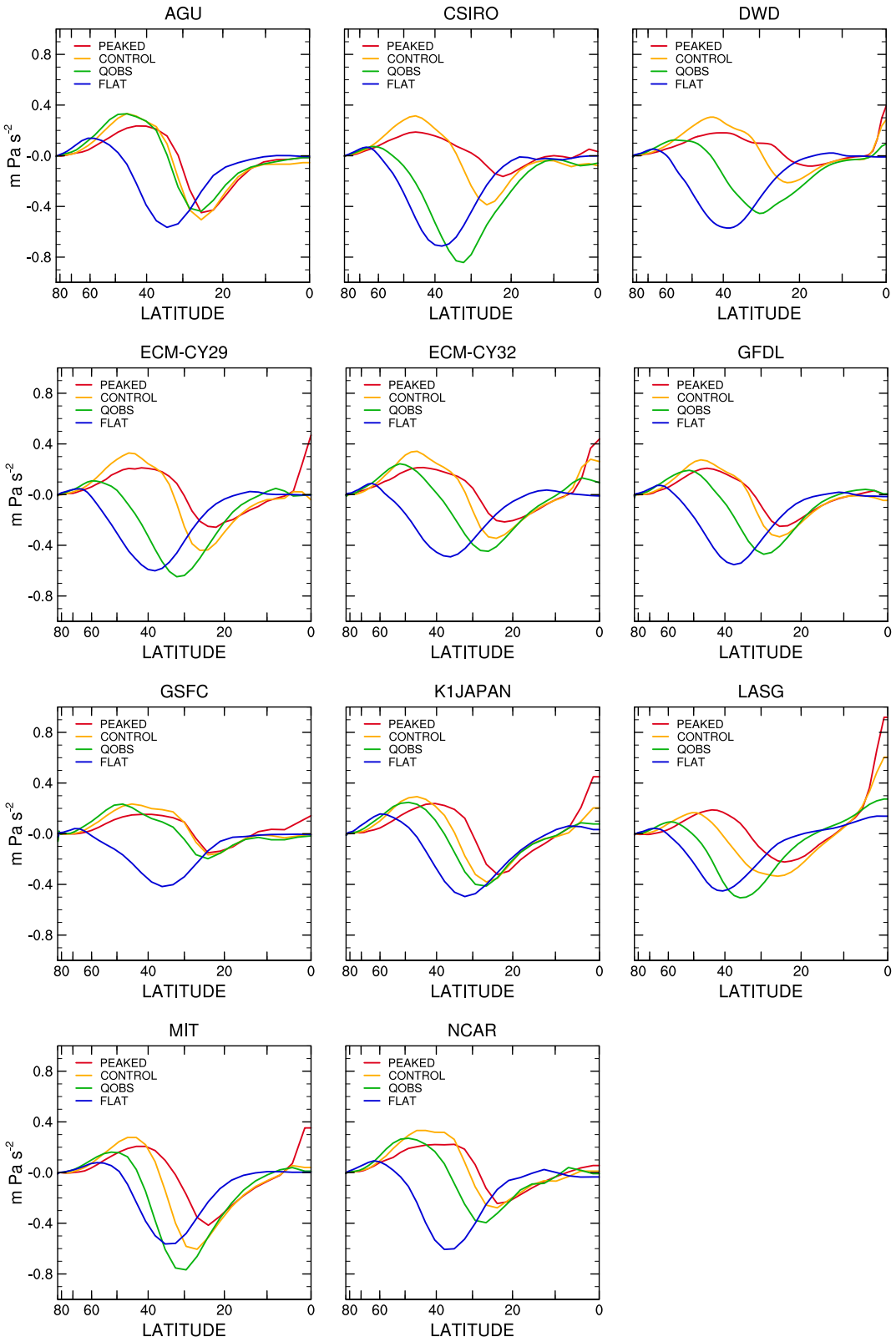

Figure 5.135: Transient eddy, te_uom, $\overline{[u]'[\omega]'}$, at 400 mb for individual models, PEAKED, CONTROL, QOBS and FLAT, m Pa s^{-2}.

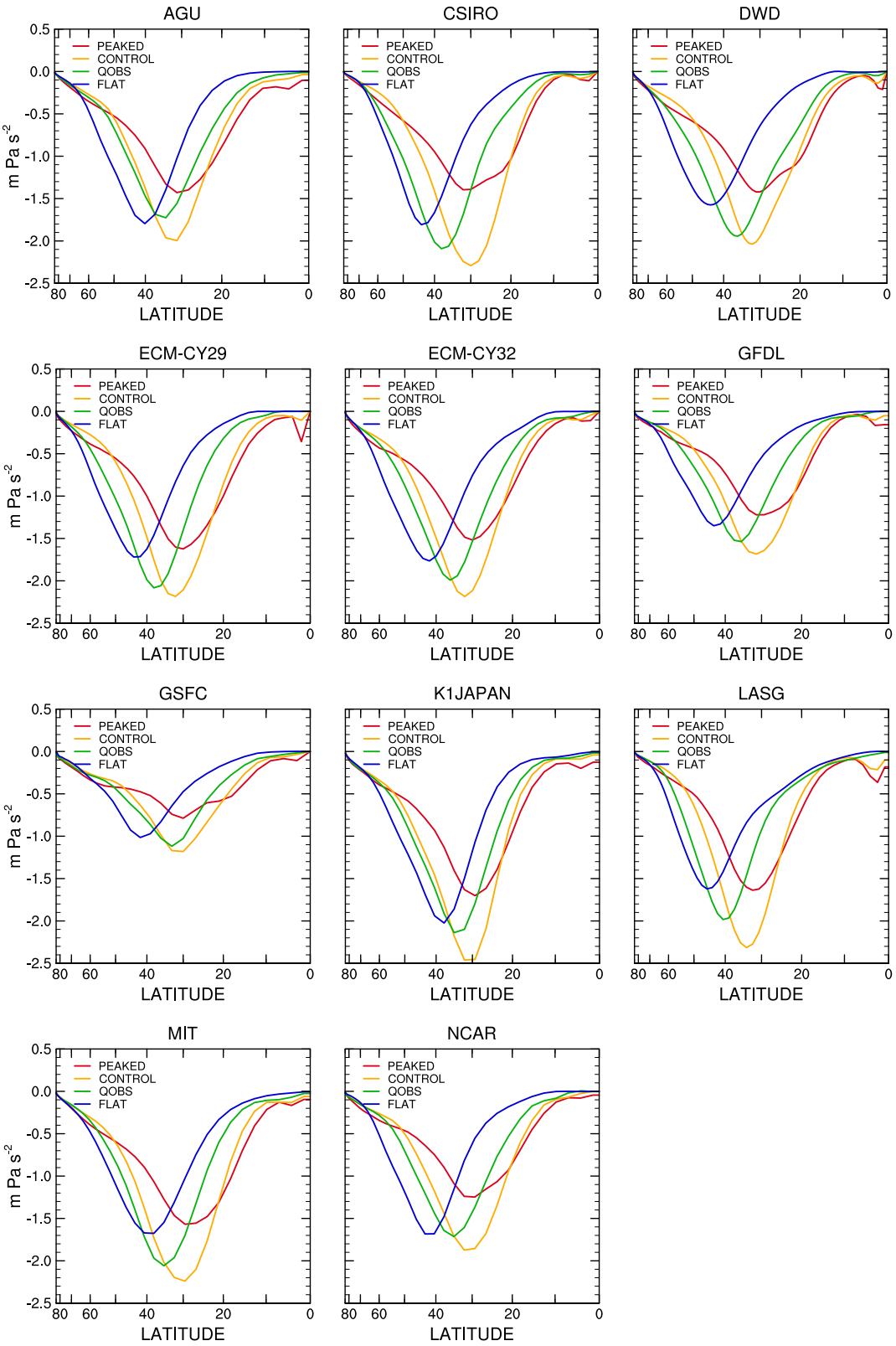

Figure 5.136: Transient eddy, te_vom, $\overline{[v]'[\omega]'}$, at 500 mb for individual models, PEAKED, CONTROL, QOBS and FLAT, m Pa s^{-2}.

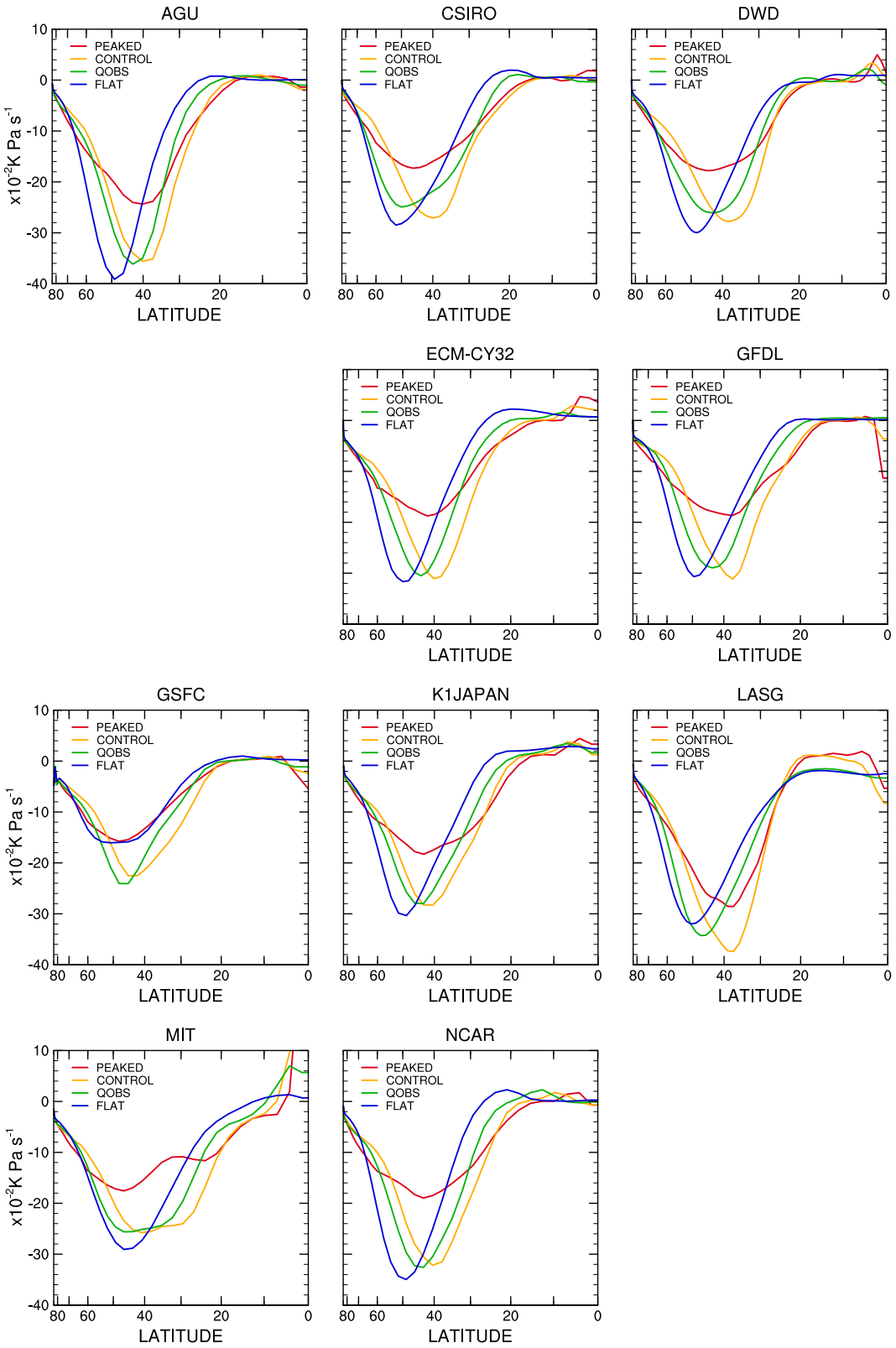

Figure 5.137: Transient eddy, te_omt, $\overline{[\omega]'[T]'}$, at 700 mb for individual models, PEAKED, CONTROL, QOBS and FLAT, 10^{-2} K Pa s^{-2}.

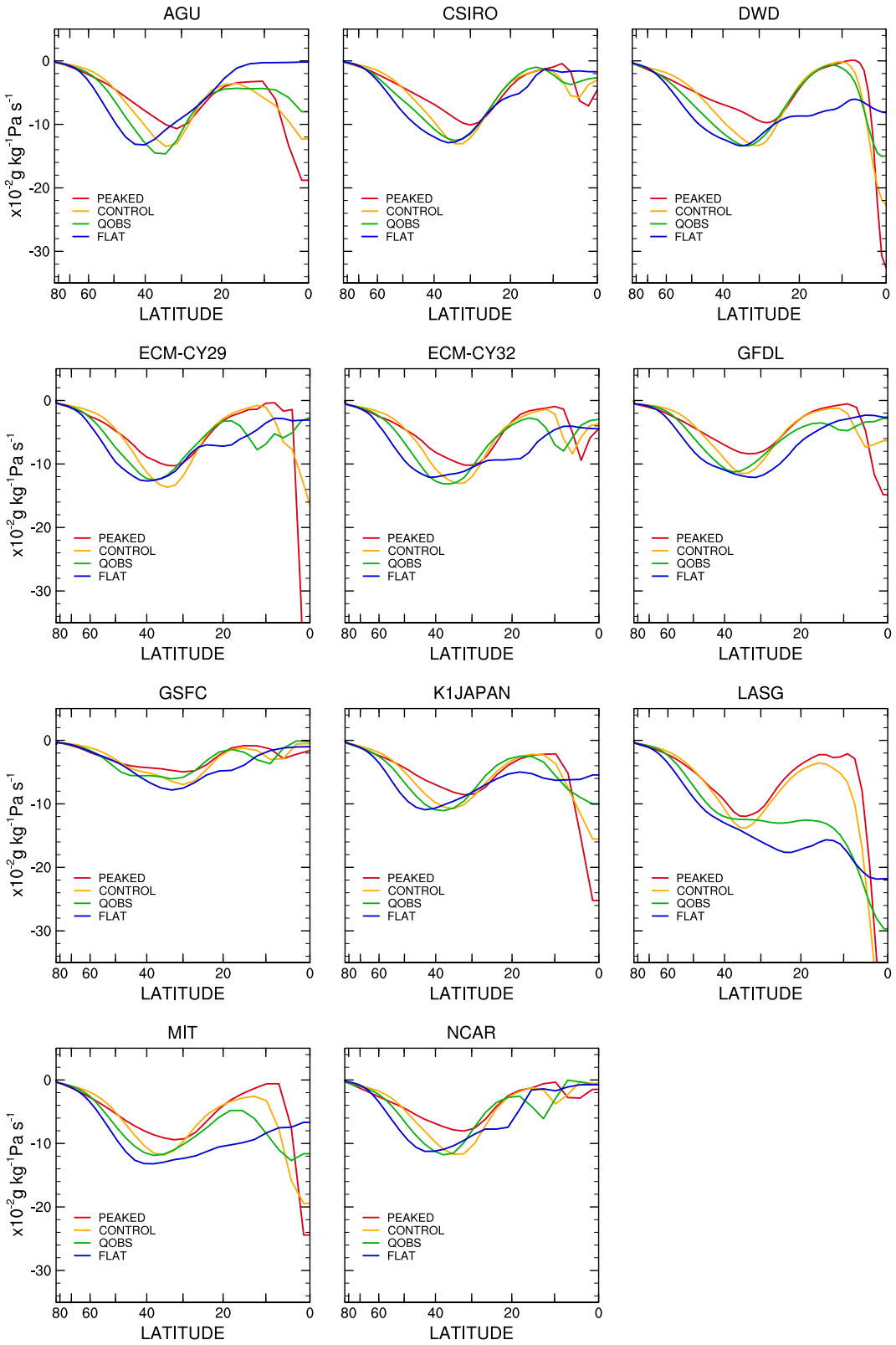

Figure 5.138: Transient eddy, te_omq, $\overline{[\omega]'[q]'}$, at 700 mb for individual models, PEAKED, CONTROL, QOBS and FLAT, 10^{-2} g kg^{-1} Pa s^{-1}.

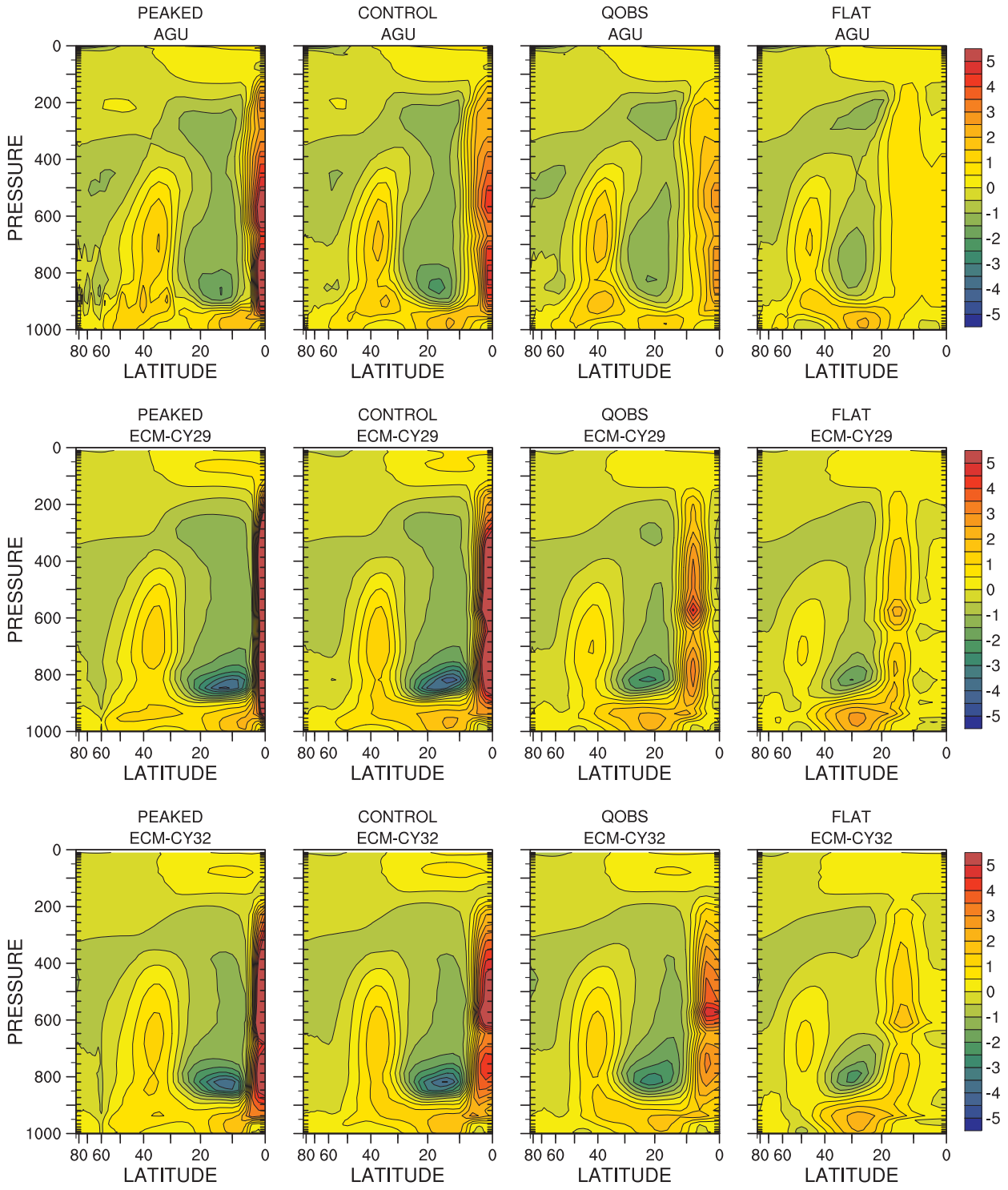

Figure 5.139: Zonal-time average total parameterized temperature tendency (t) for individual models for PEAKED, CONTROL, QOBS and FLAT, K day^{-1}.

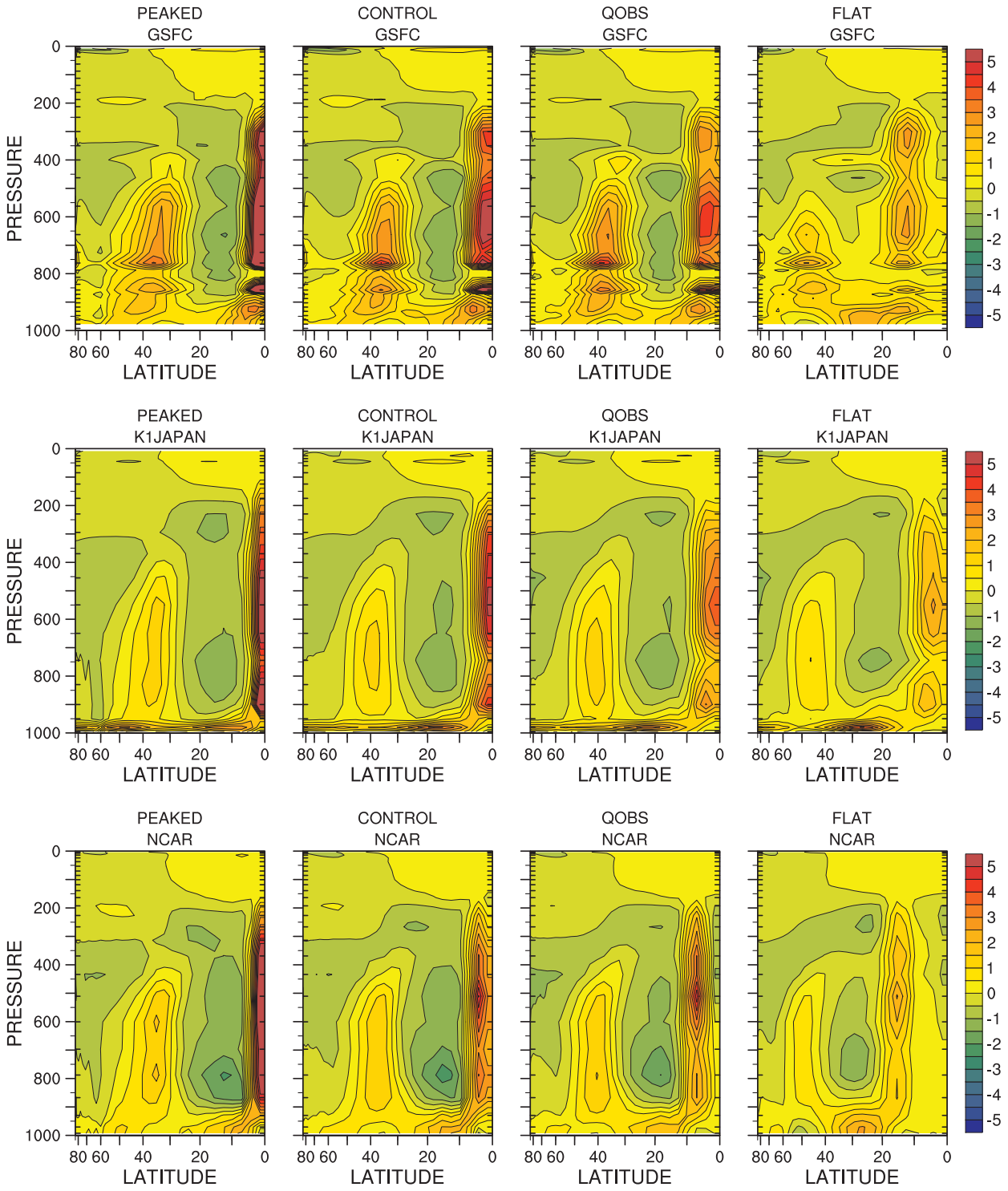

Figure 5.139 (continued): Zonal-time average total parameterized temperature tendency (t) for individual models for PEAKED, CONTROL, QOBS and FLAT, K day^{-1}.

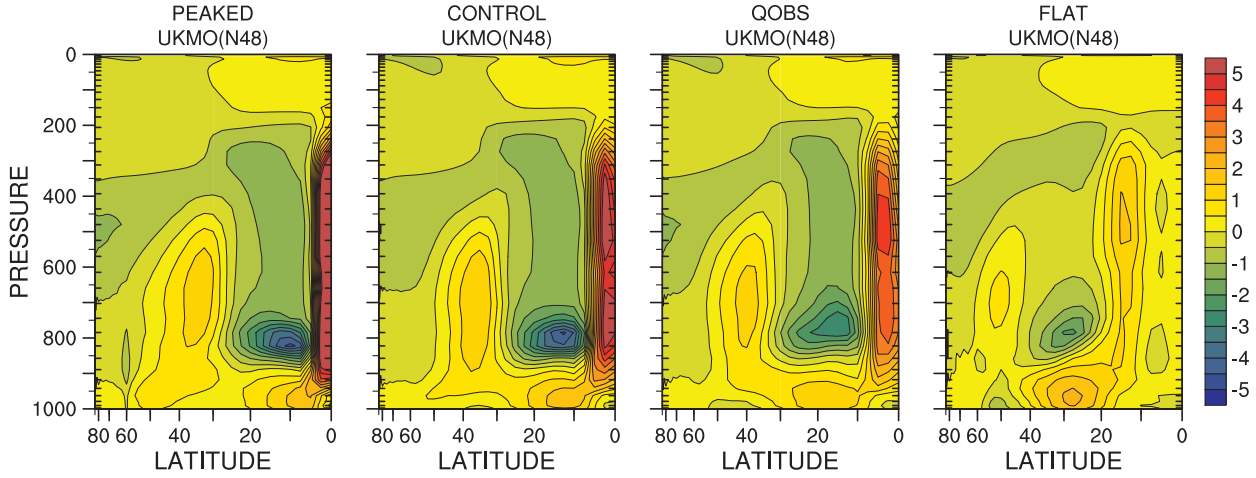

Figure 5.139 (continued): Zonal-time average total parameterized temperature tendency (t) for individual models for PEAKED, CONTROL, QOBS and FLAT, K day^{-1}.

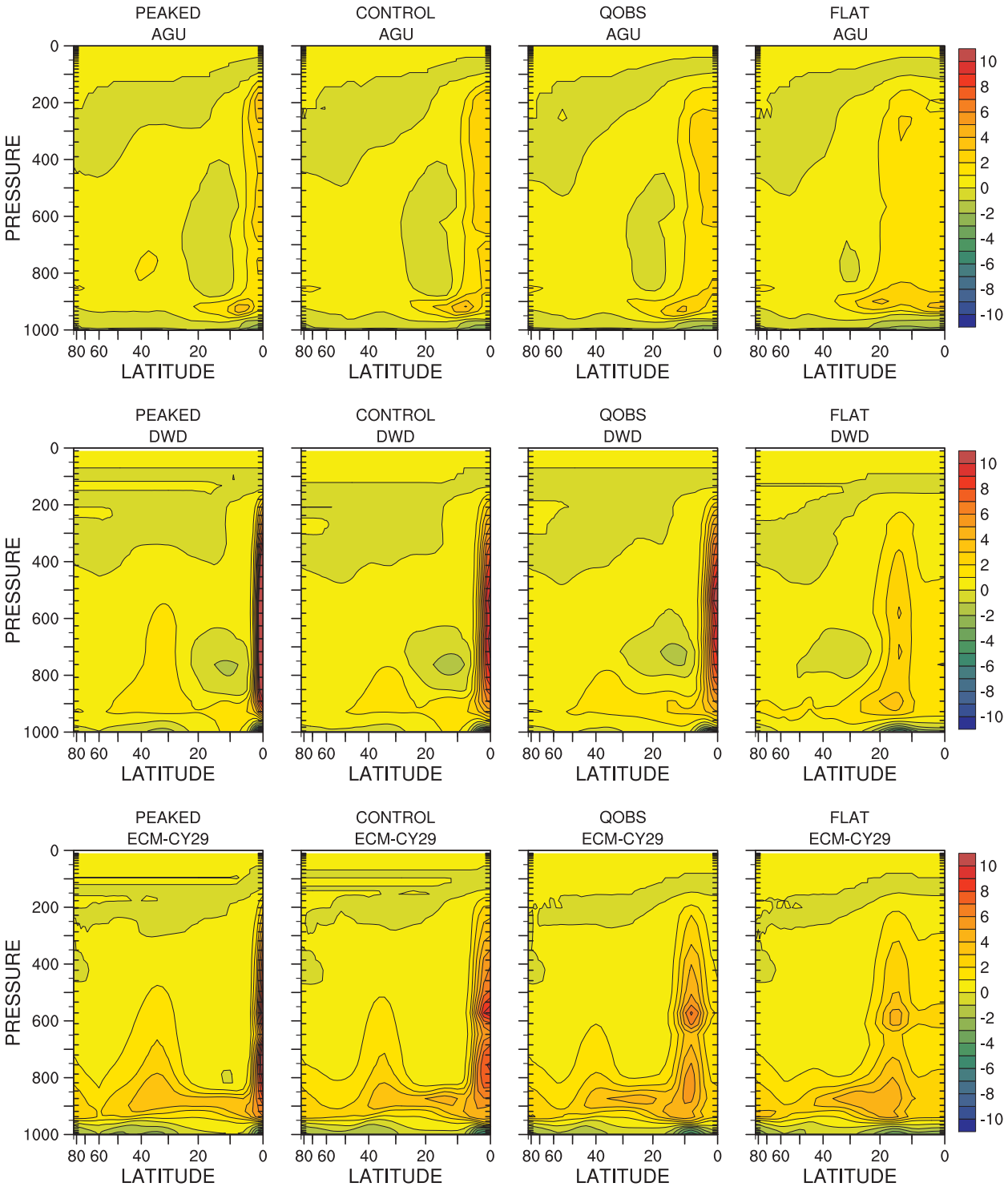

Figure 5.140: Zonal-time average parameterized convection temperature tendency (t_conv) for individual models for PEAKED, CONTROL, QOBS and FLAT, K day^{-1}.

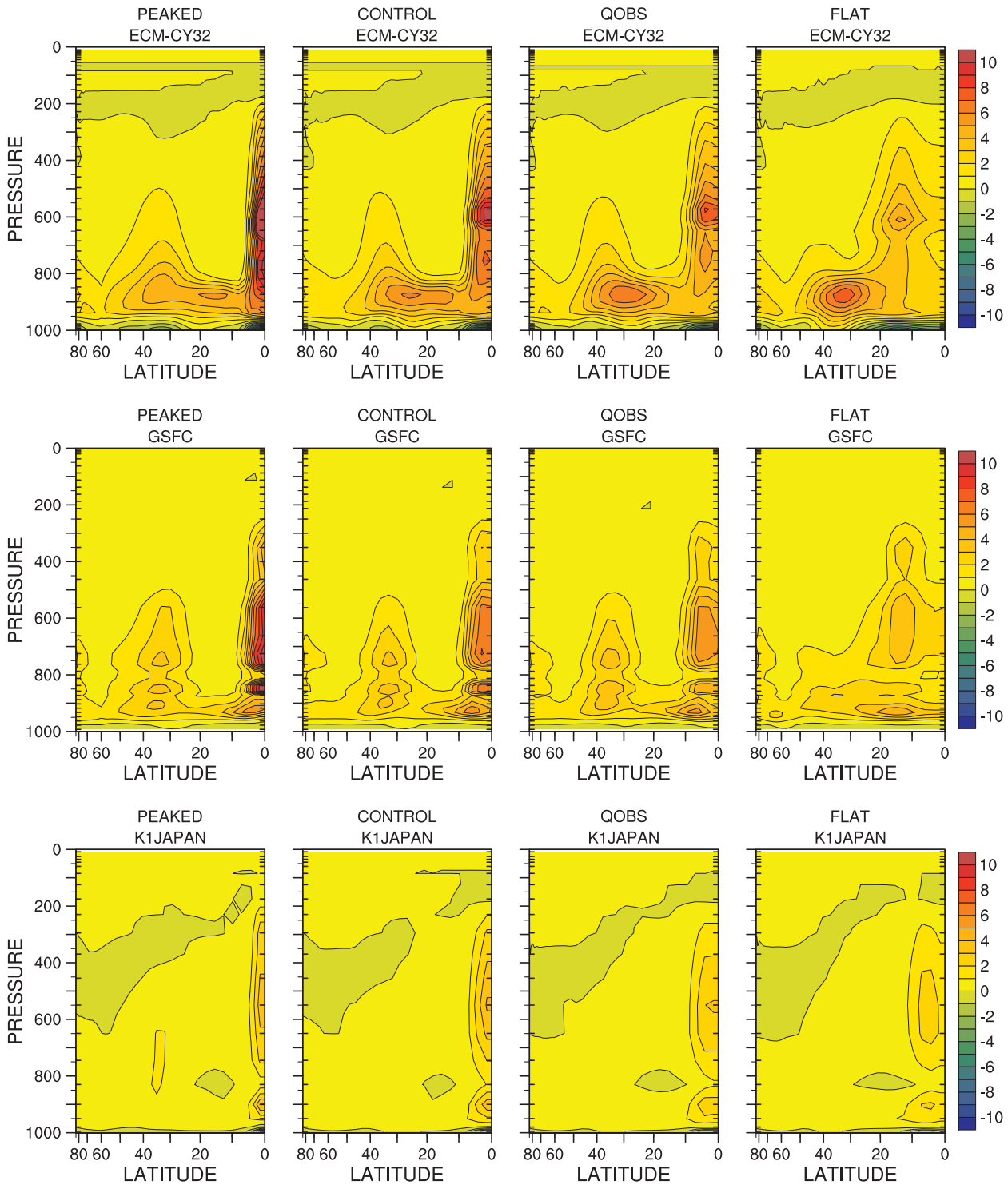

Figure 5.140 (continued): Zonal-time average parameterized convection temperature tendency (t_conv) for individual models for PEAKED, CONTROL, QOBS and FLAT, K day^{-1}.

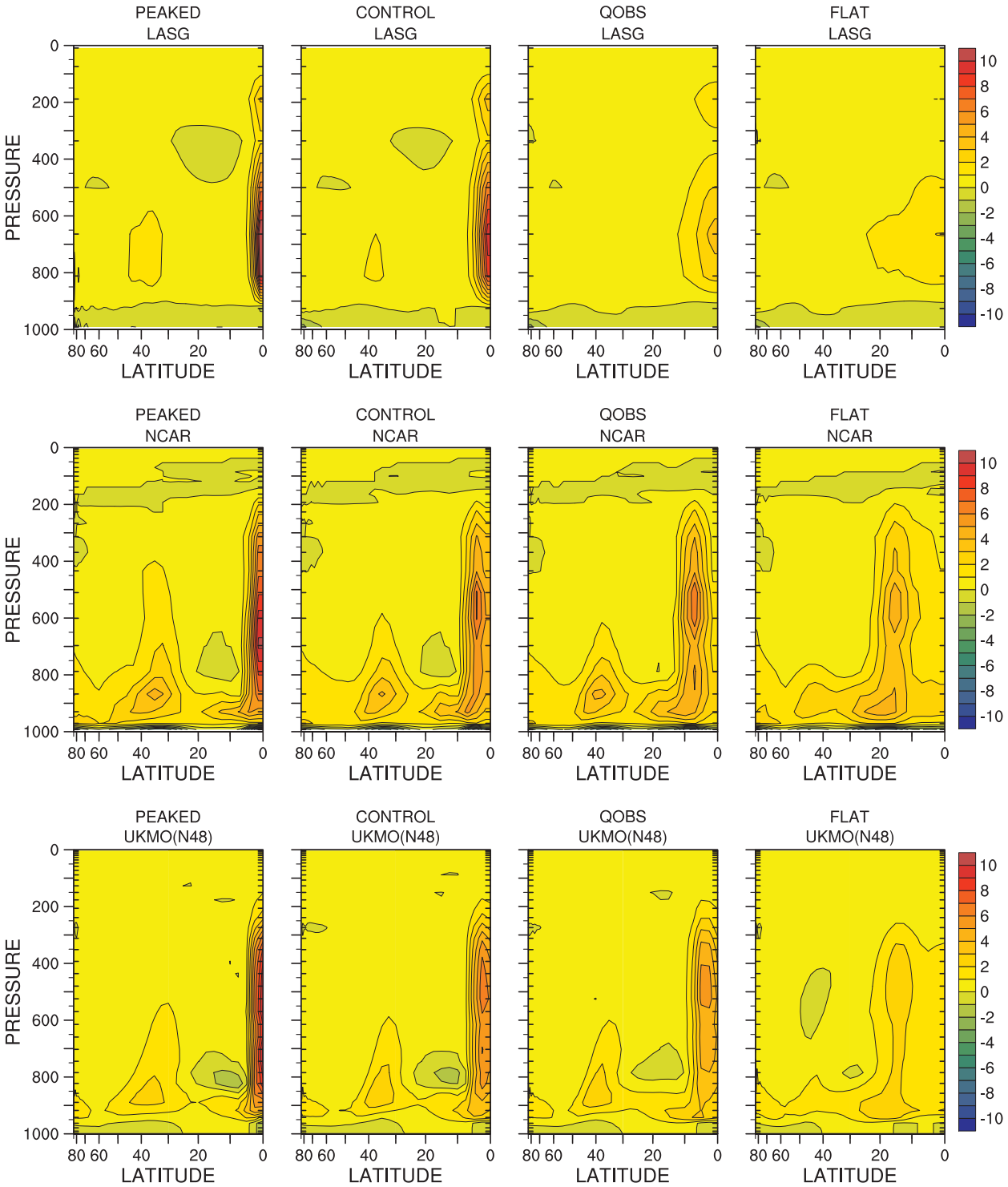

Figure 5.140 (continued): Zonal-time average parameterized convection temperature tendency (t_conv) for individual models for PEAKED, CONTROL, QOBS and FLAT, K day^{-1}.

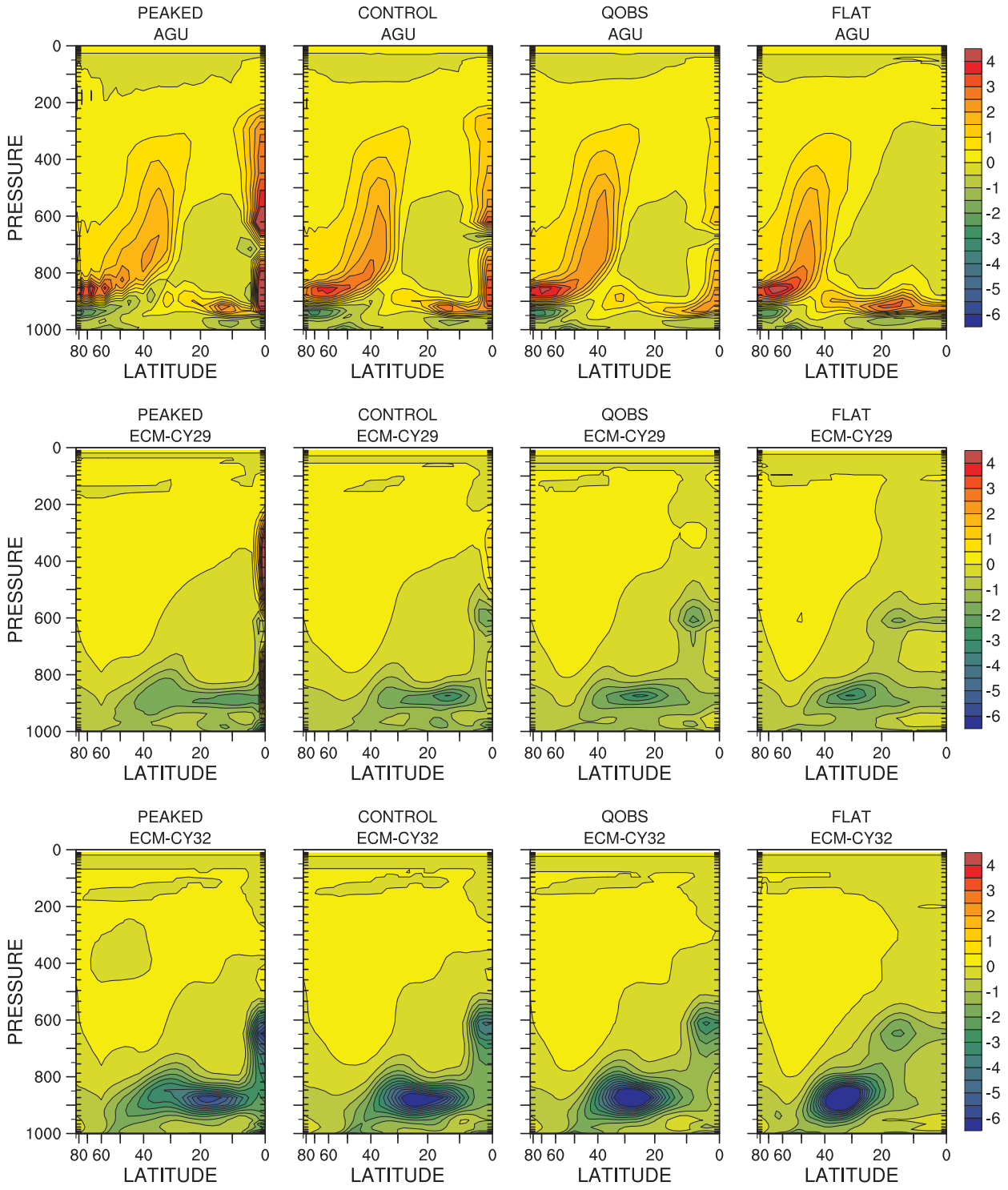

Figure 5.141: Zonal-time average parameterized cloud temperature tendency (t_cld) for individual models for PEAKED, CONTROL, QOBS and FLAT, K day^{-1}.

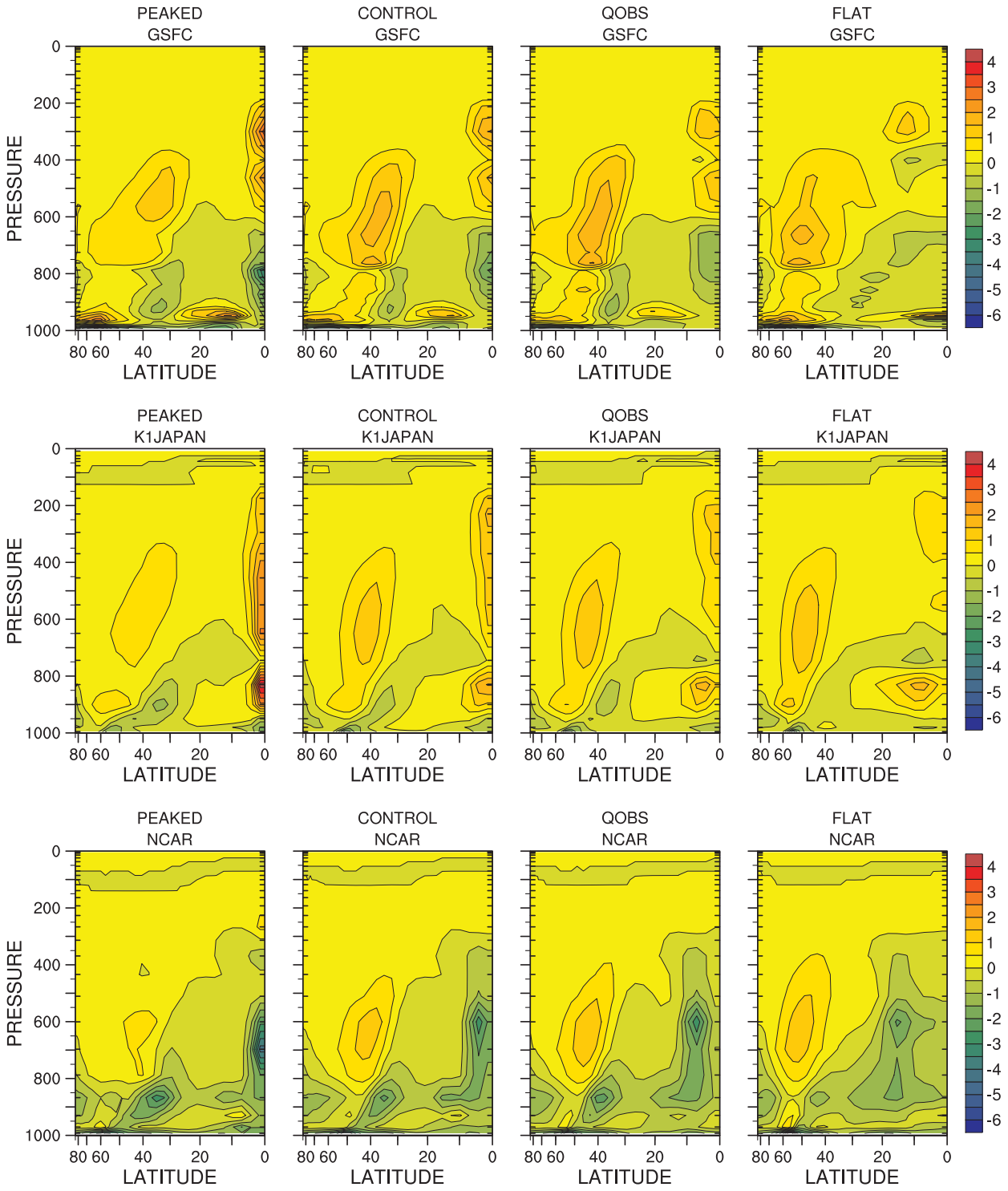

Figure 5.141 (continued): Zonal-time average parameterized cloud temperature tendency (t_cld) for individual models for PEAKED, CONTROL, QOBS and FLAT, K day^{-1}.

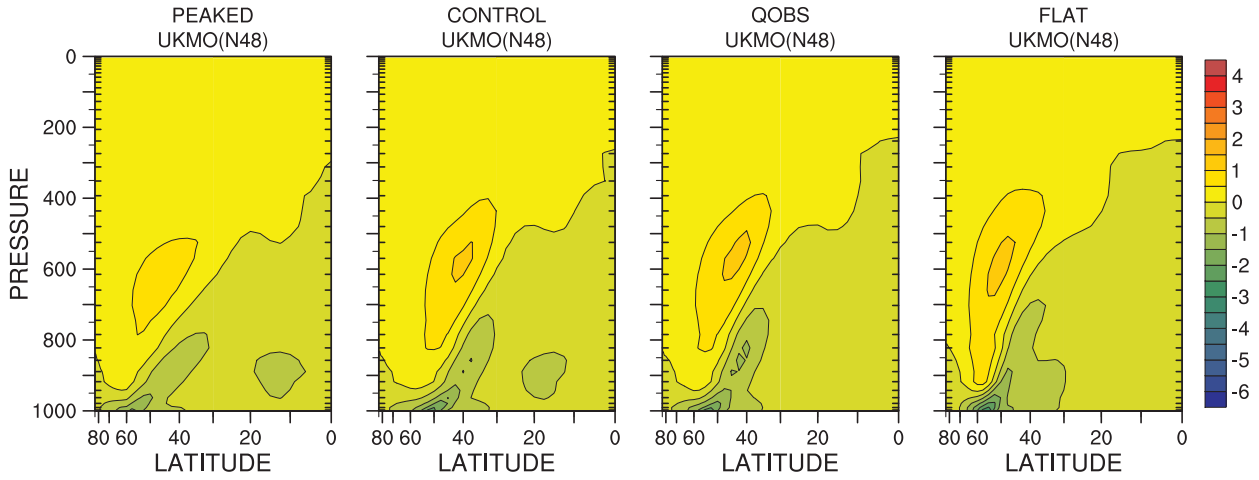

Figure 5.141 (continued): Zonal-time average parameterized cloud temperature tendency (t_cld) for individual models for PEAKED, CONTROL, QOBS and FLAT, K day^{-1}.

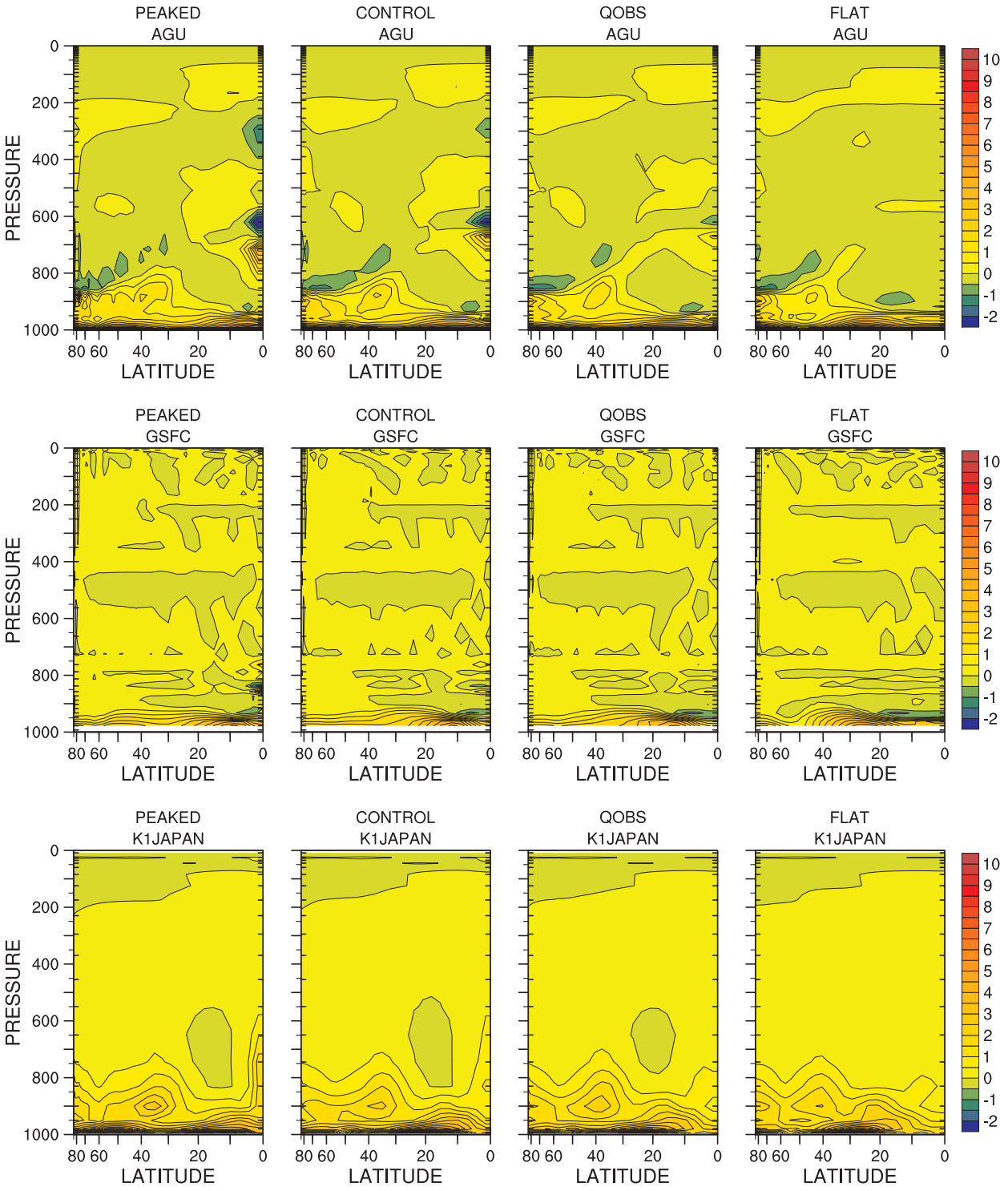

Figure 5.142: Zonal-time average parameterized turbulence temperature tendency (t_turb) for individual models for PEAKED, CONTROL, QOBS and FLAT, K day^{-1}.

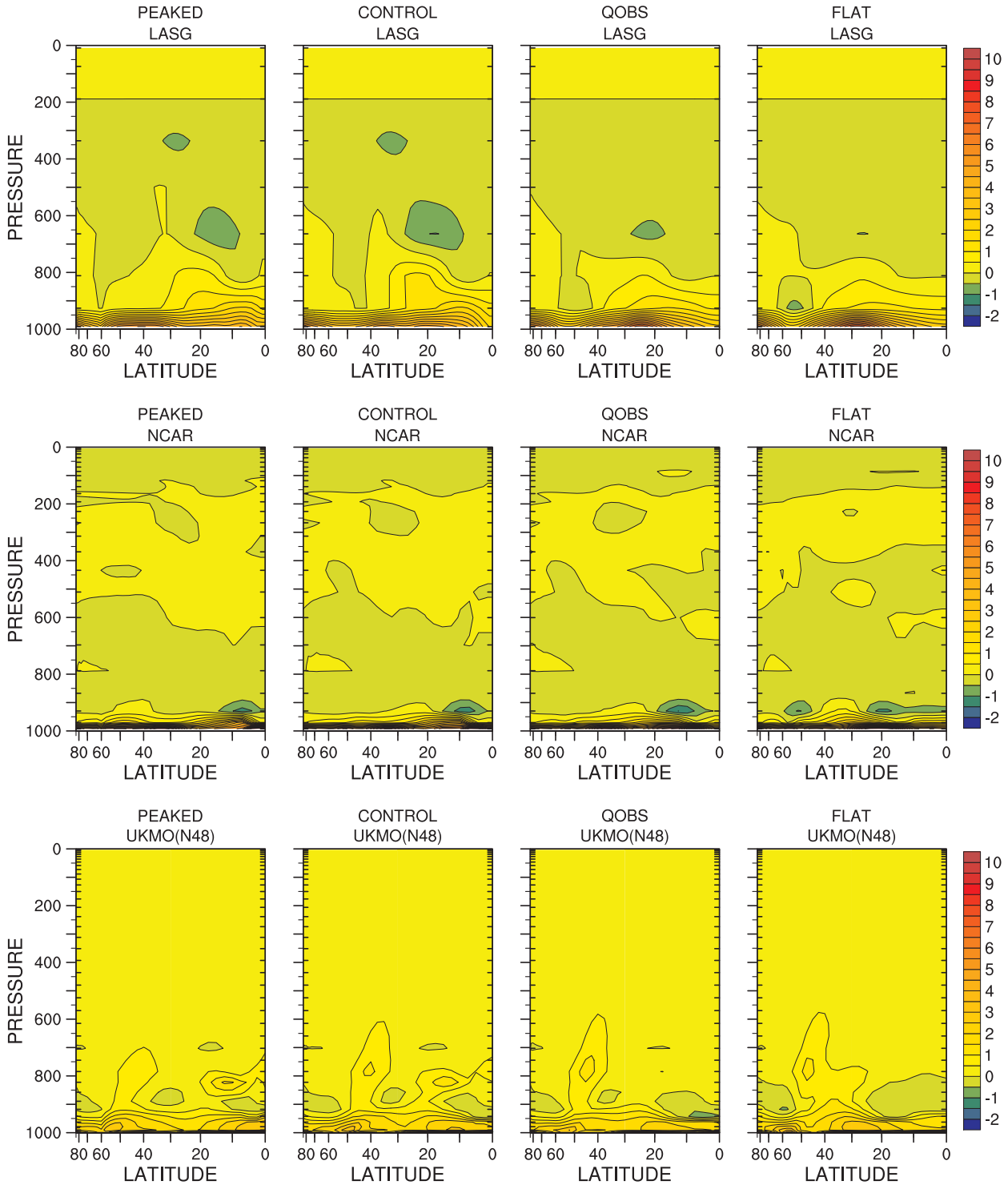

Figure 5.142 (continued): Zonal-time average parameterized turbulence temperature tendency (t_turb) for individual models for PEAKED, CONTROL, QOBS and FLAT, K day^{-1}.

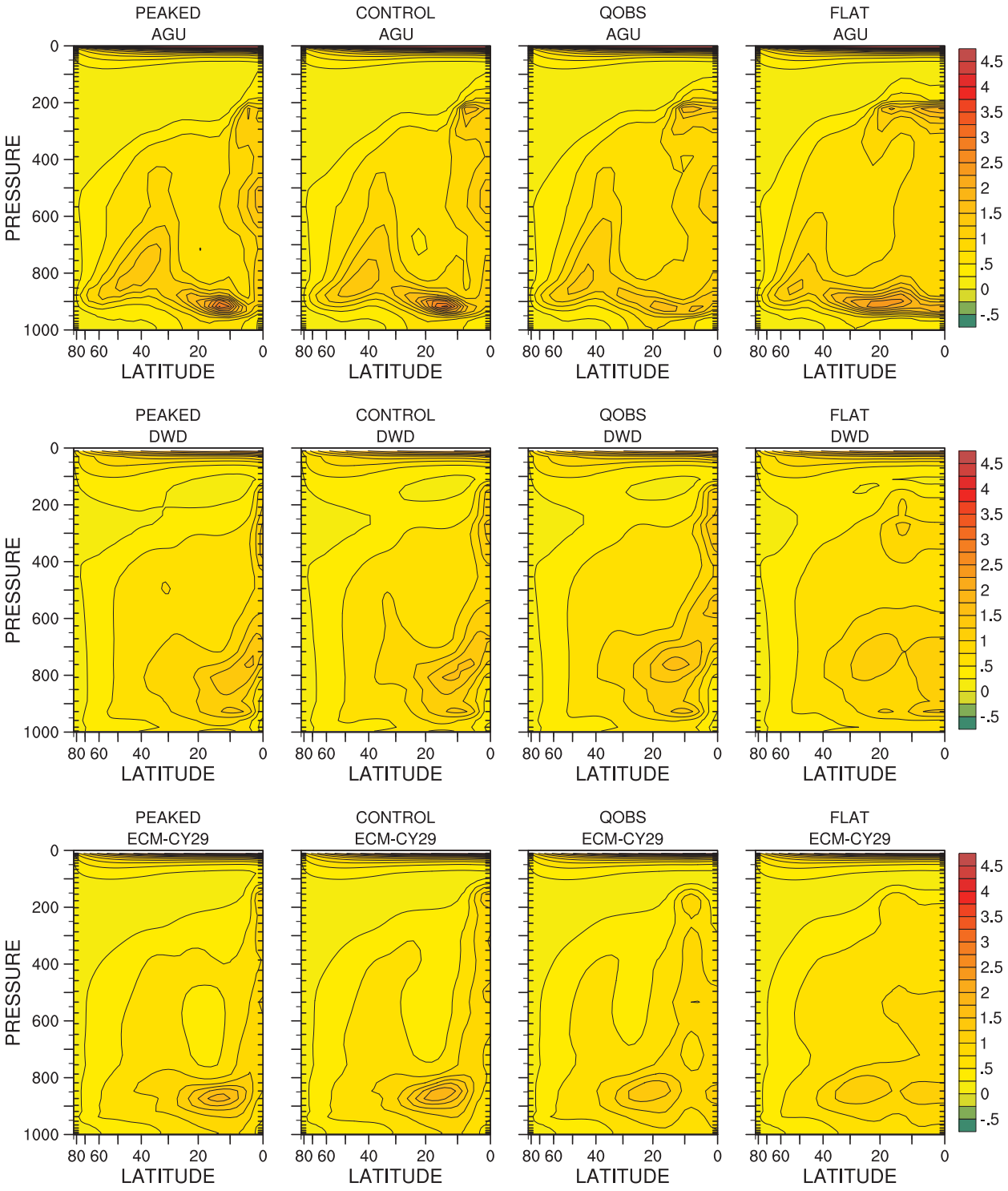

Figure 5.143: Zonal-time average shortwave radiation temperature tendency (t_sw) for individual models for PEAKED, CONTROL, QOBS and FLAT, K day^{-1}.

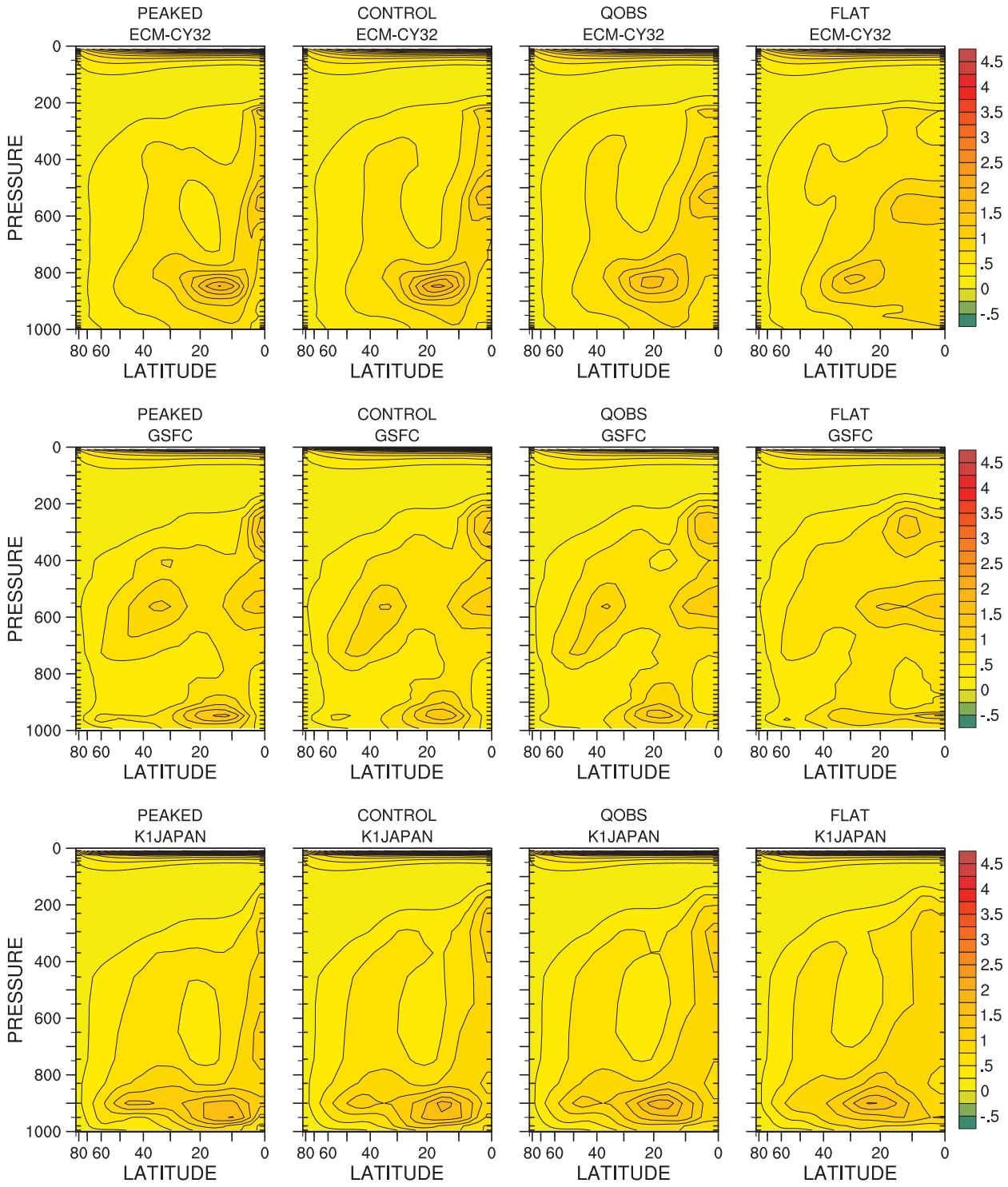

Figure 5.143 (continued): Zonal-time average shortwave radiation temperature tendency (t_sw) for individual models for PEAKED, CONTROL, QOBS and FLAT, K day^{-1}.

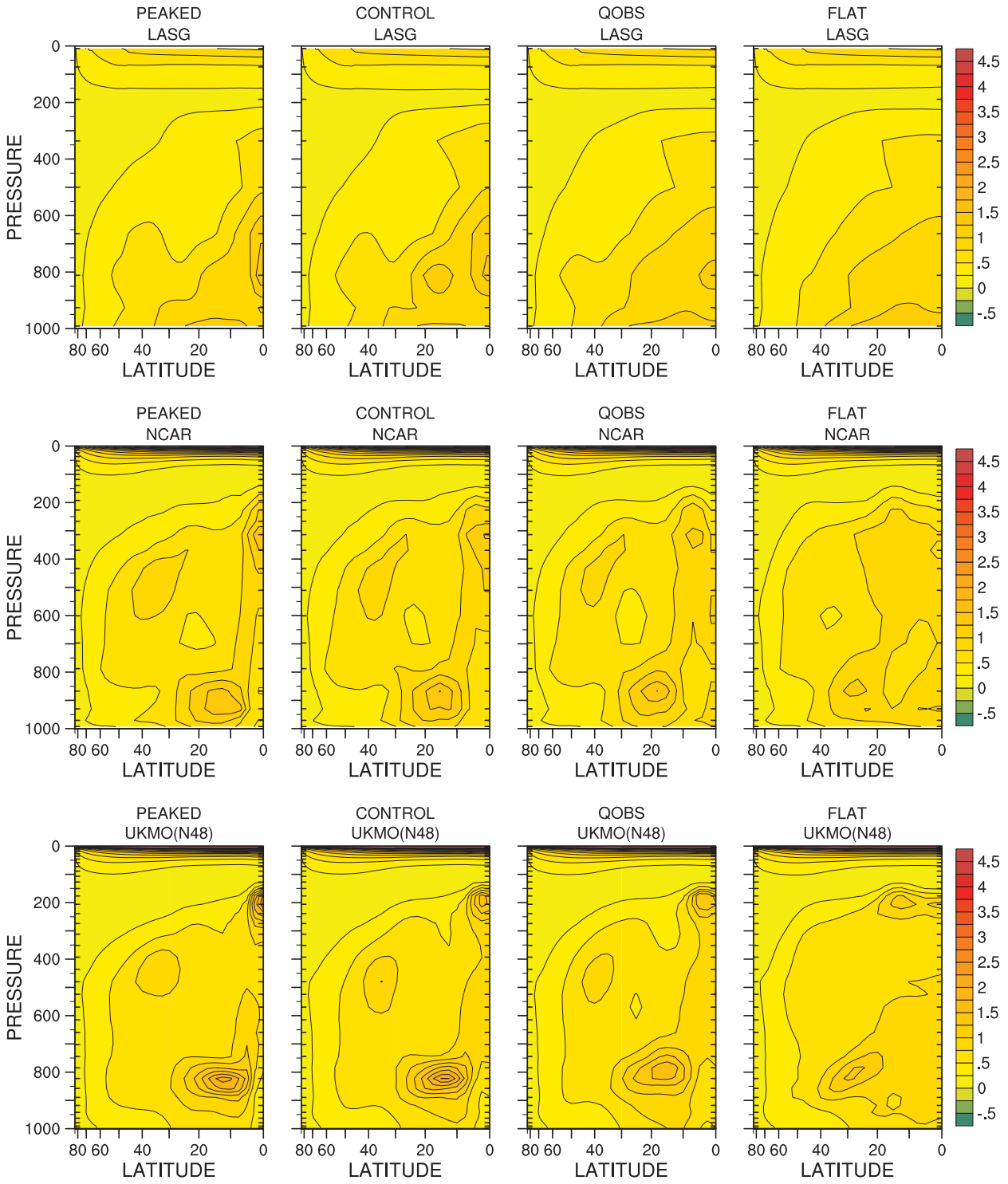

Figure 5.143 (continued): Zonal-time average shortwave radiation temperature tendency (t_sw) for individual models for PEAKED, CONTROL, QOBS and FLAT, K day^{-1}.

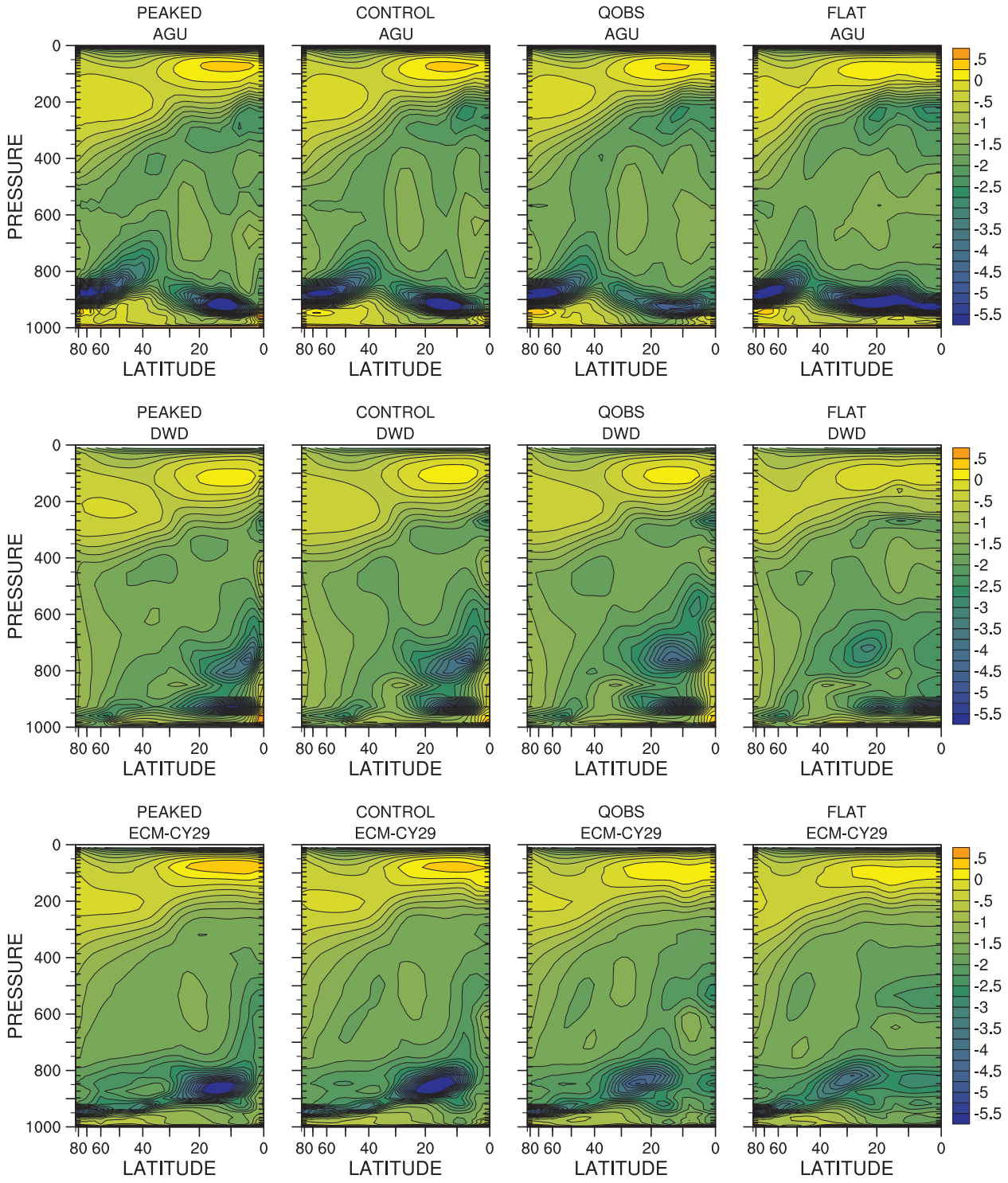

Figure 5.144: Zonal-time average longwave radiation temperature tendency (t_lw) for individual models for PEAKED, CONTROL, QOBS and FLAT, K day^{-1}.

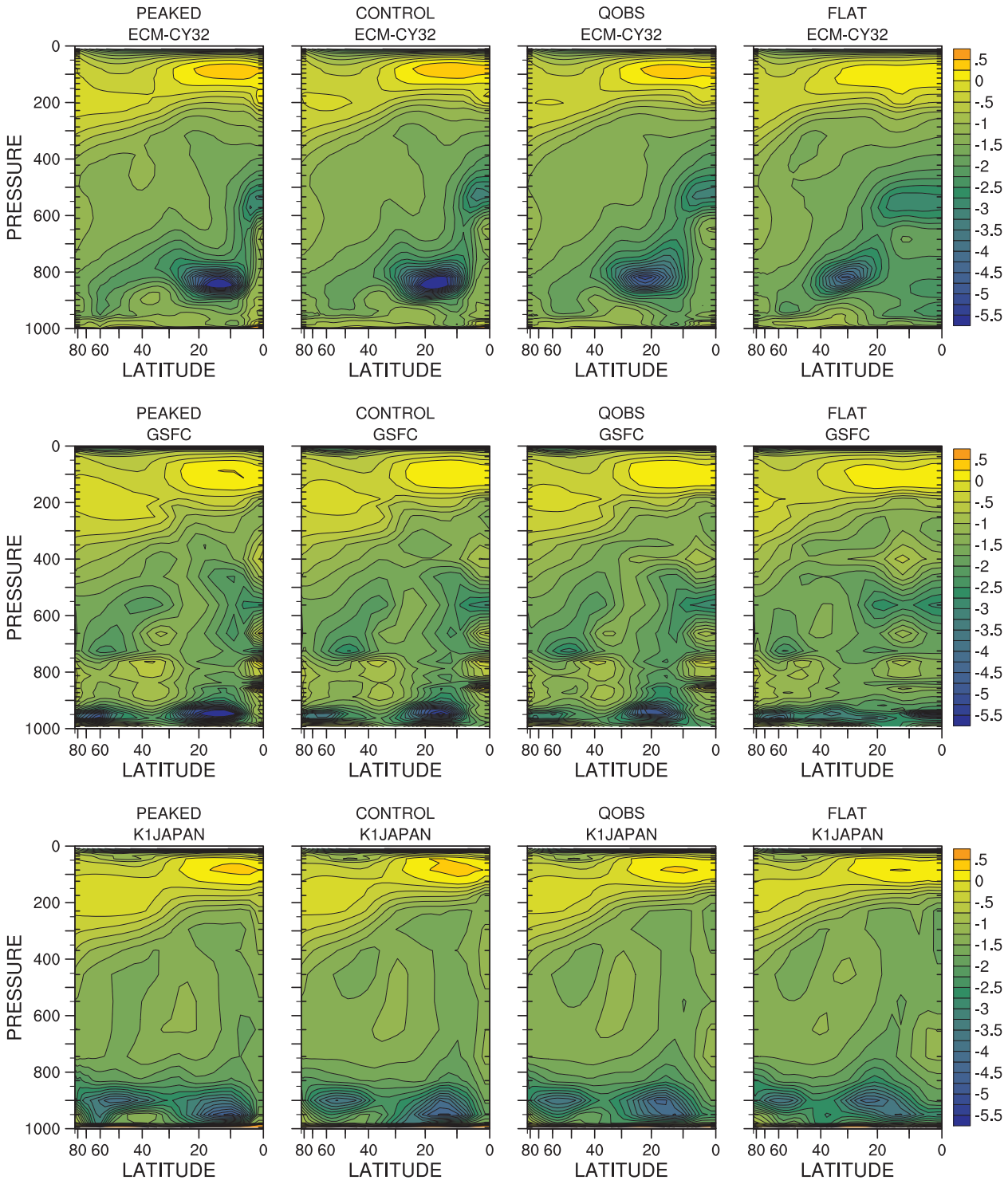

Figure 5.144 (continued): Zonal-time average longwave radiation temperature tendency (t_lw) for individual models for PEAKED, CONTROL, QOBS and FLAT, K day^{-1}.

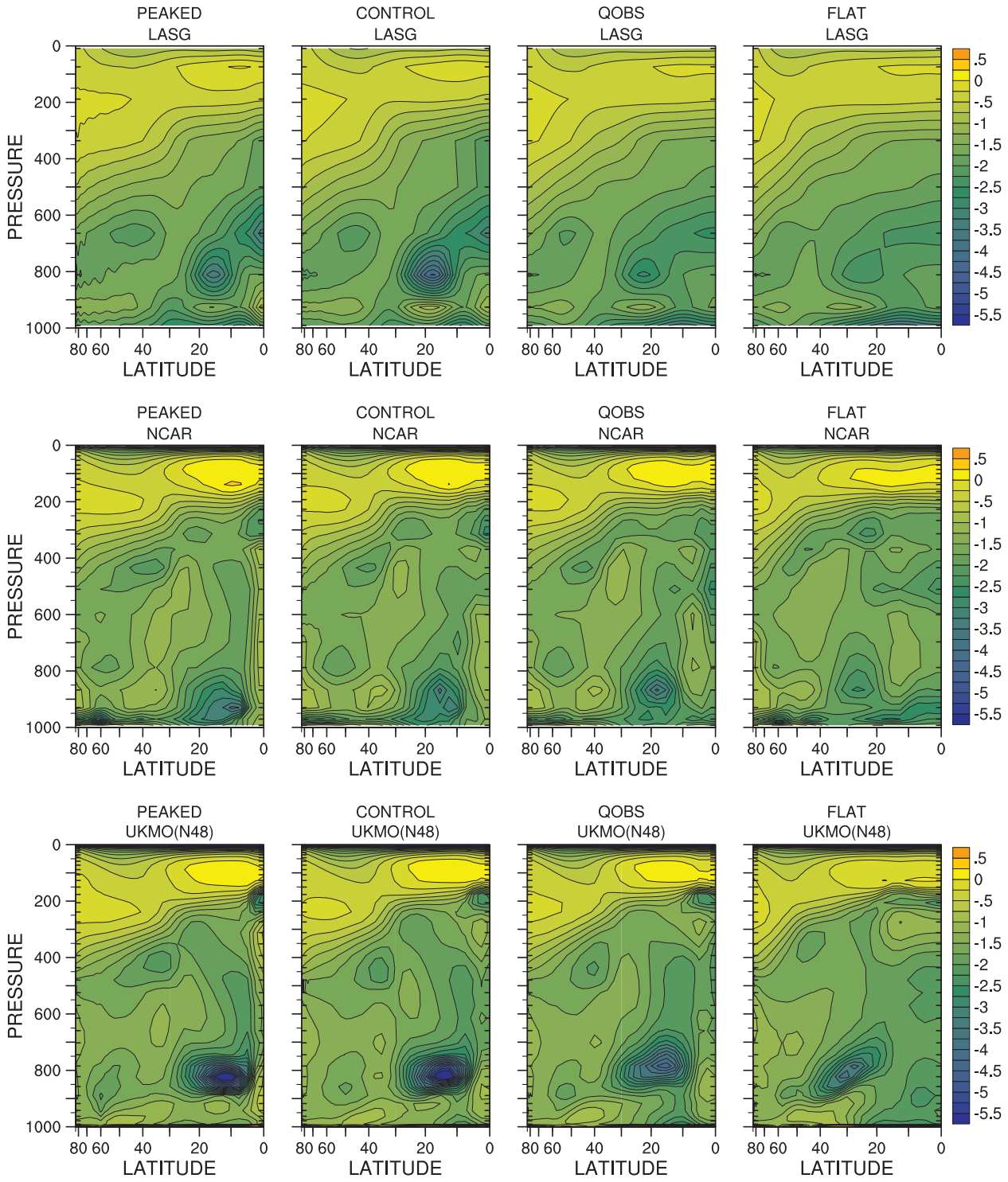

Figure 5.144 (continued): Zonal-time average longwave radiation temperature tendency (t_lw) for individual models for PEAKED, CONTROL, QOBS and FLAT, K day^{-1}.

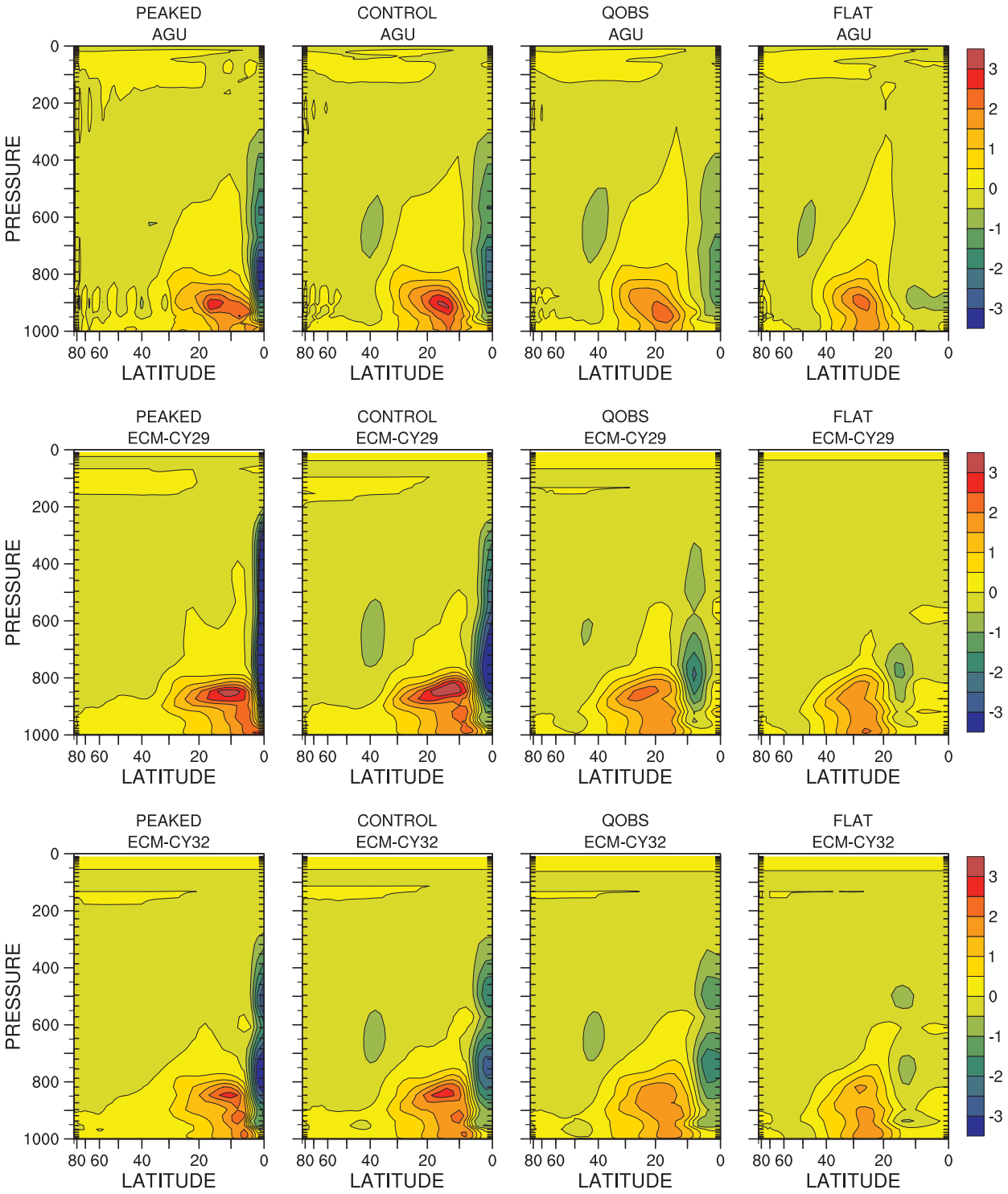

Figure 5.145: Zonal-time average total parameterized specific humidity tendency (q) for individual models for PEAKED, CONTROL, QOBS and FLAT, g kg^{-1} day^{-1}.

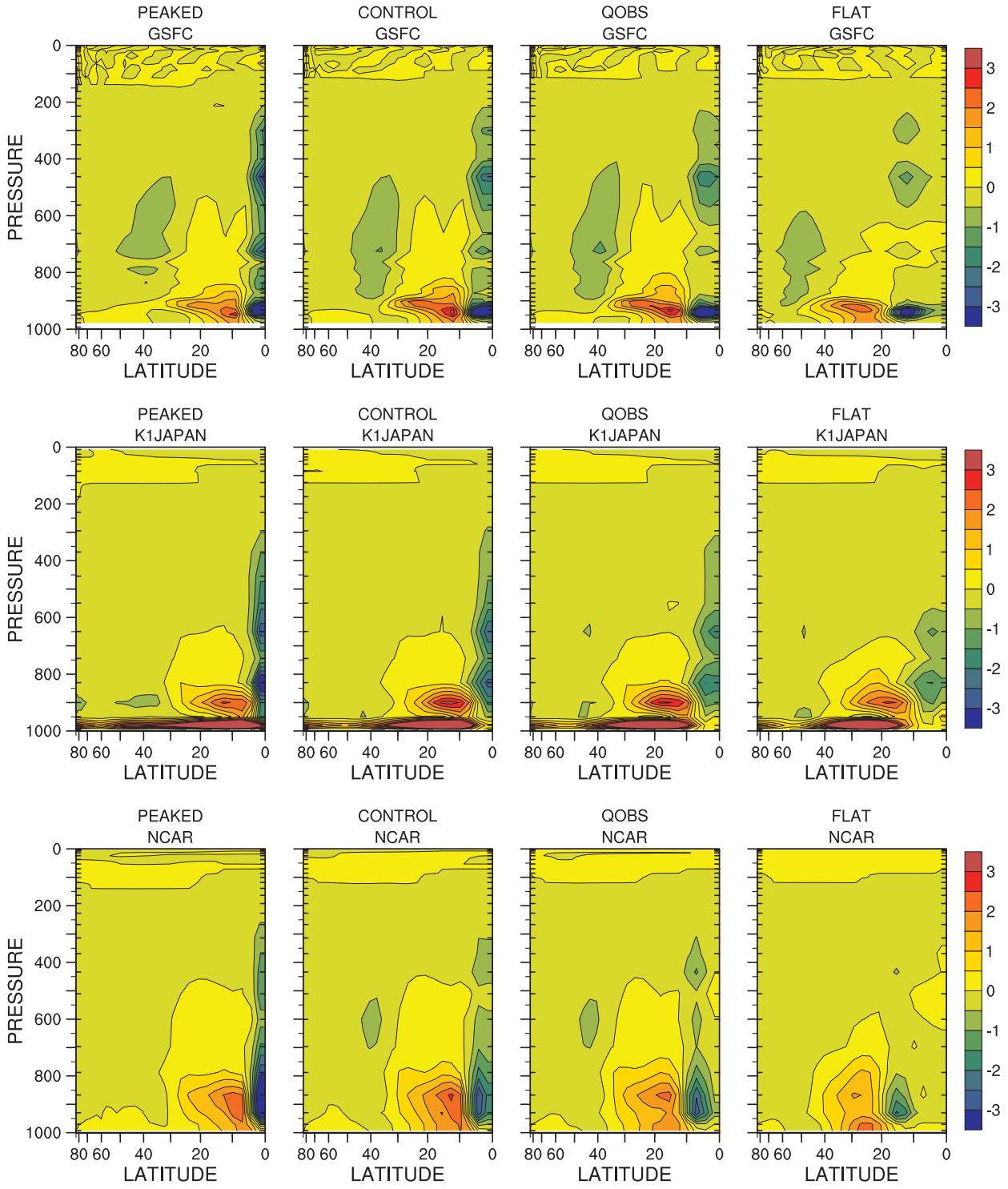

Figure 5.145 (continued): Zonal-time average total parameterized specific humidity tendency (q) for individual models for PEAKED, CONTROL, QOBS and FLAT, g kg^{-1} day^{-1}.

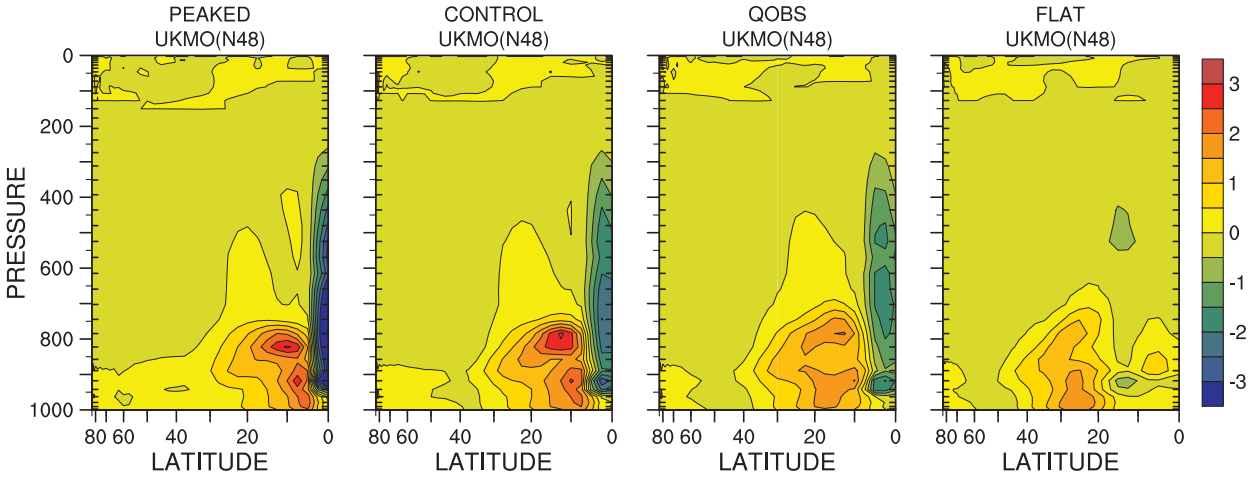

Figure 5.145 (continued): Zonal-time average total parameterized specific humidity tendency (q) for individual models for PEAKED, CONTROL, QOBS and FLAT, g kg^{-1} day^{-1}.

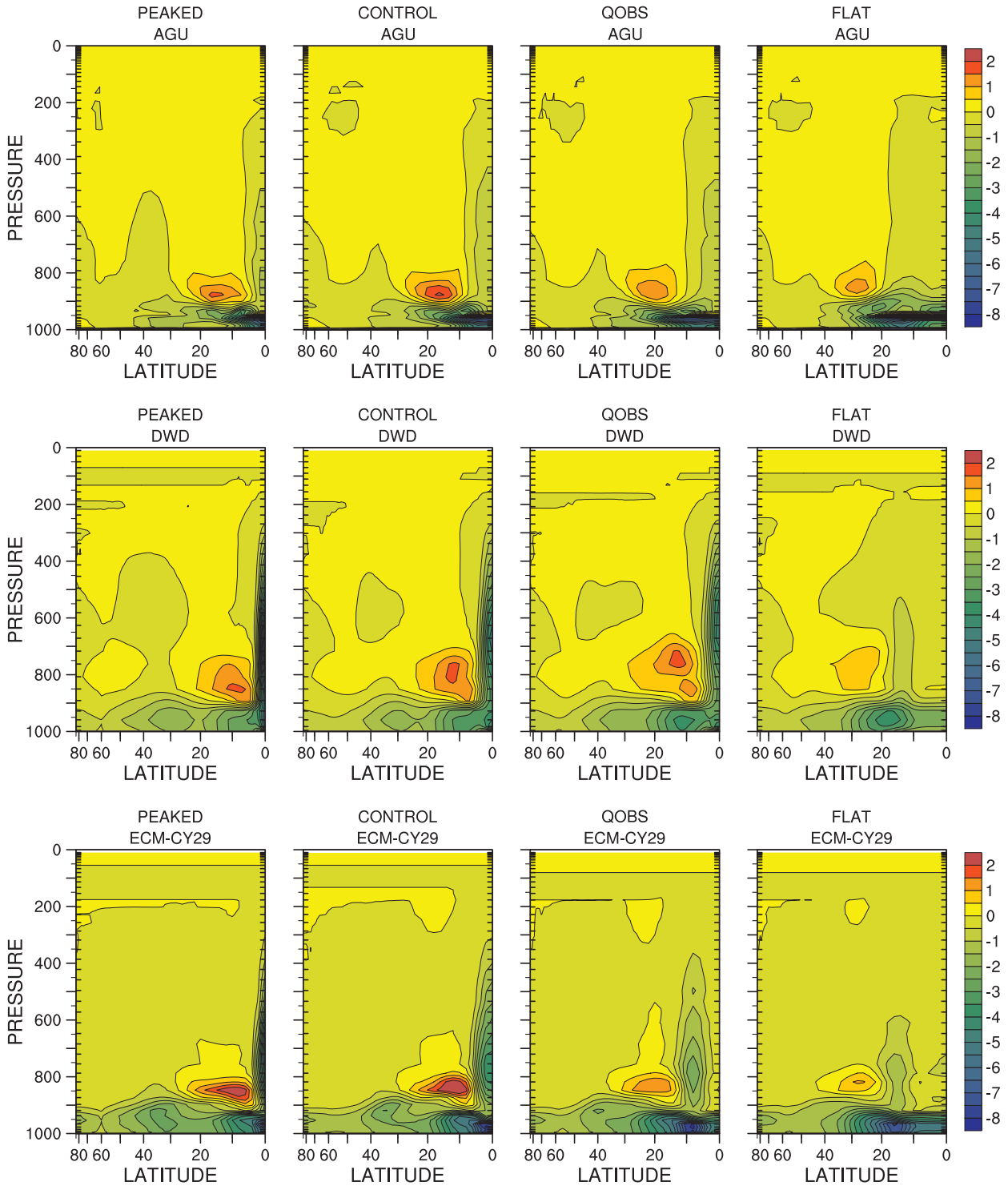

Figure 5.146: Zonal-time average parameterized convection specific humidity tendency (q_conv) for individual models for PEAKED, CONTROL, QOBS and FLAT, g kg^{-1} day^{-1}.

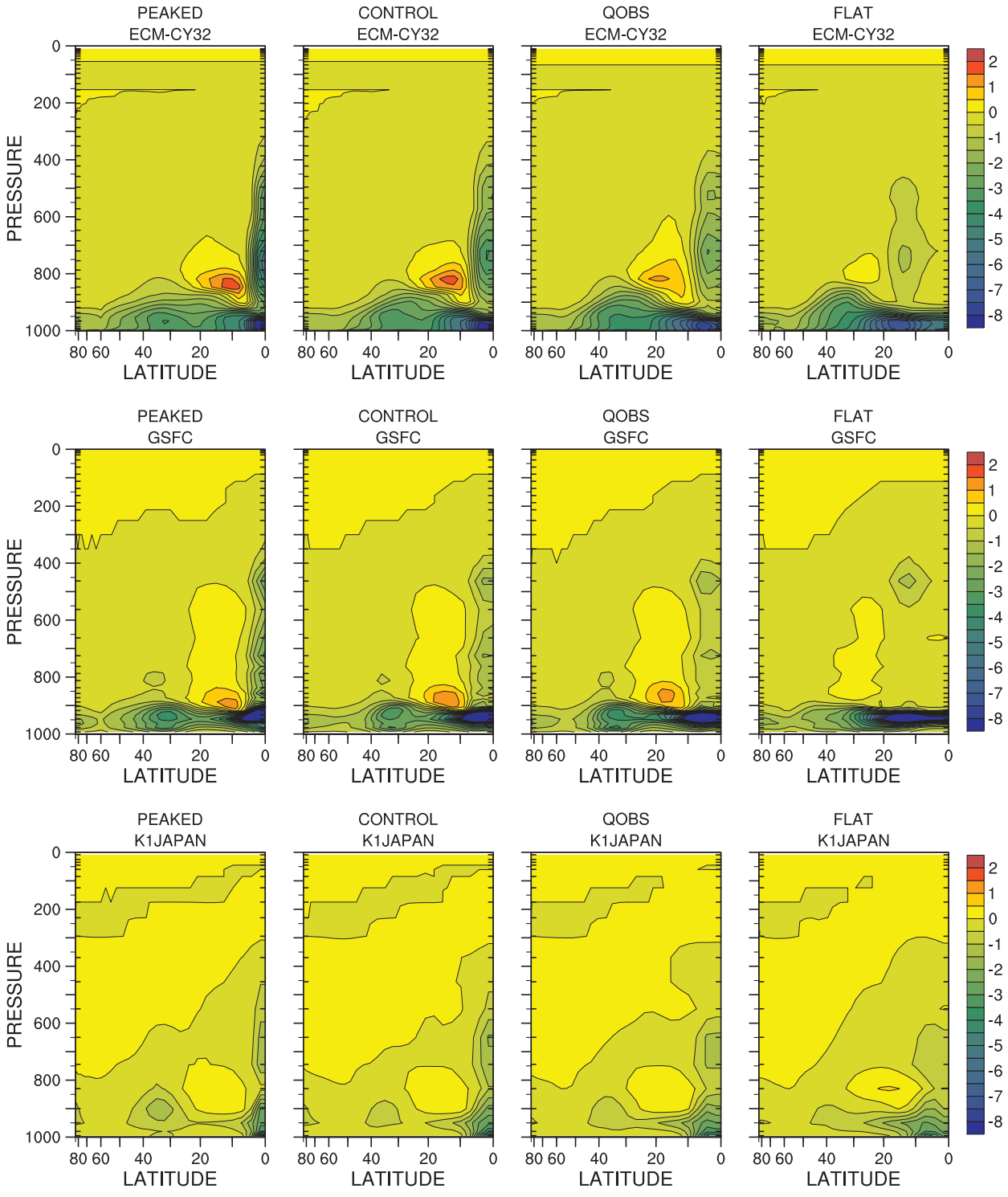

Figure 5.146 (continued): Zonal-time average parameterized convection specific humidity tendency (q_conv) for individual models for PEAKED, CONTROL, QOBS and FLAT, g kg^{-1} day^{-1}.

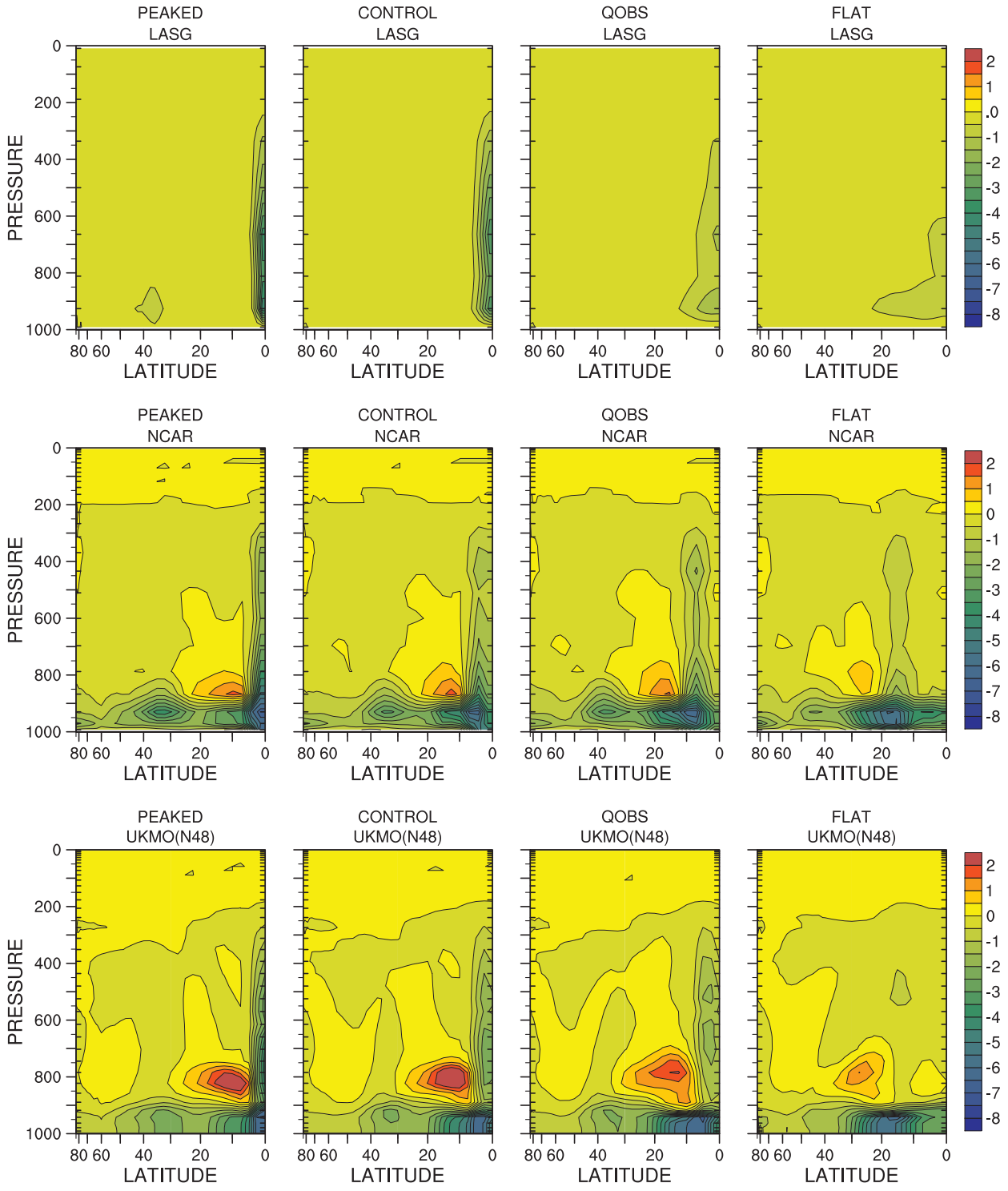

Figure 5.146 (continued): Zonal-time average parameterized convection specific humidity tendency (q_conv) for individual models for PEAKED, CONTROL, QOBS and FLAT, g kg^{-1} day^{-1}.

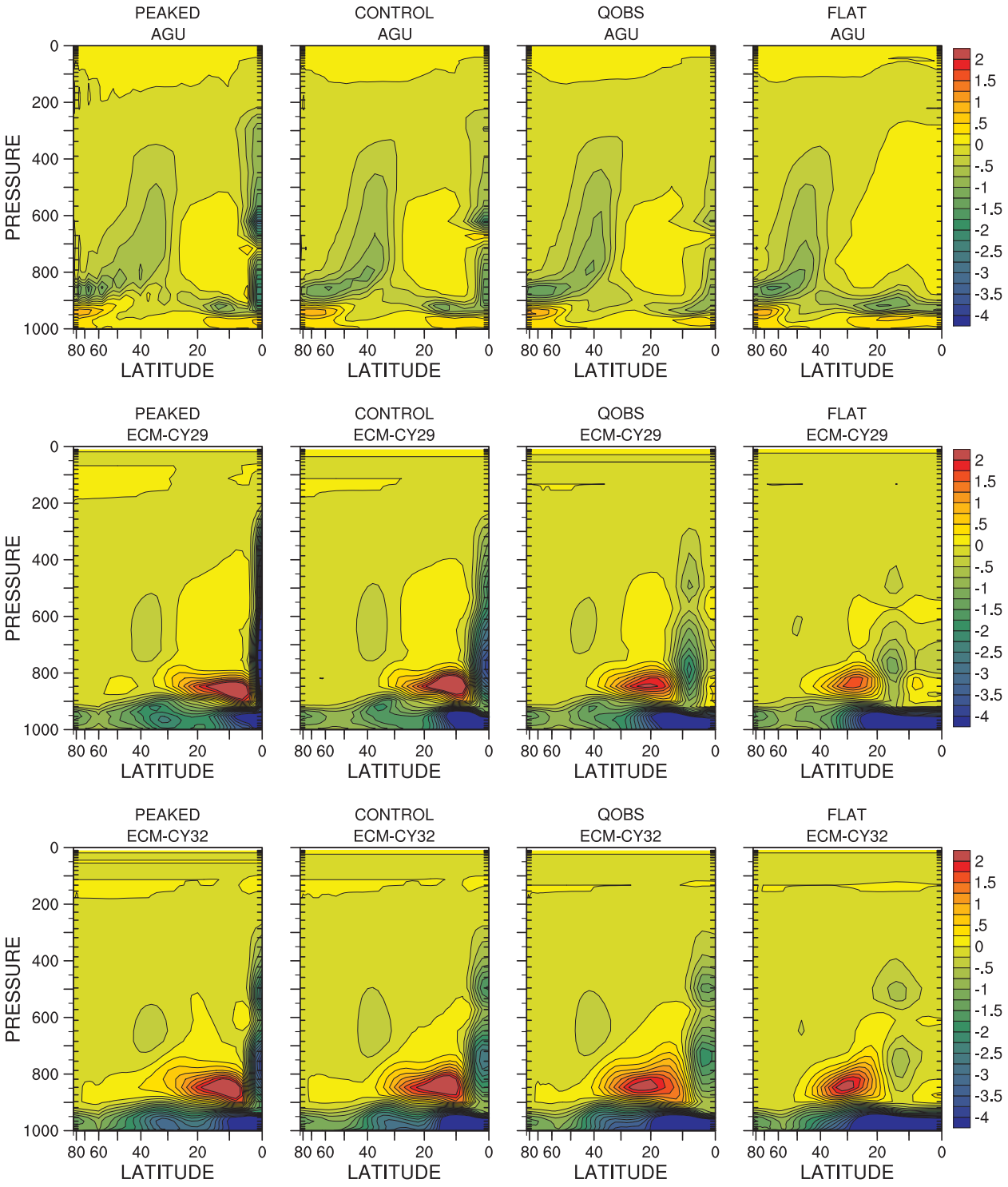

Figure 5.147: Zonal-time average parameterized cloud specific humidity tendency (q_cld) for individual models for PEAKED, CONTROL, QOBS and FLAT, g kg^{-1} day^{-1}.

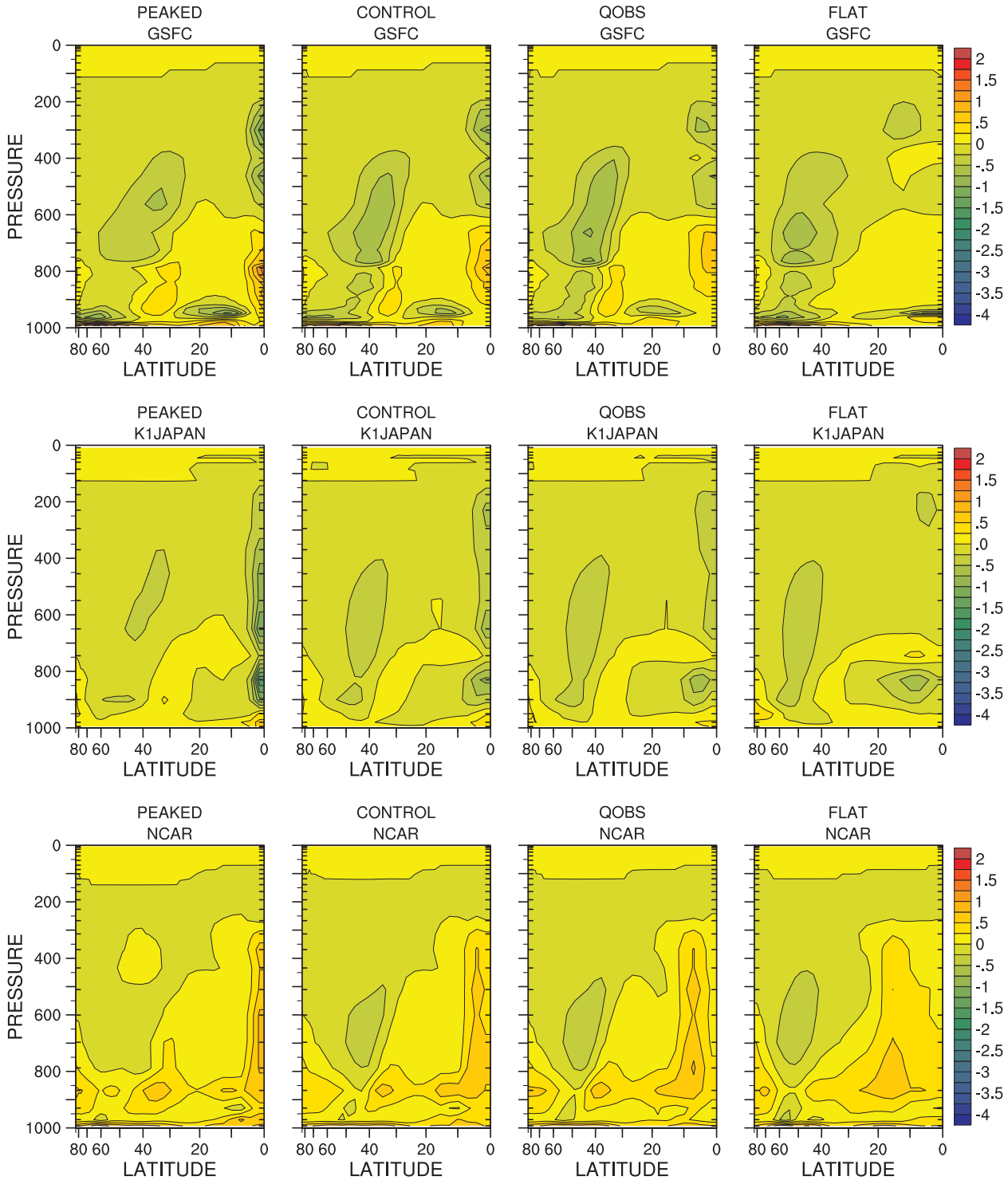

Figure 5.147 (continued): Zonal-time average parameterized cloud specific humidity tendency (q_cld) for individual models for PEAKED, CONTROL, QOBS and FLAT, g kg^{-1} day^{-1}.

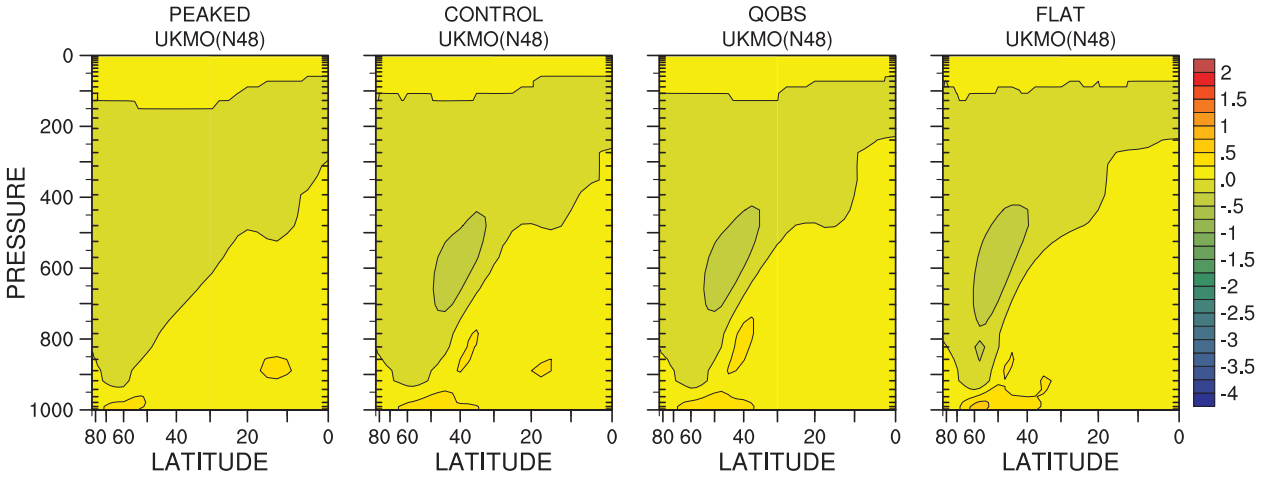

Figure 5.147 (continued): Zonal-time average parameterized cloud specific humidity tendency (q_cld) for individual models for PEAKED, CONTROL, QOBS and FLAT, g kg^{-1} day^{-1}.

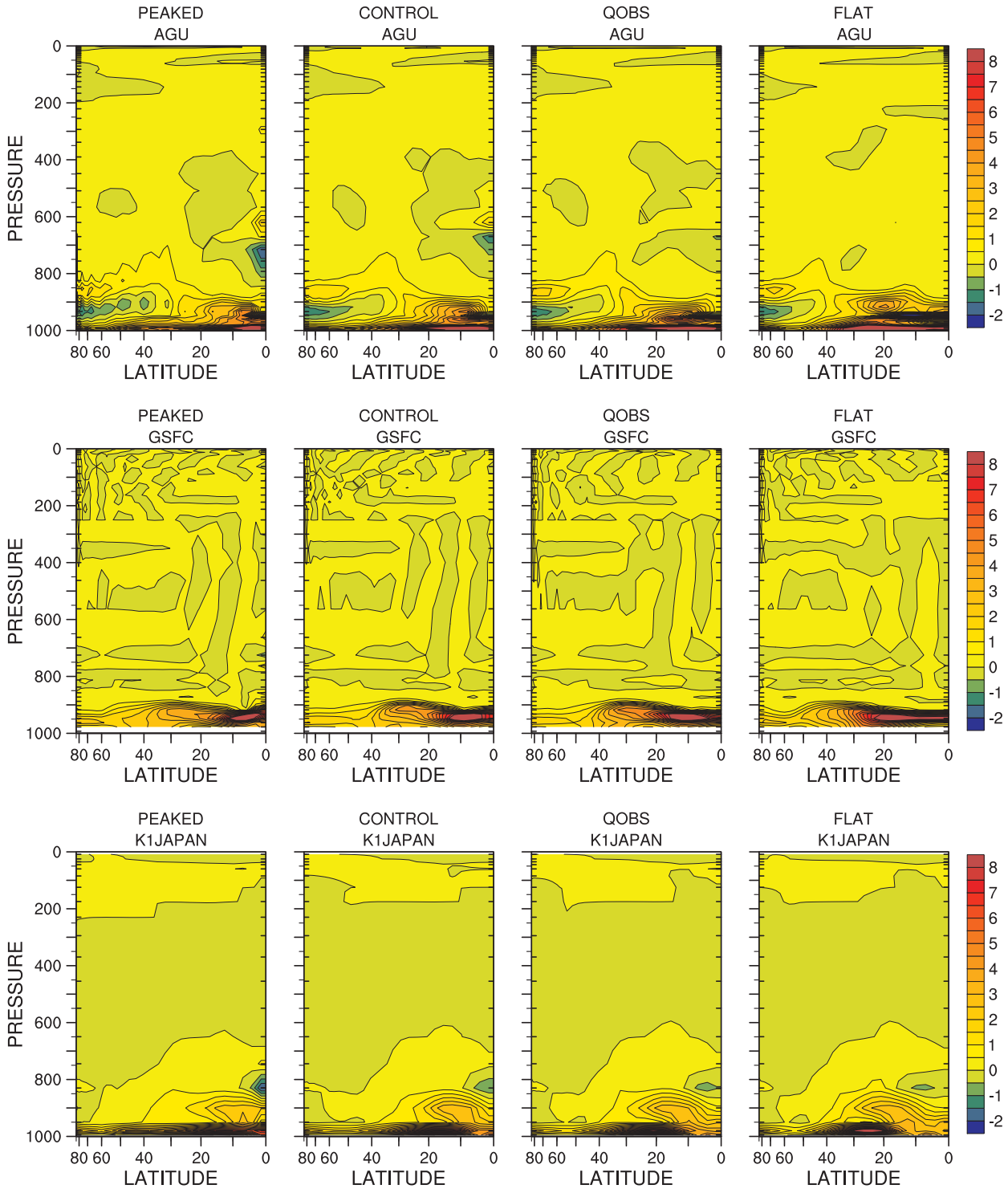

Figure 5.148: Zonal-time average parameterized turbulence specific humidity tendency (q_turb) for individual models for PEAKED, CONTROL, QOBS and FLAT, g kg^{-1} day^{-1}.

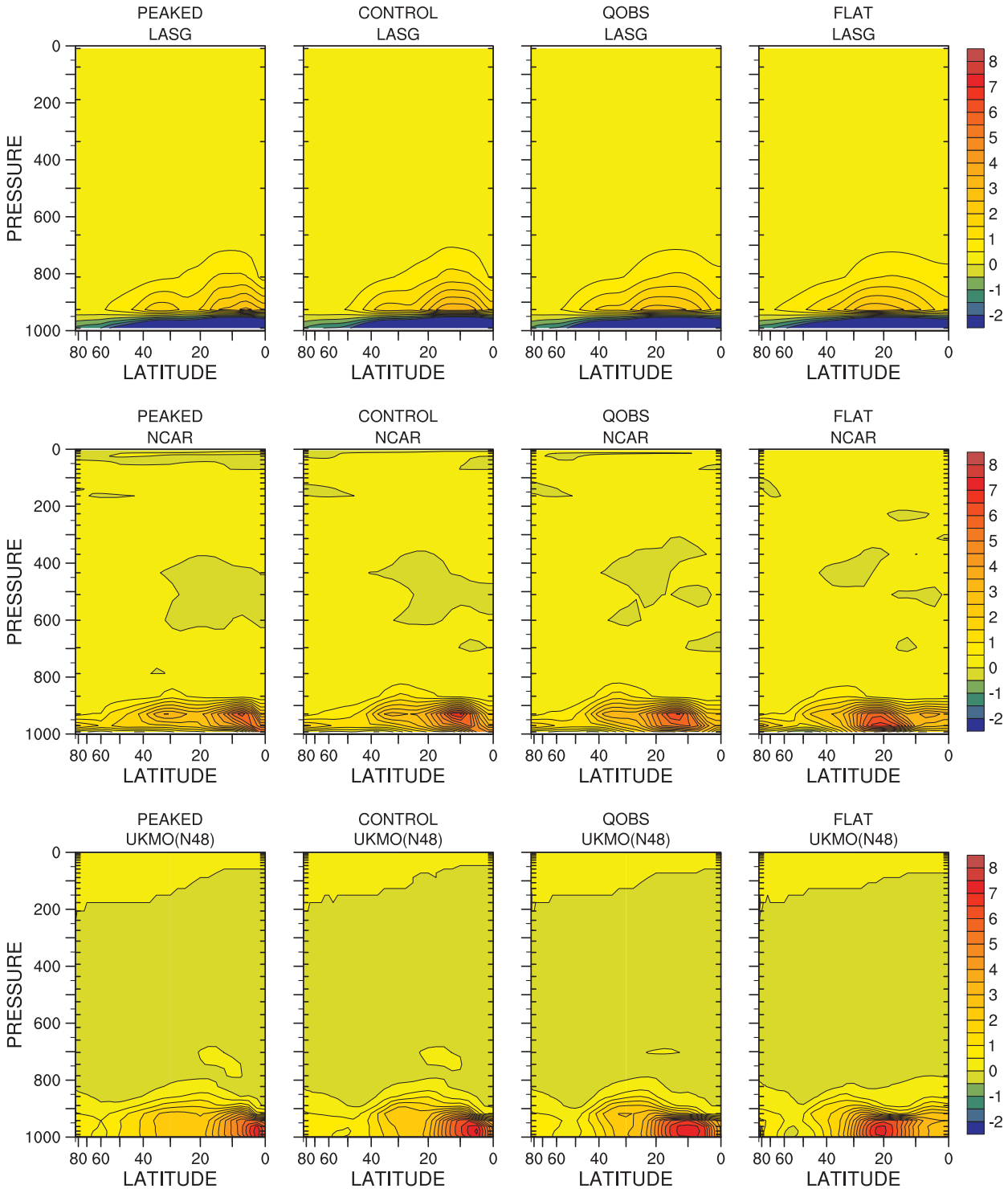

Figure 5.148 (continued): Zonal-time average parameterized turbulence specific humidity tendency (q_turb) for individual models for PEAKED, CONTROL, QOBS and FLAT, g kg^{-1} day^{-1}.

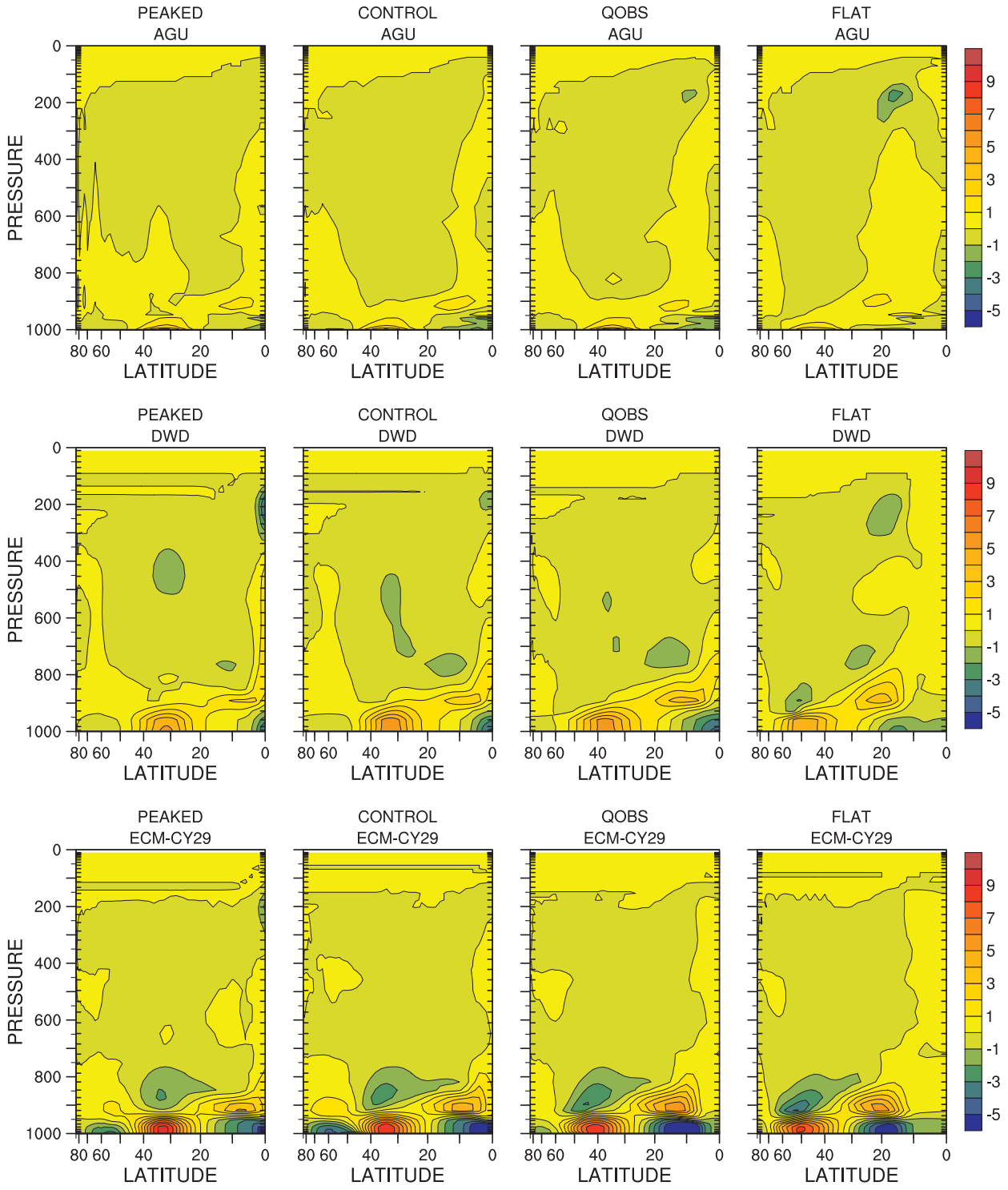

Figure 5.149: Zonal-time average parameterized convection zonal wind tendency (u_conv) for individual models for PEAKED, CONTROL, QOBS and FLAT, m s^{-1} day^{-1}.

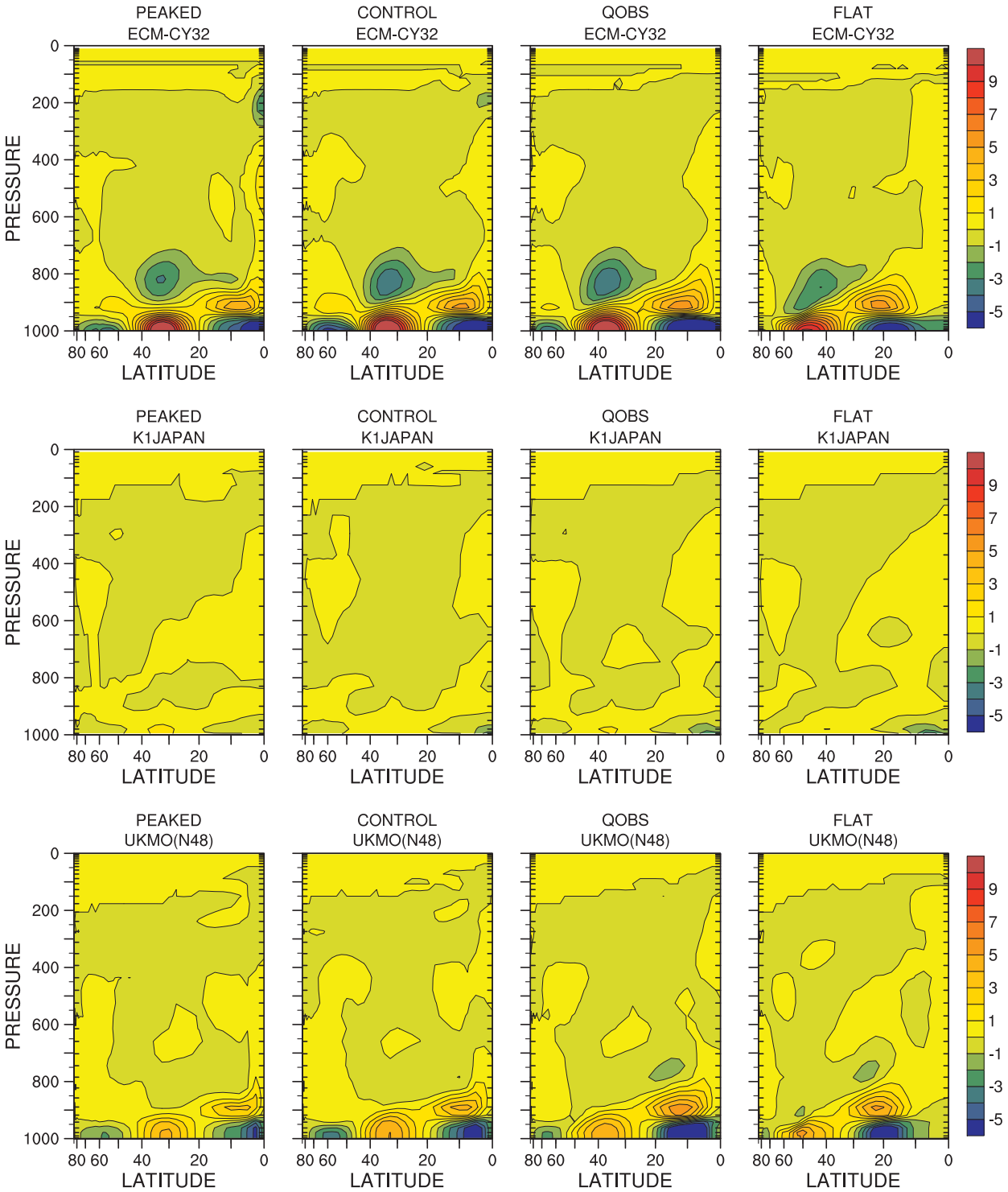

Figure 5.149 (continued): Zonal-time average parameterized convection zonal wind tendency (u_conv) for individual models for PEAKED, CONTROL, QOBS and FLAT, m s^{-1} day^{-1}.

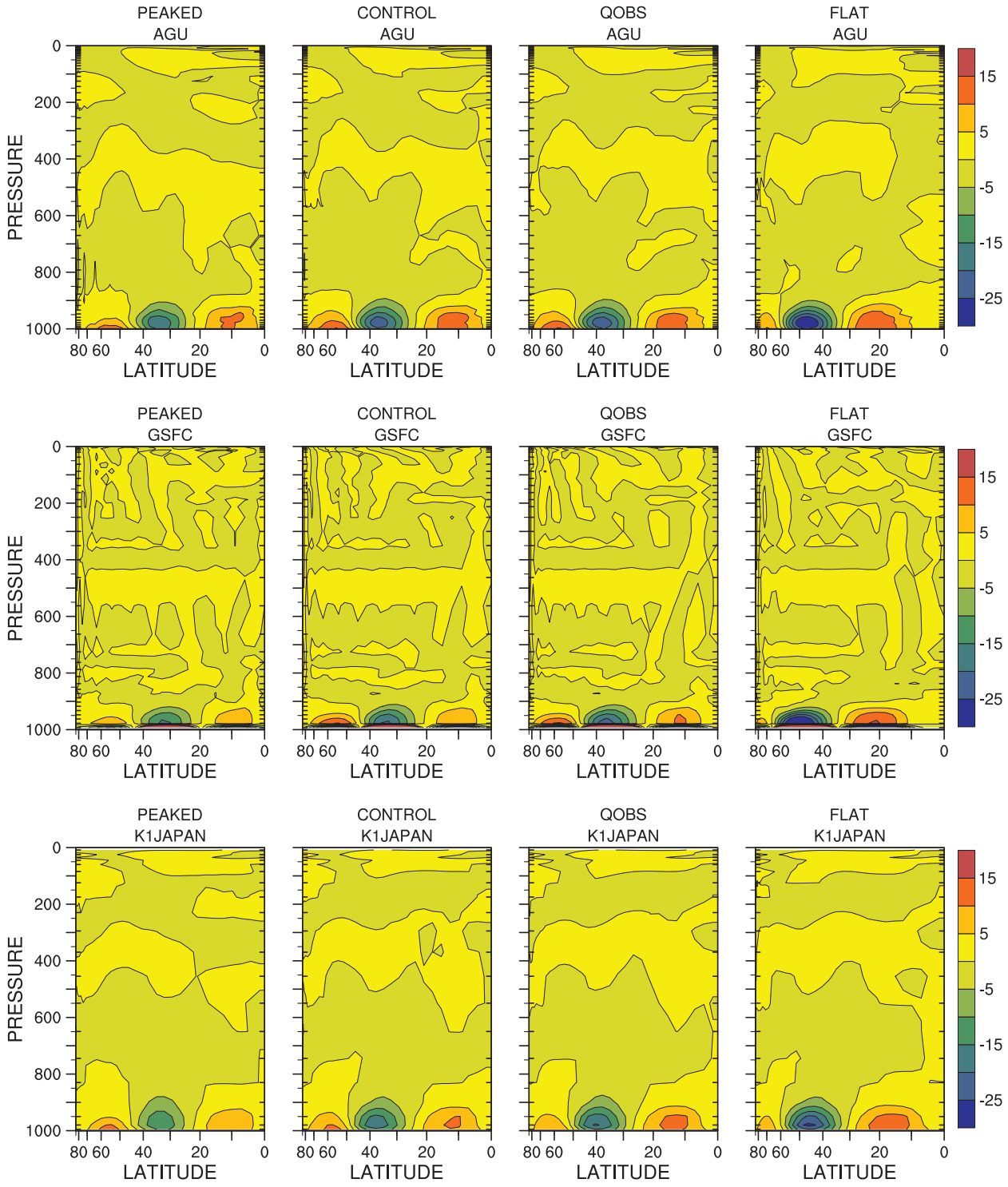

Figure 5.150: Zonal-time average parameterized turbulence zonal wind tendency (u_turb) for individual models for PEAKED, CONTROL, QOBS and FLAT, m s^{-1} day^{-1}.

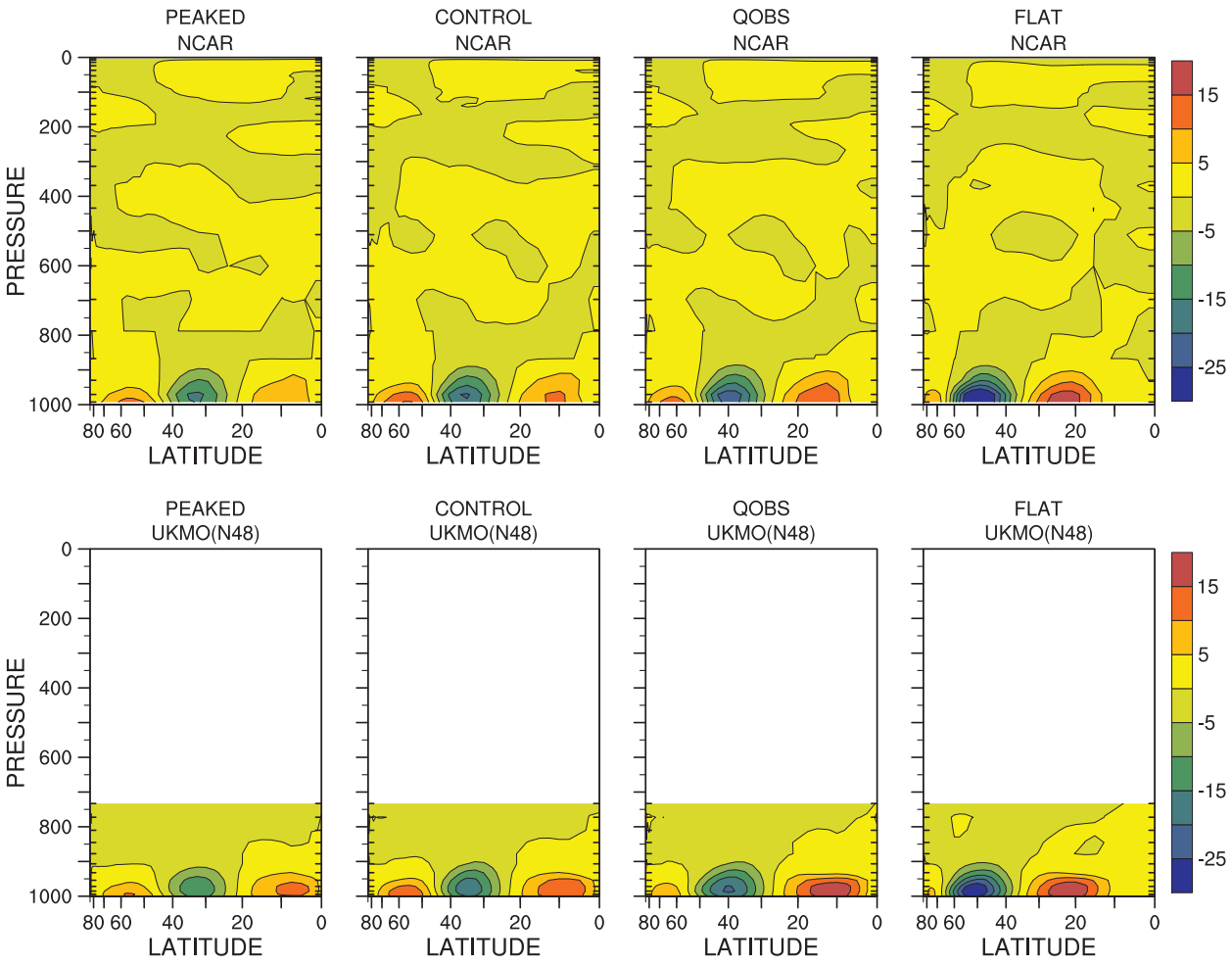

Figure 5.150 (continued): Zonal-time average parameterized turbulence zonal wind tendency (u_turb) for individual models for PEAKED, CONTROL, QOBS and FLAT, m s^{-1} day^{-1}.

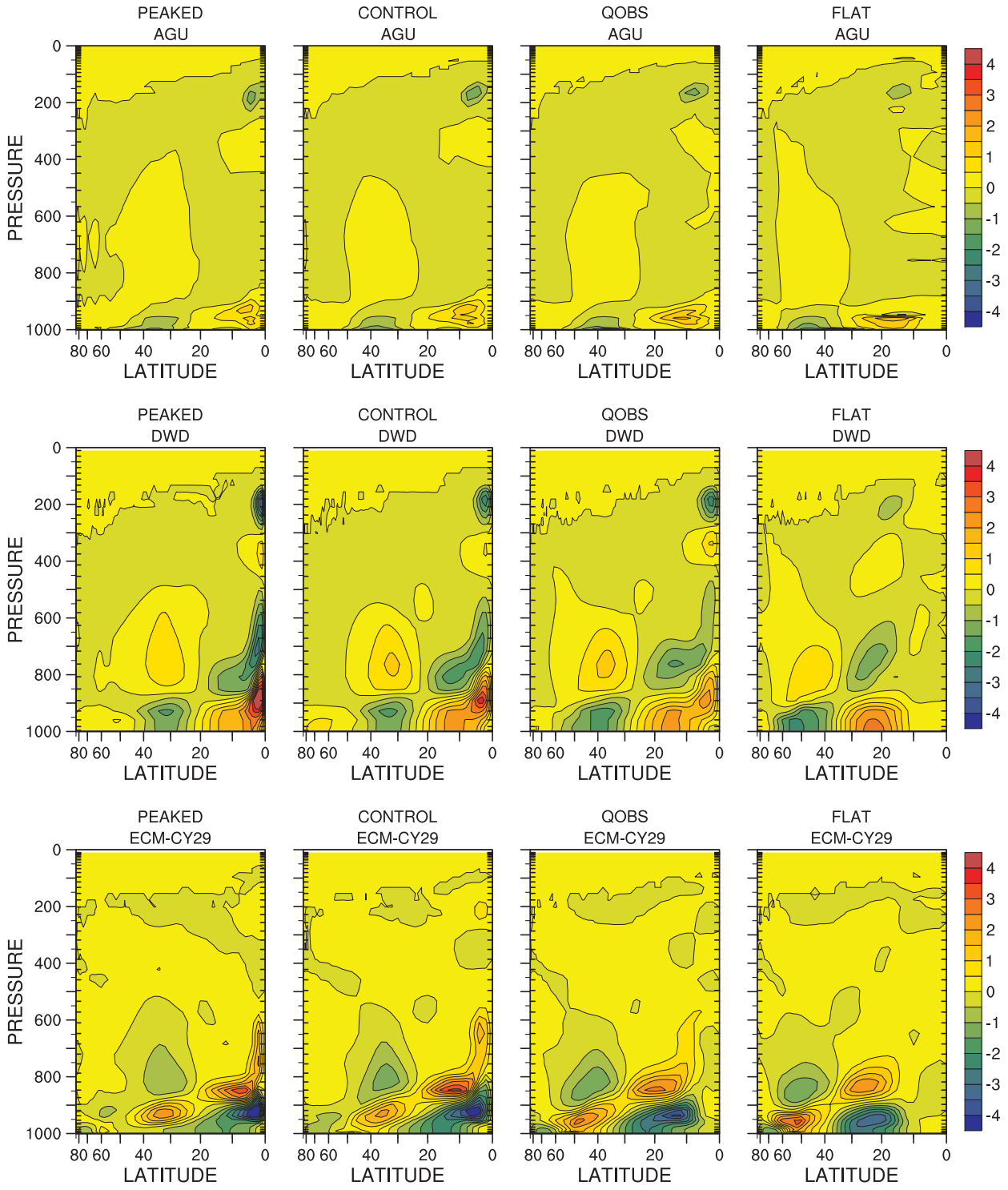

Figure 5.151: Zonal-time average parameterized convection meridional wind tendency (v_conv) for individual models for PEAKED, CONTROL, QOBS and FLAT, m s^{-1} day^{-1}.

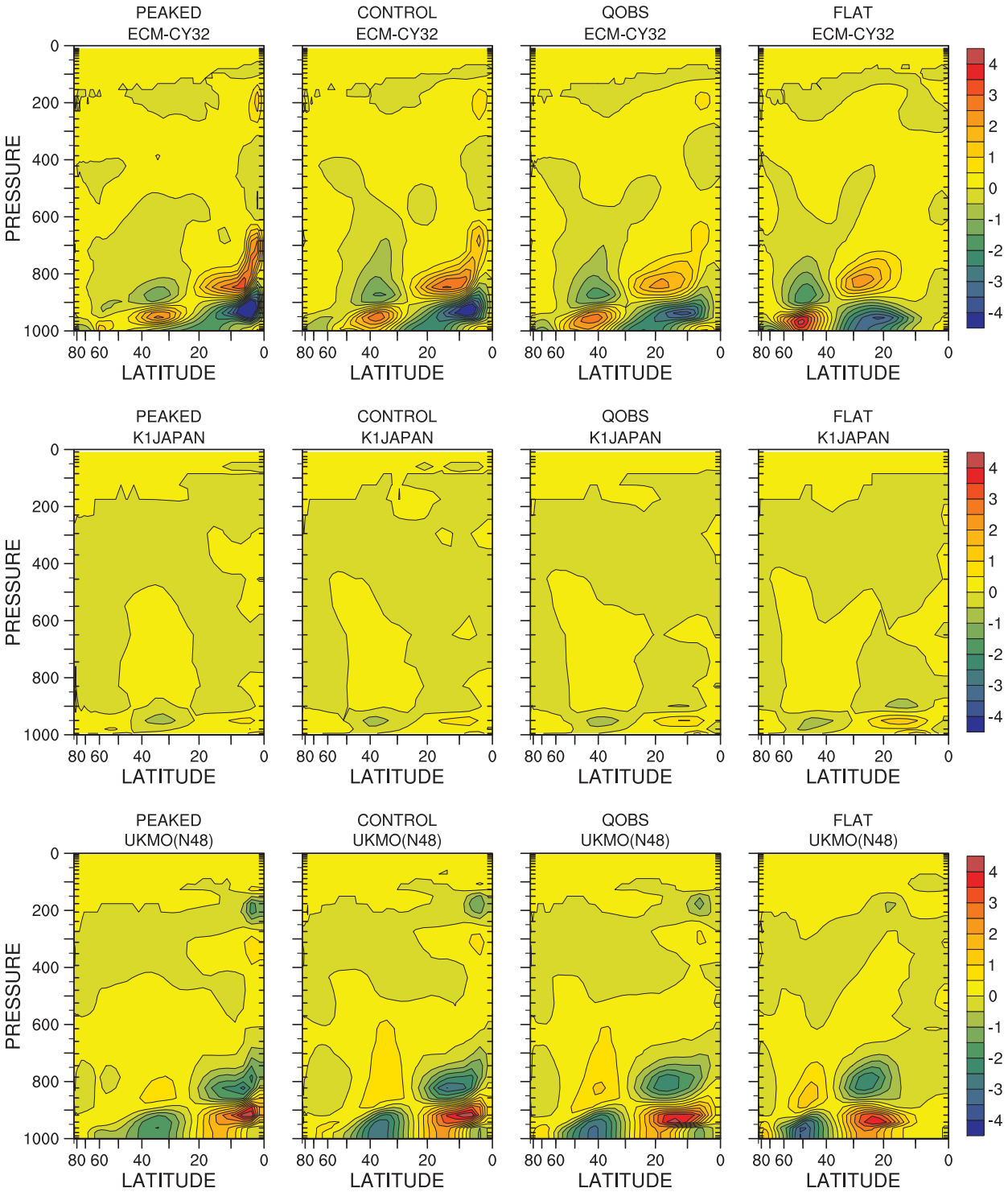

Figure 5.151 (continued): Zonal-time average parameterized convection meridional wind tendency (v_conv) for individual models for PEAKED, CONTROL, QOBS and FLAT, m s^{-1} day^{-1}.

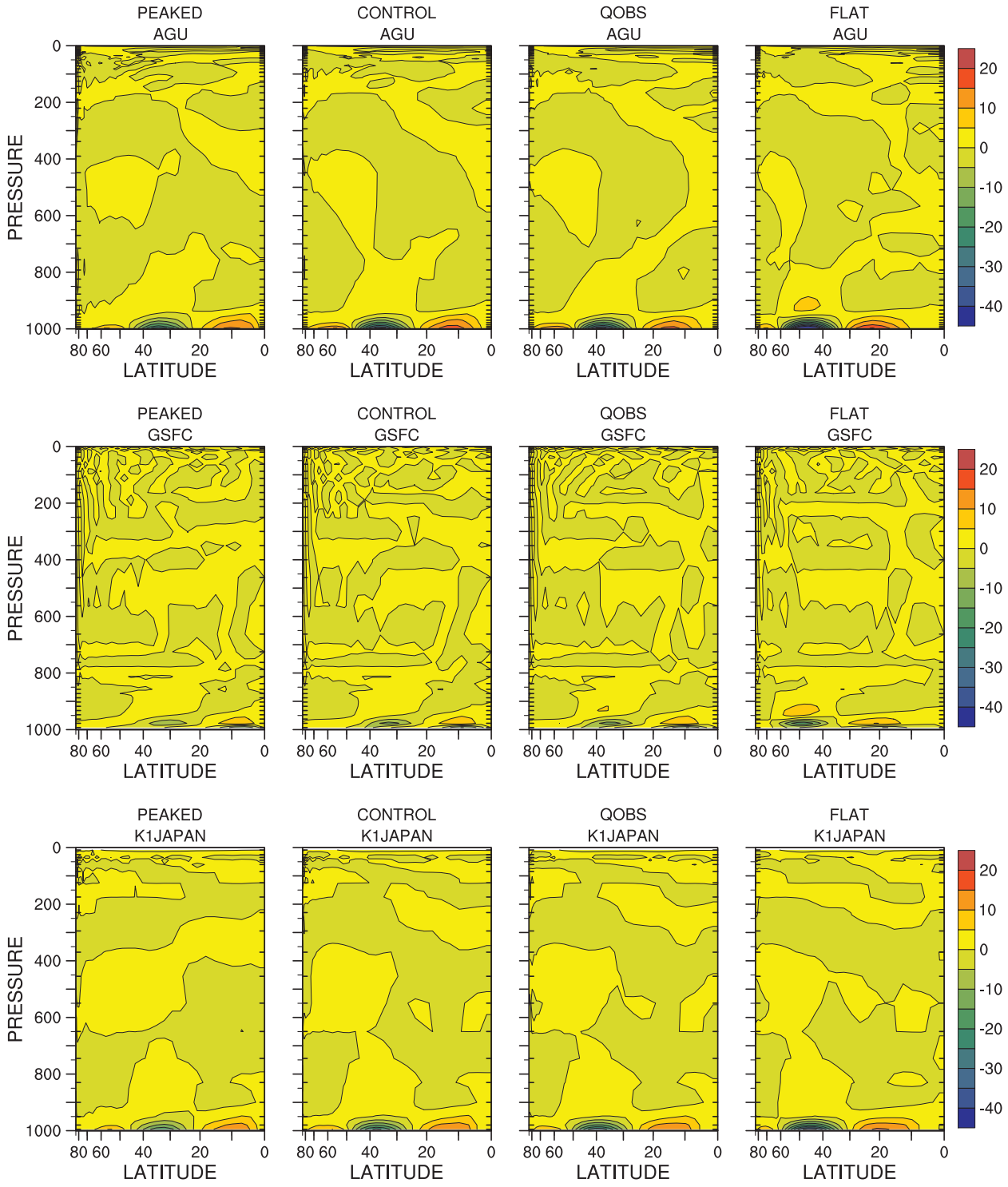

Figure 5.152: Zonal-time average parameterized turbulence meridional wind tendency (v_turb) for individual models for PEAKED, CONTROL, QOBS and FLAT, m s^{-1} day^{-1}.

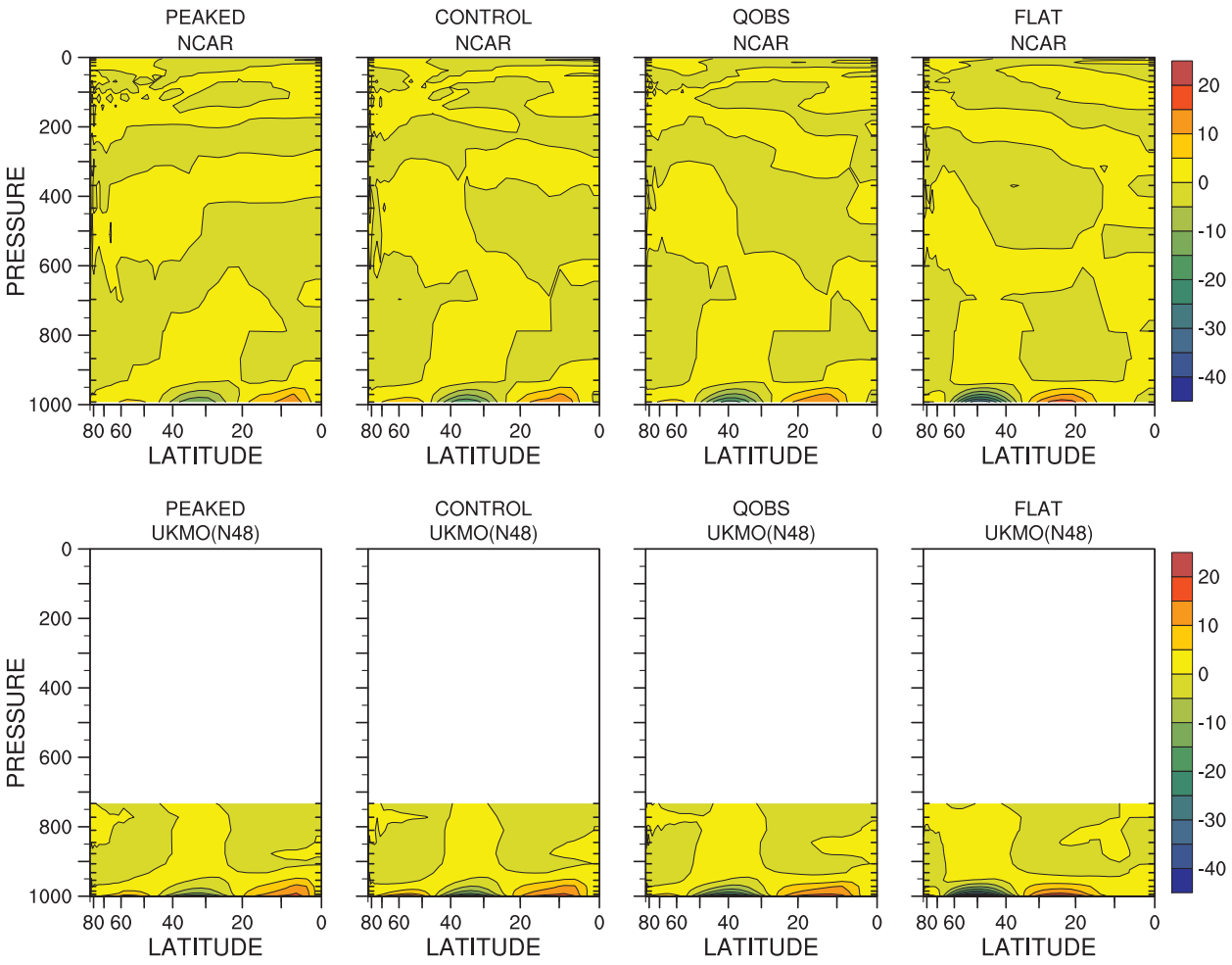

Figure 5.152 (continued): Zonal-time average parameterized turbulence meridional wind tendency (v_turb) for individual models for PEAKED, CONTROL, QOBS and FLAT, m s^{-1} day^{-1}.

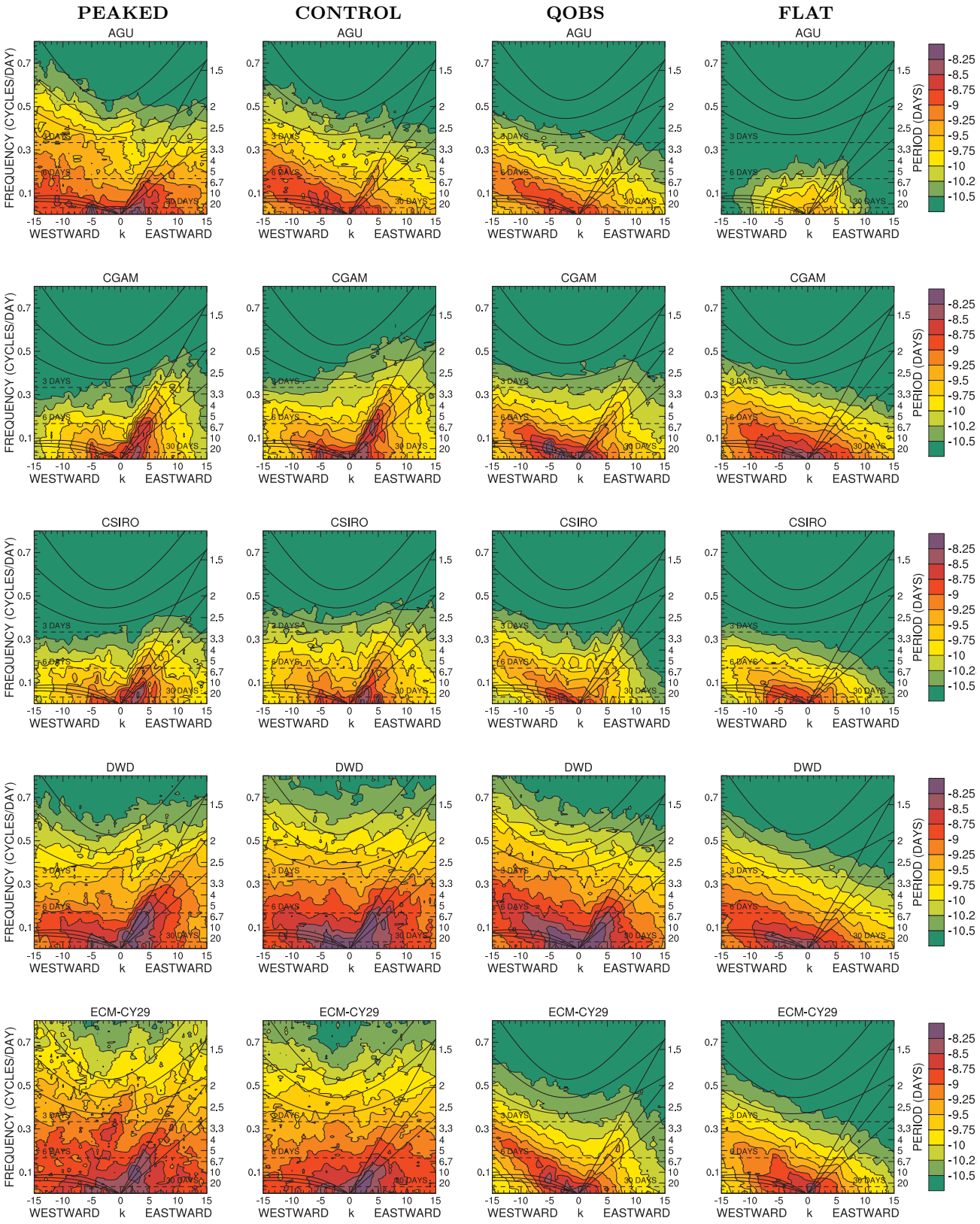

Figure 5.153: Wavenumber-frequency diagrams of log of power of symmetric modes of equatorial precipitation (tppn) for PEAKED, CONTROL, QOBS and FLAT, 20°S to 20°N.

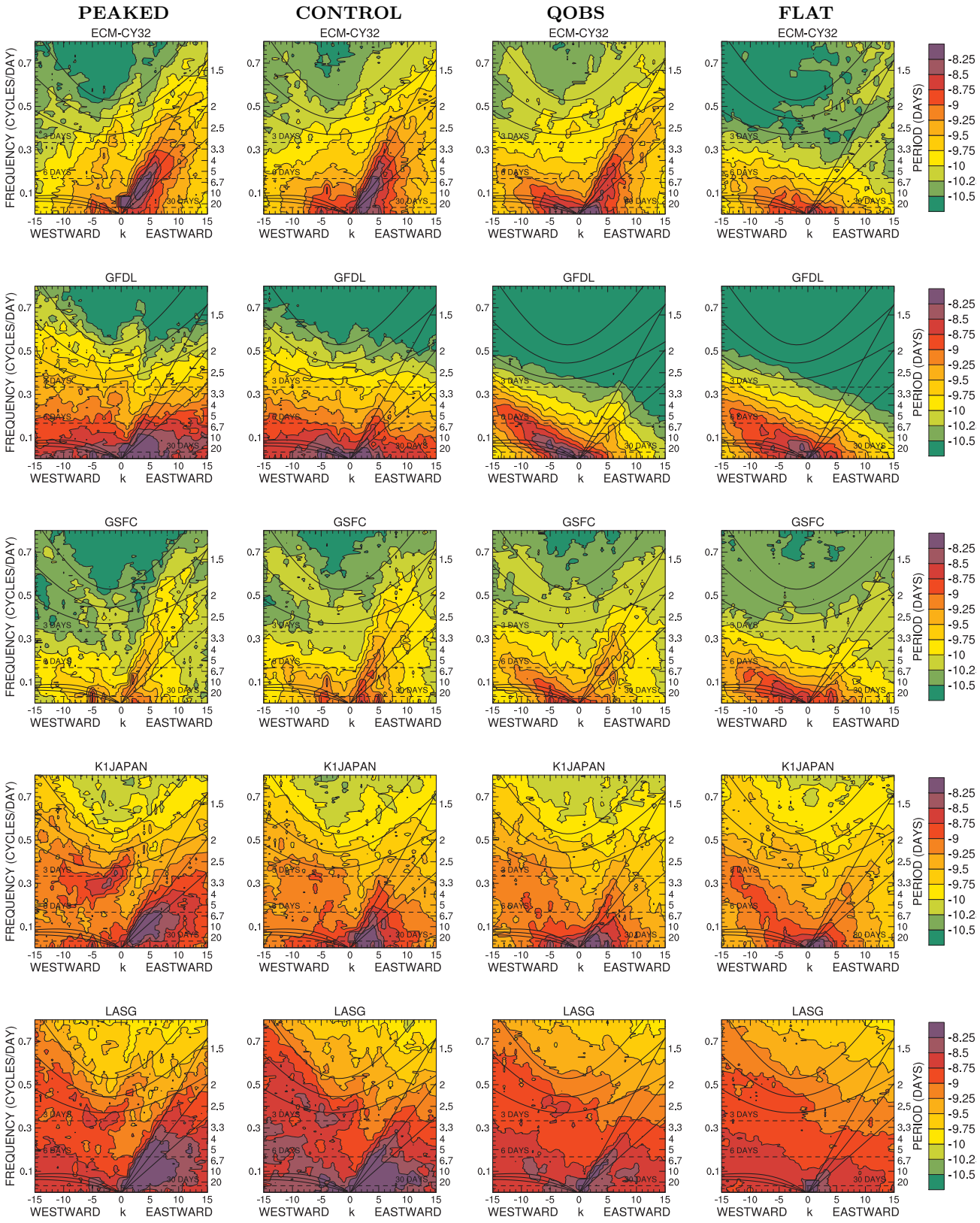

Figure 5.153 (continued): Wavenumber-frequency diagrams of log of power of symmetric modes of equatorial precipitation (tppn) for PEAKED, CONTROL, QOBS and FLAT, 20°S to 20°N.

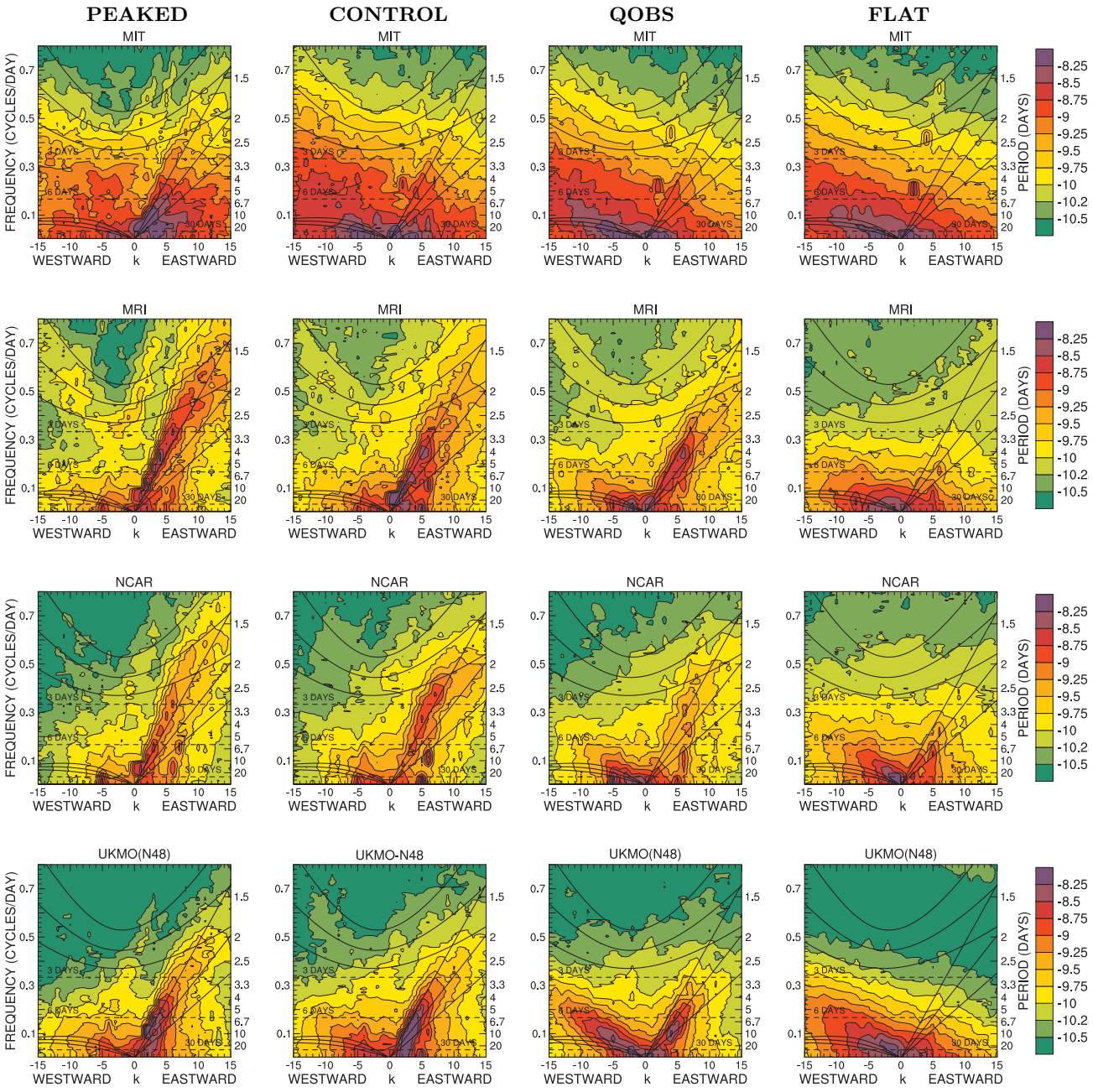

Figure 5.153 (continued): Wavenumber-frequency diagrams of log of power of symmetric modes of equatorial precipitation (tppn) for PEAKED, CONTROL, QOBS and FLAT, 20°S to 20°N.

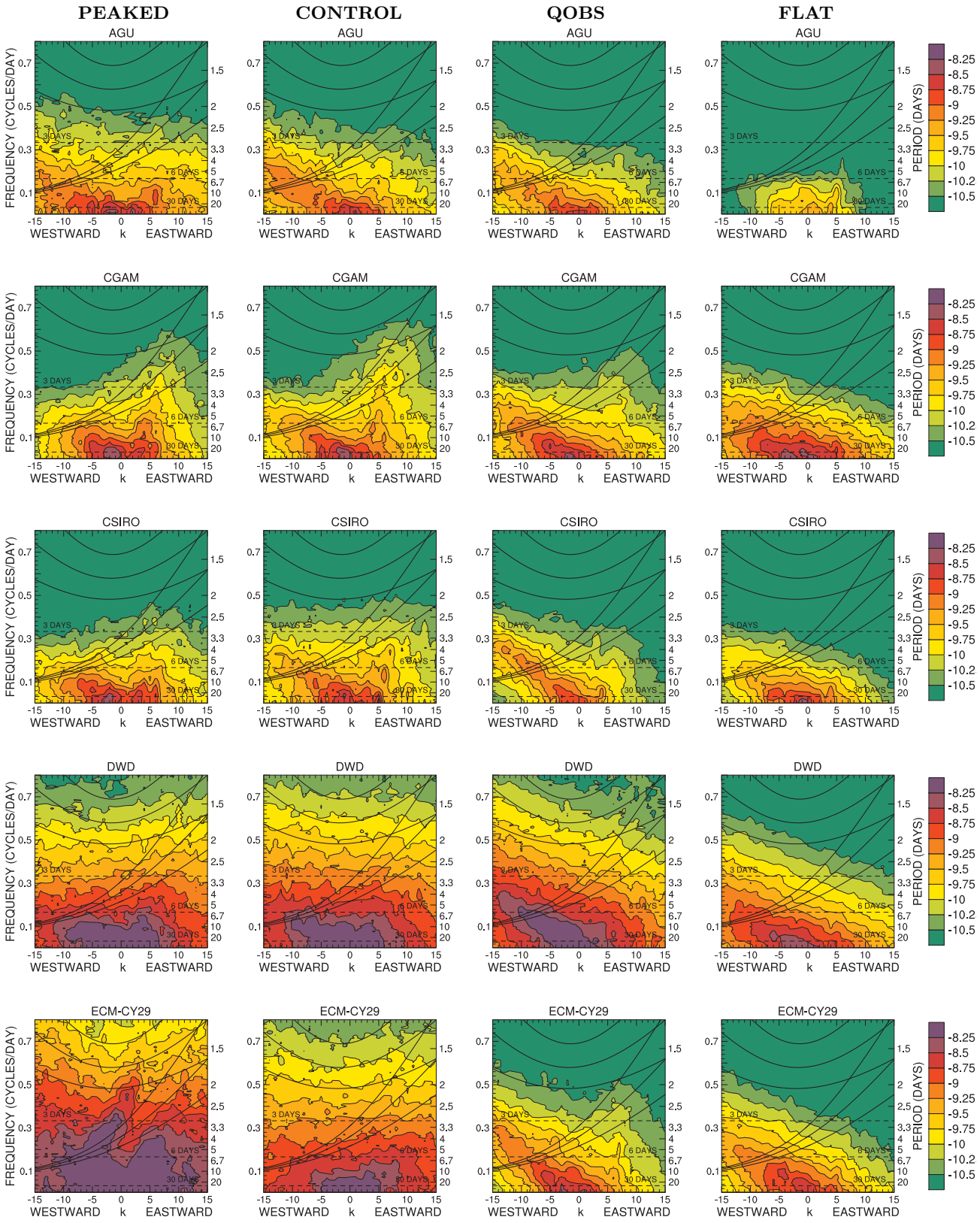

Figure 5.154: Wavenumber-frequency diagrams of log of power of anti-symmetric modes of equatorial precipitation (tppn) for PEAKED, CONTROL, QOBS and FLAT, 20°S to 20°N.

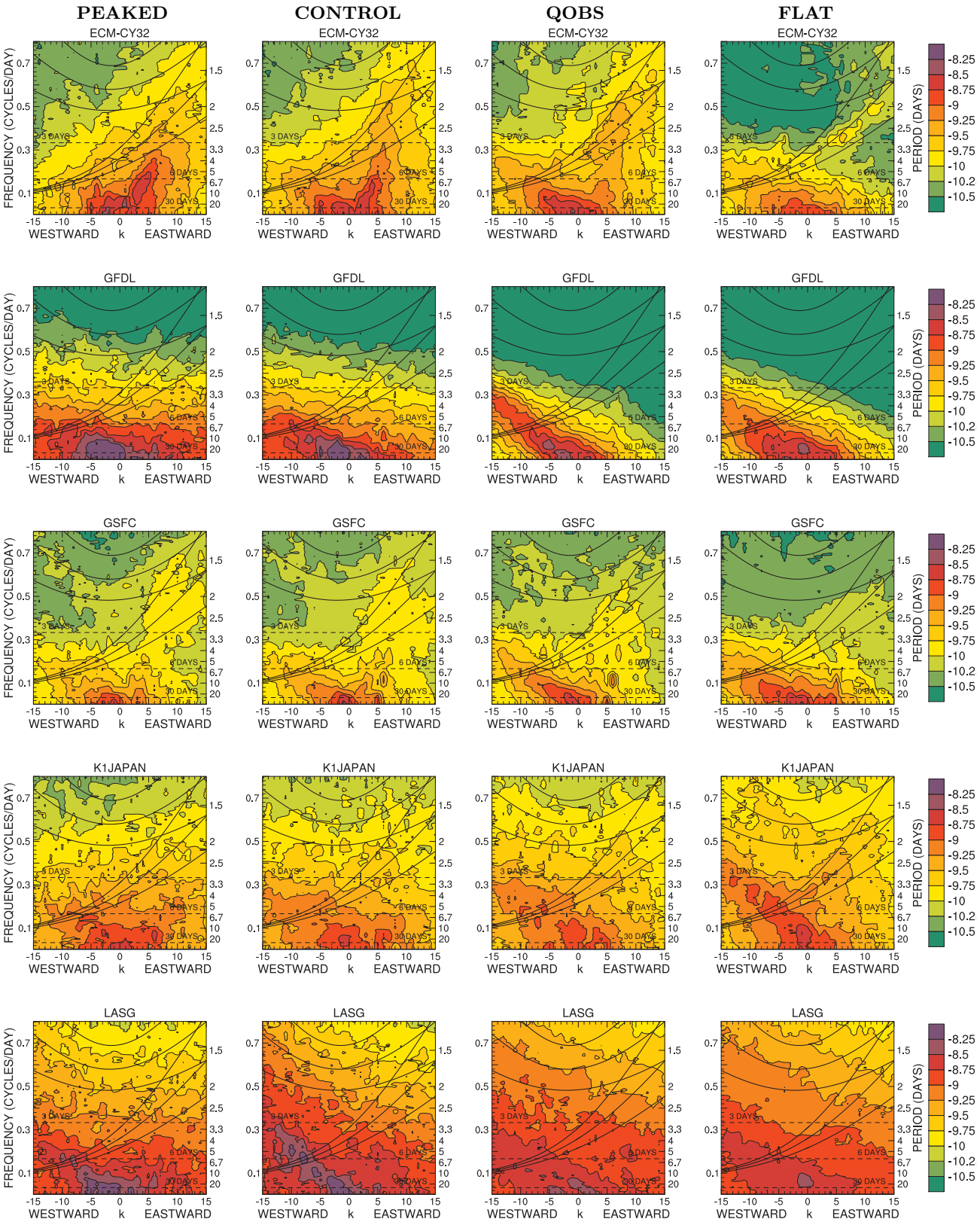

Figure 5.154 (continued): Wavenumber-frequency diagrams of log of power of anti-symmetric modes of equatorial precipitation (tppn) for PEAKED, CONTROL, QOBS and FLAT, 20°S to 20°N.

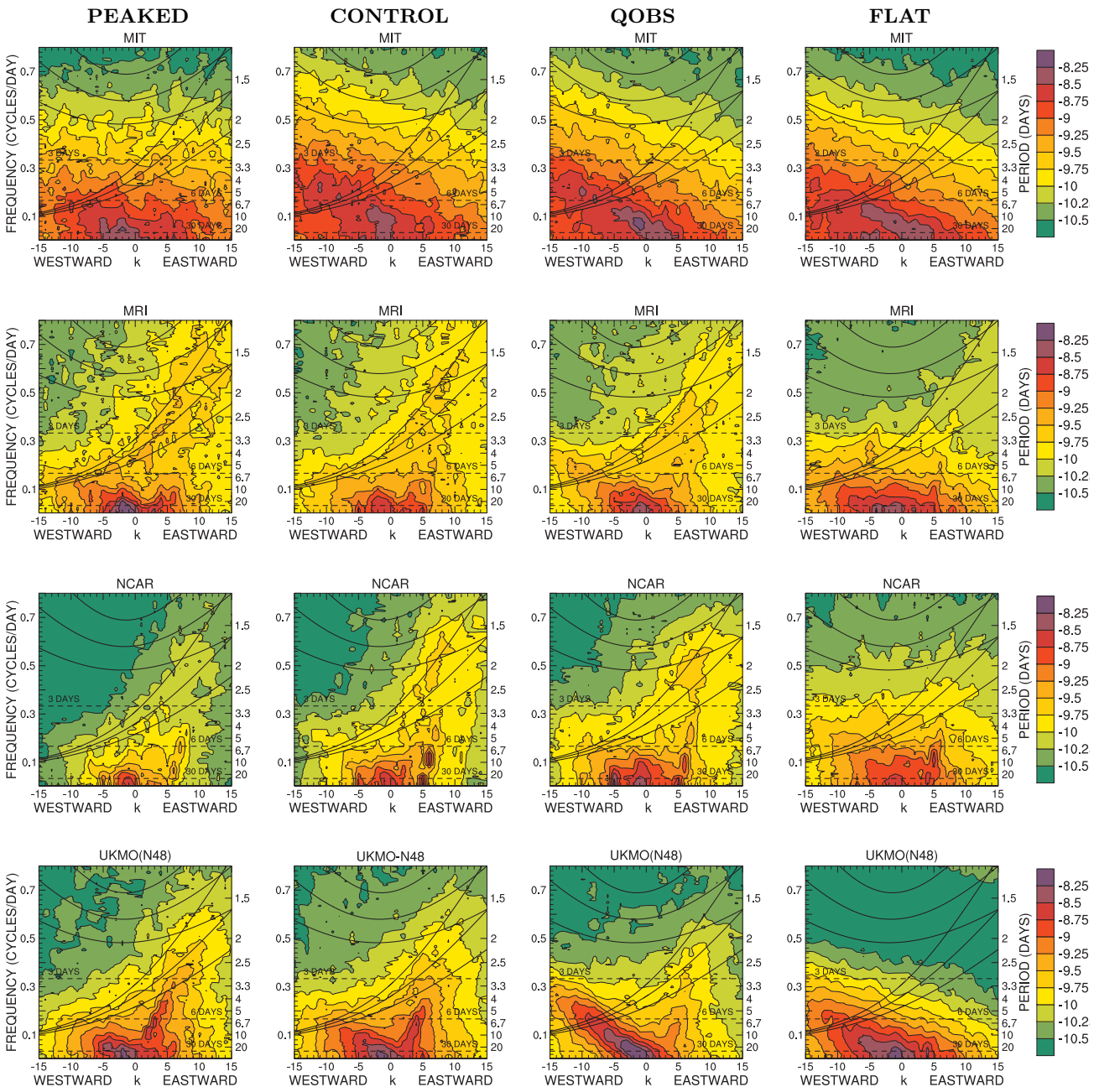

Figure 5.154 (continued): Wavenumber-frequency diagrams of log of power of anti-symmetric modes of equatorial precipitation (tppn) for PEAKED, CONTROL, QOBS and FLAT, 20°S to 20°N.

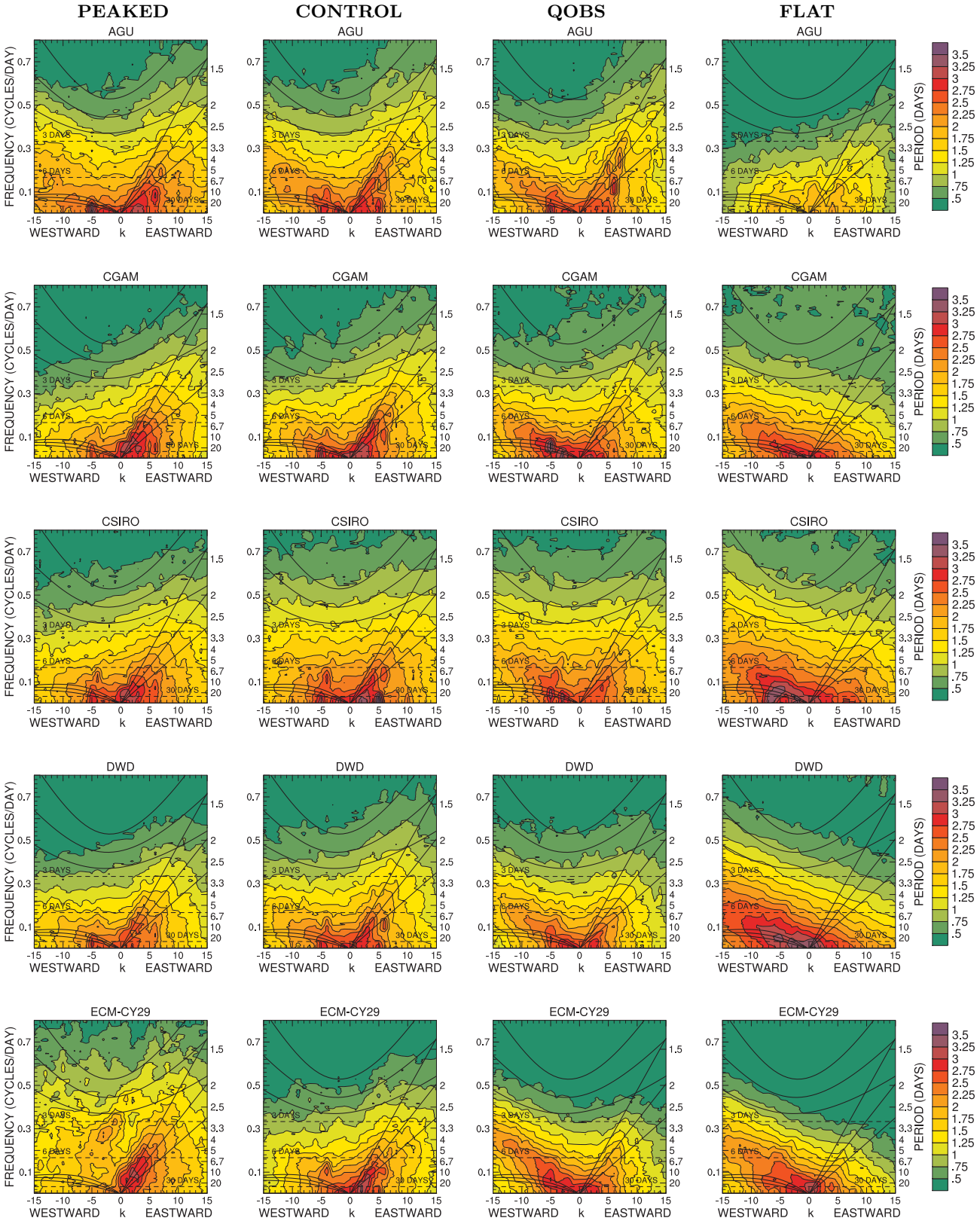

Figure 5.155: Wavenumber-frequency diagrams of log of power of symmetric modes of equatorial OLR (lw_toa) for PEAKED, CONTROL, QOBS and FLAT, 20°S to 20°N.

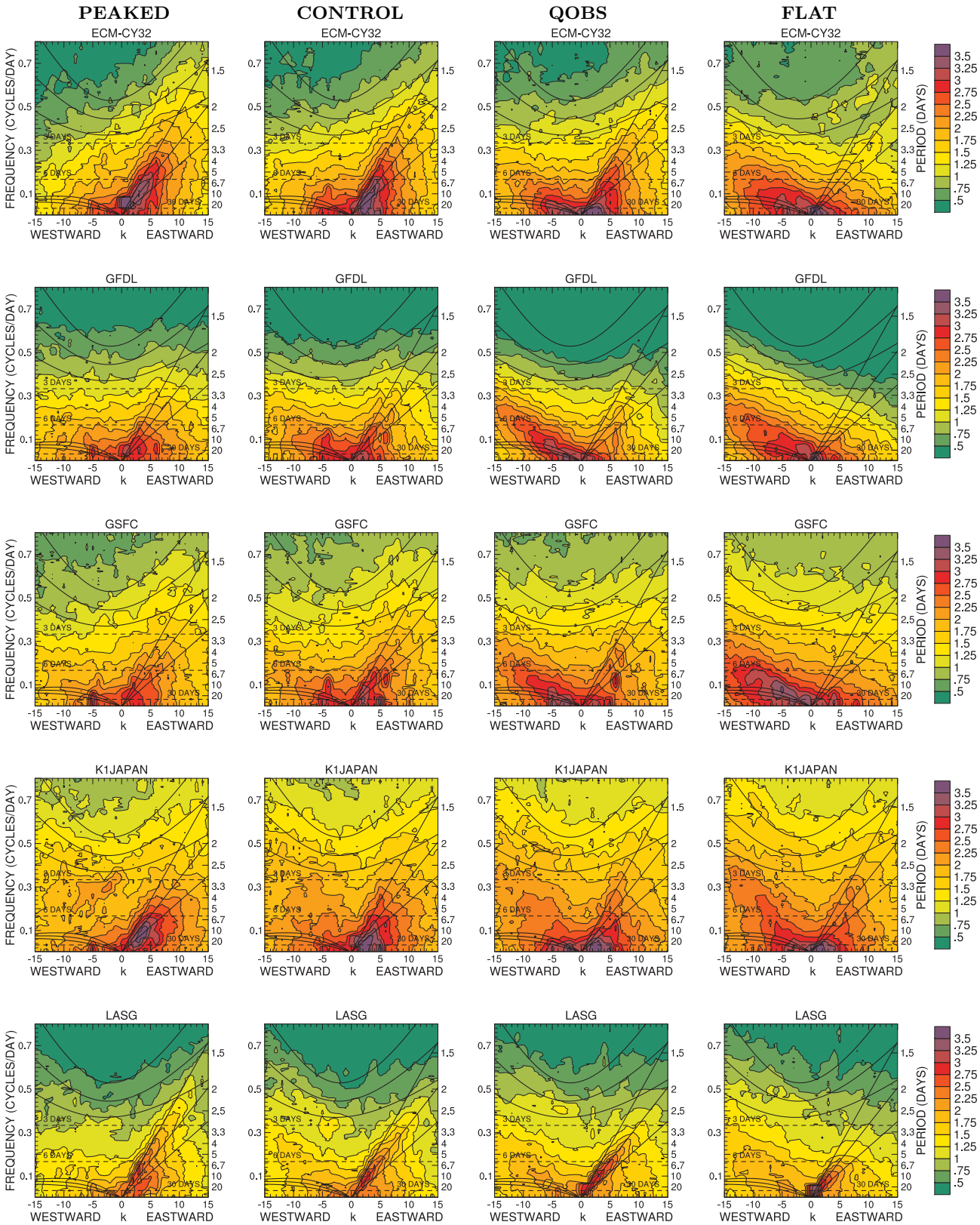

Figure 5.155 (continued): Wavenumber-frequency diagrams of log of power of symmetric modes of equatorial OLR (lw_toa) for PEAKED, CONTROL, QOBS and FLAT, 20°S to 20°N.

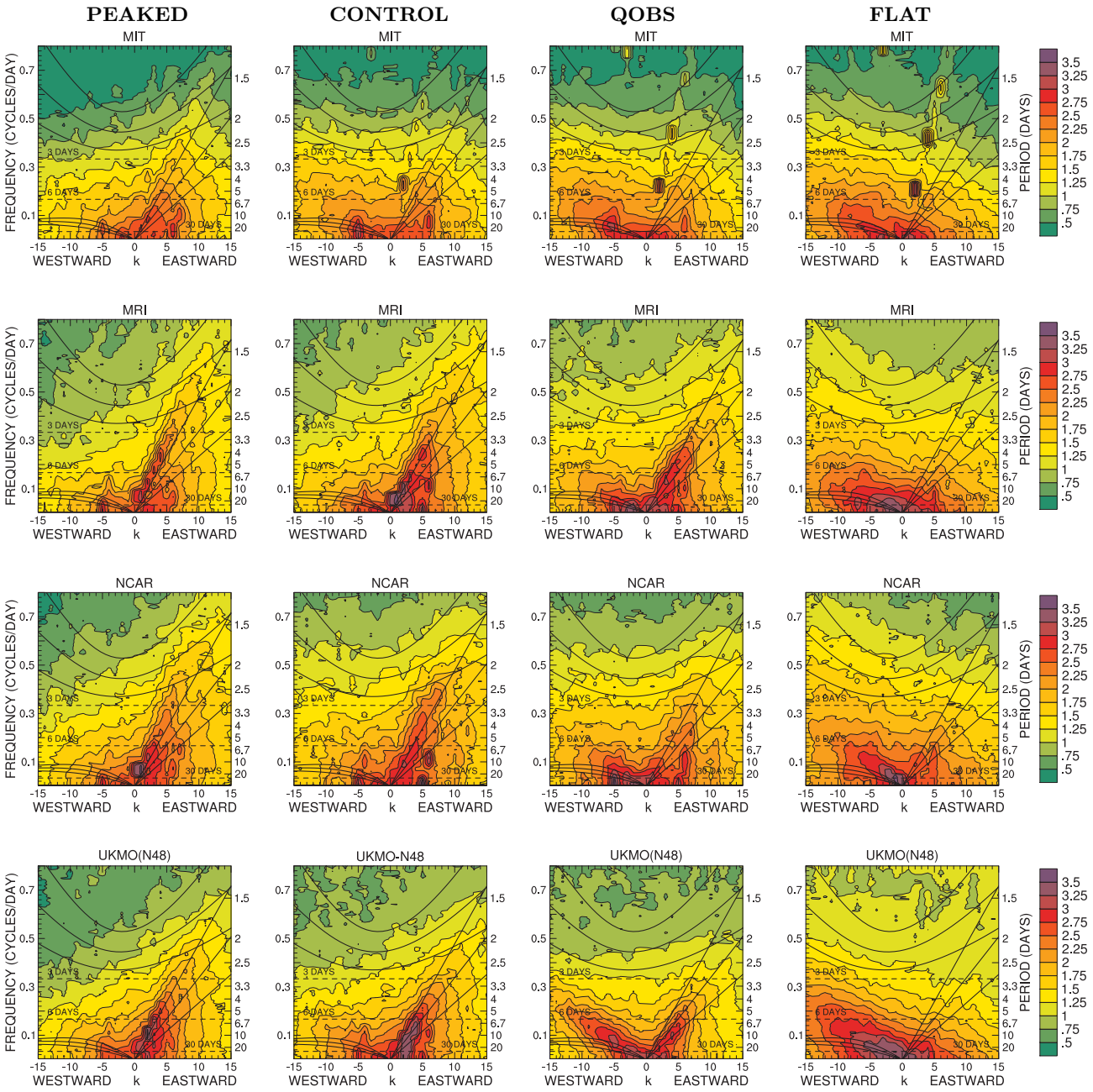

Figure 5.155 (continued): Wavenumber-frequency diagrams of log of power of symmetric modes of equatorial OLR (lw_toa) for PEAKED, CONTROL, QOBS and FLAT, 20°S to 20°N.

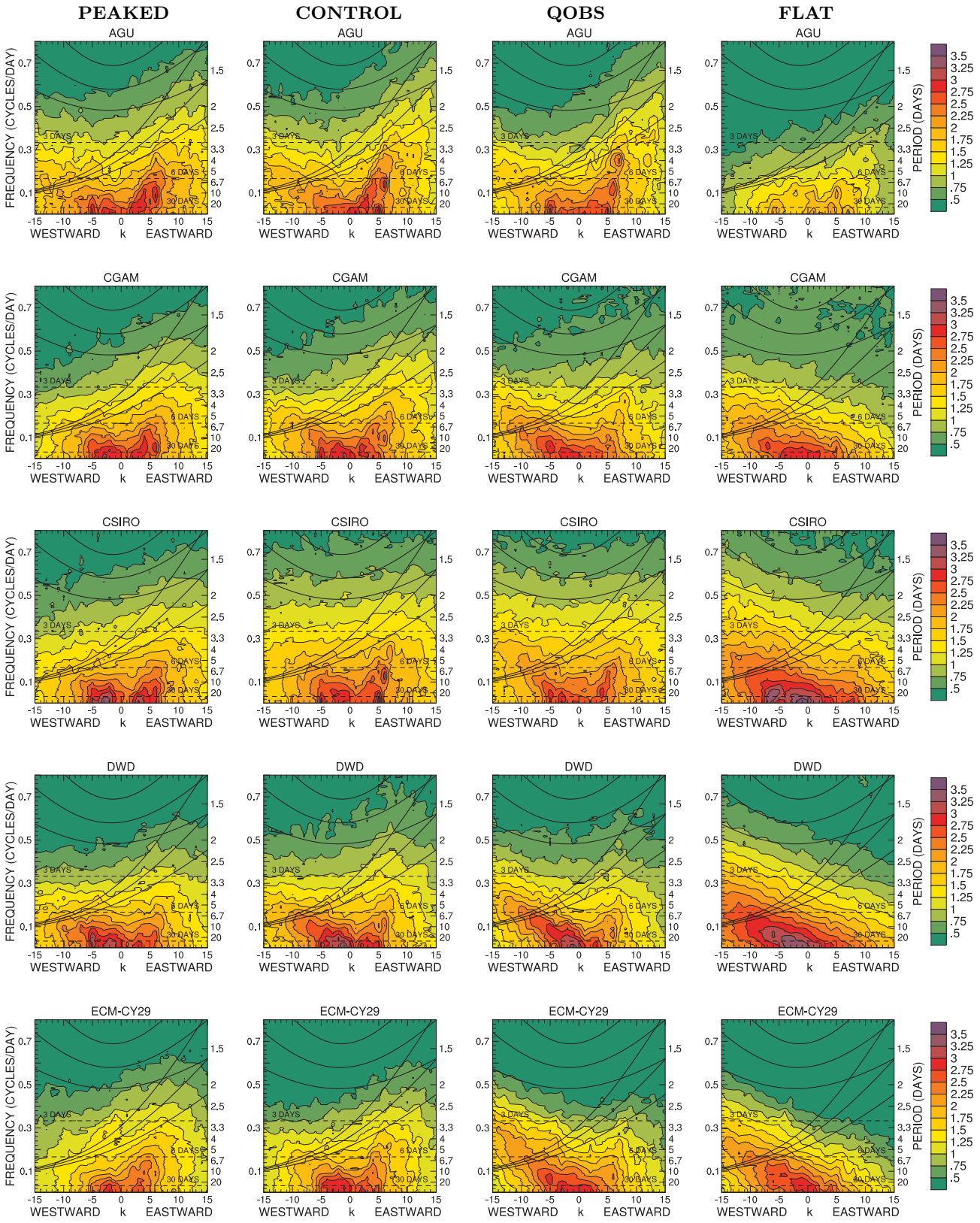

Figure 5.156: Wavenumber-frequency diagrams of log of power of anti-symmetric modes of equatorial OLR (lw_toa) for PEAKED, CONTROL, QOBS and FLAT, 20°S to 20°N.

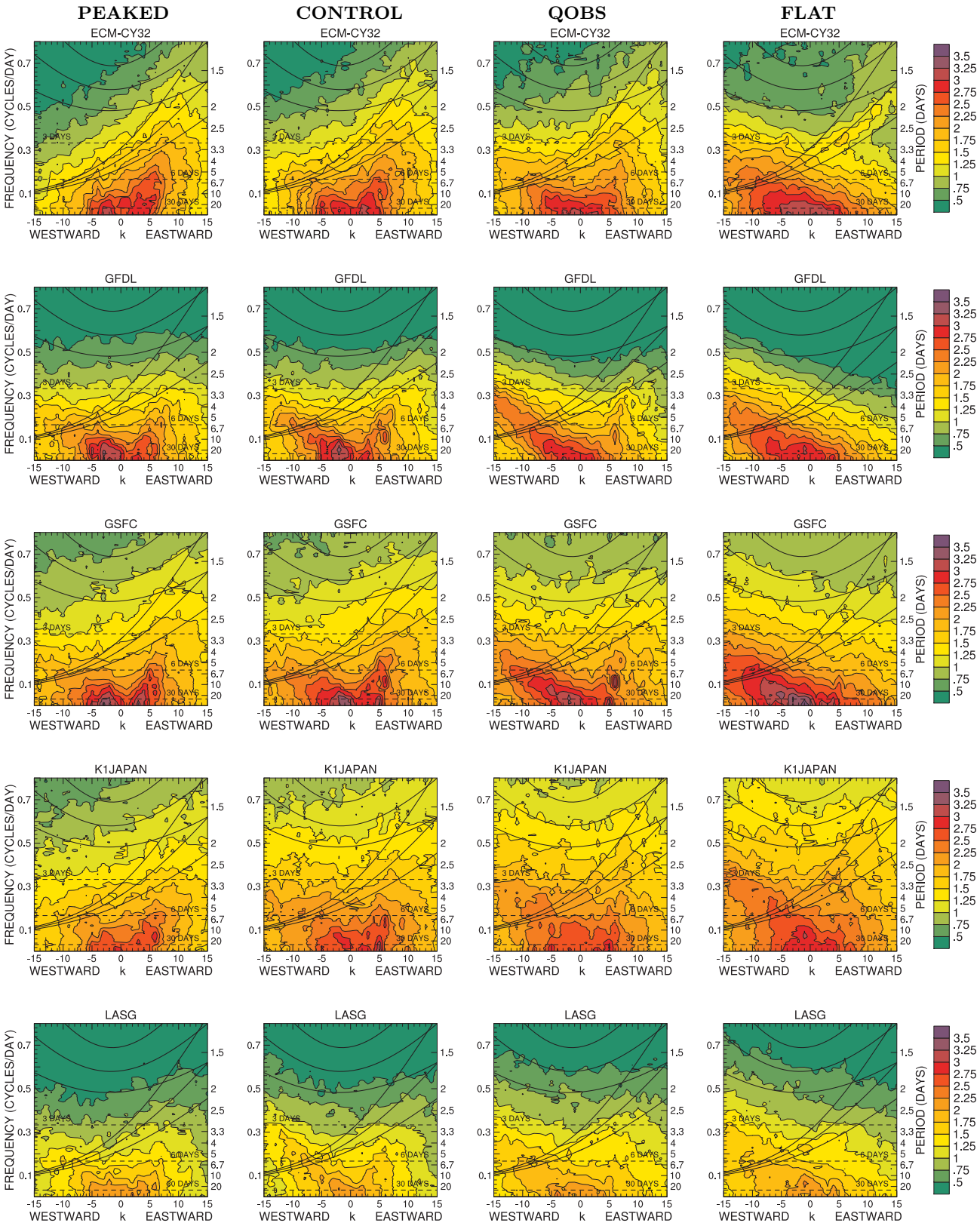

Figure 5.156 (continued): Wavenumber-frequency diagrams of log of power of anti-symmetric modes of equatorial OLR (lw_toa) for PEAKED, CONTROL, QOBS and FLAT, 20°S to 20°N.

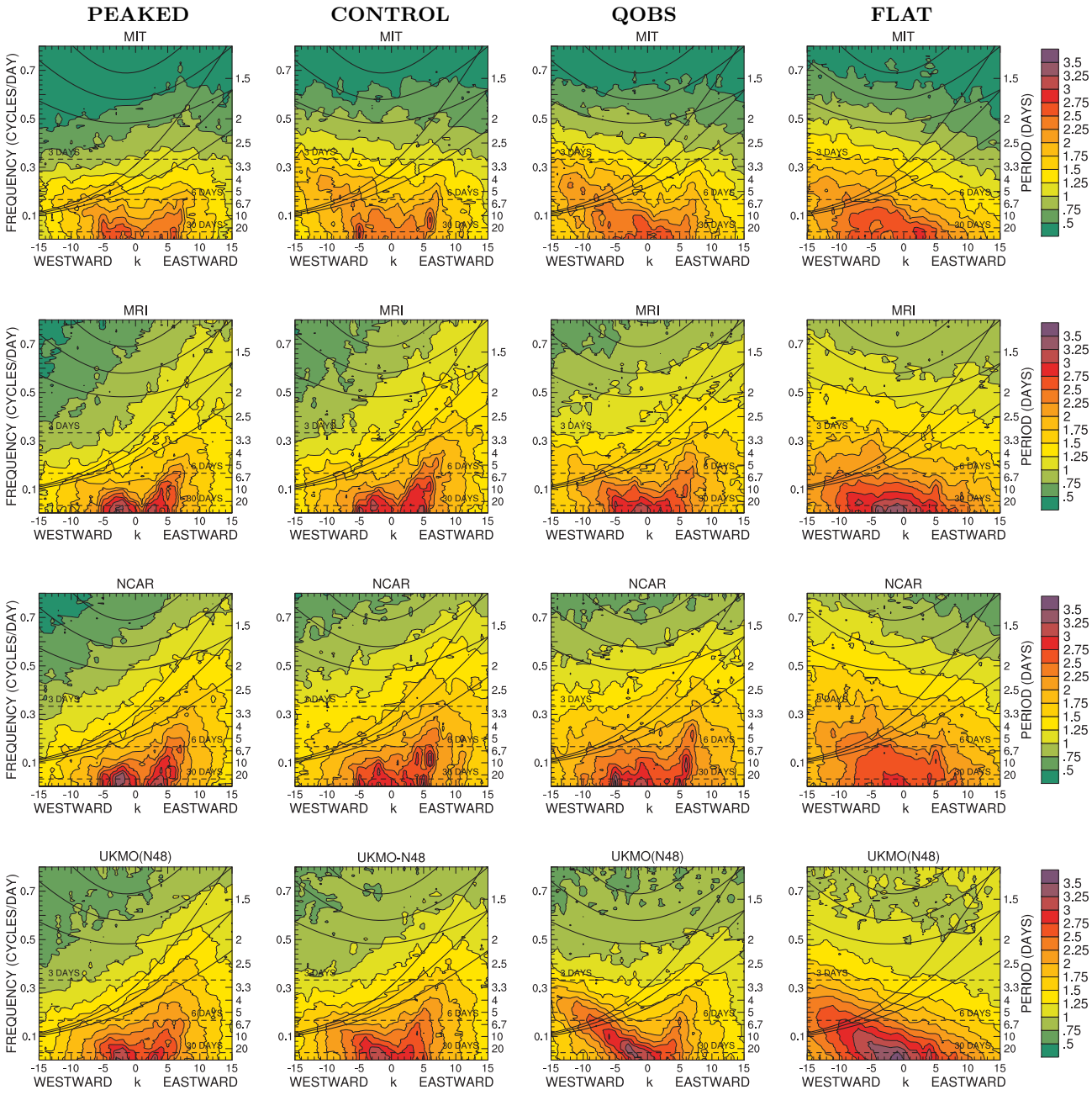

Figure 5.156 (continued): Wavenumber-frequency diagrams of log of power of anti-symmetric modes of equatorial OLR (lw_toa) for PEAKED, CONTROL, QOBS and FLAT, 20°S to 20°N.

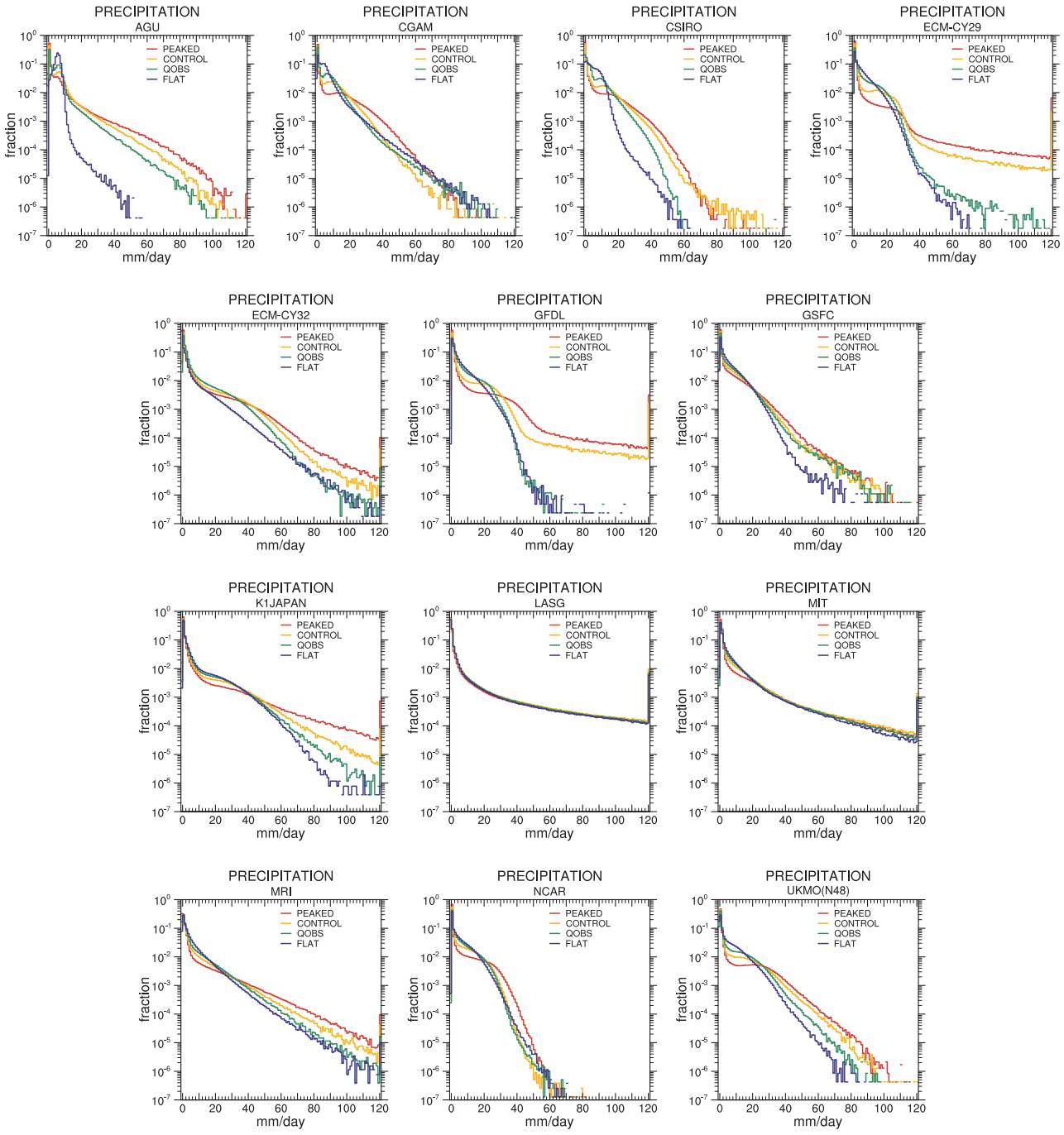

Figure 5.157: Fraction of time precipitation (tppn) from $-20°$ to $+20°$ latitude is in 1 mm day^{-1} bins ranging from 0 to 120 mm day^{-1} for individual models for PEAKED, CONTROL, QOBS and FLAT experiments.

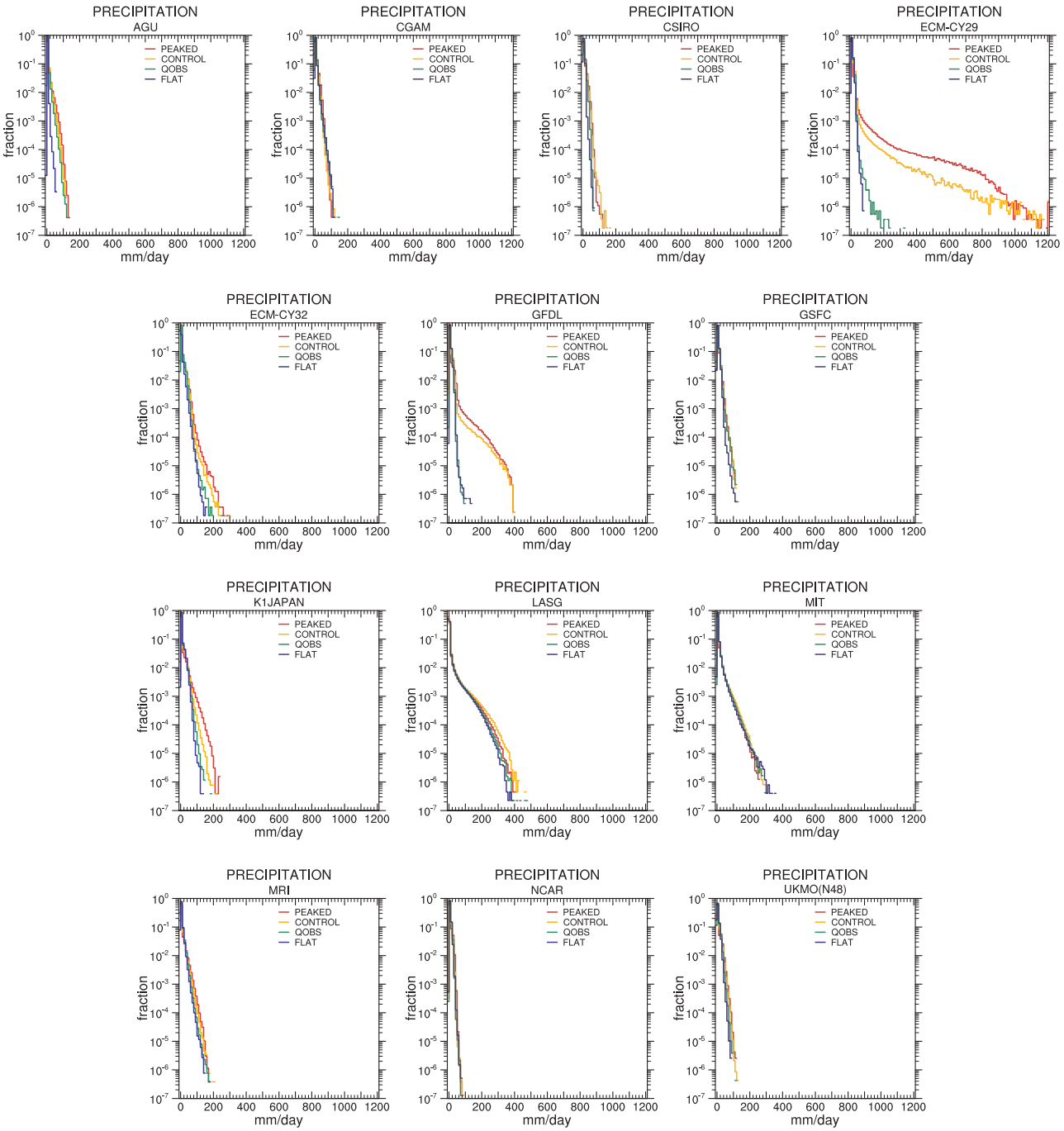

Figure 5.158: Fraction of time precipitation (tppn) from −20° to +20° latitude is in 10 mm day^{-1} bins ranging from 0 to 1200 mm day^{-1} for individual models for PEAKED, CONTROL, QOBS and FLAT experiments.

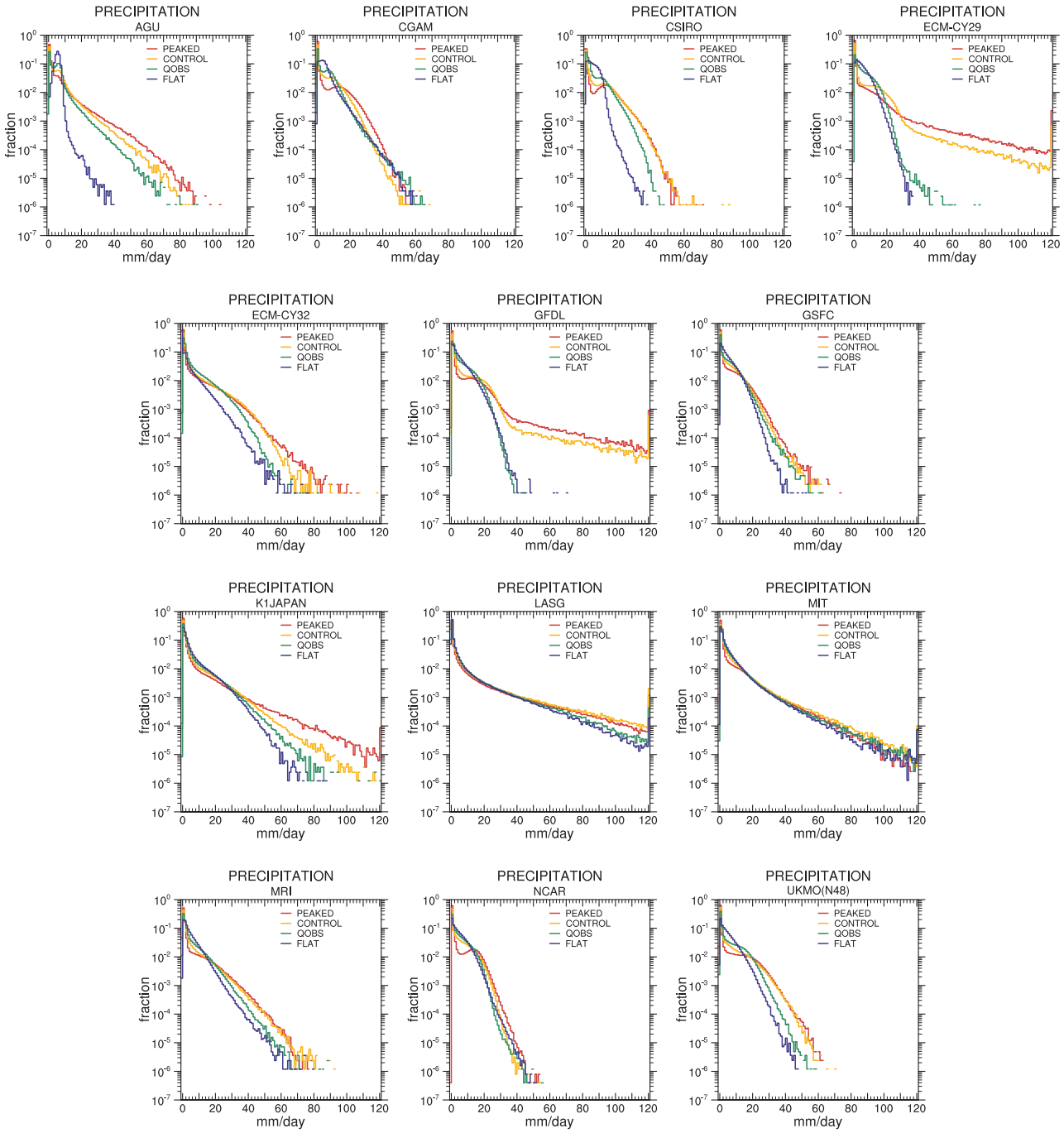

Figure 5.159: Fraction of time precipitation (tppn) from $-20°$ to $+20°$ latitude is in 1 mm day^{-1} bins ranging from 0 to 120 mm day^{-1} for individual models for PEAKED, CONTROL, QOBS and FLAT experiments. Grid values have been conservatively averaged to a 5° latitude-longitude grid.

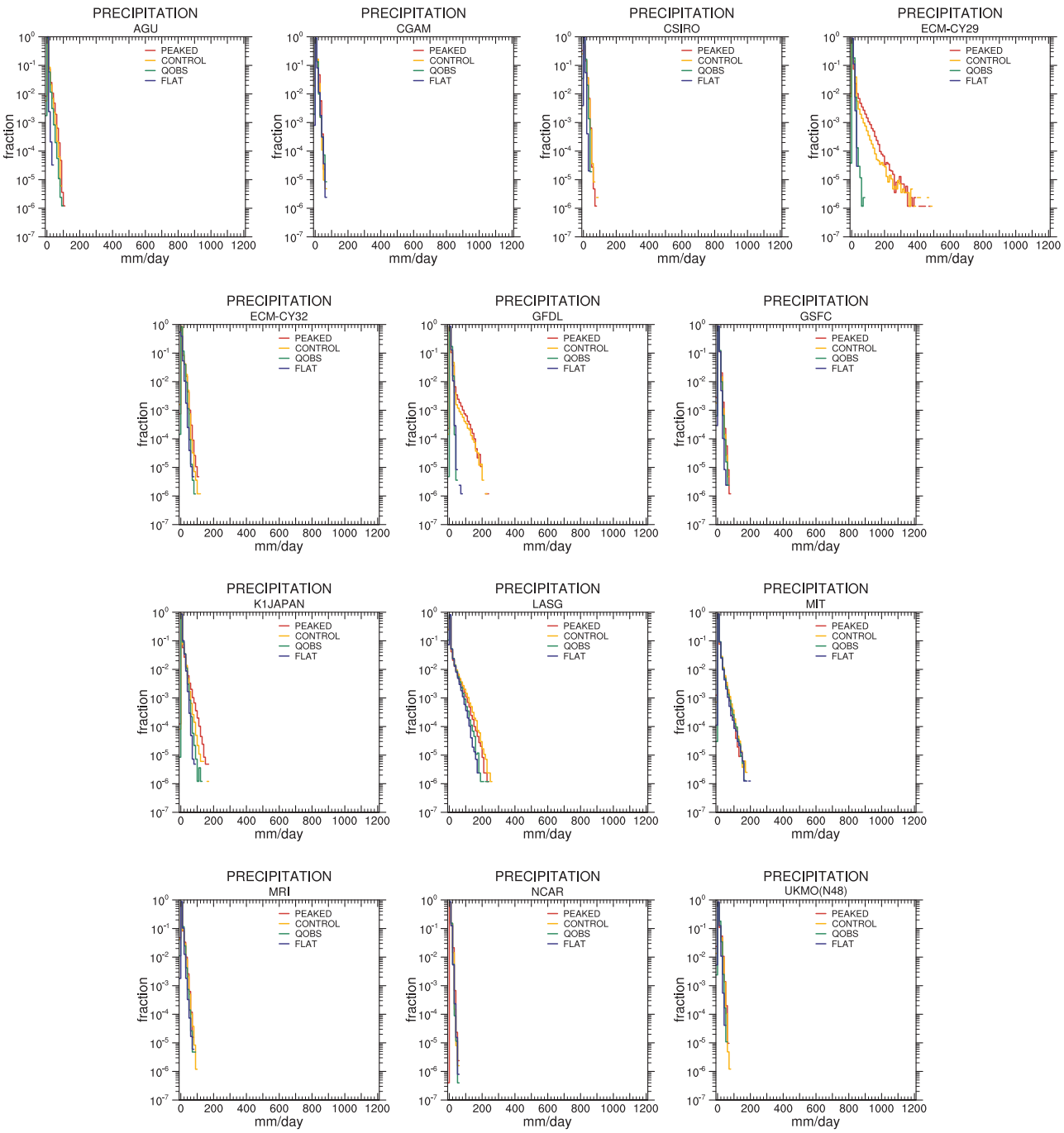

Figure 5.160: Fraction of time precipitation (tppn) from −20° to +20° latitude is in 10 mm day^{-1} bins ranging from 0 to 1200 mm day^{-1} for individual models for PEAKED, CONTROL, QOBS and FLAT experiments. Grid values have been conservatively averaged to a 5° latitude-longitude grid.

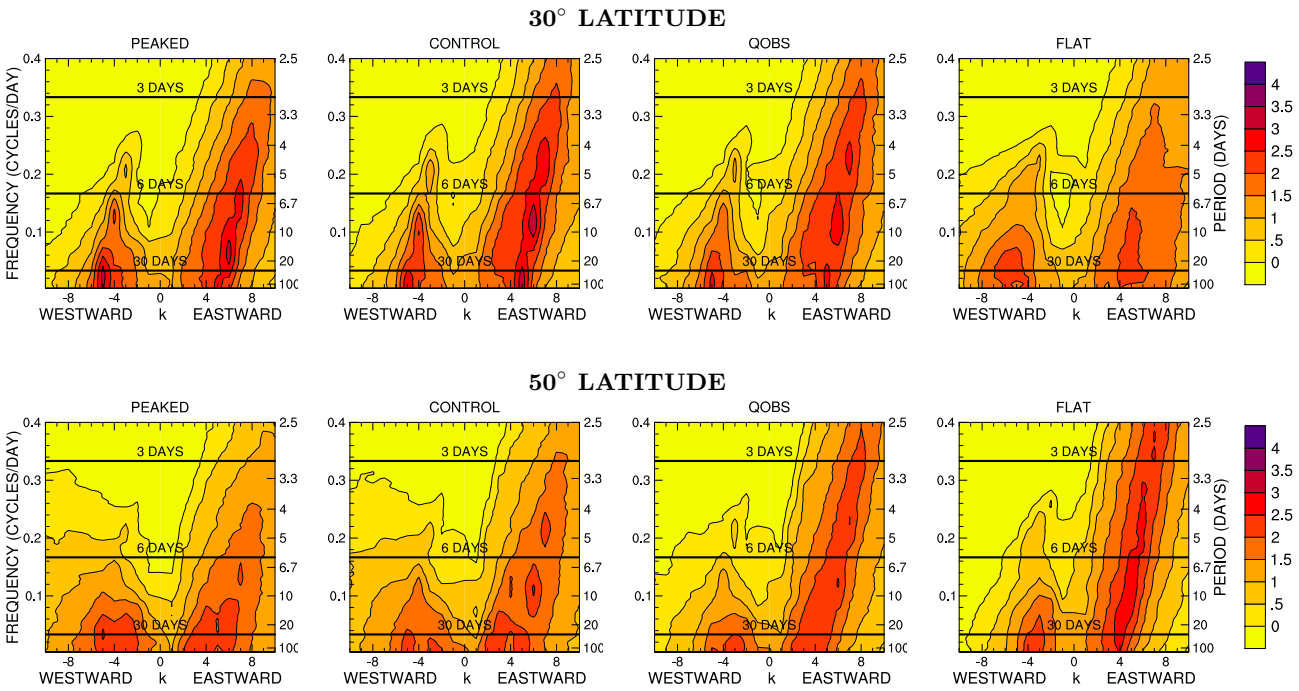

Figure 5.161: Wavenumber-frequency diagrams of log of power of symmetric modes of 250 mb meridional wind (v250) at 30° and 50° latitude for the multi-model mean.

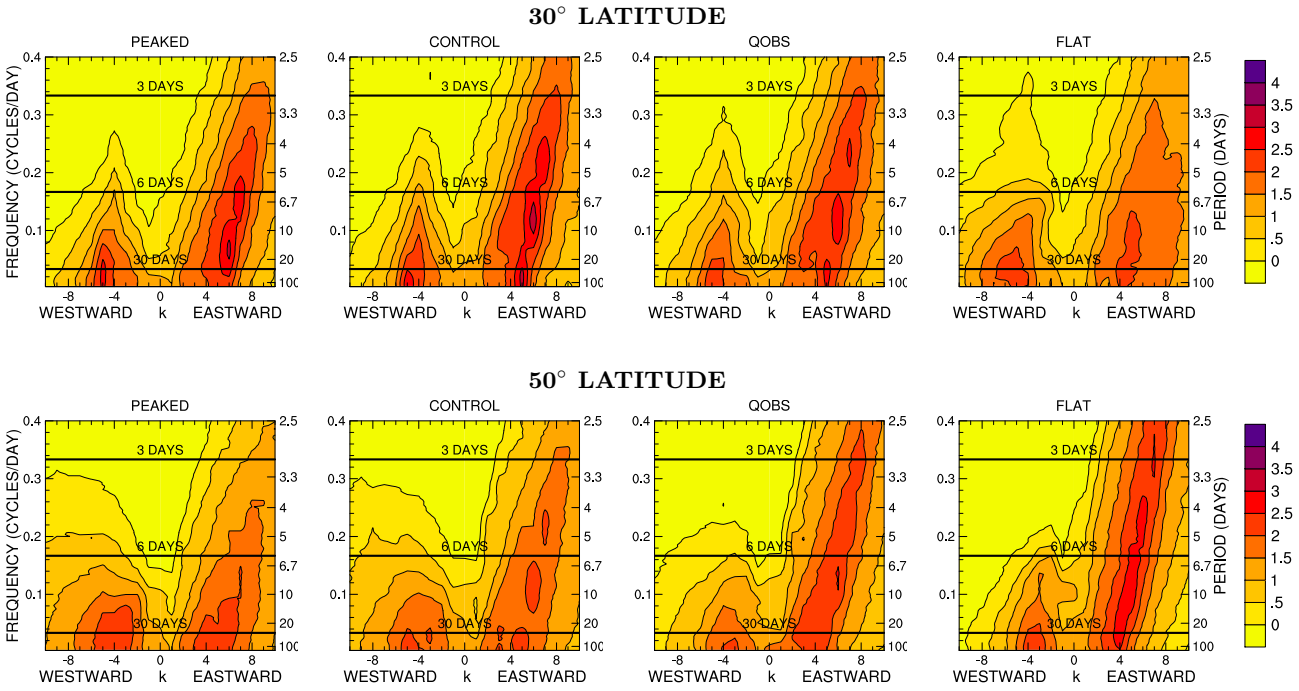

Figure 5.162: Wavenumber-frequency diagrams of log of power of anti-symmetric modes of 250 mb meridional wind (v250) at 30° and 50° latitude for the multi-model mean.